



HAL
open science

Omics on healthy and pathological placentas

Camino Ruano San Martin

► **To cite this version:**

Camino Ruano San Martin. Omics on healthy and pathological placentas. Gynecology and obstetrics. Université Paris Cité, 2022. English. NNT : 2022UNIP5014 . tel-04219800

HAL Id: tel-04219800

<https://theses.hal.science/tel-04219800v1>

Submitted on 27 Sep 2023

HAL is a multi-disciplinary open access archive for the deposit and dissemination of scientific research documents, whether they are published or not. The documents may come from teaching and research institutions in France or abroad, or from public or private research centers.

L'archive ouverte pluridisciplinaire **HAL**, est destinée au dépôt et à la diffusion de documents scientifiques de niveau recherche, publiés ou non, émanant des établissements d'enseignement et de recherche français ou étrangers, des laboratoires publics ou privés.

Thèse de Doctorat

Université de Paris Cité

École doctorale Bio Sorbonne Paris Cité (BioSPC), ED 562

Equipe "From Gametes to Birth", Inserm U1016-CNRS

UMR8104-Université de Paris (Institut Cochin)

Paris, France

Omics on Healthy and Pathological Placentas

Par Camino RUANO SAN MARTIN

Thèse de Doctorat en Reproduction

Dirigée par Céline MEHATS

Présentée et soutenue publiquement à Paris le 11 février 2022

Devant un jury composé de :

Président du jury: Nadia ALFAIDY-BENHAROUGA, DR, Université Grenoble Alpes

Rapporteur: Johanna LEPEULE, CR-HDR, Université Grenoble Alpes

Rapporteur: Cathal McCARTHY, PhD-HDR, University College Cork

Examineur: Vassilis TSATSARIS, PU, Université de Paris

Examineur: Daniel VAIMAN, DR, Université de Paris

Directrice de thèse : Céline Méhats, CR-HDR, Université de Paris

Table des matières / Table of contents

Acknowledgements.....	7
Résumé court.....	11
Résumé	11
Mots-clés :.....	16
Resume	17
Key Words:.....	18
Table of Abbreviations.....	19
Introduction	21
1 Human placenta development	23
Week 1 – Fertilization and implantation.....	23
Week 2 – Syncytiotrophoblast Invasion.....	26
Week 3 to 8 – Villi development.....	26
The syncytialization process	29
Week 8 – Maternal Spiral Arteries Remodelling.....	30
Week 10 to 12 – From Hypoxia to Normoxia.....	33
Week 12 to 18 – From First to Second trimester.....	37
Week 18 to 27 – Second trimester placental maturation	37
Week 27 to 40 – Third trimester Placenta maturation.....	37
2 Placental Functions	40
A) Transport and metabolism.....	40
B) Endocrine function.....	41
Human Chorionic Gonadotropin.....	42
Progesterone.....	42
Human Placental Lactogen	42
Estrogen	43
C) Immunomodulation	44
3 Placental Pathologies.....	46
Physiopathology of Preeclampsia.....	46
Clinical Aspects.....	46
Fetal outcomes.....	48
Maternal outcomes.....	49
Molecular Aspects.....	49
Hypothesis of Preeclampsia.....	51

a) Defective placenta	51
b) Immune Maladaptation	53
c) Genetic Factors	53
d) Primary impaired uterine perfusion	53
Physiopathology of Intrauterine Growth Restriction.....	54
Clinical Aspects.....	54
Molecular Aspects.....	54
Hypotheses of the disease	55
a) Maternal factors	55
b) Placenta.....	55
c) Genetic Factors	56
Physiopathology of Chorioamnionitis.....	56
Omics in placental research.....	56
Project Objectives	59
CHAPTER 1: DNA Methylation Analysis in Normal and Pathological Placentas	61
Introduction	61
Materials and Methods.....	65
1. Human Placental Samples.....	65
2. DNA extraction (Experimental batches 1 & 2).....	65
3. EPIC Illumina Array Methodology	66
Bioinformatic Analysis.....	67
a. Prediction of Covariates: Cell composition, ethnicity, and gestational age	68
i. Gestational Age prediction	68
ii. Ethnicity prediction.....	68
iii. Cell composition prediction	68
b. CpG quality control and filtering.....	69
c. Grouping of placentas.....	69
d. Multivariate linear regression.....	70
e. Dimensionality Reduction	70
Code Availability:	71
Results.....	71
Clinical vs Predicted Gestational Age.....	71
Cell Composition Differences between Control and Pathological Placentas	73
Ethnicity prediction: Genetics vs Epigenetics	75
Preliminary visualization and identification of covariates affecting the DNAm profile.....	75
Multivariate Linear Regression Model and Differentially Methylated CpGs	79

Discussion.....	82
Limitations.....	84
Further Perspectives	86
CHAPTER 2: Single Nuclei RNA-seq Analysis in Preeclamptic Placentas.....	87
Introduction	87
Materials and Methods.....	91
1. Sample collection	91
2. Single nuclei isolation and droplet-based scRNAseq	91
3. Bioinformatic analysis	93
a. snRNA-seq alignment and Quality control.....	93
a. Clusterization	93
b. Identification of top differentially expressed genes	94
c. Gene Enrichment Analysis	95
d. Transcriptomic dynamics and RNA velocity	95
scVelo	98
Results.....	99
Identification of major cell types in the human placenta	99
Functional characterization of the SCT nuclei	102
Analyses of the differences between Unaffected and PE-affected placentas.....	107
Differentially expressed genes between Unaffected and PE-affected placentas.....	109
Transcriptomic Dynamics.....	116
Different transcriptional dynamics in Unaffected vs. PE-affected placentas	116
Discussion.....	119
Limitations: RNA velocity Issues	122
CHAPTER 3: Alternative Splicing Dysregulation in Placental Pathologies.....	125
CHAPTER 4: The Role of Non-coding RNAs in Trophoblast Fusion and Placental Pathologies.....	155
Discussion and Future Perspectives.....	173
Conclusion.....	178
ANNEX.1	179
ANNEX.2.....	181
ANNEX.3.....	187
BIBLIOGRAPHY	233

Acknowledgements

Thank you to Celine Mehats 🍀 and Daniel Vaiman 🍷, for the opportunity they gave me to join the lab and have this 3 years journey next to them, learning, fighting and loving science. I am infinitely grateful for all the support and all the knowledge and time you have shared with me. You taught me to be a critic, to question everything and to improve, day by day all the skills necessary to succeed as a scientist. You were a true inspiration for hard work, clever ideas, and patience. Your brightness as a scientist was only surpassed by your delicacy as people. I have really enjoyed this journey with all the little chats about movies, books, politics, France, and past lab memories.

I would like to thank my two examiners: Dr Johanna Lepeule and Dr Cathal McCarthy for taking the time to read, correct and discuss this manuscript. Thank you as well to Dr Nadia Alfaidy-Benharouga, Dr Vassilis Tsatsaris and Dr Daniel Vaiman for accepting being me examiners, I am looking forward to an exciting scientific discussion.

I would like to extend my sincere thanks to Dr Collin Murdoch and his ability and hard work in the development and organization of iPlacenta. This innovative training network funded by the European Commission has been such an important part of these 3 years by stimulating networking, teamwork, and multidisciplinary training. I hope in the future more of these training networks could be developed in favour of the EU and science worldwide.

I would also thank the iPlacenta group, being part of this heterogeneous group has been such a great experience. It has been such a pleasure being able to take part in this project, and, although the circumstances did not let us meet in person very often, online support was always available.

I would like to thank to all the lab members from "Gametes to Birth": Melina Blanco 🦊, Julie Cocquet 🍷, Léa Chicoisne 🍓, Ahmed Ziyat 🍷, Côme Ialy-Radio 🍷, Sandrine Barbaux 🍷, Patrick Lores 🍷, Sophie Favier 🍷, Audrey L'Hostis 🍷, Manon Coulée 🍷, Laila El Khattabi 🍷,

Mitra Parissa Barzine 🧑‍🔬, Carole Abo 🖋️, Francisco Miralles 📊, Emma Cavarocchi 🌿, Laurence Stouvenel 🌸, Marie-Sophie Girault 🍷, Colette Blanchard 🌈, and Alberto de La Iglesia Rodriguez 🏠. Thank you very much for welcoming and making me one more of the group. All the impossible mots fleches, coffee breaks, lunches in the cloitre... thank you for your support and your help, it has been such a pleasure being able to work in such a supportive and homely environment. Merci beaucoup!!

I would like to express my gratitude to all the women who donated their placentas and all the team behind, from the collection, protection, and archive. I would like to thank especially Pr. Basky Thilaganathan and Dr Veronica Giorgione for their 6 little presents mid thesis, which let me perform and learn new techniques.

Two of the four mousquetaires, Sophie Dupuis 📷, Clara Gobé 🍷. I am so thankful for all the Friday afterlabs of support, nice food, comfort words, movies, apero, makeup and jokes. I hope this tradition keeps going for the next years. Thank you, girls, for your help and energy.

Thank you to Clara Apicella 🔑, without you my stay in Paris would have been completely different. I am so grateful you decided to continue your career in Paris and had the chance to work together doing two PhDs together. Thank you for all your constant support, all your caring words, and all the scientific discussions before the weekly lab meeting. At this time, you will be already Dr Apicella!! I am so happy and thankful I was able to witness this achievement! I wish you all the best in your future to come, and, I hope, you send me at least some of those growing in the lab foie gras for Christmas. Thank you so much for being by my side these 3 years and the ones to come.

Finally, and most importantly, thank you to my family 🚀🌟. El núcleo duro : Mi madre, mi padre y mi hermano ... Sin vuestra ternura, apoyo, infinita paciencia y amor durante todos estos años, no hubiera podido llegar a donde estoy ahora. Arturo, tus consejos y tus llamadas han sido la mejor ayuda que necesitaba para acabar a tiempo y de una pieza. Papá, Mamá, nos habéis enseñado

la importancia de la resiliencia, de pelear y de seguir adelante, de apretar los dientes y continuar. No hay dos personas más luchadoras y fuertes en este mundo y estoy infinitamente agradecida por todo lo que nos habéis dado, ofrecido y de cómo nos habéis educado. Gracias por cada beso, cada discusión, cada llamada y por cada abrazo, cada palabra de apoyo y de cariño. Os quiero ❤️.

Camino 🐱



Omics sur les placentas sains et pathologiques

Résumé court

La prééclampsie (PE) et la restriction de la croissance intra-utérine (RCIU) sont les deux pathologies placentaires les plus courantes, affectant 2 à 5% des grossesses dans le monde. Le développement correct de l'ensemble du placenta requis pour l'invasion profonde appropriée du placenta dans l'utérus maternel et le remodelage complet des artères spirales utérines. Toute perturbation dans le placenta peut conduire au développement de maladies. Ainsi, cette thèse vise à comprendre la physiopathologie du placenta au niveau moléculaire dans les états sains et pathologiques à quatre niveaux d'Omics différents:

1. Étude des changements de méthylation de l'ADN dans les placentas pathologiques pour déterminer les signatures spécifiques de la maladie dans les maladies PE et RCIU.
2. Caractérisation moléculaire détaillée des différents types cellulaires présents dans le placenta par analyse transcriptomique à l'échelle du noyau unique (single nucleus-RNA seq).
3. Étude de la dysruption d'épissage alternative du placenta souffrant de PE et / ou RCIU.
4. Le rôle des ARN non codants dans la fusion des cellules placentaires (syncytialisation).

Résumé

Le placenta humain est un organe temporaire qui se développe pendant la grossesse pour le transport des nutriments, des gaz et des déchets entre la mère et le fœtus. Au cours du développement placentaire humain, les cellules trophoblastiques (CTB) se différencient par deux voies principales : la voie villeuse où les CTB fusionnent pour former un syncytium, composé de noyaux de syncytiotrophoblastes (SCT), au contact du sang maternel et la voie extravilleuse où les CTB acquièrent un phénotype invasif et migrent pour s'ancrer dans l'utérus maternel. D'autres types

de cellules sont importants pour le bon développement et fonctionnement du placenta, comme les cellules immunitaires (cellules Natural Killer, macrophages, cellules T), les cellules stromales et les cellules endothéliales.

Le placenta doit s'adapter aux menaces environnementales tout en garantissant une bonne communication entre la mère et le bébé. Une dysfonction placentaire quel que soit le stade de la grossesse peut influencer la croissance fœtale et/ou être à l'origine d'issues défavorables de la grossesse comme un accouchement prématuré ou un petit poids à la naissance.

La prééclampsie (PE) est l'une des principales pathologies de la grossesse, touchant 2 à 5 % des femmes enceintes dans le monde. La PE est définie classiquement par une hypertension gestationnelle et une protéinurie à partir de la 20^{ème} semaine de grossesse. L'origine de la maladie serait placentaire avec deux stades distincts : le premier impliquerait une mauvaise placentation où l'organe n'est pas capable d'envahir suffisamment profondément l'utérus maternel et le deuxième stade, un stress cellulaire et un déclin de la fonction placentaire. Le retard de croissance intra-utérin (RCIU) est défini comme une *croissance* inférieure au 10^e percentile pour l'âge gestationnel. Le RCIU peut survenir en association avec la PE ou de façon isolé. Enfin, la chorioamniotite, qui affecte 9,7 pour 1000 naissances vivantes, est caractérisée par une inflammation du chorion due à une invasion microbienne. Ces trois pathologies placentaires augmentent le risque d'issues défavorables chez la mère et l'enfant et peuvent entraîner un accouchement prématuré spontané ou induit pour des raisons médicales.

Dans mon travail de thèse, j'ai abordé la question de la dysfonction placentaire, en me concentrant dans la PE, selon quatre approches distinctes, 1) une étude du méthylome placentaire à partir de 74 biopsies placentaires obtenues chez des femmes ayant une grossesse compliquée ou non par une PE ; 2) une caractérisation moléculaire détaillée des différents types cellulaires présents dans le placenta par analyse transcriptomique à l'échelle du noyau unique (single nucleus-RNA seq) à partir de 12 biopsies placentaires (8 obtenus chez des femmes enceintes au terme d'une grossesse

singleton à bas risque et 4 chez des femmes affectées par une PE) ; 3) une étude d'épissage alternatif entre les placentas contrôle et PE et 4) une étude des ARN non codants dans le processus de syncytialisation.

- 1) La méthylation de l'ADN est essentielle pour d'importants processus cellulaires, comme l'expression des gènes, la stabilité du génome, l'inactivation du chromosome X et la régulation de l'empreinte génomique. Chez les mammifères, la *méthylation* de l'ADN consiste en l'ajout d'un groupement méthyl sur les cytosines de dinucléotides CpG. Il est proposé que l'hypométhylation globale observée dans le placenta facilite les fonctions uniques de cet organe ; de faibles niveaux de méthylation améliorent la capacité du placenta à répondre aux expositions environnementales qui nécessitent des changements adaptatifs rapides. Le méthylome du placenta présente aussi des changements dynamiques au cours de la gestation afin de favoriser le développement du fœtus. Des modifications de la méthylation de l'ADN (ADNm) peuvent altérer le comportement cellulaire conduisant à des maladies. Plusieurs études ont montré des différences d'ADNm placentaires dans la PE et/ou RCIU en comparaison de grossesse à bas risque. Cependant, la reproductibilité des études de méthylation placentaire reste faible en raison de nombreux biais méthodologiques. Nous avons cherché au cours de ma thèse à identifier des « signatures mCpG » de chacune des pathologies présentes dans notre ensemble de données (prééclampsie, RCIU, PE+RCIU et chorioamniotite) en incluant une analyse approfondie de variables confondantes. Une analyse de l'ADNm a été réalisée dans 74 échantillons de placentas humains (34 témoins, 22 chorioamnionites, 12 PE, 2 RCIU et 3 PE+ RCIU) à l'aide des kits Infinium MethylationEPIC d'Illumina qui interrogent la méthylation de 750,000 CpGs. Les variables confondantes telles que l'âge gestationnel, la composition cellulaire, l'origine ethnique et le sexe du bébé ont été prédites à partir des données de méthylation. Pour écarter les CpGs influencés par les facteurs de confusion cliniques ou méthodologiques, une régression

linéaire multivariée utilisant 14 covariables a été réalisée. Ainsi, 142 CpGs ont été trouvés corrélés avec la pathologie placentaire (PE, PE+ RCIU et RCIU) (valeur de p ajustée $<0,05$, différence de valeur bêta $>5\%$). Cette approche nous permet de déterminer un sous-ensemble de CpG en corrélation avec la maladie seule, créant une « signature de la maladie » en termes de méthylation de l'ADN. Ce travail sera poursuivi par l'analyse de cette signature dans une cohorte de réplication.

- 2) Les technologies séquençage de cellule unique permettent d'effectuer une cartographie à haute résolution d'un organe grâce à l'interrogation transcriptomique de chaque cellule individuelle. Nous avons réalisé une analyse RNA-seq à l'échelle du noyau pour améliorer l'analyse du syncytium de placentas obtenus chez des femmes à l'issue d'une grossesse à bas risque ou compliquée par une PE. Douze placentas humains (8 contrôles et 4 PE) ont été analysés à l'aide de la technologie 10xGenomics. Un total de 71k noyaux individuels a été analysé, incluant 21 clusters différents et les types cellulaires suivants : SCT, CTB villeux et extravilleux, cellules stromales et fibroblastes, cellules endothéliales, et cellules immunitaires (cellules de Hofbauer, Natural Killer, cellules T). Neuf des 21 clusters contiennent des noyaux de SCT. Une analyse ontologique des gènes-marqueurs de ces neuf clusters a révélé que chaque groupe peut être associé à une fonction distincte. En effet, nous avons pu retrouver par exemple des clusters de SCT dédiés à la stéroïdogénèse, aux voies de la prolactine, ou au métabolisme du tryptophane. Ces résultats soulèvent la question de l'architecture syncytiale et la localisation des noyaux au sein de cette couche syncytiale. Les gènes exprimés différemment (DEG) entre les échantillons contrôle ou affectés par une PE ont été identifiés au niveau du type cellulaire. Nous avons observé un nombre de DEG plus élevé dans les SCT que dans les autres types cellulaires, suggérant que les SCT sont les plus affectés dans la PE. La phosphorylation oxydative, l'inflammation et les voies métaboliques liées au réticulum

endoplasmique sont les voies les plus enrichies dans les échantillons affectés par la PE. De plus, la dynamique de l'expression des gènes a été étudiée en analysant les formes d'ARNs épissés et non épissés, montrant des différences significatives entre les placentas affectés et non affectés par la PE.

3) La forme soluble du récepteur VEGF (sFLT1) est des biomarqueurs les mieux établis pour le diagnostic précoce de la prééclampsie, se trouvant à des concentrations augmentées dans le sang maternel en cas de PE. Cette molécule est produite par épissage alternatif. Cependant, une différence d'épissage globale en cas de PE n'était pas décrite à notre connaissance. Nous avons analysé le transcriptome de 37 échantillons placentaires (contrôle, PE et RCIU) par une puce d'expression Clariom D d'Affymetrix qui permet l'interrogation des sites d'épissages. Un total de 1071 gènes a été retrouvé épissé de manière différentielle entre les placentas contrôles et affectés par une PE. Parmi ceux-ci, des gènes tels que la pappalysine (PAPPA2), la sérine peptidase 4 (HTRA4) et la leptine (LEP) avaient déjà été observés comme ayant une expression augmentée dans la PE. Nous avons validé par RT-qPCR ces épissages différentiels pour 12 gènes : FLT1, CLDN1, LEP3, FSTL3, TXK, CAP2, CA10, TNFRSF1B, ACOXL, TIE1, LAGLS14 et CPXM2. Nous avons également identifié des loci de trait d'épissage quantitatif (sQTL). Les 48 gènes avec l'indice d'épissage le plus élevé étaient corrélés avec un total de 331,204 SNPs : 52 cis-QTL et 52 trans-QTL (FDR <0,05) ont été ainsi identifiés avec cette stratégie. Ces résultats mettent en évidence l'importance de l'étude de l'expression des différentes isoformes dans le contexte de la maladie placentaire et nous avons décrit les premières dérégulations globales de l'épissage dans les placentas pathologiques.

4) Les ARN non codants (ARNnc) sont des molécules d'ARN qui ne se traduisent pas en protéines mais qui peuvent réguler d'importants processus cellulaires. Pour étudier le rôle de ces molécules dans la fusion des trophoblastes à l'origine du syncytium

placentaire, nous avons réalisé une analyse transcriptomique dans les cellules BeWo de choriocarcinome humain, modèle cellulaire de CTB, capables de fusionner après traitement par la forskoline. Nous avons identifié 800 gènes avec une expression augmentée et 1281 avec une expression diminuée dans les cellules traitées à la forskoline par rapport aux cellules non traitées. Parmi ces gènes, 307 sont des ARNnc dont 8 miARN (miR-193b, miR-365a, miR-936, miR-6886, miR-7110, miR-518A1, miR-4454 et miR-1283-2) et un lncRNA (UCA1) retrouvés en commun avec le profil transcriptomique des placentas affectés par PE et RCIU. L'inhibition de l'expression d'UCA1 par interférence à l'ARN dans les cellules BeWo réduit les différences transcriptomiques observées après traitement par la forskoline dans les cellules contrôles, suggérant pour la première fois que le lncRNA UCA1 participe à la syncytialisation du trophoblaste.

Cette approche multi-« omique » des pathologies placentaires permet d'aborder les dysfonctionnements placentaires à différents niveaux moléculaires. Ces études améliorent la compréhension des pathologies placentaires et pourront servir pour l'élaboration de nouvelles stratégies de diagnostic et de traitement de ces pathologies.

Mots-clés :

Placenta, Omics, Méthylation de l'ADN, Epigénétique, Transcriptomique, Prééclampsie

Resume

Preeclampsia (PE) is one of the main pathologies of pregnancy, affecting 2 to 5% of pregnant women worldwide. The placenta is thought to be at the origin of the disease in two distinct stages: the first involved a poor placentation where the organ is not able to invade sufficiently deeply the maternal uterus and the second stage, a cellular stress which leads to a decline of the placental function. During human placental development, trophoblast cells (CTB) differentiate through two main pathways: the villous pathway where CTBs fuse to form a multinucleated syncytiotrophoblast (SCT) on contact with maternal blood and the extravillous pathway where CTBs acquire an invasive phenotype and migrate into the maternal uterus and arteries. During my thesis work, I approached the question of the placental difference in preeclampsia according to four distinct approaches, 1) a study of placental methylome from 74 placental samples of women with a pregnancy complicated or not by PE ; 2) a detailed molecular characterization of the different cell types present in the placenta by transcriptomic analysis at the scale of the single nucleus (single nucleus-RNA seq) from 12 placental samples (8 obtained from women with uncomplicated pregnancy and 4 with PE affected); 3) a study of alternative splicing between unaffected and PE-affected placentas and 4) a study of non-coding RNAs implicated in the syncytialization process. Methylome analysis allowed us to identify 142 differentially methylated CpGs in PE-affected samples, considering confounding factors such as gestational age, which could be a signature of pathology in the placenta. The snRNA-seq analysis showed an increase in the expression of genes involved in oxidative stress specifically in SCTs as well as different cell dynamics in PE-affected samples compared to unaffected placentas. We further observed global splicing differences in the disease and identified four chromosomal regions influencing splicing in the placenta. Finally, we identified two miRNAs (mir193b and miR365a) and one long non-coding RNA (UCA1) involved in the fusion of trophoblasts and deregulated in placental pathologies. These studies have helped advance our understanding of the placenta at a genome-wide scale under physiological conditions and in the context of preeclampsia.

Key Words:

Placenta; Omics; DNA methylation, Epigenetics, Transcriptomics, Preeclampsia

Table of Abbreviations

CpG	Cytosine and Guanine separated by a phosphate
C-section	Cesarean section
CTB	Cytotrophoblast
Ctrl	Control
CVD	Cardiovascular Diseases
DEGs	Differentially Expressed Genes
DNAm	DNA methylation
dS	Decidual Stromal cells
eCTs	Endovascular Cytotrophoblast
END	Endothelial cells
EOPE	Early Onset of Preeclampsia
EVs	Extracellular Vesicles
EVTs	Extravillous Trophoblast
FDR	False Discovery Rate
FSK	Forskolin
GA	Gestational Age
HELLP	Haemolysis, Elevated Liver transaminases and Low Platelet count
ITV	Interstitial cytotrophoblast
IUGR	Intrauterine Growth Restriction
IVS	Intervillous space
lncRNA	Long Non-Coding RNAs
LOPE	Late Onset of Preeclampsia
MeQTL	Methylation Quantitative Trait Loci
OS	Oxydative Stress
PCA	Principal Component Analysis
PE	Preeclampsia
Pred_GA	Predicted Gestational Age
PT/T	Preterm/Term
Pvd	Placenta vaginal delivery
QC	Quality control
SCT	Syncytiotrophoblast
SNP	Single Nucleotide Polymorphism
snRNAseq	single nuclei RNA sequencing
sQTL	splicing Quantitative Trait Loci
STB	Syncytiotrophoblast
TAC	Transcriptome Analysis Console
TB	Trophoblast
TSC	Trophoblast Stem Cells
UMAP	Uniform Manifold Approximation and Projections for Dimension Reduction
UMI	Unique Molecular Identifier
uNKs	uterine Natural Killer cells
VCT	Villous Cytotrophoblast
VSMCs	Vascular smooth muscle cells

Introduction

This PhD Thesis forms part of iPlacenta, a doctoral-level European training network founded by the European Union under the Horizon 2020 Research and Innovation Programme (Marie Skłodowska-Curie Actions) (<https://www.iplacenta.eu>). The main objective of this consortium is to support Early-Stage Researchers to study, model and visualize the placenta. Fifteen PhDs around Europe are grouped in three different work packages (WP) by their axis of interest: WP1 is focused on the development of in-vitro models to mimic the placenta; WP2 aims to understand multi-omics data using system biology and WP3 is focused on the characterization and validation of new methodologies for in vivo placenta modelling. My PhD, part of the WP2, aims for the study of the placenta through many different perspectives: genetics, epigenetics, and transcriptomics to further understand healthy and pathological placentas in the characterization of possible targets that could be used to diagnosis and treat placental pathologies.

1 Human placenta development

The placenta is the largest fetal organ and the first to develop during pregnancy. Its main functions are the fetal-maternal interchange of nutrients, gases, waste, and the production of hormones and growth factors that support fetal development and ensure a healthy 9-months pregnancy. Morphologically, it is a flat circular shape of 20 cm in diameter at term. The placenta must develop and adapt to many different environmental threats while guaranteeing proper communication between mother and baby (Gude, Roberts, Kalionis, & King, 2004).

Healthy and successful pregnancy starts at the implantation of an embryo in the maternal uterus and ends in the successful delivery of a baby after 40 weeks of gestation. Human pregnancy is divided in three trimesters: first trimester (0 to 13 weeks), second trimester (13 to 27 week) and third trimester (27 to 40 weeks). Three subsequential and discrete events are necessary for a healthy pregnancy: implantation, decidualization and placentation (Mendes, Timóteo-Ferreira, Almeida, & Silva, 2019). A proper placentation, defined as the formation and a controlled invasion of the placenta in the maternal tissue, is critical in pregnancy.

Week 1 – Fertilization and implantation

Fertilization of the oocyte with sperm occurs in the maternal oviduct creating the zygote, in which the maternal and paternal genome will fuse. After 30 hours, the zygote undergoes a series of mitotic divisions, in which each cell or blastomere reduces in size every time a division occurs. These blastomeres will be compacted together inside the zona pellucida. On the 3rd day post-fertilization, 12 to 32 blastomeres constitute a compact mass denominated the morula. During the 4th day post-fertilization, the morula travels throughout the fallopian tube towards the uterine cavity. Cells located in the morula's outer line start to secrete a fluid inside the cell clump, creating an intracellular space (blastocoel). The hydrostatic pressure produced by this liquid gives rise to a shallow monolayer sphere of cells (trophoblast), protecting an inner cell mass (embryoblast) (**Figure**

1). While the embryo will develop from the inner cell mass, the placenta will arise from these trophoblast cells composing the external monolayer (Shahbazi, 2020).

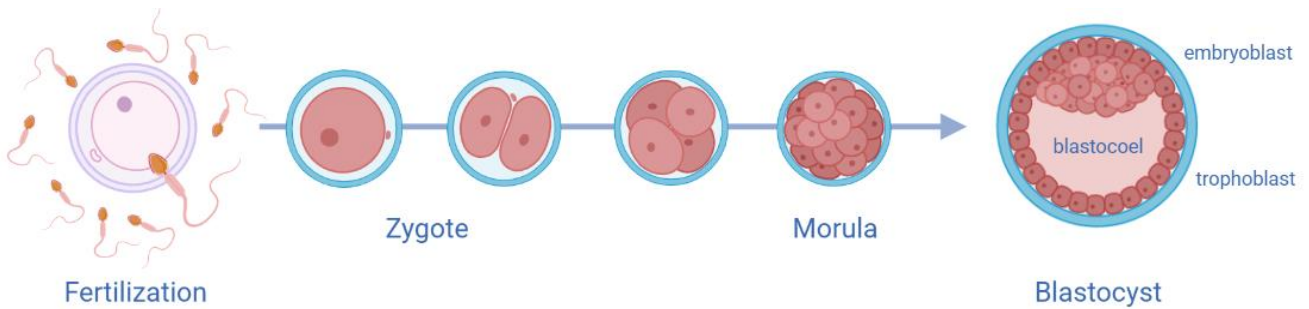


Figure 1: After the fertilization of the egg with a spermatozoid, a one-cell zygote is formed. Several divisions after, a morula will arise. These cells will rearrange in the blastocyst, where the inner cell mass or embryoblast will develop into the fetus while the outside cell monolayer, the trophoblast; will form the placenta.

During day 5 post-fertilization, the blastocyst arrives at the uterine cavity and hatches from the degraded zona pellucida. Around the 6th day post-fertilization, the blastocyst gets activated and acquires implantation competency, implanting into the receptive uterine lining or endometrium. The endometrial tissue has previously undergone a differentiation called decidualization, which occurs during the second part of the ovarian cycle, right after ovulation. When the egg is released from the ovaries, the empty follicle left in the ovary reorganizes and becomes an endocrine cyst or the so-called, the corpus luteum. This cyst is the major source of steroid hormones, such as progesterone, which is one of the main drivers of the decidualization process (S.-W. Ng et al., 2020; Reynolds & Redmer, 1999). Decidualization prepares the maternal uterus to tolerate the invasion of the activated blastocyst (S.-W. Ng et al., 2020). The main changes are increased vascularization, stromal cell differentiation into decidual secretory cells, extracellular matrix remodelling and increase in specific subsets of immune cells (macrophages and uterine natural killer cells).

Moreover, the decidua is key to supply nutrients to the embryo during the first trimester. Since the placenta has not yet been developed, the embryo nutrition is achieved through the secretions of the uterine glands. This process is denominated histotrophic nutrition, and it is critical in the supply

of carbohydrates, amino acids, proteins, and ions to the developing embryo (Cooke, Spencer, Bartol, & Hayashi, 2013).

Once the embryo gets in contact with the maternal decidua, trophoblast cells (Chorion Frondosum) differentiate into the two main placental cells: cytotrophoblasts (CTB) and syncytiotrophoblasts (SCT). The SCT, formed by fused cytotrophoblast cells on the first line, creates a primary syncytium that protrudes and invades the endometrium. In contrast, in the second line, a mononuclear cytotrophoblast layer retains the primitive trophoblast morphology sphere. Therefore, SCT develops from the CTB, and it is continuously renewed through CTB division and syncytialization. In this stage, named the pre-lacunae stage, the syncytiotrophoblast protrusions, filled with digestive enzymes, break down the maternal decidua and erode the uterine glands making nutrients available to the fetus. As a result, the blastocyst not only invades but also gets completely encapsulated into the maternal tissue by the proliferation of uterine stromal cells around it (Carter, Enders, & Pijnenborg, 2015; Staun-Ram & Shalev, 2005) (**Figure 2**).

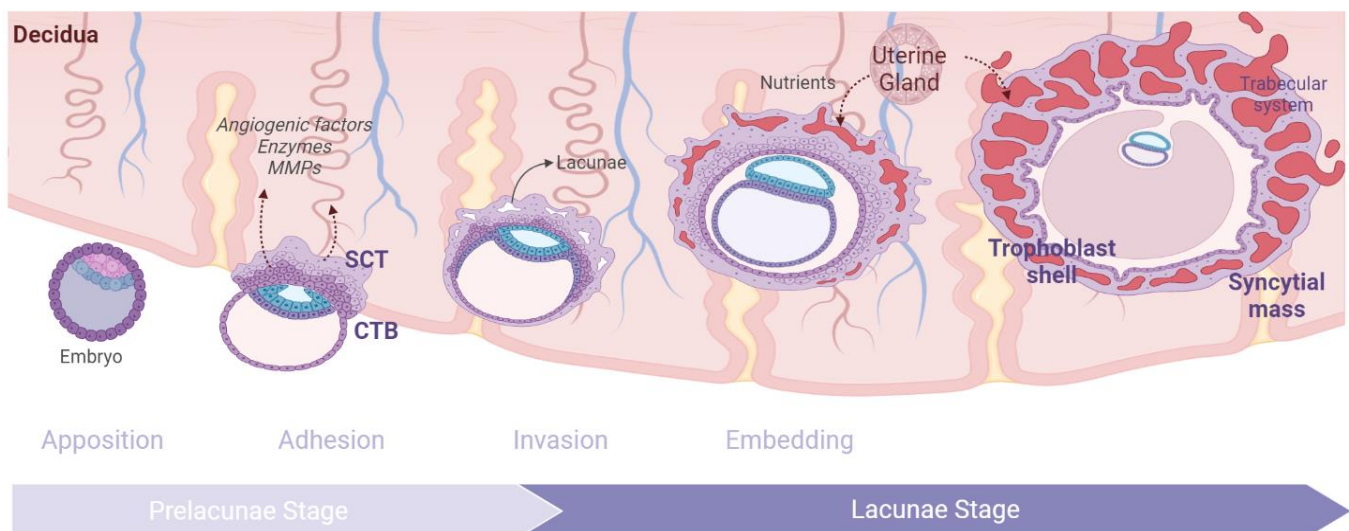


Figure 2: Embryo implantation and early placenta development: After the embryo gets in contact with the decidualized uterine wall, the cytotrophoblast cells (CTB) start to fuse creating the syncytiotrophoblast (SCT). SCT secretes digestive enzymes and metalloproteases (MMPs) which modify the uterine tissue leading to the invasion of the fetus. The embryo gets embedded in the uterus and the SCT produces spaces within the syncytium (lacunae), where nutrients from the remodelled uterine glands will be supplied to the embryo. The early placenta is composed by a syncytial mass with a trabecular system of lacunae and a trophoblast shell formed by the cytotrophoblast cells surrounding the developing embryo.

Week 2 – Syncytiotrophoblast Invasion

In the middle of the 2nd week of gestation, irregular spaces appear within the syncytium; these fluid-filled cavities, called lacunae, establish the trabeculae placental system. The syncytium erodes into the uterine glands, filling these cavities with nutrients and bathing the syncytial mass. The development of these lacunae gives rise to the lacunae stage of the placenta (Hertig, Rock, & Adams, 1956).

Around day 14, post-fertilization CTB formed the initial shell around the embryo proliferates and projects into the syncytium in column-like structures (villous CTB), forming the **primary villi** (**Figure 3**). The placenta enters into the placental villous stage. CTB cells undergo a proliferation pressure. While moving through the villi they change their repertoire of matrix metalloproteases (MMPs) and start the expression of immunotolerant antigens. Once the CTB villi reach the syncytium, they differentiate in SCT, maintaining and renewing the syncytium that surrounds the villi or in CTB, maintaining the CTB pool. Moreover, these nucleated trophoblast cells invade the uterine tissue and create an exterior cytotrophoblast shell between villi and decidua (Turco & Moffett, 2019). Further villi's growth and branching lead to more complex tree-like villi structures. The space between these villi, the former lacunae, will become the intervillous space (IVS) (Kingdom, Huppertz, Seaward, & Kaufmann, 2000; Knöfler et al., 2019; Turco & Moffett, 2019).

Week 3 to 8 – Villi development

Around day 17-18 post-fertilization, fetal mesenchymal cells penetrate the CTB columns, forming the **secondary villi**. Some of these extraembryonic mesenchymal cells can differentiate into placental macrophages or so-called Hofbauer cells. These cells are highly numerous at this stage of pregnancy. They have essential roles in releasing proangiogenic factors that will guide the fetal endothelial cells towards the tips of the placental villi. Moreover, they stimulate the production of human Chorionic Gonadotropin and human Prolactin by the trophoblast. Thus, Hoffbauer cells are

highly important in fetal defence, and their phagocytic activity engages them in tissue remodelling by breaking down collagen fibrils present in the villi (Aplin, Lewis, & Jones, 2018).

After 18 days, fetal capillaries start to invade the mesenchymal core of the secondary villi, leading to the **tertiary villi**. As a resume, tertiary villi are formed by fetal capillaries surrounded by fetal mesenchymal stromal cells embedded inside the cytotrophoblast villi, which is surrounded by the syncytiotrophoblast layer (**Figure 3**). The top tip of some of the placental villus reaches the maternal decidua, allowing the cytotrophoblast to invade the maternal tissue. Thus, each placenta villi act as a wall between two intervillous spaces, where the maternal blood will be allocated in the coming weeks of pregnancy once the invasion of the spiral maternal arteries is achieved (Kingdom et al., 2000; Knöfler et al., 2019; Turco & Moffett, 2019).

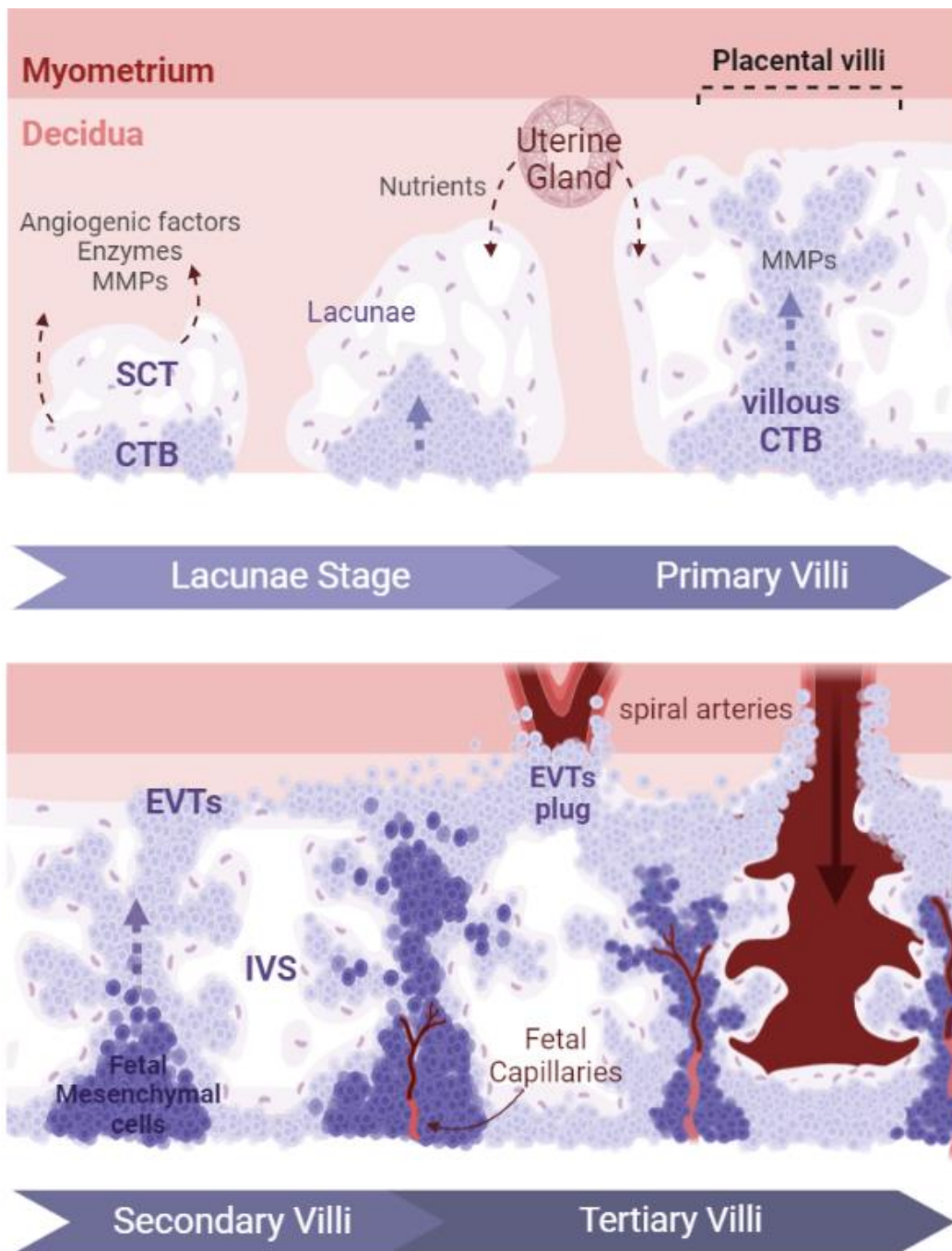


Figure 3: Placental villi development. The Syncytiotrophoblast (SCT) invades the maternal decidua. SCT develops further forming a syncytial mass with empty spaces called lacunae. The cytotrophoblast (CTB) below the SCT starts proliferating towards the syncytium. This CTB releases Metalloproteases (MMPs) continues proliferating creating tree-like structures, the primary villi. Fetal mesenchymal cells invade the villi, creating the secondary villi. Some trophoblast cells from the SCT keep proliferating outside the villous column, becoming extravillous trophoblast (EVTs). The previous lacunae from the syncytial mass have merged creating the intervillous space (IVS). Fetal capillaries invade the secondary villi, transforming it into the tertiary villi. EVT's keep invading the decidua, remodelling the maternal spiral arteries, and creating a plug (EVTs plug) which blocks the maternal blood flow into the IVS. At the end of the first trimester, these plugs are dissolved, and the blood can bath the intervillous space, allowing the exchange of nutrients between the mother and the fetus, being the placental villi the filter and wall between both blood streams.

The syncytialization process

Syncytialization is an important hallmark of placentation, tightly regulated by numerous molecules and pathways. Although the full understanding of the process is still under debate, this process can be divided in three main steps:

- 1) **Biochemical differentiation:** increasing levels of intracellular cyclic AMP (cAMP) induce the activation of multiple signalling pathways implicating transcription factors such as ELF5, TP63, ID2 and TEAD4 and epigenetic modifications. These changes induce CTBs to exit the cell cycle, lose their ability to proliferate and become fusion-competent cells (**Figure 4**) (Jaremek, Jeyarajah, Jaju Bhattad, & Renaud, 2021; Lu et al., 2017).
- 2) **Morphological differentiation of competent CTBs:** competent CTBs suffer a modified epithelial-mesenchymal transition, resulting in the loss of cell-cell junctions and the reorganization of the cytoskeleton. This morphological differentiation is mainly achieved by the downregulation of E-cadherins through ADAM12 and the increased expression of fusogenic proteins such as syncytin-1 (HERVW-1) and syncytin-2 (HERVFRD-1) (Aghababaei, Hogg, Perdu, Robinson, & Beristain, 2015; Omata, Ackerman IV, Vandre, & Robinson, 2013; Wheelock & Johnson, 2003). Syncytins are envelope proteins of human endogenous retroviruses which were integrated in the human genome through evolution (Rawn & Cross, 2008). While syncytin-1 is expressed in the STB during all pregnancy, syncytin-2 is observed only in the villous trophoblast and its expression decreases as pregnancy progresses. However, recent single-cell analysis, syncytin-2 transcripts are observed in subpopulations of syncytiotrophoblast, contradicting the immunohistochemistry, where syncytin-2 is observed mainly in the extravillous trophoblast (Roberts et al., 2021).
- 3) **Fusion:** cytotrophoblast cells fuse with the overlaying syncytiotrophoblast rather than with neighbouring cytotrophoblast (**Figure 4**). The fusion process is triggered by the interaction of the fusogenic proteins with the membrane phospholipids such as

phosphatidylserine or cardiolipin found in temporary complexes in the cells to be fused (Pötgens et al., 2002).

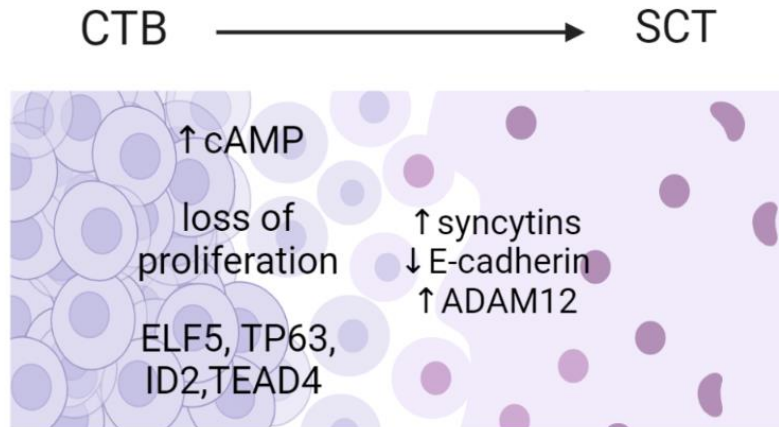


Figure 4: The syncytialization process: CTB differentiate into fusion competent cells through the increase of cAMP and the activation of different transcription factors. Loss of proliferation and the expression of fusogens leads to the fusion of the CTB cells into the syncytial layer.

Week 8 – Maternal Spiral Arteries Remodelling

As mentioned previously, Extravillous cytotrophoblast (EVTs) differentiate from the column CTB once they reach the maternal decidua. EVT cells which lose their proliferative activity, are differentiated into invasive interstitial cytotrophoblast (ITV). ITVs invade and remodel the tissue stimulating the profound expansion of the placenta in the uterus and the recruitment of maternal arteries. These uterine arteries are narrow muscular vessels that need to be remodelled into dilated, flaccid sinuses without maternal vasomotor function. The final transformed vessels will perfuse high quantities of blood at a low resistance towards placental intervillous space, achieving the proper distribution of nutrients and gases to the fetus for its correct development and growth (Kaufmann, Black, & Huppertz, 2003; Pijnenborg, Vercruyse, & Hanssens, 2006). Thus, a strong and deep spiral artery remodelling is a critical step in the placentation process.

This remodelling can be described in 4 different stages, based on the extent of maternal vessel disruption and loss (S. D. Smith, Dunk, Aplin, Harris, & Jones, 2009):

1) Intact arterioles with full vascular smooth muscle layer (VSML)

The uterine arteries supply blood to the uterine musculature, the myometrium. They penetrate through the muscular tissue and supply blood to the uterus and the endometrial tissue walls. The human uterus has around 1500 arteries, and only 150 of these will take part in the placental blood supply. Initially, these arteries are highly muscular and composed of two tissue layers: an internal layer of endothelial cells supported by an elastic lamina and a medial layer of tightly compacted vascular smooth muscle cells (VSMCs) (**Figure 4**) (Sweeney, Jones, Greenwood, Baker, & Taggart, 2006).

2) Initiation of the VSMC layer disruption and misalignment independently of ITVs

Invasion of the ITVs into the uterine tissue leads to the recruitment of uterine arteries towards the placental. It is hypothesized that the uterine Natural Killer cells (uNKs), a specific set of NK cells located in the decidua characterized by reduced cytotoxicity, are key players in early spiral artery remodelling (Robson et al., 2012). As early as the decidualization process occurs, uNKs migrate towards the uterine arteries and start to express pro-inflammatory cytokines (Interferon- γ), to produce proangiogenic factors (Angiopoietin-1, Angiopoietin-2 and VEGF), and to secrete proteolytic enzymes (Metalloproteases-7 and -9) into the vessel vicinity (**Figure 4**). The array of these molecules leads to the impairment of the VSMC and the endothelial layer below, causing endothelial barrier dysfunction. The ability of uNKs to destabilize the VSMC layer is crucial and facilitate the further invasion of the ITVs in the latter stages of remodelling (Robson et al., 2012).

3) Major disorganization and clearance of the vessel structural cells

EVTs will reach those maternal spiral arteries located in the remodelled tissue. Once the trophoblast cells contact the VSMCs, these muscle cells get detached from the walls.

ITVs differentiate into endovascular cytotrophoblasts, substituting this muscle layer (**Figure 4**).

There are two main hypotheses on this substitution process. **a)** ITVs stimulate the apoptosis of the VSMCs throughout the ligation of the tumour necrosis factor receptor (TNF-R) family, namely Fas/CD95, TNF-R1, death R-3/TRAMP, TNF- α -related apoptosis-inducing ligand (TRAIL-R1, and TRAIL-R2 (Harris et al., 2006) and **b)** VSMCs get detached from the vessel and migrate away from the spiral artery to the endometrial tissue, where they further dedifferentiate (Bulmer, Innes, Levey, Robson, & Lash, 2012).

4) Fully remodelled vessels without VSMC

The spiral artery VSML is completely substituted by a fibrinoid material containing endovascular trophoblast cells (*Figure 4*). As a result, these vessels are now wide-bore channels independent of maternal vasoconstriction.

From week 8 to the end of the first trimester, these spiral arteries keep being invaded until the junctional zone of the myometrial layer. This invasion is the deepest placental invasion in all placental animals and could be caused by the high necessity of nutrients the embryo requires for the early brain development observed in humans (Burton, Moffett, & Keverne, 2015).

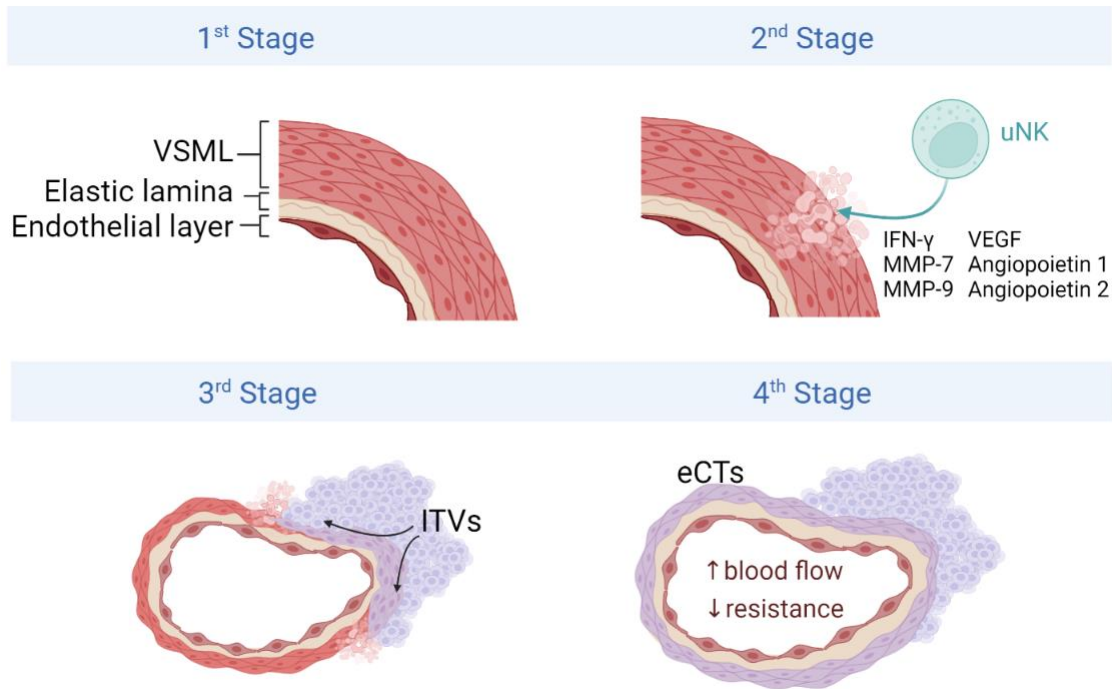


Figure 3: Four stages of the maternal spiral artery. **Stage 1**, intact arterioles formed by the vascular smooth muscle layer (VSML), the elastic lamina and the endothelial layer. **Stage 2**, immune cells such as the uterine Natural Killer cells (uNK) express pro-inflammatory cytokines which induce the impairment of the muscular cells. **Stage 3**, invasion of the interstitial cytotrophoblast (ITVs) in the muscular layer induce the detachment of the muscular cells and the differentiation of the trophoblast cells into endovascular cytotrophoblast (eCTs). **Stage 4**, the complete invasion of the trophoblast cells in the maternal arteries produces a blood vessel with increased blood flow and decreased resistance.

Week 10 to 12 – From Hypoxia to Normoxia

Vasculogenesis and angiogenesis are two consecutive important processes in the creation and development of blood vessels in the human placenta. Firstly, vasculogenesis induces the novo production of a primitive vascular network through the differentiation of precursor cells (pluripotent mesenchymal cells) into endothelial cells. Secondly, angiogenesis is described as the growth of capillaries from pre-existing blood vessels (Risau, 1997). Two of the main genes implicated in vascular development are Vascular Endothelial Growth Factor (VEGF) and Placental Growth Factor (PIGF). While VEGF stimulates the mobilization and circulation of endothelial progenitor cells, inducing the novo vessels and the growth of existing ones (Szmitko et al., 2003). PIGF, a VEGF

subfamily member, acts on endothelial cells and trophoblast cells stimulating VEGF expression and the development and branching of the existing vasculature (Torry, Ahn, Barnes, & Torry, 1999).

EVTs cells form plugs inside the vessel lumen during all these remodelling processes, preventing the flow of oxygenated blood into the placental intervillous space. This creates a physiologically hypoxic environment (oxygen tension 2.5%) required for a successful trophoblast differentiation and migration (James, Stone, & Chamley, 2006). At low oxygen tension, the placenta maintains its stemness throughout activated hypoxia-inducible factors (HIF-1 α and HIF-2 α). These two transcription factors bind to specific DNA sequences called Hypoxia Response Elements (HREs), present in more than 200 genes. HIF-1 and HIF-2 are heterodimeric proteins composed of an oxygen-sensitive subunit (HIF-1 α /HIF-2 α) and an oxygen-independent subunit (HIF-1 β) (Fryer & Simon, 2006) (**Figure 4**). Only in a hypoxic environment, the α subunit is functional, stimulating the expression of key genes in vasculogenesis, such as the previously mentioned Vascular Endothelial Growth Factor (VEGF).

VEGF has a pivotal role in embryonic vasculogenesis, angiogenesis, vascular permeability, anti-apoptosis of endothelial cells and cell migration promotion (Melincovici et al., 2018). VEGF upregulates the expression of the two isoforms of Nitric Oxide Synthase (NOS), the inducible NOS (iNOS) and the endothelial (eNOS) in the endothelial cells, SCT and EVTs (Martin & Conrad, 2000). While eNOS induces an intrinsic synthesis of Nitric Oxide (NO) which leads to the maintenance of the vascular tone and inhibits a pro-inflammatory state by blocking the adhesion of leukocytes and platelets in the vascular endothelium, iNOS produces a proinflammatory temporary excess of NO (Matsubara, Higaki, Matsubara, & Nawa, 2015). In normal pregnancies, NO is key in the delay and inhibition of trophoblast apoptosis, increasing trophoblast proliferation, migration, and invasion. Moreover, increased levels of NO upregulate the VEGF gene enhancing the HIF-1 activity, these reciprocal relations between NO and VEGF regulate angiogenesis in normal tissues (**Figure 4**).

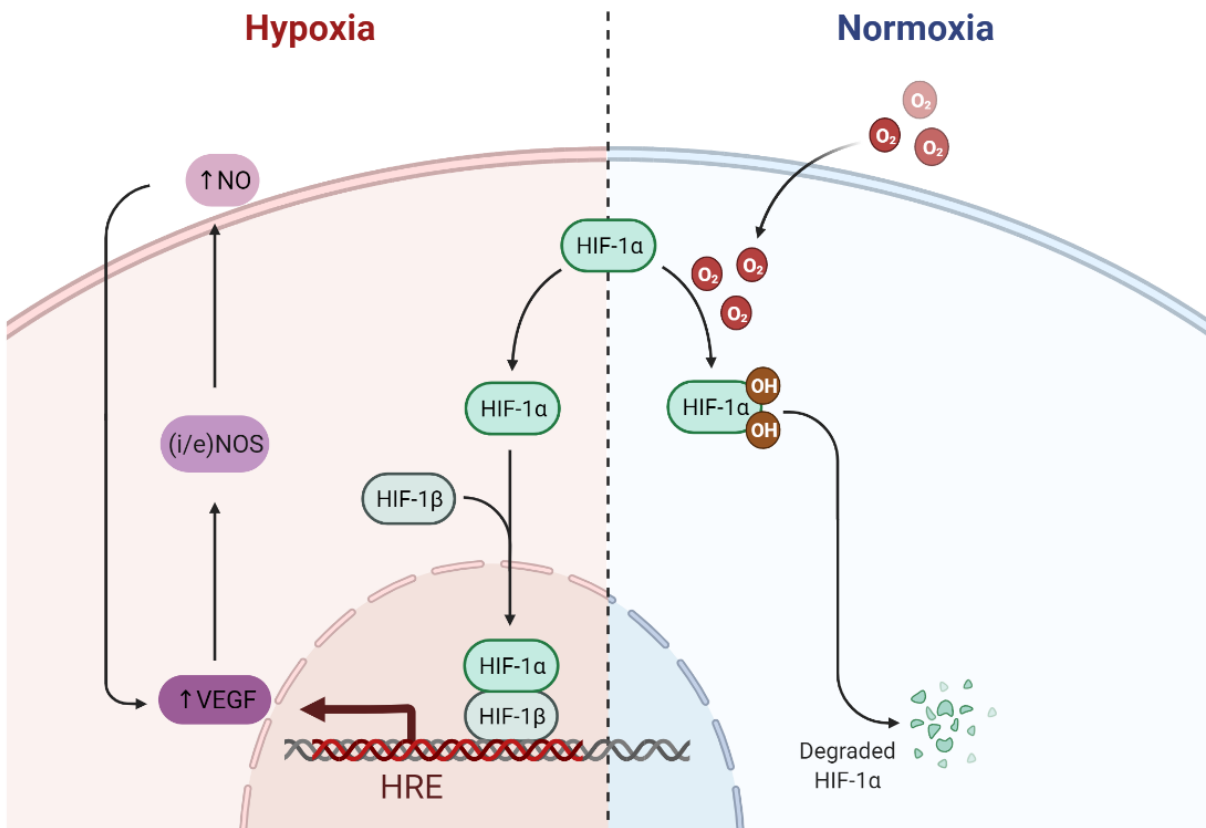


Figure 4: HIF regulation in Hypoxia and Normoxia in the placenta. The HIF1- α heterodimer is degraded in normal oxygen concentrations (Normoxia). During hypoxia, HIF1 is active and activates the transcription of genes that have Hypoxia Response Element in their sequence. One of these genes is VEGF, a proangiogenic protein that upregulates the expression of Nitric Oxide Synthases, which increase the production of Nitric Oxide (NO) leading to a positive loop in which VEGF is upregulated by high concentrations of NO.

As pregnancy progresses, the embryo metabolic requirements increase, thus, a more efficient maternal to fetal supply system is necessary. Increased uteroplacental circulation is enhanced by the removal of the trophoblast plugs around weeks 10-12 of pregnancy. Once these cell clumps are dissolved, the maternal blood bathes the intervillous placental spaces and continuous low perfusion of oxygenated circulation is established. Oxygen tension increases to normoxic levels (8.5% O₂) leading to a dramatic reduction in markers of trophoblast stemness (ELF5, CDX2), the loss of growth factors (Chiarello et al., 2020) and the activation of oxygen sensors, such as NAD(P)H oxidase, which regulates the differentiation from CTB to SCT (Poston & Raijmakers, 2004).

Higher O₂ availability increases fetal metabolic rate and placental mitochondria increase their activity. Due to this increased activity, incomplete reduction of oxygen and nitrogen molecules occurs, leading to the release of high quantities of free radicals such as Reactive Oxygen Species (ROS) and Reactive Nitrogen Species (RNS) into the maternal circulation. Increased concentrations of RNS and ROS produce an imbalance between oxidants and antioxidants denominated oxidative stress (OS). OS induces cell damage through lipid peroxidation, incorrect protein conformational modifications, DNA lesions and even DNA methylation errors. As a defence mechanism against ROS and RNS, the placenta expression of antioxidants is stimulated. There are two different types of antioxidants: enzymatic-antioxidants (manganese superoxide dismutase (MnSOD), superoxide dismutase (SOD), glutathione peroxidase (GSH-Px) and catalases (CAT)) and non-enzymatic antioxidants (vitamin C, vitamin E, lipoic acid, ubiquinone, and uric acid). These molecules metabolize free radicals into innocuous by-products returning the OS burst to baseline levels (Chiarello et al., 2020).

OS is necessary for the maturation of the placenta and the development of the fetus in healthy pregnancies. However, excessive OS can also exert a critical effect on pathological processes. This increase of OS induces a proinflammatory state in which maternal neutrophils and endothelial cells are active and expressing inflammatory cytokines through the activation of key transcription factors such as nuclear factor-kappa B (NF- κ B). The most vulnerable cell type in this environment is the SCT. SCT is the first layer in contact with maternal oxygen tension, it has a high mitochondrial activity, a reduced expression of antioxidants and a high concentration of fatty acids in the cytoplasm. Moreover, SCT mitochondria are highly implicated in steroidogenesis, specifically progesterone production, which starts in the mitochondria and leads to lipid peroxide production (Chatuphonprasert, Jarukamjorn, & Ellinger, 2018). Consequently, a higher ROS production rate is observed in this layer, favouring apoptosis, and shedding of syncytial fragments into maternal circulation

Week 12 to 18 – From First to Second trimester

The end of the first trimester of pregnancy is characterized by the complete placenta formation and maturation, the establishment of the maternal circulation to the placenta and the achievement of a correct intrauterine environment for the further development of the fetus. To note, trophoblast invasion, unlike cancer, is tightly regulated spatiotemporally. This invasion ceases by the 18th week of gestation and is limited to the inner third of the myometrium (Y. H. Ng, Zhu, & Leung, 2012).

Week 18 to 27 – Second trimester placental maturation

As the placenta matures and increases in size in the second trimester, the villi become smaller and more vascular. The syncytiotrophoblast cell layer draws up into “syncytial knots” which are small clusters of nuclei, leaving a single cytotrophoblast layer (Sultana et al., 2017). This leaves the core of the villi is exposed to the maternal blood temporary (Loukeris, Sela, & Baergen, 2010). Detachment of the syncytial knots can occur, producing syncytial aggregates which are transcriptionally active and circulate in the maternal bloodstream.

Week 27 to 40 – Third trimester Placenta maturation

During the third trimester, the more prevalent villi are mature intermediate and terminal villi with a thin stromal layer. Increased concentration of vasculo-syncytial membranes, characterized by the fusion of fetal capillaries with the syncytiotrophoblast layer are produced due to the thinned of the syncytial layer caused by the increased mass of the placenta. All these maturation changes result in an optimal materno-fetal transfer of nutrients and gases for the increased conductance of oxygen diffusion (Fox, 1997).

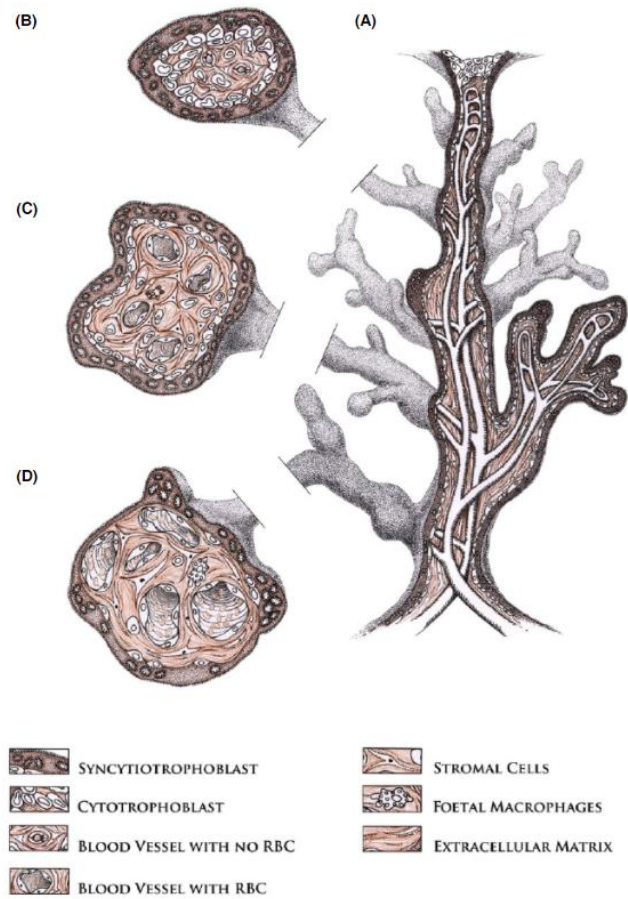


Figure 5 : Development of the human placental villi: a) Primary villi arborization b) First-trimester villi c) second trimester villi d) third trimester villi. Figure from Sultana et al., 2016.

2 Placental Functions

The placenta has 3 main functions throughout pregnancy: 1) the transport of nutrients, gases from the mother to the fetus and waste from the fetus to the mother, 2) generation of hormones to maintain the pregnancy and 3) the participation to an immunotolerance state to avoid being attacked by the maternal immune system.

A) Transport and metabolism

Three main groups of molecules are transported through the placenta: gases, nutrients, and waste.

The placenta is highly permeable to respiratory gases allowing rapid diffusion of oxygen from maternal to fetal blood and of carbon dioxide from fetus to mother. To note, fetal haemoglobin has a much higher affinity to oxygen than maternal haemoglobin, favouring the transfer of oxygen to the fetus (Souza, McDaniel, & Baum, 2011).

The main source of energy for the placenta is glucose. Trophoblast cells express a high number of Glucose transporters (GLUT). Once in the SCT, glucose is transformed into placental glycogen and transported into the fetus. Eight different GLUT have been described in the placenta and GLUT1, considered the primary placental glucose transporter, is only observed to be expressed in the SCT (Baumann, Deborde, & Illsley, 2002). Interestingly, GLUT1 is a bidirectional transporter, but its asymmetric expression, 6-fold higher in the apical part of the syncytium (the maternal-facing membrane) than in the basal, allows the maximal gradient for glucose flux into the fetus and prevents the transport of glucose from the fetus to the mother in the event of maternal hypoglycemia (Knipp, Audus, & Soares, 1999).

Lipids are hydrolysed before crossing the placenta by several lipases, such as lipoprotein lipase (LPL), endothelial lipase (EL) and hormone sensitive lipase (HSL), expressed by the

placenta (Barrett et al., 2014). Placenta uptakes long-chained fatty acids through five different Fatty acid transporter proteins (FATPs) (Gaccioli & Lager, 2016). Although the placenta can produce enough lipids to maintain the plasma membrane function and morphology, cholesterol is key to producing hormones. Therefore, high internalization of cholesterol bound to Low-Density Lipoproteins (LDL) is transported from the mother to the placenta by endocytosis (Gude et al., 2004; Martinez, Olvera-Sanchez, Esparza-Perusquia, Gomez-Chang, & Flores-Herrera, 2015).

Amino acid transport across the placenta is active and mediated by specific transporters found in the syncytiotrophoblast membrane and in the basal membrane. Fifteen different transporters are observed across the placenta with high stereospecificity and can be divided in Na⁺-dependent and Na⁺-independent systems. The concentration of free amino acids in the placental tissue is higher than the concentration both in fetal and maternal plasma, thus, the transport of these amino acids across the syncytiotrophoblast always requires energy to act against concentration gradient while in the basal membrane amino acid exchangers are observed (Avagliano, Garò, & Marconi, 2012).

Ions, minerals, and vitamins are as well transported across the placenta from the maternal blood and their demands increase during the gestational period. While sodium and chloride ions are transferred across the placenta by passive diffusion, calcium, magnesium, iron, zinc, copper, manganese, and vitamins are transported by active carrier-mediated transport and determine the proper growth and development of the fetus (Griffiths & Campbell, 2015).

B) Endocrine function

Pregnancy is characterised by a tight hormonal control, involving steroid hormones such as progesterone, produced by the ovaries in the beginning of pregnancy, then by the placenta after the 9th week of gestation. The placenta produces endocrine, paracrine and autocrine factors such as oestrogen, progesterone, chorionic gonadotrophin, placental lactogen, placental growth hormone

and several growth factors, cytokines, chemokines, and many others. The production of these hormones is necessary for the development and maintenance of pregnancy and also for the labour process (Costa, 2016) and their concentrations vary across the pregnancy (**Figure 6**).

Human Chorionic Gonadotropin

Produced mainly in SCT cells, human Chorionic Gonadotropin (hCG) stimulates in early pregnancy the production of progesterone from the corpus luteum to maintain pregnancy before the placenta takes over, also has a role in immunomodulation and angiogenesis stimulation. hCG in the uterine microenvironment binds to its cognate receptor (LHCGR) stimulating leukaemia inhibitor factor (LIF) production and inhibiting Interleukin-6 (IL-6) in the endothelial endometrial cells enhancing embryo implantation and trophoblast invasion. Hofbauer cells respond to high concentrations of this hormone by protecting the fetal tissues against maternal immune cells (Gridelet et al., 2020).

Progesterone

At the beginning of pregnancy, the corpus luteum is the main producer of progesterone until the placental syncytium layer is developed. Then, the hormone is produced in the SCT's mitochondria by a two-step process in which maternal cholesterol is transported into the organelle by the metastatic lymph node 64 (MLN64) protein (Martinez et al., 2015). Progesterone levels increase throughout pregnancy, peaking at the 4th week. This hormone is implicated in the decidualized process by activating the PKA signalling pathway, immunotolerance through the inhibition of uterine Natural Killer (uNK) cells and the inhibition of myometrial contractility through the control of Ca²⁺ levels (Martinez et al., 2015; Tuckey, 2005).

Human Placental Lactogen

Human Placental Lactogen (hPL) is produced by the syncytiotrophoblast in a constant rise until the 34th week of gestation. It modulates the maternal metabolisms inducing peripheral insulin resistance to reduce maternal glucose usage. Moreover, it stimulates maternal lipolysis, increasing

the dependency of the mother on the fatty acids and ketones and increasing concentrations of lipids in the bloodstream as a substrate for hormones production (Johnson, Jackson, & Schust, 2018).

Estrogen

Fetal and maternal androgens are supplied to the placenta, where the placental aromatase converts these into the 3 main estrogens (estradiol, estrone and estriol). Estrogen production in the placenta is dependent of the fetal and maternal adrenal cortex, where androgenic C19 steroid (dehydroepiandrosterone (DHEA)) is produced (Kaludjerovic & Ward, 2012). Elevated estrogens concentrations suppress Follicular-Stimulating hormone and Luteal hormone production, blocking the development of ovarian follicles. Estrogens stimulate uterus growth leading to vascular proliferation and remodelling and an increased uteroplacental blood flow (Johnson et al., 2018). Moreover, they are involved in appetite regulation, insulin and glucose homeostasis and mammary

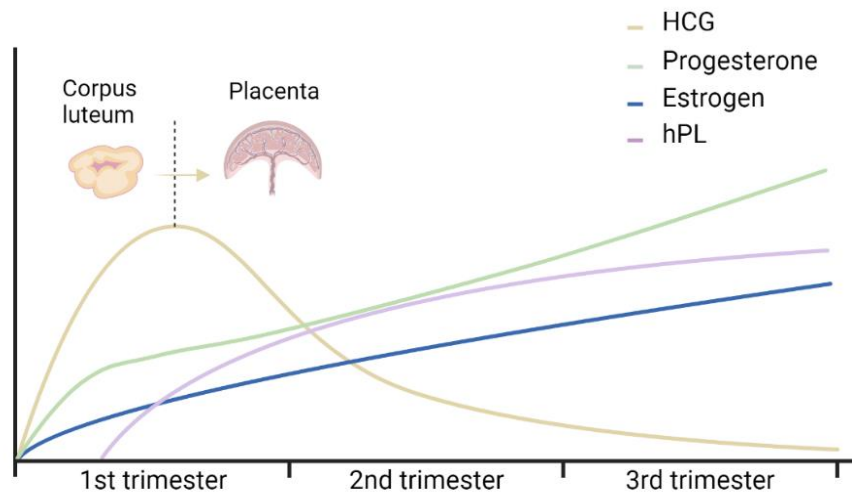


Figure 6: Hormone trends during pregnancy. Human Chorionic Hormone (HCG) is produced by the maternal Corpus luteum until the placental production takes place. Progesterone and estrogen maintain a constant rise from the beginning till the end of pregnancy while human Placental Lactogen (hPL) starts to be secreted after the 4th week of pregnancy.

gland development (Napso, Yong, Lopez-Tello, & Sferruzzi-Perri, 2018).

C) *Immunomodulation*

Immunology of pregnancy is a vast subject which goes beyond the subject of my thesis. I will not go into details on this part and will only mention a few key elements.

Pregnancy is characterized by a very specific immunological timing denominated “pregnancy immunological clock” (Mor & Cardenas, 2010). This clock is characterized by a shift from a proinflammatory state in the first trimester, to an anti-inflammatory state in the second trimester towards a pro-inflammatory state at the end of pregnancy leading to the baby’s delivery.

During the first half of pregnancy, a pro-inflammatory state stimulates embryo implantation, invasion, placental development, and spiral artery remodelling. High concentrations of pro-inflammatory cytokines are expressed, and the maternal immune cells are activated, the pregnancy resembles an “open wound”. Maternal immune cells, such as Natural Killer (NK) cells, dendritic cells and macrophages accumulate in the decidua, surrounding the invading trophoblast. SCTs are devoid of HLA I molecules, while EVT expresses non-classical HLA class Ib molecules, HLA-E and HLA-G low amounts of the polymorphic HLA-C, HLA-Ia molecules (Slukvin, Lunn, Watkins, & Golos, 2000). These molecules are key in blocking alloreactivity of the placenta by inhibiting MHC class I receptors in maternal lymphocytes and myelocytes (Slukvin et al., 2000). Moreover, HLA-G and HLA-C expression can enhance communication between trophoblast and endometrial NK cells, the most abundant immune cells in the decidua, a key element to achieving a proper placental invasion (Small, Cornelius, Guzik, & Delles, 2017). During the first trimester, remodelling and invasion caused by the placenta produced cell debris and high levels of apoptotic cells. Removal of these components must be quick and effective to prevent the release of paternal antigens. Endometrial macrophages are the main actors in this task, although Hofbauer cells engulf some apoptotic bodies from the placental side (Reyes, Wolfe, & Golos, 2017). Moreover, the placenta expresses Fas Ligand (FasL), which is responsible for maternal immunotolerance to the paternal alloantigens by the induction of apoptosis in maternal lymphocytes (Bamberger et al., 1997). Interestingly, some studies suggest the

role of the placenta in controlling maternal T cells through the regulation of tryptophan availability in the maternal-fetal interface (Munn et al., 1998).

3 Placental Pathologies

Preeclampsia (PE) and Intrauterine Growth Restriction (IUGR) are the two most common placental pathology affecting 3 to 5% of the worldwide pregnancies and 24% of new-borns respectively. PE and IUGR are separate disease entities that can be seen alone or together, with more unfavourable outcomes for the mother and/or foetus when they occur together.

Physiopathology of Preeclampsia

Clinical Aspects

Preeclampsia is described by the International Committee of the International Society for the Study of Hypertension in Pregnancy (ISSHP) in 2018 as the new onset of hypertension (blood pressure of ≥ 140 mmHg systolic and/or ≥ 90 mmHg after 10 weeks of gestation accompanied by one or more of the following new-onset conditions at or after 20 weeks' gestation (Bouter & Duvekot, 2020):

1. Proteinuria or presence of proteins in the urine
2. Maternal organ dysfunction including:
 - renal insufficiency (creatinine $> 90\mu\text{mol/L}$; 1 mg/dL)
 - liver involvement (increased level of transaminases with or without right upper quadrant or epigastric abdominal pain)
 - neurological complications (eclampsia, altered mental status, blindness, stroke, severe headaches)
 - hematological complications (thrombocytopenia with platelet count below 150,000/dL, DIC, haemolysis)
3. Uteroplacental dysfunction (fetal growth restriction, abnormal umbilical artery Doppler wave)

In the most severe cases, PE can lead to HELLP syndrome, a pregnancy-associated liver disease characterized by haemolysis (H), elevated liver transaminases (EL) and low platelet count (LP). HELLP syndrome constitutes the main predisposing factor to the development of eclampsia (Alese, Moodley, & Naicker, 2021). Severe PE can also progress in eclampsia, characterized by maternal seizures leading to cardiovascular accidents, liver rupture, pulmonary oedema and acute renal failure that can result in maternal death (Ghulmiyyah & Sibai, 2012) (**Figure 9**).

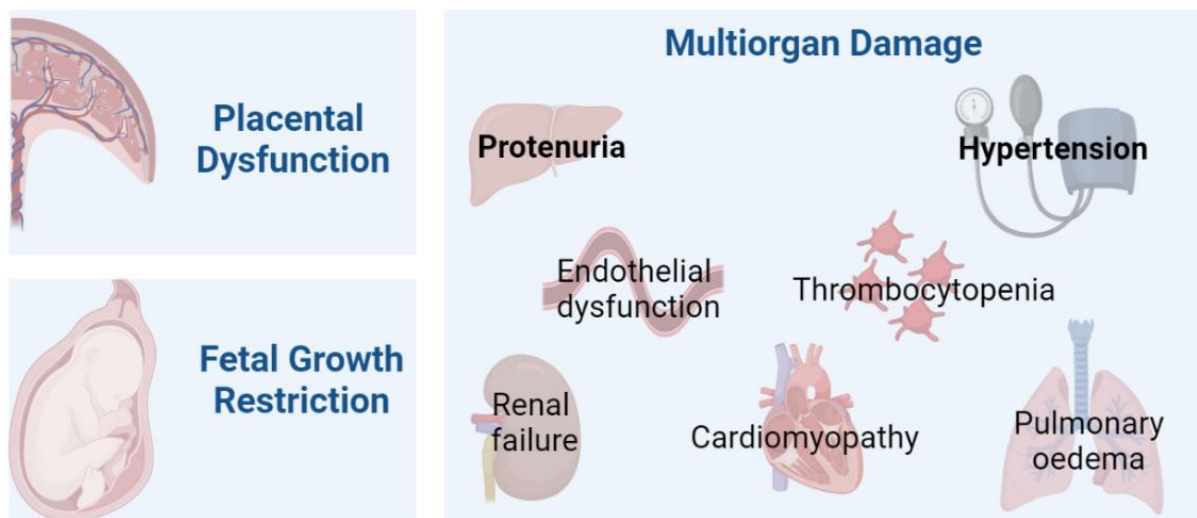


Figure 7: Main clinical symptoms and comorbidities observed in PE

PE can be subdivided into Early-onset of PE (EOPE) when the symptoms appear before 34 weeks of gestation or Late-onset of PE (LOPE) when they appear after 34 weeks. EOPE is generally associated with defective placentation and as a result, most of these pregnancies will lead to preterm delivery since the early delivery of the baby is induced to avoid further system damage in the mother and/or the fetus. On the other hand, late onset of preeclampsia (LOPE), which corresponds to 85% of the preeclamptic pregnancies, is less severe, and it is generally associated with defective placental interaction and maternal predisposition to cardiovascular diseases (Burton, Redman, Roberts, & Moffett, 2019).

Treatment for pre-eclampsia focuses on lowering blood pressure and managing the other symptoms, sometimes with medication, such as labetalol (200–1200 mg/day), methyldopa (0.5–3 gm/day) as first-line agents and oral nifedipine (10–30 mg) and Verapamil (80 mg) as second-line agents (Brown & Garovic, 2014). Low dose of aspirin (81mg/day) is recommended as prophylaxis in women with high risk of PE (with more than one risk factors for PE) and should be initiated in early stage of pregnancy (12-28 weeks of gestation) and continued daily until delivery (Odigboegwu, Pan, & Chatterjee, 2018). Early diagnosis of the disease is also key to reducing the progression of PE into eclampsia and the risk of death from the condition (Zakiyah, Postma, Baker, van Asselt, & Consortium, 2015). Early prediction in high-income countries has reduced the mortality rate associated with PE by 90% from the early 1900s to 1980. However, in low-income countries, PE is responsible of the 98% of fetal and maternal deaths (Goldenberg et al., 2014). Moreover, sequelae related to this multiorgan syndrome can highly affect the long-term health of the mother and the fetus. Mothers suffering from PE have a 14-fold higher risk of suffering cardiovascular diseases (CVDs) later in life and are more likely to be treated for primary hypertension within the following 10 years of delivery (Lin et al., 2011). Babies may also suffer from comorbidities associated with the brain, heart, liver, kidney, hormonal changes and delayed physical development (Turbeville & Sasser, 2020).

Fetal outcomes

PE represents a significant risk factor for intrauterine fetal death of about 21 stillbirths per 1000 in severe cases, while in mild cases, fetal demise is observed 9 out of 1000 cases (MacDorman, Munson, & Kirmeyer, 2007; L. L. Simpson, 2002). Babies suffering from PE are observed to have reduced fetal growth, birth asphyxia, neonatal thrombocytopenia (platelet count less than 150,000/ μ L), bronchopulmonary dysplasia, neurodevelopmental outcomes (cerebral palsy, autism, attention deficit hyperactivity disorder) and increased risk of developing adult diseases such as hypertension, obesity and diabetes due to the “Fetal Origins of Adult Disease” (Backes et al., 2011).

Maternal outcomes

Within the first 6 weeks after the infant's delivery, mother's blood pressure and other symptoms go back to normal. However, several studies have shown that women who had PE are at a 4-times higher risk of developing hypertension and 2-times higher risk of developing ischemic heart disease, blood clots in vein and stroke compared to women who did not have PE (Andrus & Wolfson, 2010). Less commonly, women suffered from PE experience permanent damage to the kidneys and liver, fluid in the lungs and eclampsia and seizures after delivery (M. Smith, Waugh, & Nelson-Piercy, 2013).

Molecular Aspects

The aetiology of PE has not been yet fully elucidated, probably due to its complexity. It is likely that multiple insults converge on a common pathophysiology in which endothelial disruption and an anti-angiogenic response is observed. However, the placenta seems to be a main actor in the development of the disorder, since after delivery, the symptoms remit.

Although there are still debate as to whether improper placentation results in either a hypoxic environment, an increased oxygenation (Huppertz, Weiss, & Moser, 2014) or a cycle of ischemia and reperfusion, a burst of oxidative stress (OS) is produced in the preeclamptic trophoblast. Increased levels of OS induce trophoblast damage and the release of factors such as sFLT1, angiotensin II type-1 receptor autoantibody (AT1-AA) and inflammatory cytokines (TNF- α and IL-6, IL-10), C-reactive protein (CRP), creating an inflammatory environment in the maternal blood (**Figure 8**). Disruption of the delicate balance between antioxidants and oxidants, increases free radicals in the maternal circulation. High levels of Reactive oxygen species (ROS) and Reactive nitrogen species (RNS) leads to lipid peroxidation, protein degradation and ultimately cell death and endothelial dysfunction (ED) (Burton & Jauniaux, 2011; O'Brien, Baczyk, & Kingdom, 2017).

ED can be characterized as increased vascular resistance, vasoconstriction, leukocyte adherence, increased oxidative stress and vascular inflammation. All these abnormalities lead to the leakiness of the blood vessels, the active infiltration of immune cells into the tissues and ischemic injury. Some of the molecules upregulated during the pathological process include Endothelin 1 (ET-1), IL-8, Endothelial Leukocyte Adhesion-Molecule 1 (ELAM-1), etc (Lamarca, 2012) (**Figure 8**). Interestingly, ET-1 is a vasoconstrictor whose antagonism has been linked with improvements in gestational hypertension in animal models, suggesting this molecule as the main link between ED and hypertension (George & Granger, 2011; Lamarca, 2012). ET-1 with decreased expression of VEGF adversely affects the expression and distribution of podocyte foot, leading to proteinuria (Wagner, Craici, Grande, & Garovic, 2012). Endothelial function is largely based on endothelial Nitric Oxide Synthase (eNOS) activity. Although there are ambiguous results, eNOS expression and activity has been shown to be increased in the preeclamptic maternal endothelium (Sutton, Gemmel, & Powers, 2020). Increased expression elevates the local NO concentration, leading to vasoconstriction. However, in high OS, oxidation of eNOS cofactors, such as tetrahydrobiopterin (BH4), induces the uncoupling of eNOS. Dysfunction of eNOS triggers an activity switch in the production of superoxide instead of NO (Guerby et al., 2021).

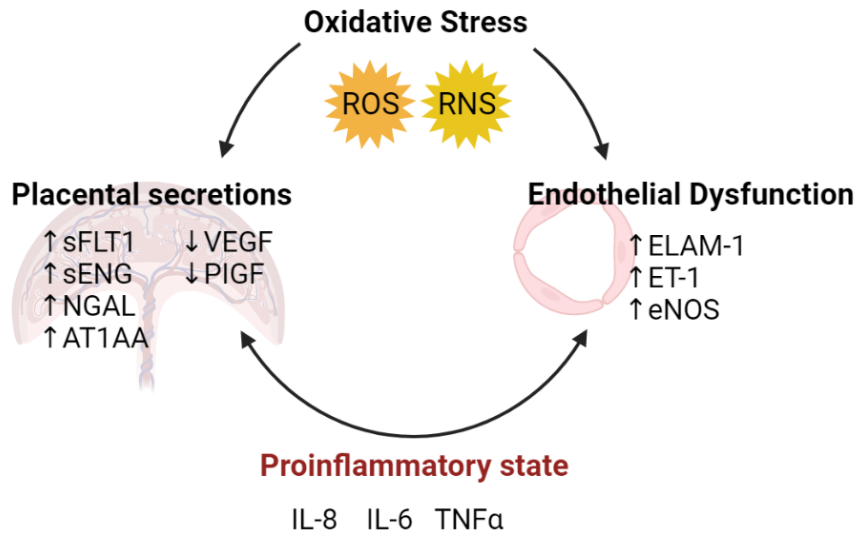


Figure 8: Main mechanisms implicated in the developmental of PE. Elevated Oxidative stress due to poor placental invasion is increased production of Reactive Oxygen and Nitrogen Species (ROS and RNS). This oxidative stress leads to secretion of placental molecules into the maternal circulation increasing endothelial dysfunction and creating a proinflammatory state.

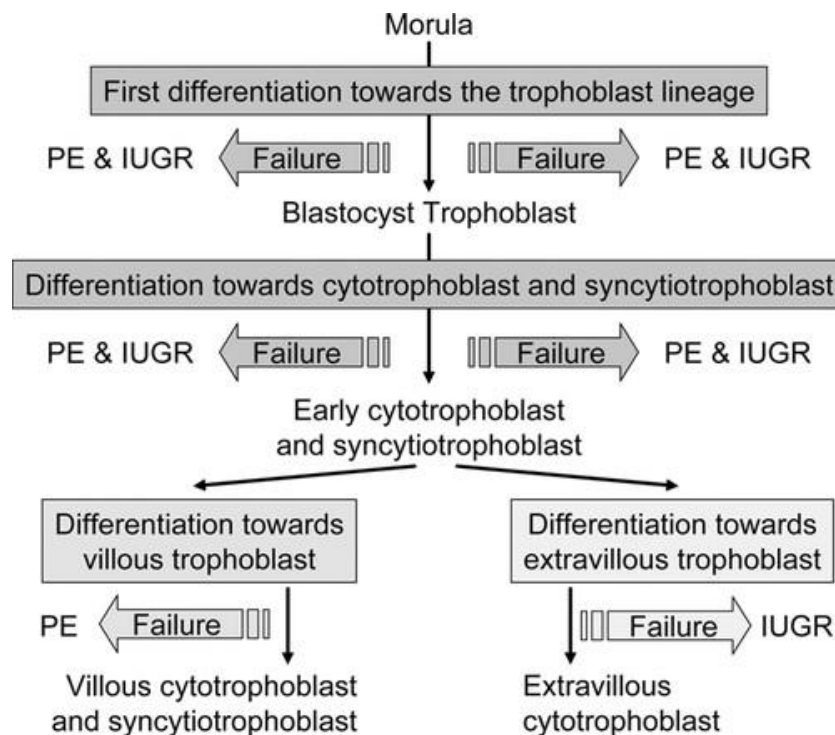
Hypothesis of Preeclampsia

Although the molecular physiopathology of PE is well described, the ultimate cause of the disease development is not well established. Several hypotheses have been developed; however, continuous contradictory findings maintain the disease aetiology as a mystery. A constellation of non-specific features ends up in the development of preeclampsia.

a) Defective placenta

The classical hypothesis of PE is the inability of the placenta to properly invade deep into the maternal myometrium. This hypothesis sets placental defects in trophoblast lineage specification. If insults occur in early placental development, PE and IUGR occur at the same time (**Figure 9**). However, if defects are produced in late stages the diseases can be seen separately. The onset of PE occurs if all villous trophoblast cell types are affected (SCT and VCT) while the onset of IUGR is produced if only EVT shows defects in the second trimester of pregnancy (Huppertz, 2008).

It is mostly EOPE, typically associated with IUGR that is linked to defective EVT. The placenta is unable to invade the spiral arteries and leading to an impaired response to oxidative stress. This, in turn, causes the release of antiangiogenic factors that induce endothelial dysfunction and inflammation. Several studies pinpoint the role of the defective expression of trophoblast factors in the development of PE, being sFLT1 and PIGF the most studied (Agrawal, Shinar, Cerdeira, Redman, & Vatish, 2019; Sheridan et al., 2019). While sFLT1 is upregulated, PIGF is downregulated in PE placentas. Low concentrations of PIGF, mainly through its sequestration by sFLT1, contribute to abnormal placentation and abnormal growth in the latter half of pregnancy (Chau, Hennessy, & Makris, 2017; Dover, Gulerman, Celen, Kahyaoglu, & Yenicesu, 2013). Other studies suggest the inability of the syncytiotrophoblast to sense and generate ROS possibly due to the abnormal regulation of NADPH oxidase in this cellular layer



(Pereira & Martel, 2014).

Figure 9: Trophoblast Development diagram and placental pathologies associated. *Insults in early placental lineage specification led to a combination of PE and IUGR, while late insults can lead to either PE (if it affects the villous trophoblast) or IUGR (if it affects the extravillous trophoblast). Image extracted from Huppertz et al. 2008.*

b) Immune Maladaptation

First pregnancies have a higher risk of developing PE while second pregnancy with the same partner decreases the risk, second pregnancy with a new partner has the same risk of PE as first pregnancies. This multiparity problem has been explained by the maternal immune system mechanisms to recognize paternal alloantigens. Several immunomodulatory mechanisms seem to be dysregulated in the preeclamptic placenta. As an example, HLA-G, an important molecule that confers protection to the fetus from the maternal immune system, is reduced in PE placentas (Saito, Shiozaki, Nakashima, Sakai, & Sasaki, 2007).

Another immune hypothesis involves the catabolism of Tryptophan. Tryptophan catabolic pathway produces different metabolites that exert a potent immunoregulatory function by inducing apoptosis in T-cells. The first step of the catabolic pathway requires indoleamine-2,3-dioxygenase (IDO), which expression is decreased in PE placentas (Keaton et al., 2019).

c) Genetic Factors

PE has a strong genetic component, with a recurrent risk of 20-40% in daughters of either eclamptic or preeclamptic mothers. African American mothers have a higher rate of PE than the general population of the United States, suggesting an ethnicity impact on the incidence of PE. Twin studies estimate that 22% to 47% of PE risk is heritable (Chappell & Morgan, 2006). Several studies suggest that the transmission method of PE is complex, involving non-Mendelian transmission, numerous variants, gene interactions and environmental variables. Moreover, since the disease is already characterized by its non-specificity, the genetic variants will not induce the disease, rather reduce the threshold at which the mother will develop the condition (Ayorinde & Bhattacharya, 2017).

d) Primary impaired uterine perfusion

Although placental dysfunction is necessary for the development of PE, its aberrant function is secondary to a maternal vascular maladaptation to pregnancy. Dramatic changes in the

cardiovascular system occur throughout gestation, intending to increase blood flow delivery to the fetus. In these terms, PE is more likely to be related to a hemodynamic adaptation to the pregnancy, where the maternal vasculature leads the end-organ damage (Thilaganathan, 2018).

Physiopathology of Intrauterine Growth Restriction

Clinical Aspects

Intrauterine Growth Restriction (IUGR) is defined as the inability of the baby to reach its full growth potential due to an abnormal growth rate. There are two main types of IUGR: asymmetrical IUGR (70% of the IUGR cases), symmetrical IUGR and mixed IUGR. Symmetric growth restriction implies a foetus whose entire body is proportionally small while asymmetric growth is characterized by a foetus who is undernourished and only the vital organs maintain a normal growth at the expense of liver, muscle, and fat (Peleg, Kennedy, & Hunter, 1998).

Many acute neonatal problems develop from IUGR babies, such as perinatal asphyxia, hypothermia, hypoglycaemia and polycythaemia (Sharma, Shastri, & Sharma, 2016). IUGR babies are at increased risk of growth retardation, neurodevelopmental handicaps, and have increased risk to develop of metabolic syndrome later in life, obesity, arterial hypertension, hypercholesterolemia, cardiovascular disease, impaired glucose tolerance, or diabetes mellitus type 2 (Kanaka-Gatenbein, Mastorakos, & Chrousos, 2003).

Molecular Aspects

Fetal growth depends purely on the maternal supply of nutrients through the placenta into the umbilical circulation. The placental transport of glucose, the most important nutrient, seems to be maintained in IUGR. However, alterations in the glucose fetal availability have been observed, which in turn lead to fetal chronic hypoglycemia (Sharma et al., 2016). This mismatch can be explained by the ability of the placenta to maintain a normal glucose uptake to ensure its survival at expense of a decreased growth rate in the fetus.

Reduction in the concentration of amino acids in the placental plasma have been also observed (Economides, Nicolaides, Gahl, Bernardini, & Evans, 1989). Several amino acids transporters, such as system A and taurine transporters, have a reduced activity in the IUGR placenta (Glazier et al., 1997; Norberg, Powell, & Jansson, 1998). In some cases, not only reduction in amino acid ratios is observed due to impaired transport, but due to an increase of protein catabolism. Regarding fatty acids, changes in the ratios of specific fatty acids have been reported, which can be linked with damage in the brain of the fetus suffering this pathology. Moreover, lipoprotein receptors and lipases are significantly altered in IUGR placentae (Gauster et al., 2007).

Due to the limited nutrients, IUGR embryos develop a low uptake of oxygen, IUGR fetus becomes progressively hypoxic and lacticemic, leading to metabolic changes which can develop into long-term effects (Marconi, Paolini, Zerbe, & Battaglia, 2006).

Hypotheses of the disease

a) Maternal factors

Maternal status has been linked with the development of IUGR, especially age. Women aged below 20yrs have a 25% increased risk of developing IUGR while women over 35yrs account for 3% of IUGR cases. Socioeconomic status, nature of the occupation, low maternal weight before pregnancy and parity are as well correlated with the risk of developing IUGR (Manandhar, Prashad, & Pal, 2018).

b) Placenta

As mentioned before, IUGR can arise from the early insult in placenta development or the later impairment of the extravillous trophoblast. Defects in all differentiating trophoblast pathways seem to be related to the early onset of IUGR, implicating an early defect in trophoblast differentiation (Chaddha, Viero, Huppertz, & Kingdom, 2004). Electron microscopy of IUGR placental villi indicates abnormal villi development. More specifically, a lack of formation of terminal villi may account for the reduced gas and nutrient exchanging

ability of the villi (Krebs et al., 1996). Peripheral villous maldevelopment is a prominent feature in the early development of IUGR.

c) Genetic Factors

Fetuses with chromosomal disorders, such as trisomy and autosomal abnormalities, frequently show suboptimal growth restriction. Approximately 20% of the IUGR fetuses have an abnormal karyotype and the percentage is higher if growth failure is detected before 26 weeks of gestation (Monk & Moore, 2004). This may be linked with impairments in cell division leading to a reduction in cell number and fetal growth. Moreover, genomic imprinting syndromes, such as Silver-Russell syndrome (SRS) leads to growth restriction.

Physiopathology of Chorioamnionitis

Clinical Chorioamnionitis has been defined as a broad clinical syndrome with a heterogeneous array of conditions characterized by infection and inflammation or both, the so-called “Triple I”. On histopathological settings, chorioamnionitis is defined as diffuse infiltration of neutrophils into the chorioamniotic membranes, affecting the villous tree in an acute manner (acute villitis)(Jain, Willis, Jobe, & Ambalavanan, 2022). Chorioamnionitis is a common cause of preterm birth and may cause adverse neonatal outcomes, including neurodevelopmental, cardiorespiratory, retinal and renal sequelae (Galinsky, Polglase, Hooper, Black, & Moss, 2013; Peng, Chang, Lin, Cheng, & Su, 2018). Current therapies of this pathology rely on antibiotics, progesterone and antenatal corticosteroids (Jain et al., 2022).

Omics in placental research

Omics technologies, described as the study at a wide-genome level of different molecules in a non-target and unbiased manner aim to understand the biology of healthy and pathological organs using large scale data on DNA, RNA, proteins, etc (**Figure 10**). Proteomics, Epigenomics, Genomics and Transcriptomics among other “omics” large datasets are organized by computational tools to

provide a framework for the hierarchical contribution of integrated cellular pathways (Jaremek et al., 2021).

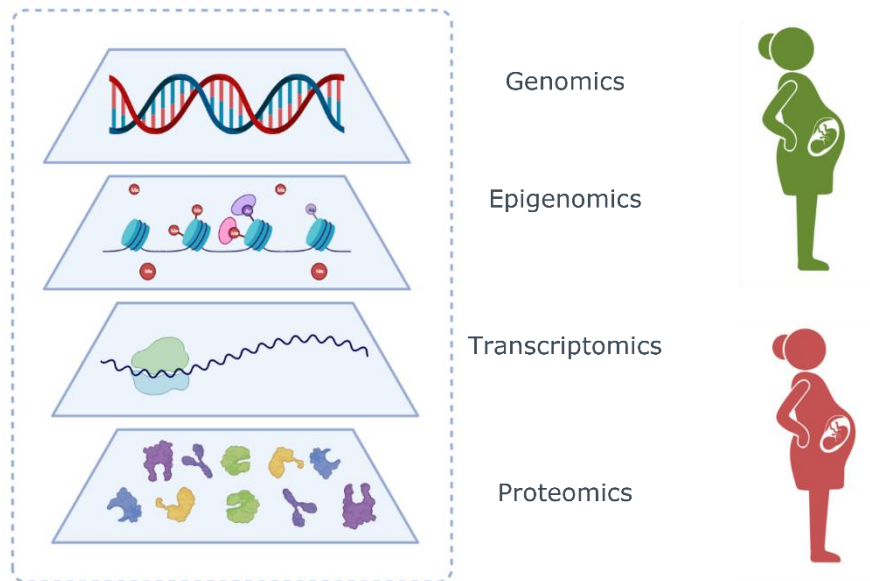


Figure 10: Omics to understand health and disease. Genomics, the study of the gene sequence; Epigenomics, the study of DNA methylation and histone modifications; Transcriptomics, the study of gene expression and Proteomics, the study of the proteins are the main large-scale studies used in omics to understand the biology in health and pathology.

Omics studies regarding the placenta have been focused on placental development using both cellular models that recapitulate trophoblast differentiation and early human embryonic cells (Jaremek et al., 2021). The most common techniques used have been DNA arrays and RNA-seq to understand gene transcription and the molecular pathways implicated in placental cells differentiation (Jaremek et al., 2021; Yong & Chan, 2020). Epigenomic approaches have focused on DNA methylation using bisulfite-pyrosequencing, histone marks using ChIP-seq and microRNAs using microarray-based miRNA profiling. Epigenetic network dynamics have been observed in the placenta during development, during oxygen tension changes and during drug treatment, giving more understanding the epigenome and its associations with the transcriptome. Proteomics and metabolomics using mass-spectrometry or nuclear magnetic resonance spectroscopy have been

developed to understand placental metabolic rate, hormone biosynthesis and nutrient transport in both healthy, pathological pregnancies.

Although Omics approaches in the placenta and its pathologies have given unprecedented details about the formation and function of the organ, several challenges and limitations arise from these studies. Inconsistency in the patient's description, sampling procedures, patient population, placental cell composition, data management differences and the fragility of the organ itself. Omics technologies are fastly advancing, entering into the multi-omics stage for the integration of different omics strategies for a better understanding and characterization of the placenta.

Project Objectives

Given the role of the placenta in these two pathologies and the remaining gaps in knowledge on healthy and pathological placentas, we aimed to continue studying the placenta to find distinct traits which can potentially help in the understanding of PE and IUGR. We developed four different perspectives to study the placenta and pathologies associated:

- 1) Identification of DNA methylation signatures in placental pathologies through the assessment of 850k CpGs using EPIC Illumina array.
- 2) Molecular characterization of the placental cell types using single-nuclei RNAseq transcriptomics and the study of lineage specifications through computational analysis.
- 3) Investigation of global splicing alterations in pathological placentas using transcriptomic from microarrays and genetic information from Single Nucleotide Polymorphisms.
- 4) Investigation of trophoblast fusion through the analysis of key long-non-coding RNAs involved in the syncytialization process and key in the development of a pathogenic phenotype

CHAPTER 1: DNA Methylation Analysis in Normal and Pathological

Placentas

Introduction

Epigenetics constitutes all the heritable changes in gene activity without alteration of the DNA sequence. These epigenetic modifications include histone modification, DNA methylation, DNA acetylation and production of non-coding RNAs. The plasticity of certain epigenetic modifications can be followed throughout development and differentiation and in response to environmental stimuli. Changes in methylation can be also associated with aging, oncogenesis, and other diseases.

One of the most studied epigenetic modifications is DNA methylation (DNAm). In mammals, DNAm is defined as the addition of a methyl group to the C5 of a cytosine to form a 5-methylcytosine (5mC). These methyl groups are generally added to specific symmetrical CpG dinucleotides found all around the genome. These CpGs can be found individual or clustered in small regions of the genome, creating CpG islands, which are often associated with the promoter regions of a gene. It is generally thought that, when the promoter of a gene is methylated, the transcription is inhibited, due to promoter being compacted and the transcription factors not able to bind to this region. However, a growing number of studies has challenged this simple model of gene expression control as hypermethylation of promoters may also be associated with induction of transcription (J. Smith, Sen, Weeks, Eccles, & Chatterjee, 2020). Epigenetic contributions to transcriptional regulation occur in a complex and dynamic manner, also involving regions outside genes such as enhancers. DNAm is heritable through mitosis, consequently, when a CpG is methylated in a cell, it remains methylated in all its descendants (Goll & Bestor, 2005). This cell-to-cell transmission makes DNAm a long-term stable epigenetic modification (Handy, Castro, & Loscalzo, 2011). DNA methylation is vital for important cellular processes including gene expression, genome stability, X chromosome dosage composition and regulation of imprinted genes.

After fertilization, global DNA methylation of both the maternal and paternal pronuclei is erased, except on imprinted regions in which methylation is maintained. The genes in these specific regions are only transcribed from one parental copy and their expression is directly governed by methylation. While the paternal genome seems to undergo active demethylation driven by the demethylase TET3, the maternal demethylation process is slower and passive through cell division, caused by the inactivation of the methyltransferase DNMT1 in the daughter cells (Guo et al., 2014; Kobayashi et al., 2012; Okae et al., 2014; Smallwood et al., 2011). Once this global demethylation is achieved, the embryo genome is activated towards an epigenetic state compatible with totipotency.

During embryo development, cell fate decisions are pursued to determine how cells develop into different cell types. This is a complex process that involves many different signals, such as the position and location of the cell, mechanical constraints, epigenetic modifications, and changes in gene expression. These combined signals will end up to specific cell types, units of specific organs. The first cell lineage differentiation event is a new wave of de-novo methylation in the blastocyst. Trophectoderm cells are primarily distinguished from the inner cell mass cells by their global hypomethylated status, showing a 14-25% less global methylation than embryoblast (**Figure 1.1**) (Gamage et al., 2018). This hypomethylated profile will be maintained during all pregnancy.

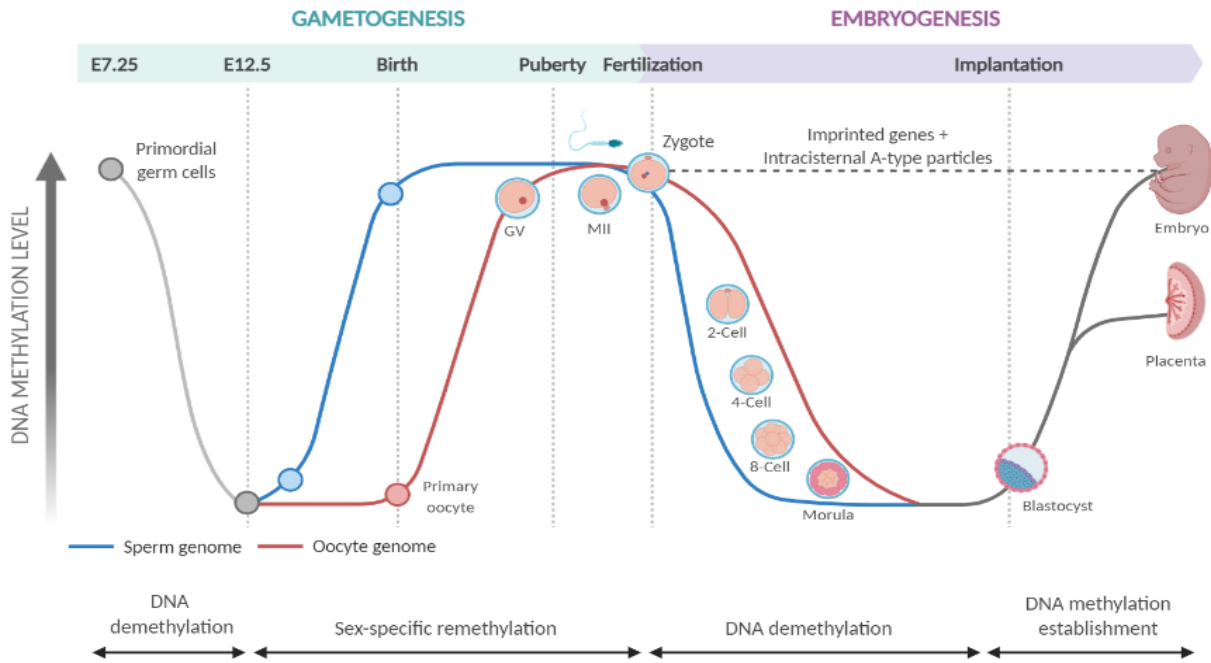


Figure 1.1: DNA methylation levels along gamete formation, fertilization, and embryo development. During gametogenesis. After fertilization, removal of DNA methylation signatures (except those on the imprinting regions) is produced. After implantation, re-methylation takes place giving the embryonic tissue higher methylation levels than the placenta.

Global hypomethylation in the placenta is hypothesized to support the unique functions of the organ. Low methylation levels enhance the ability of the placenta to respond to environmental exposures that require fast adaptive changes in the cell composition. In addition, the placenta methylome undergoes dynamic changes during gestation in order to promote fetal development and adapt to the different requirements of each month. Increased methylation levels are observed from the first to the third trimester, especially on genes implicated in immunomodulation (Novakovic et al., 2011). Some studies have detected increased inter-individual variation comparing beginning to end of pregnancy, supporting the effect of environment or stochastic changes in DNA methylation pattern during pregnancy (Vlahos, Mansell, Saffery, & Novakovic, 2019). Interestingly, DNA methylation in the placenta shows highly similar patterns as tumoral cells, which can explain the similar phenotypic behaviour: invasive, immunomodulatory and angiogenic (Costanzo, Bardelli, Siena, & Abrignani, 2018).

Aberrations in DNA methylation can modify cell behaviour leading to diseases. Several studies have associated DNAm differences between PE/IUGR and control samples (Blair et al., 2013; Sundrani et al., 2013; van den Berg et al., 2017; Zhu et al., 2015). However, there is a general inconsistency in the results and most findings have not been replicated. Although same ontology terms are found between different studies (oxidative stress, cell proliferation and inflammation), sites that show differentially DNAm are not (Wilson, Leavey, Cox, & Robinson, 2017). Small sample size, intrinsic heterogeneity of the diseases samples and different statistical and methodological approaches have led to different results with minimal overlap. Some of the genes that have been correlated with lower methylation levels in PE are VEGF, MAPK1, PRDX5, LEP, INHBA, etc. On the other hand, observed hypermethylated genes are ACAP2, CLIC6, GATA4 and PCFH9 among others.

Biological and technical confounders contribute to DNA methylation value variation. One of the most known confounding factors in PE is gestational age (GA) since, in severe PE cases, babies (and ipso facto placenta) are delivered in earlier gestational terms than in non-PE affected pregnancies. Some DNAm in PE and IUGR studies have addressed the effect of gender, batch, and GA in their analyses, however, other confounding factors, such as cell composition, ethnicity and other technical errors are not always considered.

The scope of our work was to identify “CpG signatures” from each of the pathologies present in our dataset (Preeclampsia, Intrauterine Growth Restriction, PE+IUGR and Chorioamnionitis) by removing CpGs influenced by other covariates. Clinical, technical, and inferred covariates were used. Herein, we aimed to identify CpGs, linked with the disease status with minimal influence of other clinical, biological, known or predicted, and technical covariates.

Materials and Methods

1. Human Placental Samples

This study includes a total of 73 placental DNAm datasets issued from 3 different series of placental datasets. We generated the DNAm datasets from two of these series—in two separate experimental batches—and DNAm dataset of the third series was retrieved for the public functional genomics data repository Gene Expression Omnibus (GSE115508) (**Table 1.1**). Series 1 is composed of placental biopsies obtained from women who were delivered at the Maternité Port Royal, Hospital Cochin (Paris). Series 2 is composed of placental biopsies obtained from women who delivered at the St George’s Hospital (London). Two control samples from GSE115508 were considered outliers after principal component analysis and thus removed from the dataset. Clinical features can be found in the **Annex 1.1**.

Table 1.1: Samples used in the experiment

Subject group/Series (Experimental batch)	Hospital/GEO	Ctrl	PE	IUGR	PE+IUGR	Chorioamnionitis
Series 1 (Batch 1/Batch 2)	Cochin	6/8	6/0	0/2	3/0	0
Series 2 (Batch 2)	St Georges	0	6	0	0	0
Series 3	GSE115508	20	0	0	0	22
	Total (73)	34	12	2	3	22

2. DNA extraction (Experimental batches 1 & 2)

Human placental tissue was collected after delivery, cleaned and a few biopsies of the villous fetal in different parts of the placenta were collected, snap-frozen and stored at -80°C until use. Tissues were powdered using a pestle and mortar on dry ice and resuspended on sample Lysis buffer (10mM Tris HCl pH8, 10mM EDTA, 50mM NaCl, 0.5% NaCl, 0.5% SDS, Proteinase K (Invitrogen #25530-049) used at 1:3000) overnight in shaking water bath at 58°C. DNA was precipitated using absolute ethanol. Pellet was collected and washed with 70% ethanol. After the pellet was air-dried, DNA was resuspended in Tris-EDTA.

3. EPIC Illumina Array Methodology

Five ng of placental DNA were analysed by EPIC Illumina array. This array assesses 850k CpGs located all along the genome: CpGs located in CpG islands and outside the islands, in DNase hypersensitivity sites, and miRNA promoter regions, CpGs differentially methylated in tumour cells vs. control cells and, also, additional non-CpG methylated sites observed in human stem cells.

After assessing DNA quality and quantity, DNA is sequenced after bisulfite treatment, which converts the unmethylated cytosine into uracil. Briefly, after a whole genome amplification, DNA is fragmented enzymatically, purified from dNTPs, primers, and enzymes, and hybridized onto the array. Fluorescent staining (red fluorochromes for Adenine and Thymine bases (unmethylated CpGs) and green fluorochromes for Cytosine and Guanine (methylated CpGs) is then recorded. Methylation level, reported as a β -value (ratio of unmethylated/methylated value for one given CpG), can have a value range from 1 if the CpG is completely methylated to 0 if there is no methylation (**Figure 1.2**).

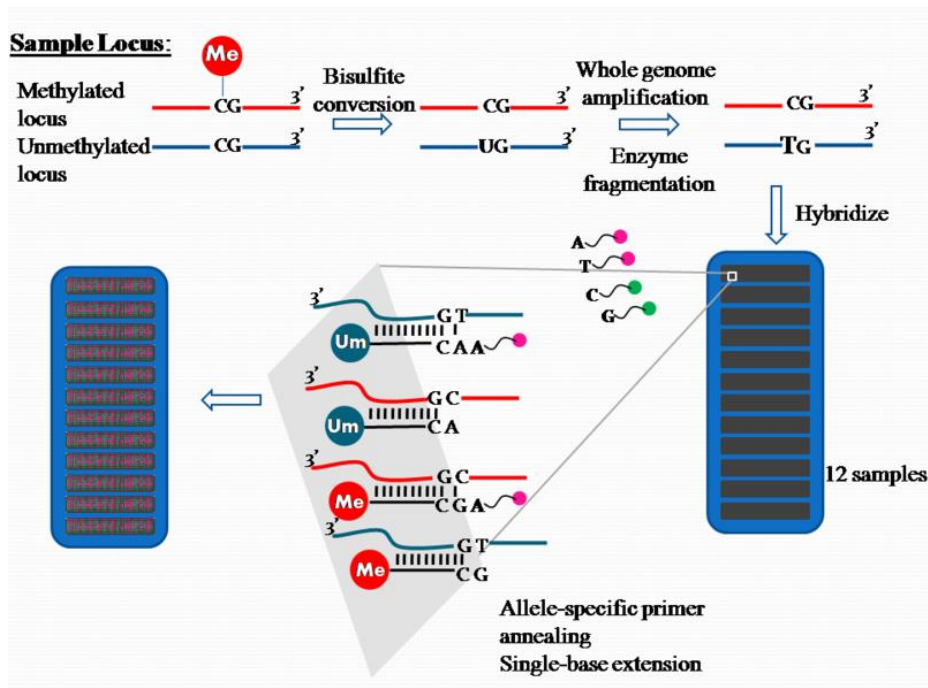


Figure 1.2: DNA methylation array methodology. After bisulfite conversion, enzyme fragmentation and whole genome amplification, hybridization of the fragments to the chips is performed. Single base extension adds a red fluorochrome to Thymine and Adenine bases and a green one to Cytosine and Guanine bases. Beta values

are obtained from the fluorescence scan of the chip. Image obtained from <http://www.nxt-dx.com/epigenetics/infinium-methylation-epic-array/>

Bioinformatic Analysis

Since our aim is to obtain CpG signatures for each disease, we attempted to select CpGs which are correlated with the disease status with minimal contribution to any other confounding factors. To achieve this, we first gathered as much information as possible about the different series in terms of clinical data and technical confounding factors and also inferred ethnicity/ancestry, GA, and cell composition using the PlanetR package (PlaNET —Placental DNAmE Elastic Net Ethnicity Tool—) developed by Yuan et coll. (Yuan et al., 2019) (**Figure 1.3**). Once these covariates were inferred, CpG filtering and quality control of the raw data was performed, removing low quality CpGs, CpGs located on sex chromosomes or aligned to multiple locations and CpGs influenced by SNP. Next, multivariate linear regression was performed against each individual CpG in to remove CpGs influenced by these covariates. CpGs significantly correlated with the disease status and with minimal influence of the other covariates were then selected. Finally, CpGs with a mean beta value difference of more than 5% between the disease and the control samples were considered as “CpG

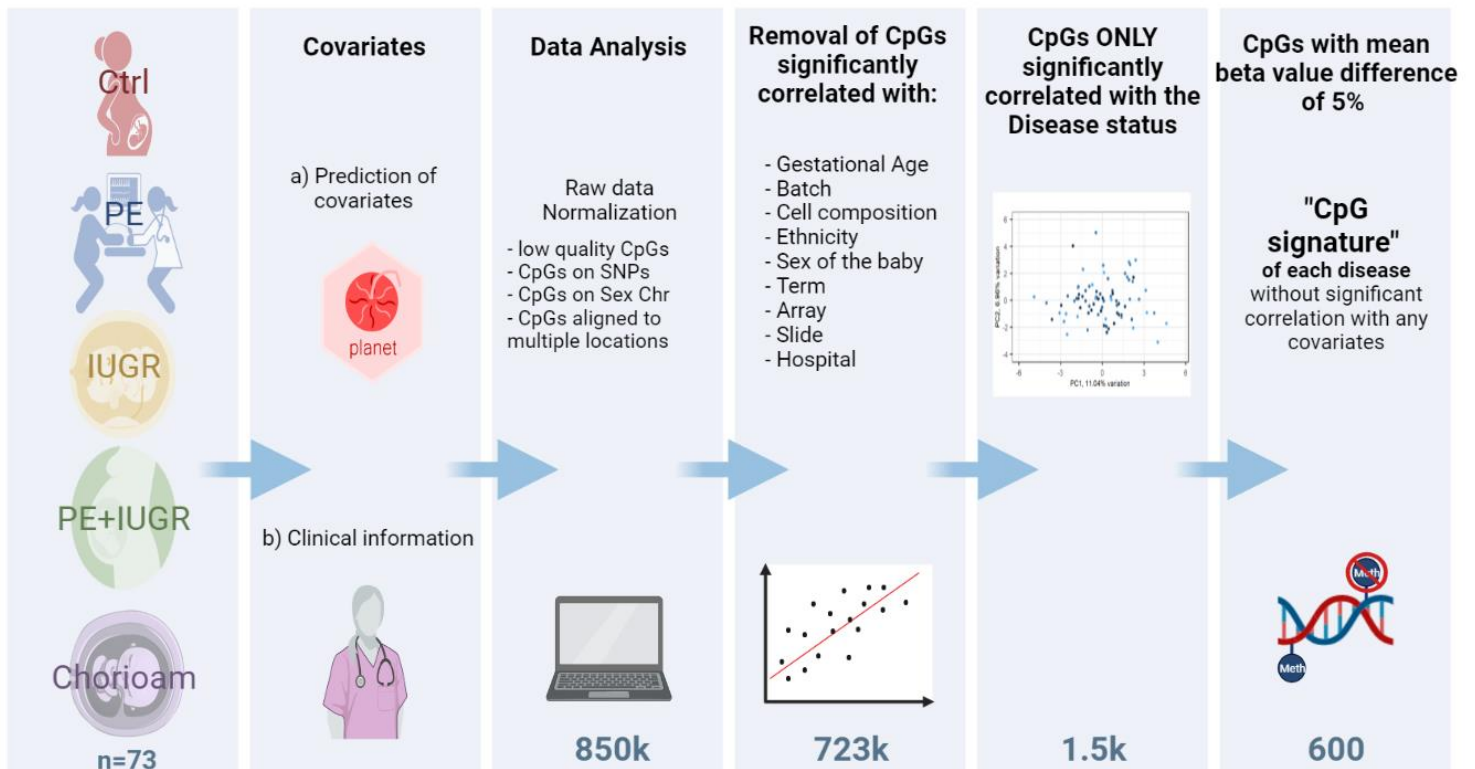


Figure 1.3 : Bioinformatic Analysis workflow

signatures”.

a. Prediction of Covariates: Cell composition, ethnicity, and gestational age

The raw β -values were normalized using the Beta-Mixture Quantile Normalization (*BMIQ*) method from the *Watermelon* R package, in which the beta value is fitted correcting for possible bias of type-2 probe values. Unfiltered normalized data was then used with the *PlanetR* package to infer information about GA, ethnicity, and cell composition.

i. Gestational Age prediction

Three different GA clocks from Lee Y. et al. 2019 are used to infer GA on the placenta (Lee et al., 2019): 1) a robust placental clock (RPC, 558 CpGs) which is unaffected by common pregnancy complications (e.g., gestational diabetes, preeclampsia), and 2) a control placental clock (CPC, 546 CpGs) constructed using placental samples from pregnancies without known placental pathology, and 3) a refined RPC (395 CpGs) for uncomplicated term pregnancies, GA >36 weeks. The results of the three clocks were averaged to produce the “Predicted GA” covariate of our dataset.

ii. Ethnicity prediction

Ethnicity prediction is based on an ethnicity classifier in placenta samples. *PlaNET* utilizes a total of 1860 ethnicity-predictive sites. Categorical labels (Caucasian, Asian, Eurasian, Ambiguous, Afro-European, or African) was applied using the probability of being African, Asian or European as predicted by the model.

iii. Cell composition prediction

Cell composition prediction for trophoblast (TB), syncytiotrophoblast (STB), nucleated red blood cells (nRBC), Hofbauer, endothelial cells (END) and stromal cells (Stromal) was obtained through three different cell deconvolution methods from the *minfi* package using, as reference data, DNAm profiles of third-trimester placentas from the *PlanetR* package *pCellCpGsThird*. This reference data was obtained by assessing term and preterm placenta cell populations separated by FACs and

enzymatically isolated STB (Yuan et al., 2021). The average of the three different estimations (Houseman, Epidish partial correlations and Epidish Cibersoft) was used as the percentage of each cell type present in the sample and added as a covariate. Comparisons between diseased placentas (PE, PE+IUGR and IUGR samples) vs. control placentas (Control and Chorioamnionitis samples) were compared using T.test to assess if the differences were significant.

b. CpG quality control and filtering

Filtering of low-quality CpGs was performed using the function '*champ.load*' of the Champ Package. CpGs located in SNPs (93,970 CpGs based on Zhou's paper 2016), located in the X or Y chromosomes (15,576 CpGs), 11 CpGs which align to multiple locations (11 CpGs), probes with a beadcount <3 in at least 5% of the samples (1173 CpGs), non-cg probes (2,774 CpGs) and those CpGs whose detection p-value was above 0.01 in at least 1 sample (28,675 CpGs) were removed. A total of 723,680 CpGs were used for downstream analysis. Zeros from the dataset were replaced to the smallest positive value and the ones were replaced by the largest value below 1. The beta-mixture quantile normalization method was used for the correction of the bias observed in the type-2 probes. Finally, to get better statistical power, normalized β -values were logarithmically transformed into M-values:

$$M \text{ value} = \log_2\left(\frac{\beta \text{ value}}{1 - \beta \text{ value}}\right)$$

To note, all statistical analyses were performed using M values, however, β -values were used for figure visualization.

c. Grouping of placentas

All statistical models were performed three times, differing the grouping of the samples as follows:

- **"Group"** → Ctrl, chorioamnionitis, PE, PE+IUGR, IUGR, all considered individually

- **“Unaffected_Diseases”** → Unaffected groups (Ctrl and chorioamnionitis, together) vs. PE, PE+IUGR, or IUGR, considered individually
- **“Unaffected_affected”** → Unaffected groups (Ctrl and Chorioamnionitis, together) vs. Affected (PE, PE+IUGR, IUGR groups considered together)

d. Multivariate linear regression

To determine which CpGs were influenced by the pathology, the M-values of a total of 723,680 CpGs were linearly regressed towards 16 clinical, technical, and predicted covariates using the limma R package under the following model:

$$\{M \text{ value} \sim GA+Sex+Term+Batch+Series+Pathology+Array+Slide\dots$$

$$\dots+Ethnicity+TB+Stromal+Hofbauer+ENT+nRbC+STB+Pred_GA \}$$

This model has been performed in “Pathology” groupings described before: Group, Unaffected_Diseases, Unaffected_affected.

eBayes function from limma package was used to perform the statistical analysis and p. values corresponding with the significance of each individual regression coefficient towards the regression model. Thus, when the p.value is <0.05 the regression coefficient of the covariate is significantly different from zero meaning the covariate has a significant effect in the DNA methylation level of the CpG. To obtain CpGs linked with the pathology status with minimal influence of the other covariates, removal of significantly correlated CpGs (p.val <0.05) for each of the remaining 15 covariates were removed. From these, only significantly correlated CpGs with the pathology status were collected for downstream analysis.

e. Dimensionality Reduction

Principal Component Analyses were performed using PCAtools R package, after standard removal of the lower 10% of variance based on variance. In order to determine the correlation

between the Principal Components (PCs) and the covariates was performed using the eigencorplot function of the same package.

Code Availability:

All code repositories are available in <https://github.com/CaminoRuano?tab=repositories>

Results

Clinical vs Predicted Gestational Age

Predicted GA of all the samples was inferred with the PlaNet package and the linear relationship between predicted and clinical GA was evaluated by *linear regression t-test*. These tests were significant for the control ($R^2=0.92$, p value= $2.14e-18$) and for the chorioamnionitis cases: ($R^2=0.91$, p value= $2.84e-12$) (**Figure 1.4**), and the lines did not differ between the two groups (Control and chorioamnionitis equations: $y=4.7+0.86x$ and $y=4.6+0.86x$, respectively). In contrast, the linear relationship was not significant for the placentas affected by PE, $R^2: 0.097$, p value: 0.325 (equation; $y=27+0.24x$). Especially, for the earlier GA, diseased placentas have a higher predicted GA than the clinical GA, suggesting that the methylation pattern on these placentas is much similar to older placentas.

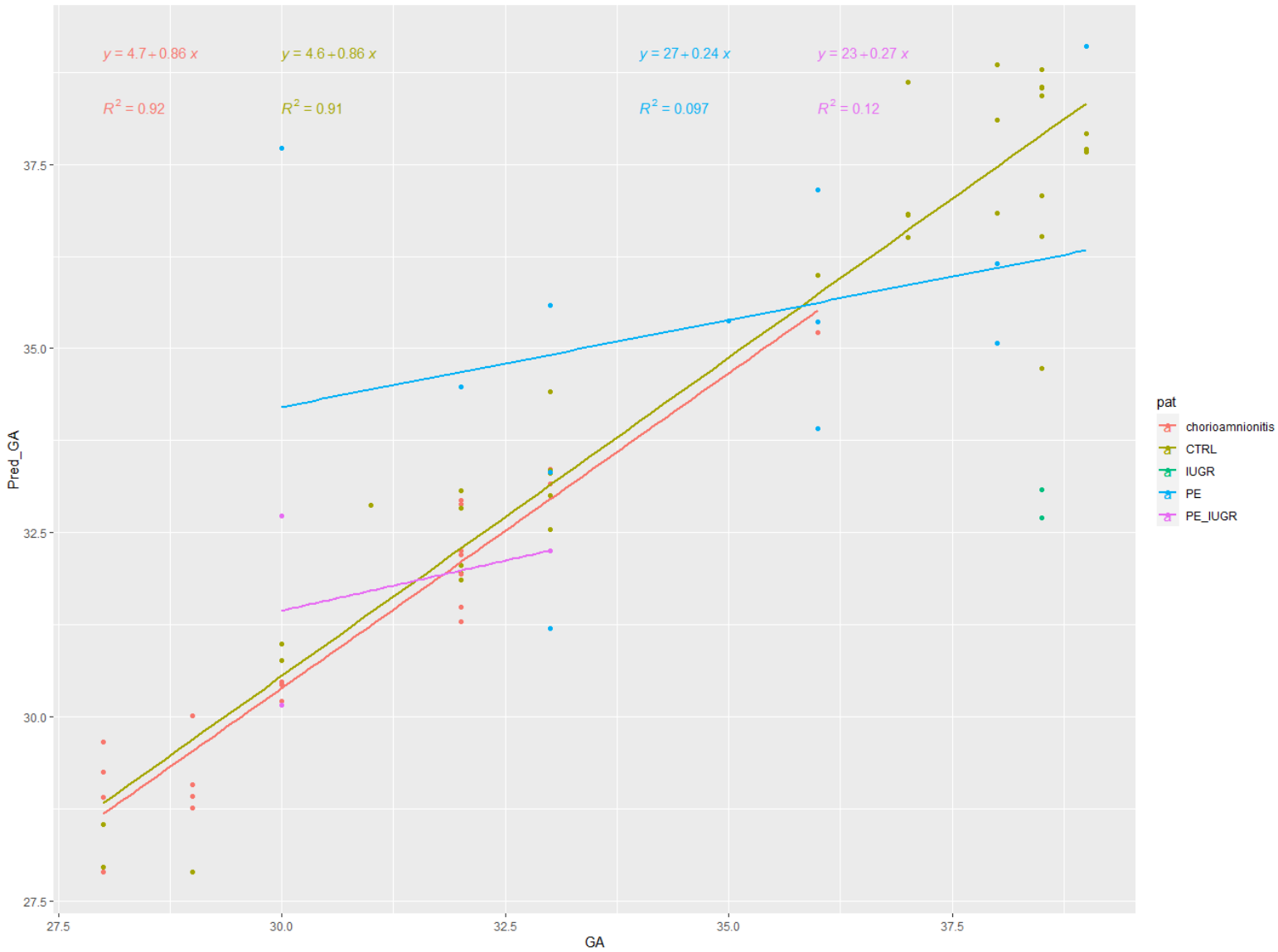


Figure 1.4: Clinical GA (x-axis) vs Predicted Gestational Age (y-axis). Colour code: Ctrl in light green, chorioamnionitis in red, PE in blue, IUGR in dark green, PE+IUGR in purple.

Cell Composition Differences between Control and Pathological Placentas

Since cell type composition is a major contribution to DNAm pattern, it can easily confound important findings in placenta such as true difference occurring at the cellular level (Avila et al., 2010; Jones, Islam, Edgar, & Kobor, 2017). The main inferred cell type was Syncytiotrophoblast (>50% of the cells), as expected from term placentas, followed by Trophoblast cells (20-30%) (**Figure 1.5**). We can also observe some differences among the sample groups in terms of proportion. However, because there is interaction between cell composition, GA, disease and, DNAm pattern, we did not perform any statistical analysis to compare the proportion between groups.

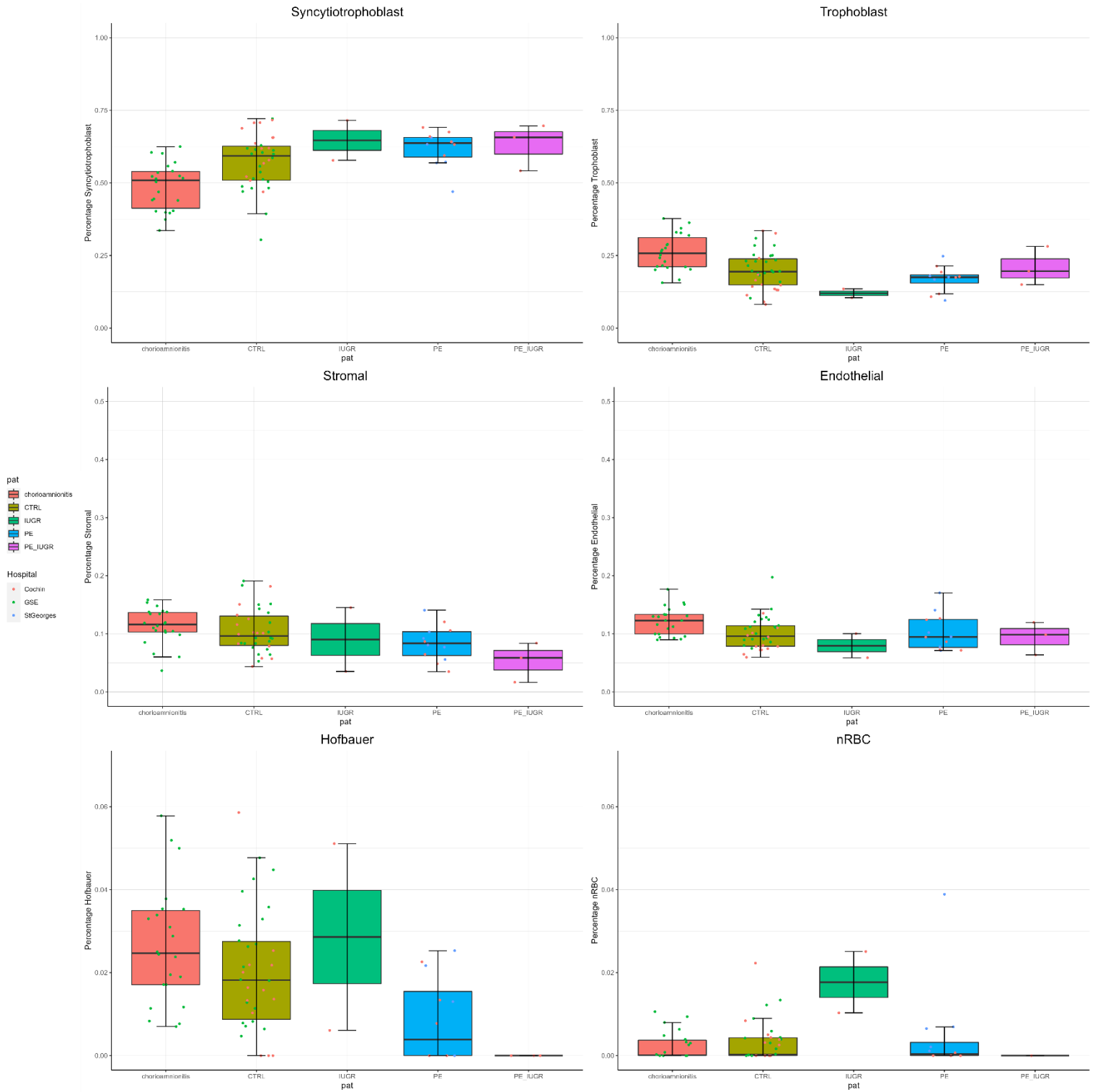


Figure 1.5: Cell composition differences between control and diseased placentas: Colours of dots represent the Series: red Series 1 (Cochin), blue Series 2 (St. Georges) and green Series 3 (GSE).

Ethnicity prediction: Genetics vs Epigenetics

Because in France, it's forbidden by law to collect statistics on ethnicity, we do not have access to this information through clinical reporting. However, DNAm pattern can be used to address population stratification and we were able to infer the ethnical origin of our samples: 31 Caucasian, 12 Asian, 6 Eurasian, 8 Ambiguous, 4 Afro-European and 12 African (Figure 1.6).

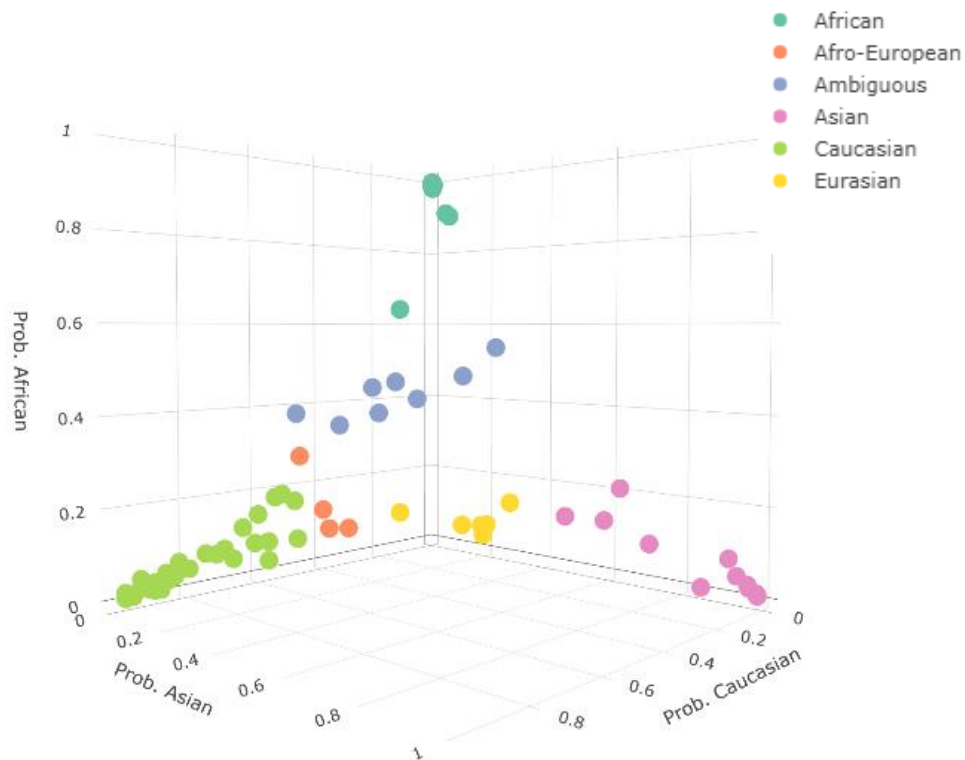


Figure 1.6: Ethnicity Prediction of the placental samples. Probability of being African, by the probability of being Asian by the probability of being Caucasian. African, Caucasian and Asian are considered when the percentage of the respective ethnicity was >60%. Mixed ethnicities (Afro-European and Eurasian) were considered when the second top ethnicity had a probability >20%. Ambiguous ethnicities were considered when neither of the three probabilities reached the 50%.

Preliminary visualization and identification of covariates affecting the DNAm profile

As an assessment of the global variability in our different datasets, principal component analysis (PCA) was performed. The two main principal components (which explain the 24% and 8%

of the global variability) segregate the samples from series 1 and 2 to the samples from series 3 (Figure 1.7a). PCA without the 42 samples of series 3 segregates series 1 and 2 samples by experimental batches (Figure 1.7b).

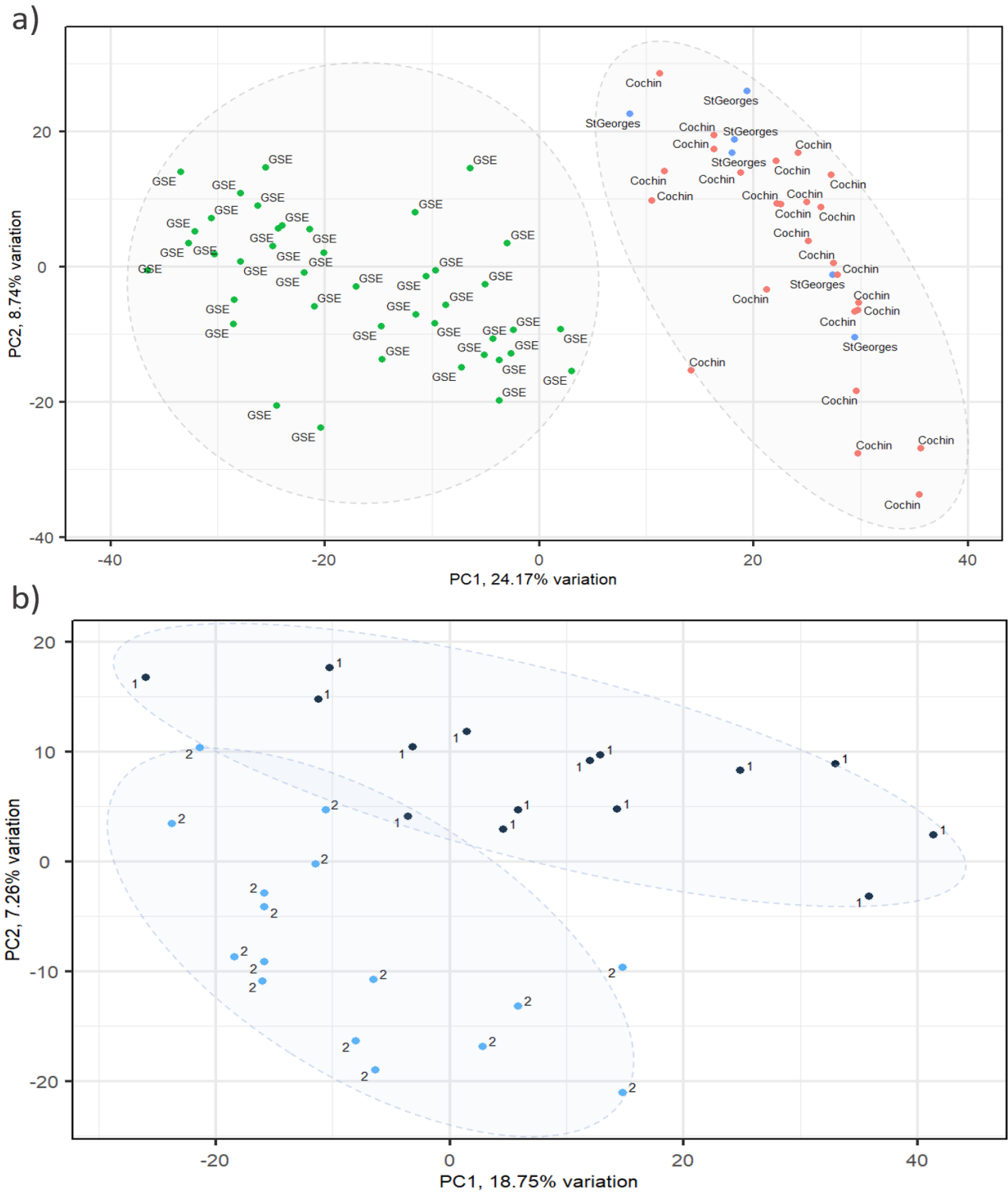


Figure 1.7: Visualization Normalized 723,680 CpGs. a) PCA plot of all 73 samples showing the two groups by Series. Series 1 (Cochin), Series 2 (St Georges), Series 3 (GSE). b) PCA plot of the samples from Batch 1 and Batch 2.

To further gain insight on the sources of variation in the DNAm profile of these three series, a correlation plot between the 10 first PCs and our observed and predicted covariates was performed **Figure 1.8**. The covariates ranged from continuous variables (GA, cell composition) and discrete values (ethnicity, PT/Term (delivery before or after 37 weeks of gestation based on the clinical data, baby sex, Series, Groups, Unaffected_Diseases, Unaffected_Affected, Batches, Array). These covariates were classified in the following subgroups: Technical (Batch, Array, slide), Grouping (Unaffected/Affected, Unaffected/Disease, with PE, PE_IUGR and IUGR taken into account individually, and Group, with the sample group taken into account separately), Inferred covariates (Cell composition, ethnicity, predicted GA), and clinical data (GA, Infant sex, PT/term, and Series). As depicted in Figure 1.8, all covariates, but Array, nRBC, ethnicity, and sex, are significantly correlated with PC1. Batch presents the highest correlation coefficient, following by slide and group. So, a distinct DNAm signature could not be inferred with this analysis.

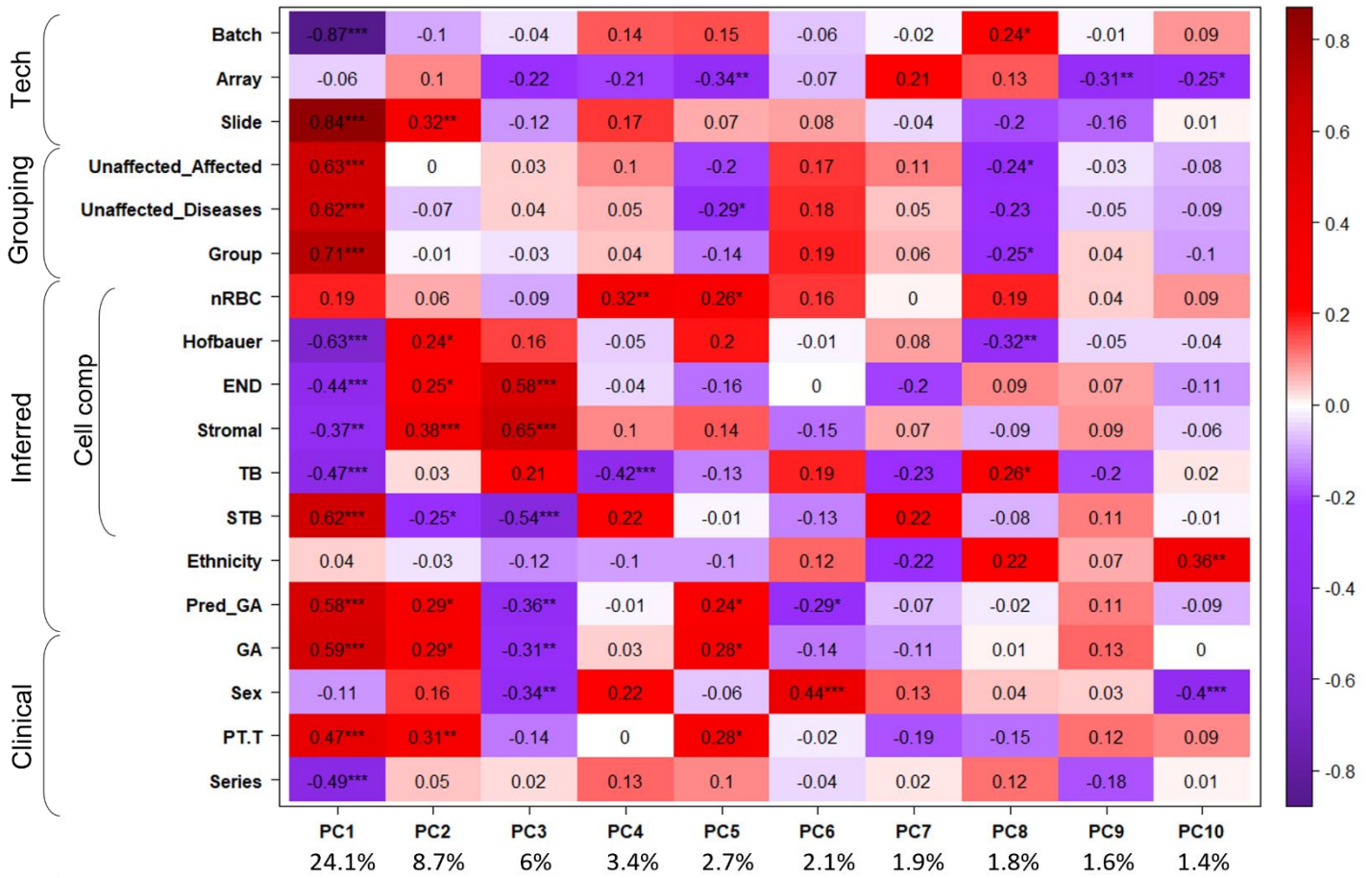


Figure 1.8: Correlation plot between the main 10 PCs and the 16 covariates of interest. Pearson coefficients of correlation between the covariates and the first Principal components. Negative correlations are in purple and positive correlations in red. Significance is stated as F-statistic where * pvalue ≤ 0.05 , ** pvalue = 0.001, *** pvalue = 0.0001, **** pvalue = 0.00001. Percentage of variance explained by each PC is annotated in the bottom.

Multivariate Linear Regression Model and Differentially Methylated CpGs

We next performed a multivariate analysis using a multivariate Linear Regression model, since it considers more than one factor of independent variables that influence the variability of dependent variables. To create our regression model, the Pearson correlation coefficient between the covariates was calculated (**Figure 1.9**). Because all the covariates, but the ones describing the grouping of the samples, have a correlation coefficient $<|0.9|$, they were not considered as colinear and, thus, added in the regression model.

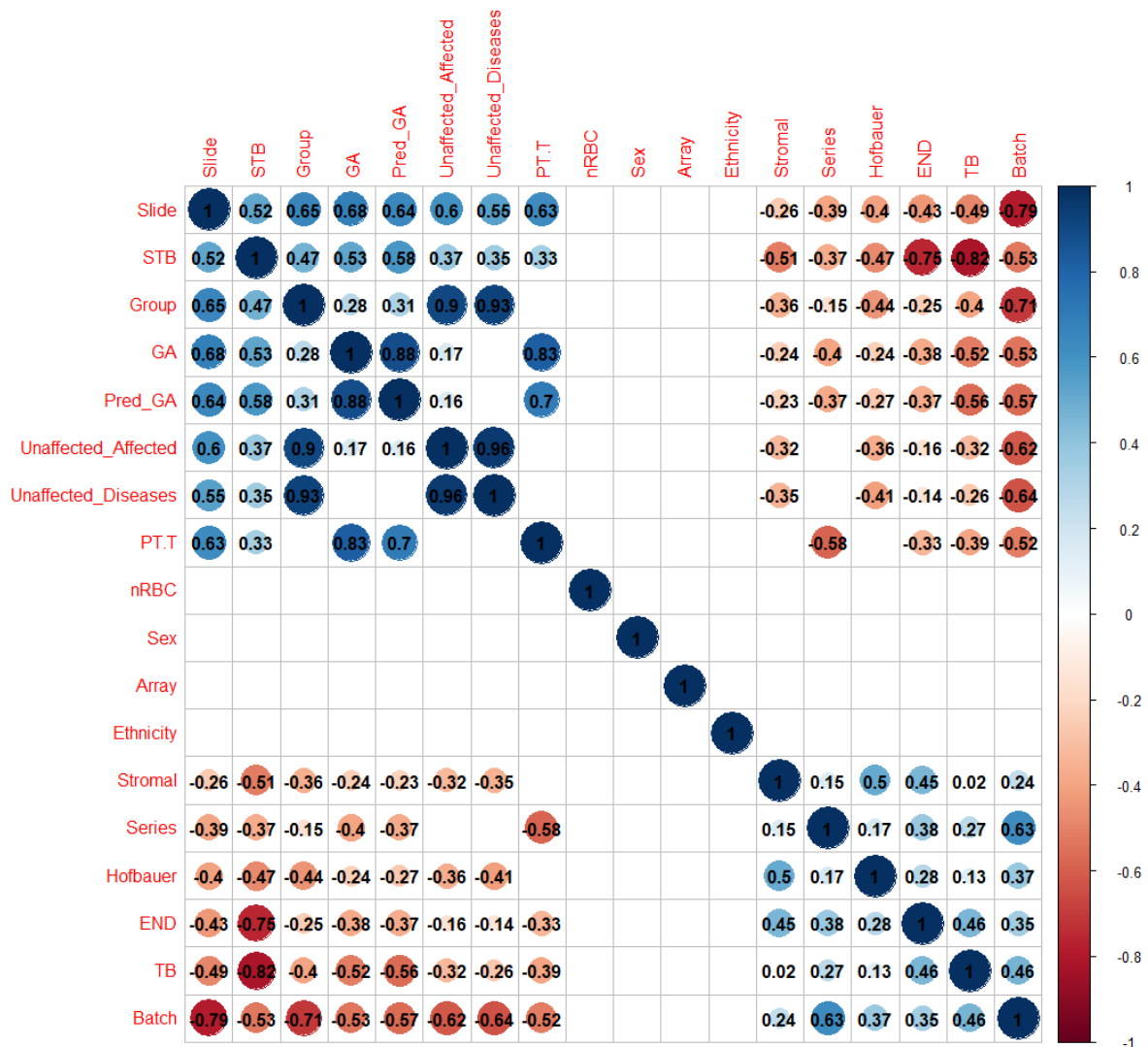


Figure 1.9: Correlation coefficients between the experimental, clinical and predicted variables. Each dot is the correlation coefficient with a significance $p\text{-value} \leq 0.05$. The dot area corresponds to the correlation coefficient. Negative correlation is in red, while positive correlation is in blue.

We next performed the multivariate linear regression model analysis with a total of 16 covariates on the M-value of each CpG. All the CpGs that were significantly influenced ($p.val < 0.05$) by any of the 15 covariates — clinical GA, Predicted GA, Sex, Term, Batch, Array, Slide, Ethnicity, TB, Stromal, Hofbauer, Endothelial cells, nRBCs, STB, and Hospital— were then discarded. As result, 1,713 CpGs correlated with the “group” category ($p.val < 0.05$), when considering all the different pathologies, 1,666 with the “Unaffected_Diseases”, and 1,760 with the “Unaffected_Affected” category. CpGs showing a β -value difference $> |5\%|$ between unaffected and affected groups were further filtered (**Table 1.3**).

Table 2.3: Results of the multivariate linear regression: Significant CpGs were considered when $pval < 0.05$. Beta value difference was performed on Control vs Diseased placentas.

	CpGs only correlated with the disease	Beta value difference $> 5\% $
Group	1713	614
Unaffected_Diseases	1666	691
Unaffected_Affected	1760	698

As depicted in **Figure 1.10**, 142 CpGs are common to the three grouping categories, with 90 associated with a gene. Unsupervised clustering of our placenta samples, based on the methylation status (β -value) of the 142 CpGs placed 14/17 diseased placentas in two subgroups on the far left, clearly separating them from the healthy placentas. Heatmap displaying the methylation status in relation to the pathology status showed the trend toward a disease (PE and PE+ IUGR) signature, with two main groups of hypermethylated CpG and two main groups of hypomethylated groups. A PCA analysis was next performed and the two groups, Unaffected and PE-affected placenta, are clearly separated on PC1, which explains 27% of the total variance.

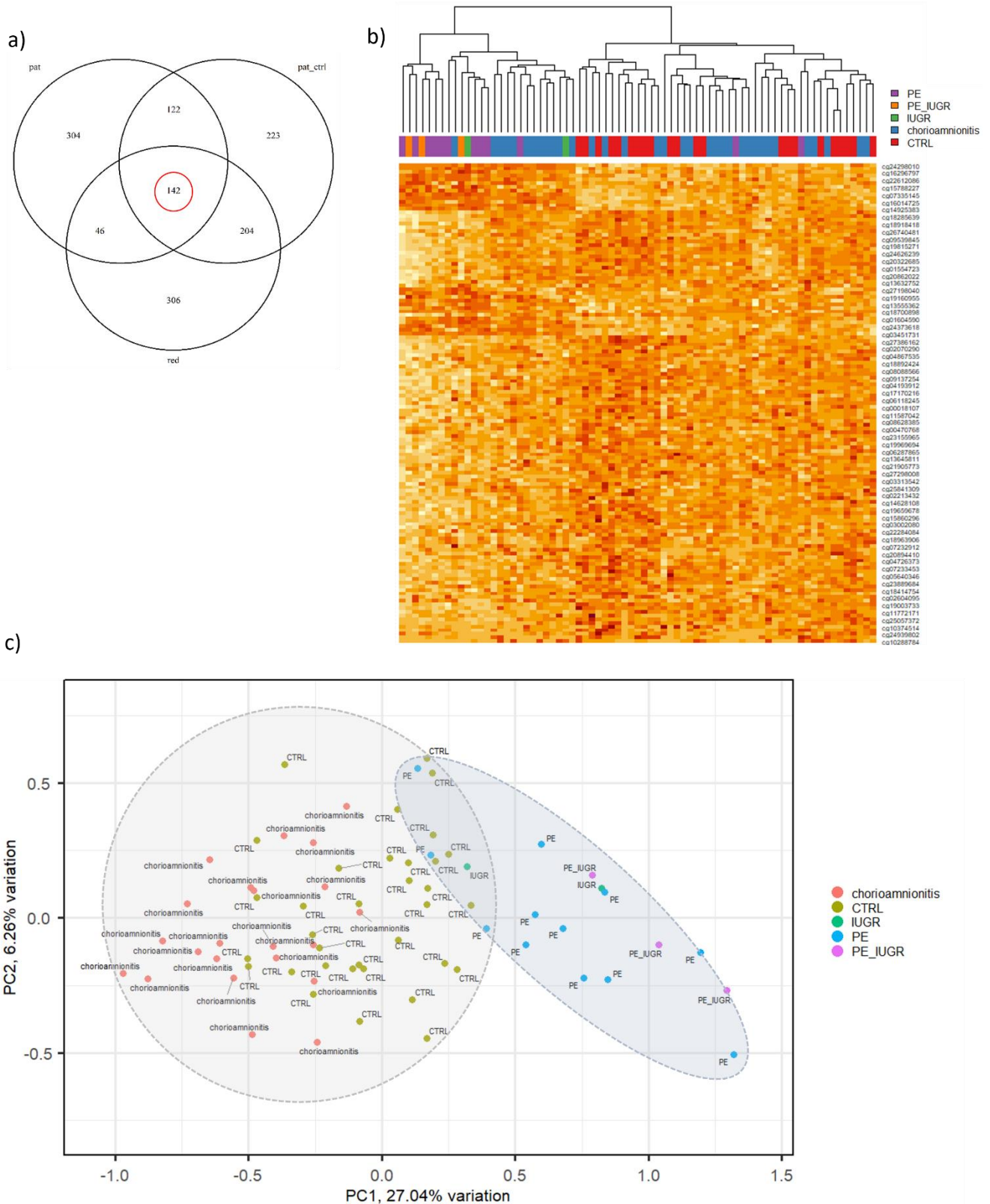


Figure 1.10: Final Set of CpGs with biological significance in the development of pathologies in the placenta. A) overlap between the different analysis performed lead to the identification of 142 common CpGs correlated with only the disease and with a difference β -value $\geq |5\%|$. **B)** Heatmap of the β -values of the 142 CpGs and the 73 samples (annotation of the 73 samples is not in the figure). **C)** Plot of the PC1 (which explains 27.04% of the variation between samples) against the PC2 (explaining the 6.26%). Color of the points represent the pathology.

Discussion

DNA methylation (DNAm) is an important epigenetic mechanism of gene regulation and has critical role in cellular processes and fates. Herein, we were interested in identifying differential mCpGs purely driven by the pathology, intending to find “CpG signatures” for each of the pathologies across our dataset. We analysed the methylome of 73 placental samples across unaffected, and chorioamnionitis, PE, PE_IUGR or IUGR-affected groups using the Illumina EPIC methylation array, which quantifies DNAm at > 850,000 CpGs. After quality control and filtering, multivariate linear regression was performed using 16 covariates including clinical, technical, and inferred variables. A total of 1.7k CpGs were found to be more influenced by the PE state — considering separately the PE, PE_IUGR or IUGR-affected groups— than by any other covariates. Among these 1.7k CpGs, a focus on those with a β -value difference of at least 5% between unaffected and pathology-affected placentas further filters ~600 CpGs, of which 142 were common to the PE, PE_IUGR or IUGR-affected groups. Hierarchical clustering and PCA confirmed that the methylation levels of these 142 CpGs effectively separated unaffected and PE-affected placentas.

PE and/or IUGR constitute heterogeneous conditions, with many different factors contributing to these phenotypes. To date, five published studies have reported genome-wide changes in DNAm associated with PE (Hogg, Blair, von Dadelszen, & Robinson, 2013; Smallwood et al., 2011; Sundrani et al., 2013; van den Berg et al., 2017; Xiang et al., 2013). However, differences between PE subtypes, the inclusion or not of confounding factors and different statistical analysis led to lists of CpGs with minimal overlap between these studies. Indeed, there is challenge in reproducing genome wide DNAm hits. Hence, the use of covariates to adjust the methylation signal is essential for the finding of CpGs driven by the disease. For example, DNAm cell-specific differences and variability in the cell-type mixture can have a strong effect on the DNAm level observed in mixed tissue samples. Furthermore, in placenta samples, other factors, such as age, maternal comorbidities, fetal characteristics, sex, ethnicity have also to be considered in the statistical model.

Although many of the published studies introduced gestation age and experimental batch as possible confounders, only one (van den Berg et al., 2017) performed a side analysis with 8 covariates (batch-effect of the bisulphite-plate, gestational age, birth weight, fetal gender, maternal comorbidity, mode of delivery and moment of inclusion for the study) which were not further considered in their statistical model.

Since one of the main confounding variables in PE is GA, we decided to add unaffected placental dataset from early GA from a publicly available database into our analysis. Although half of these new samples were associated with chorioamnionitis, a preliminary analysis showed that samples of the chorioamnionitis-affected group have a similar DNAm profile to those of the unaffected samples in that dataset. Thus, we decided to consider in our subsequent analyses, chorioamnionitis-affected and unaffected samples at the “series” level without considering the chorioamnionitis parameter. In addition to increase the number of “control” samples to be analysed, these early GA samples proved to be key to discriminate CpGs influenced by GA from those influenced by the disease. Since the gestational age prediction was highly similar using the three different methylation clocks, a mean Notably, the prediction of gestational age using a DNAm clock was as accurate in samples affected by chorioamnionitis as in healthy placentas. This was not the case with PE-affected samples, where the DNAm clock inferred older gestational ages for the most severe cases; this is in line with the hypothesis of premature aging of the placenta in PE (Mayne et al., 2017).

We also performed cell deconvolution analysis to infer underlying cell type proportions, because DNA methylation patterns can serve as distinctive cell type markers (Baron et al., 2006). We obtained results comparable to a recent study addressing this issue in healthy placentas (Yuan et al., 2021). These proportions were included in our linear model, but we did not formally test the cell composition difference in unaffected vs. PE-affected placentas since cell proportions may also be influenced by GA and the location of the placenta biopsy within the whole organ. However, a

strongly correlation was observed between cell subpopulations and the first 3 PCs in our PCA, especially for the STB component, suggesting that STB proportion/composition is an important source of variation in the global placental DNAm profile.

We are also able to estimate the ethnicity of the placenta donors with a good precision. The results obtained with DNAm profiles were confirmed for the samples of series 1 and 2 by analysing the genotype using Illumina human genotyping arrays (*data not shown*). We were able to differentiate not only Caucasians, Africans, and Asians, but mixtures of these ethnicities, giving a high spectrum of genetic variability within our sample set. However, the interindividual epigenetic variation is not only determined by genetic ancestry but also by environmental/cultural influences (Busche et al., 2015; Gunasekara et al., 2019; Wilson & Robinson, 2018). Nevertheless, considering the ethnicity prediction adds another layer of information in our dataset.

In conclusion, although we did not achieve to produce “CpG signatures” for each of the placental pathologies, our statistical approach led to the identification of a small subset of CpGs with a stronger influence of the PE disease rather than discrete or continuous confounding factors. However, we can hypothesize that either a) all the covariates explain the pathology, leading to an insignificant number of CpGs correlated with the disease alone which, at the same time can be still influenced by the other covariates at a non-significant level b) the effect of the disease cannot be detectable at the DNAm level, which can be due to strong DNAm changes at specific cell-type level are blurred into the bulk DNAm data or c) we did not have enough number of samples to develop this type of analysis accounting with both, the strong heterogeneity found in the disease and the strong heterogeneity that represents the placenta itself.

Limitations

- Known risk factors for PE, such as maternal characteristics and comorbidities (maternal age, BMI, hypertension, parity) and fetal characteristics (birthweight) were not available and, thus, could not be added to the model. These variables, although they could be collinearly

correlated with other covariates, e.g. birthweight and GA, should also be considered, especially due to their high relevance in the development of PE (Ogunwole et al., 2021).

- When using of Combat package, although being a standard step in DNAm analyses, on a small subset of the samples, we observed inflation of the β -values. Several studies have pointed out how batch normalization approaches can increase the false discovery rates and hyperinflated differences between conditions (Zindler, Frieling, Neyazi, Bleich, & Friedel, 2020). We thus choose to filter CpGs correlated with batch experimental effect rather than applying a batch correction.
- This strategy aims to identify only CpGs whose effect is highly specific to the pathology; thus, we have discarded probes which could be associated with both the pathology and other covariates. These CpGs are still interesting in the development of the disease and should be taken in account for further studies, such as the case of sex-specific probes which can increase the development of placental dysregulations.
- Some covariates of interest, such as maternal blood pressure, environmental factors, diabetes, the use of drugs, smoking or other covariates may have an effect in the development of the disease but have been discarded due to incomplete information within our samples. This is a highly common problem in big data analysis in which several datasets have been used. Curation of the metadata file and the homogenization of the patient and disease information is a common requirement for the development of these type of research.
- Placental collection and variations in the biopsy location and the protocol used can impact the DNA methylation level and, although batch effect could explain some of this difference, other variations should be considered.
- As mentioned before, the low number of samples, the high heterogeneity between the patients, the disease and within the placenta itself made this DNA methylation analysis a

complicated task. Increase the number of samples and adding new PE dataset could benefit in the robustness of the analysis.

Further Perspectives

We will further test the robustness of our 142-CpG signature by a Monte Carlo approach, with a random shuffling of the group labels to assess whether this enrichment is random. Moreover, validation of this signature in replication cohorts is mandatory.

CHAPTER 2: Single Nuclei RNA-seq Analysis in Preeclamptic Placentas

Introduction

As described in the introduction, the placenta is an organ composed of a mix of cell subpopulations, including trophoblasts in differentiated states —VCT, SCT, EVT—, stromal and endothelial cells and resident placental macrophages (Hofbauer cells). Trophoblasts arise from the trophoctoderm, while stromal, endothelial, and immune cells derive from the extraembryonic mesenchyme that originates from the inner cell mass (**Figure 2.1**).

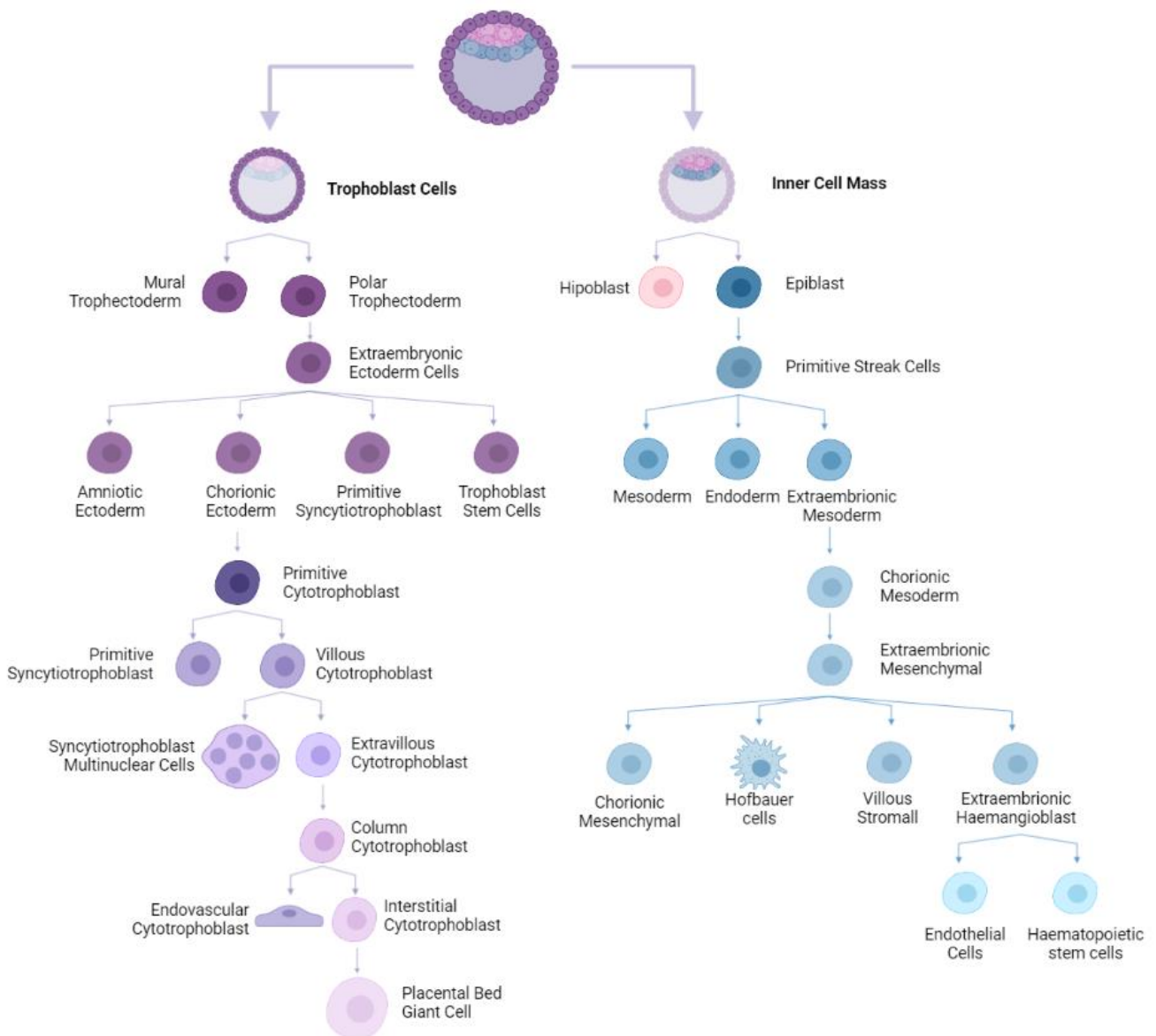


Figure 2.1: Trophoblast cell lineage specifications (Edgar et al., 2013).

Briefly, during the placentation process and throughout the 9 months of pregnancy. VTB differentiates into EVT, when it reaches the tip of the placental villi, or into SCT if the fusion process takes place. SCTs form a syncytial layer that covers all the placenta villi (**Figure 2.2**). Over time, nuclei in this layer age and decay, creating structures denominated syncytial knots which are released into the maternal circulation (Loukeris et al., 2010). The CTB layer is continuously renewing the syncytial layer by dividing and fusing to maintain a proper syncytial layer during all the development of pregnancy (Jaremek et al., 2021).

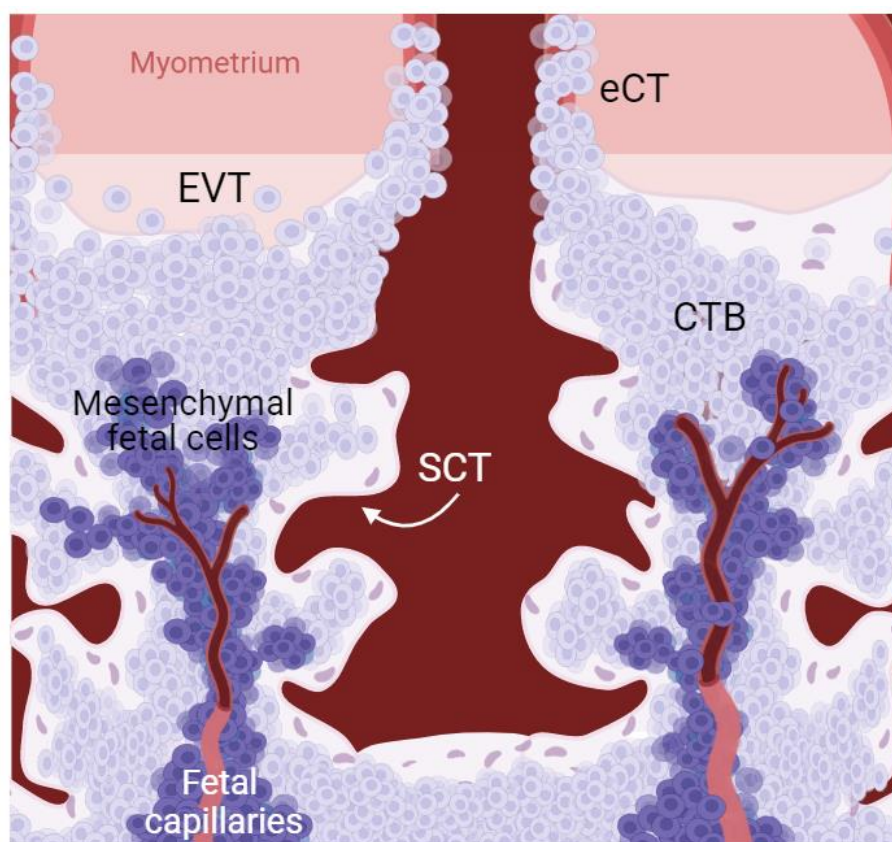


Figure 2.2: Main placental cellular populations found in the villi of the organ. Extravillous trophoblast (EVT), syncytiotrophoblast (SCT), cytotrophoblast (CTB), endovascular cytotrophoblast (eCT).

Improvements in microfluidic devices, substantial reductions in sequencing costs, developments of ready-to-use kits and bioinformatic pipelines have made experiments at the single-cell level increasingly feasible and affordable. These experiments have opened the possibility to map

cell types, subsets and cell states in health and disease at a high degree of resolution. Single-cell RNA sequencing (scRNA-seq) has been used to describe the placenta [20,518 captured cells from 6 full-term placenta villi (Tsang et al., 2017), 11,055 cells from 4 full-term placenta villi and 8,195 cells from 3 midterm placenta villi (Pique-Regi et al., 2019)] and the maternal-fetal interface in early pregnancy [18,547 captured cells from 5 early term placenta villi (Vento-Tormo et al., 2018), 14,341 cells from 8 early term placenta villi (Suryawanshi et al., 2018)]. These datasets captured a significant number of trophoblastic cells, ranging from 36% to 51%, with VCT being the most abundant captured trophoblast subtype, followed by SCT and EVT —90%, 7.7% and 2.3%, respectively in early placenta (Suryawanshi et al., 2018) and —82%, 1.3%, and 16.9%, respectively in late term placenta (Pique-Regi et al., 2019). However, earlier stereological analyses of full-term placenta found that VCT cells are less than 20% of SCT; the average placenta contains 6.4×10^{10} trophoblast nuclei of which 90% are located within the syncytium (Mayhew, 2014; R. A. Simpson, Mayhew, & Barnes, 1992). scRNA-seq technology relies on enzymatic dispersion of live cells and multinucleated cells show poor recovery after tissue digestion. Single nucleus RNA-seq (snRNA-seq) approach achieves comparable gene expression detection to scRNA-seq, but presents substantial advantages as it allows the reduction of cell dissociation bias, it is compatible with frozen tissue samples, and it avoids the stress response induced by the dissociation procedures (Habib et al., 2016; Wu, Kirita, Donnelly, & Humphreys, 2019). Grindberg et coll. described that 98% of the transcripts which are found in whole cells are found at similar levels in the nuclei (Grindberg et al., 2013). Therefore, snRNA-seq applied to the term placenta paves the way for the identification of transcript profiles and inference of functions, cell trajectories, signaling interactions in nuclei embedded in the SCT layer.

Thus, in order to further understand the cellular complexity of this heterogeneous tissue, we performed snRNA-seq analysis from 8 healthy and 4 PE-affected late-term placentas. We captured a total of 71,719 isolated nuclei and analysed their transcriptomes to evaluate the diversity of placental cell subpopulations. Also, transcriptomics differences were assessed at the single nucleus level between healthy and pathological placentas as well as the differential transcriptomic dynamics.

Collectively, we established a comprehensive map of trophoblasts in human late-term placenta and provided a resource to better understand how preeclampsia conditions can affect the molecular profile of the human placenta.

Materials and Methods

1. Sample collection

Placental villi biopsies were obtained from 4 women affected with late onset of PE and 8 placentas from women with uncomplicated pregnancies (control) between 35 to 40 weeks of gestation (**Table 2.1**). All tissue samples used for this study were obtained with written informed consent from all participants in accordance with the guidelines in The Declaration of Helsinki. These placentas were obtained from either the Maternité Port Royal- Hospital Cochin, Paris, France or St. George's Hospital, London, UK, and snap-frozen in less than 30 minutes after C-section delivery or vaginal delivery.

Sample name	Hospital	Gestational age	Delivery	Sex of the baby
pces1	Hospital Cochin	39	C-section	F
pces2	Hospital Cochin	38	C-section	M
pces3	Hospital Cochin	39	C-section	F
pces4	Hospital Cochin	39	C-section	M
pvb1	Hospital Cochin	40	Vaginal delivery	F
pvb2	Hospital Cochin	41	Vaginal delivery	F
pvb3	Hospital Cochin	40	Vaginal delivery	M
pvb4	Hospital Cochin	41	Vaginal delivery	M
ppreeclamp1	St. Georges Hospital	35	C-section	M
ppreeclamp2	St. Georges Hospital	36	C-section	M
ppreeclamp3	St. Georges Hospital	36	C-section	F
ppreeclamp4	St. Georges Hospital	38	C-section	M

Table 2.1: Samples used in the experiment

2. Single nuclei isolation and droplet-based scRNAseq

Frozen placental tissue was minced in small pieces with scissors and homogenized using an ice-cold (Lysis Buffer 10 mM TrisHCl, 10 mM NaCl, 3 mM MgCl₂ and 0.1% NP40 solution) for 10 min at 4°C. The solution was completed with washing buffer containing 1X PBS, 2% bovine serum albumin (BSA) and 0.2 U/μL of RNase inhibitor, and dounced 15 times before to be filtered through 70 μm, 40 μm and 20 μm cell strainers. Nuclei suspensions were centrifuged at 800G for 10 min at 4°C and

the pellet was resuspended in washing buffer. This operation was done twice followed by the nuclei counting. Nuclei were then incubated with antibodies against the nuclear pore complex (Mab414, BioLegend) at 2 $\mu\text{g}/\mu\text{l}$ for 15-20 min at 4°C and washed, before to be sorted using an ARIA3 flow cytometer. For the extraction of nuclei, all the products (except indicated) came from Sigma Aldrich (St. Louis, MO).

Further encapsulation and snRNA-seq were performed using the 10X Genomics technology (Figure 2.3). Briefly, 10,000 Mab414-positive nuclei are sorted and individually encapsulated in an oil drop together with an individual microbead using the 10XGenomics Chromium Controller. The surface of each bead is covered with tags, which contains three different oligos: a Unique Molecular Identifier (UMI), a 10X Barcode and a poly(d)-T-tail. Each 10X Barcode sequence is specific for each bead, thus it will mark an individual nucleus. Each tag has a specific UMI, which will individually identify each mRNA molecule from the nuclei. A total of 750,000 different barcodes is used as UMI. The 10x-Genomics v3.1 libraries were prepared as per the manufacturer’s instructions. Libraries were sequenced, aiming at a minimum coverage of 50,000 raw reads per cell, on an Illumina HiSeq

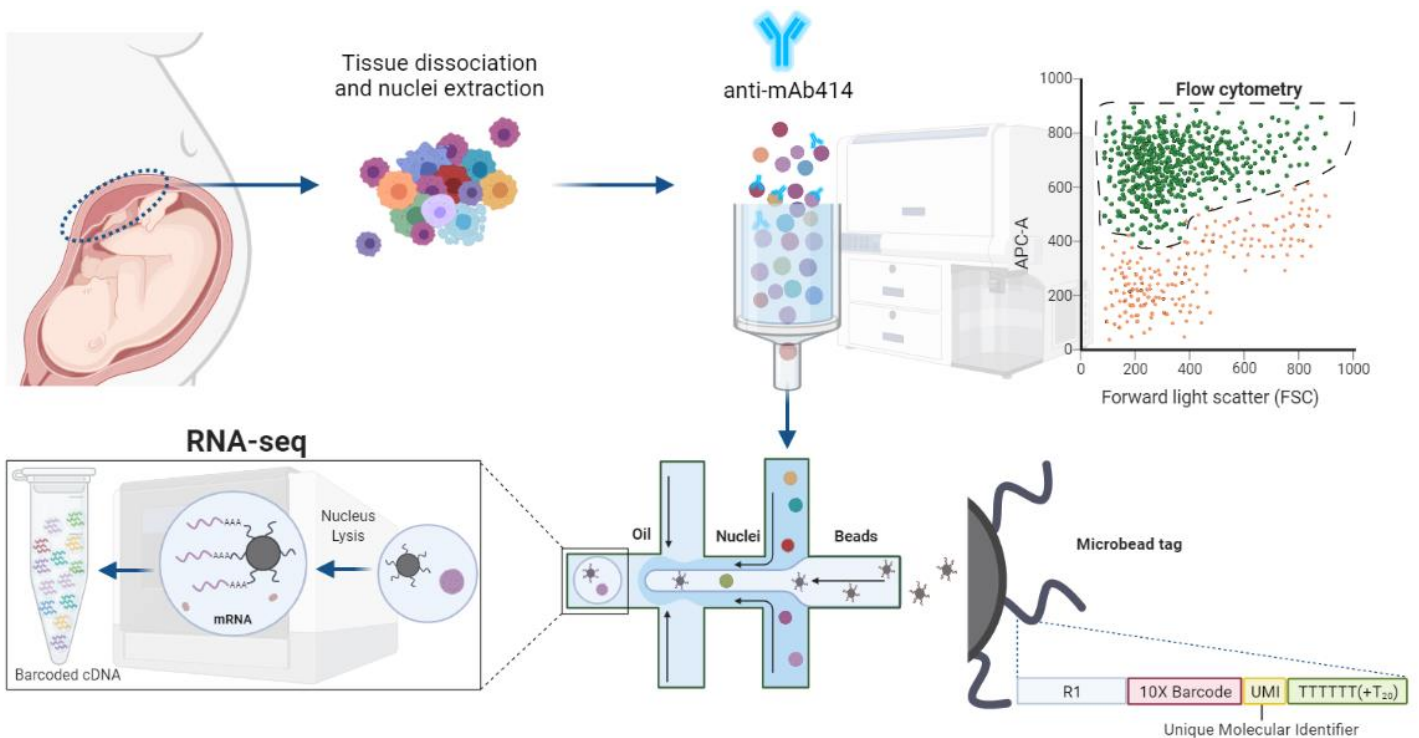


Figure 2.3: Single Nuclei scheme from tissue collection to barcoded cDNA. Placental tissue is dissociated until nuclei isolation. These nuclei are marked with anti-nuclear pore antibody (anti_mAb414) and sorted by flow cytometry. Each nucleus is inserted in an oil droplet with an individual microbead whose surface is covered in tags. Nucleus lysis of each oil drop releases mRNA which are bound to the microbead tag by the poly-A tail. Reverse retro-transcription produces barcoded cDNA to be sequenced.

4000.

3. Bioinformatic analysis

a. snRNA-seq alignment and Quality control

Droplet-based sequencing data were aligned and quantified using the Cell Ranger Single-Cell Software Suite (version 4.0, 10x Genomics) against the GRCh38 human reference genome provided by Cell Ranger. We counted reads mapping to introns as well as exons, as this results in a greater number of genes detected per nucleus, more nuclei passing quality control and better cell type identification (Bakken et al., 2018). Single-cell feature counts for every single library were produced and used for permissive quality control (QC) step using the Seurat package. Gene expression was determined by the number of UMI observed per gene. The percentage of mitochondrial and ribosomal RNA was determined through a percentage of either mitochondrial or ribosomal genes by the total gene counts of each nucleus. Only high-quality nuclei were retained using the following criteria: **1)** between 250 and 6000 detected genes per nuclei; **2)** percentage of mitochondrial RNA lower than 5%; **3)** percentage of ribosomal RNA lower than 7.5%; **4)** percentage of haemoglobin RNA lower than 3%. Doublets and/or multiplets were determined using the *'scDbfFinder'* function. Nuclei that passed these quality control standards were used for the downstream analysis. Normalization and regression against mitochondrial mapping percentage, cell cycle and RNA counts were performed using the function *'SCTransform'* using the 3000 most variable genes.

a. Clusterization

For each sample, counts were scaled and normalized using *'ScaleData'* and *'NormalizeData'*, respectively, with default settings using the 3000 most variable genes as input for all future analyses obtained through the *FindVariableFeatures* function from Seurat.

Several cluster resolutions were generated (res0.4, res0.6, res0.8, res1.0, res1.2) using the *'FindClusters'* function and Silhouette R package was used to determine which of the resolutions had the best score resolution. Finally, res0.4 was selected because it had the best Silhouette R score, and

all 21 obtained clusters have a balanced distribution of nuclei per sample. Visualization of the different cell clusters was performed using Uniform Manifold Approximation and Projections for Dimension Reduction (UMAP) algorithm implemented by Seurat *'runUMAP'* function using the first 20 principal components. Cell type of each cluster was determined by gene enrichment analysis using as reference placenta gene expression database (<https://placentacellenrich.gdcb.iastate.edu/>) generated using ref data from Suryawanshi et al., 2018 and Vento-Tormo et al., 2018. SingleR package was also used to label new cells from a test dataset based on similarity to the reference (Aran 2019); this allows the inspection of the confidence of the predicted labels across the dataset.

Comparison of cell composition between preeclampsia and control samples was assessed by T-test. For downstream analyses, trophoblast nuclei were merged to create two “mega-clusters”: SCT merged SCT_1, SCT_2, SCT_3, SCT_4, SCT_5, SCT_6, SCT_7 and SCT_8 clusters and Trophoblast merged EVT_s_1, EVT_s_2, EVT_s_3, SCT_EVT_s, VCT_s_1, VCT_s_2 clusters.

b. Identification of top differentially expressed genes

Pseudobulk aggregation method from Muscat R package has been performed to determine the differentially expressed genes (DEG). Aggregation methods are implemented to control for both zero-inflation and within-sample correlation, but are conservative in unbalanced situations (Crowell et al., 2020). This method is based on the aggregation of the RNA-seq data by each specific cluster, thus, mimicking RNA-bulk by cell type, similar to if the tissue has been separated by cell type through FACS and then RNA-seq has been performed in each cell type. This aggregation method accounts for the intrinsic cell composition variation and heterogeneity between the biological samples, aiming to decrease the false discovery rate on DEGs between conditions. DEGs were obtained through the *'pbDS'* function from the Muscat package under the *'DeSeq2'* method and under design (gene_expression ~ 0 + group_id) and the contrast matrix comparing the samples of interest. Several contrasts have been studied to determine DEGs at different levels: a) C-section vs. vaginal birth in PE-unaffected samples, b) PE-unaffected samples from C-section birth, only vs. PE-

affected samples, c) PE-unaffected samples from C-section and vaginal birth, together vs. PE-affected samples. Because no DEG was found with the comparison C-section vs. vaginal birth in PE-unaffected samples (data not shown), we next only considered the comparison: PE-unaffected samples from C-section and vaginal birth, together vs. PE-affected samples in the differential state analyses.

c. Gene Enrichment Analysis

Gene enrichment and ontology was performed using several online resources such as Enricher (<https://maayanlab.cloud/Enrichr/enrich>), String (<https://string-db.org/>).

d. Transcriptomic dynamics and RNA velocity

Gene activity is orchestrated by transcriptional regulation. Globally, when the transcription of a particular gene is induced, newly transcribed precursor mRNA (unspliced mRNA) is rapidly produced, following by the splicing process and the subsequent production of a mature, spliced, mRNA. When transcription is stopped due to gene repression, unspliced mRNA is no longer produced, and the amount of spliced mRNA decreases (**Figure 2.4**). Spliced (s) and unspliced (u) mRNA amounts for a dedicated gene can be retrieved from snRNA-seq data. La Manno et coll. showed that RNA velocity—the time derivative of the gene expression state—can be directly estimated by distinguishing between unspliced and spliced mRNAs (La Manno et al., 2018). A simple model for transcriptional dynamics can be determined by the balance of the transcription (α), splicing (β), and degradation (γ) rates. Unspliced (u) and spliced (s) mRNA abundance with respect of time (t) can be described by the following equations:

$$\frac{du(t)}{dt} = \alpha_k(t) - \beta u(t) \qquad \frac{ds(t)}{dt} = \beta u(t) - \gamma s(t)$$

When the transcription rate is constant, the unspliced and spliced forms abundance reach a plateau or “steady state”. According to the above model, when the transcription rate is constant, the

spliced and unspliced molecules can be constrained to a fixed-slope relationship, where $u=\gamma s$. Considering a line from (0,0) towards the steady-state nuclei where $u=\gamma s$, a regression line with a slope $k=\alpha/\beta$ denominated “steady state ratio” can be drawn. RNA velocity for a particular gene in a particular nucleus can then be described as the deviation of the nucleus towards the expected “steady-state ratio”, which equation is:

$$u(t) - \frac{\gamma}{\beta}s(t) \propto \frac{ds(t)}{dt}$$

The combination of velocities across genes can then be used to estimate and model the future state and fate of an individual cell. Off note, RNA velocity model assumes constant rates of splicing and degradation across cells for each gene. When considering nuclear mRNA instead of whole cell mRNAs, nuclear export replaces degradation. The assumptions such as constant degradation and nuclear export have not been conclusively verified, so this model may be limited. However, the existing RNA velocity model show promising results in mouse placenta snRNA-seq study (Marsh & Blelloch, 2020).

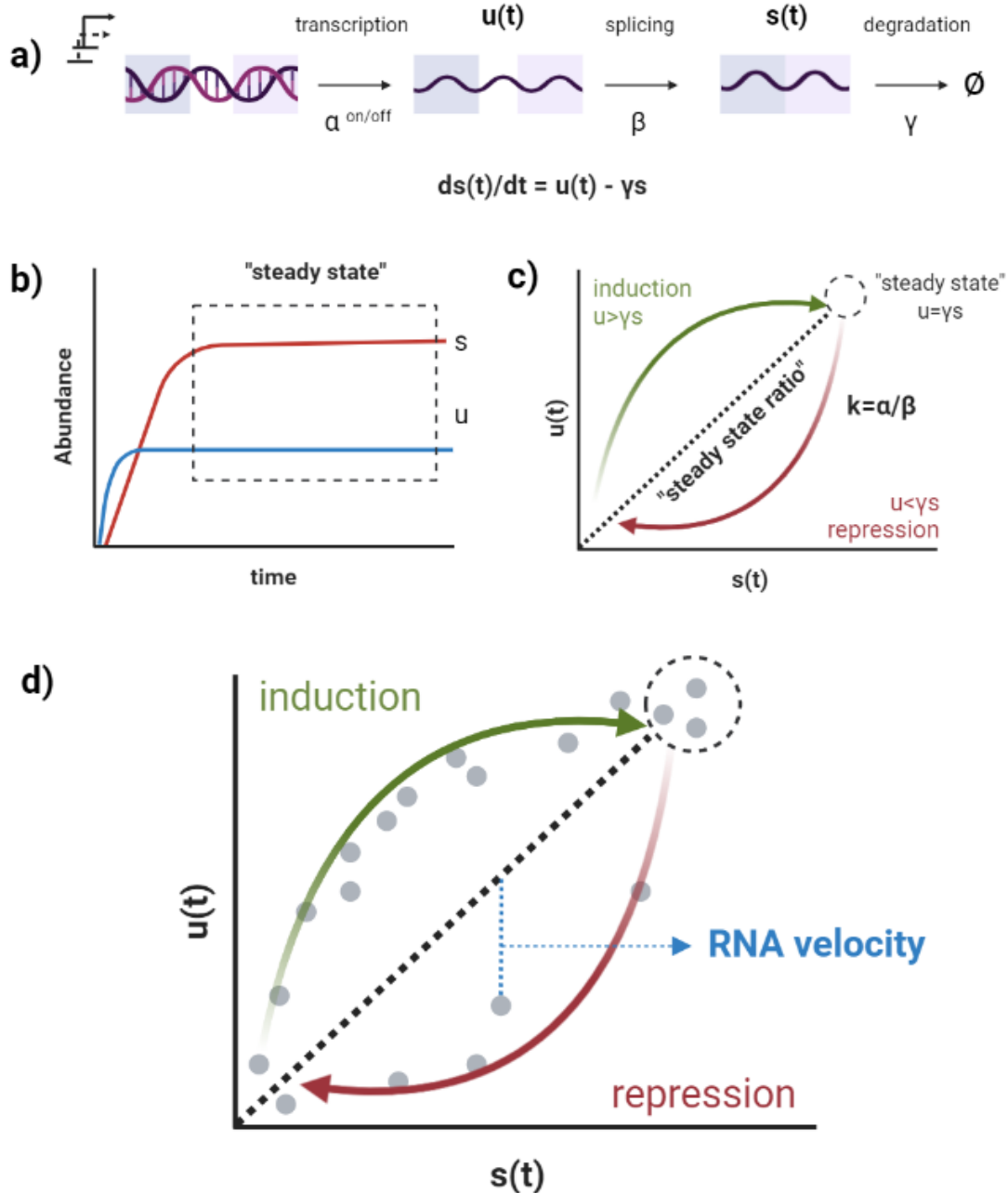


Figure 2.4: Scheme of RNA-velocity. **a) Velocity parameters.** Each gene is transcribed at a specific transcription rate (α) which depends on the cell state. Transcription generates unspliced mRNA at a specific time point ($u(t)$), which is spliced at a constant rate (β) to produce spliced ($s(t)$) forms. This spliced mRNA is degraded at a specific rate (γ). **b) Abundance trajectory example of spliced and unspliced forms.** Once transcription takes place, unspliced mRNA is created, following spliced mRNA. There is a point when both spliced and unspliced abundances reach a plateau or the so-called 'steady-state'. **c) The steady-state ratio is the line from the steady-state to (0,0) and which slope is equal to γ/β .** **d) RNA velocity of each individual nuclei (grey dots) for a specific gene is the deviation of the nuclei towards the modelled steady-state ratio.** Induction of transcription can be described as the increase of unspliced forms compared to spliced forms while repression of the transcription can be described as the reduction in the number of unspliced mRNAs compared to spliced mRNA.

scVelo

Spliced and unspliced mRNA counts were obtained using the scVelo Python package (<https://scvelo.org>). Data was pre-processed and normalized using the standard *'pp.filter_and_normalize'* function. To infer the future states of each nucleus, the velocity of each nucleus was calculated by performing the function *'tl.velocity'* under the *stochastic* method in PE-unaffected samples (from C-section and vaginal birth, together) and PE-affected samples. Top dynamical genes were selected by ranked spearman correlation.

We next ran a subset analysis on a total of 22,924 trophoblast nuclei from PE and 33,948 from control placentas coming from the clusters EVT_s_1, EVT_s_2, EVT_s_3, SCT_1, SCT_2, SCT_3, SCT_4, SCT_4, SCT_5, SCT_6, SCT_7, SCT_EVT_s, VCT_s_1 and VCT_s_2). Recalculation of spliced and unspliced mRNA abundance of 25,039 genes was performed using the *'tl.velocity'* under the dynamical mode. Full transcriptional dynamics were then computed using the *'scvelo.tl.recover_dynamic'* function which infers the transcription, splicing and degradation rate for a given gene in a given nucleus. Pseudotime, a function that estimates the root cells and the cells that have reached their final state, was also computed using *'tl.pseudotime'* function.

Results

Identification of major cell types in the human placenta

A total of 71,719 nuclei passed the quality control standard, ranging from 4664 to 8429 nuclei across the three placental sample groups (**Annex 2.1**). We next performed graph-based clustering of the data (UMAP) and used cluster-specific marker genes to automate cell type assignment based on the expression of previously reported marker genes of the early maternal-fetal interface in humans (Vento-Tormo et al., 2018). A total of 21 clusters were resolved by UMAP (**Figure 2.5**; nucleus abundance per cluster and per sample in **Supplemental table 2.2**). Automated annotation assigned these clusters in the following cell subpopulations, ranked from the most to the less abundant: trophoblasts (SCT, VTB, and EVT), structural cells (decidualized stromal cells, fetal endothelial cells and fibroblasts) and immune cells (Hofbauer cells and NK cells) (**Figure 2.5**; list of the 10 most significant markers per cluster in **Supplemental table 2.3**). Although most of the clusters are clearly resolved, this automated assignment failed to identify some clusters (e.g. mixed population of SCT and EVT) or identified a T Cells subset embedded in the trophoblast subpopulation. To further resolve these clusters, we constructed a heatmap with the unsupervised assignment scores across all cell-label combination using Single R (Aran et al., 2019) (**Figure 2.6**). This analysis identified that most of the captured nuclei are highly related to first trimester SCTs. Other cell types presenting high scores are EVT and VCTs, Fetal Endothelial cells (Endo (f)), decidual Stromal cells (dS), Hofbauer (HB) cells and, with lower scores, decidual macrophages. Off note, very few NK and T cells were identified with this reference set. Overall, our term placental villi dataset contains mostly SCT, that cannot be differentiated in subtypes using the first trimester reference dataset. To further explore the SCT heterogeneity, we compared gene signatures amid our 9 clusters of SCT. As illustrated in **Figure 2.7**, the number of overlaps between clusters is low. The most similar clusters, SCT_4 and SCT_2 only share 33 markers, suggesting a high functional heterogeneity of the SCT nuclei.

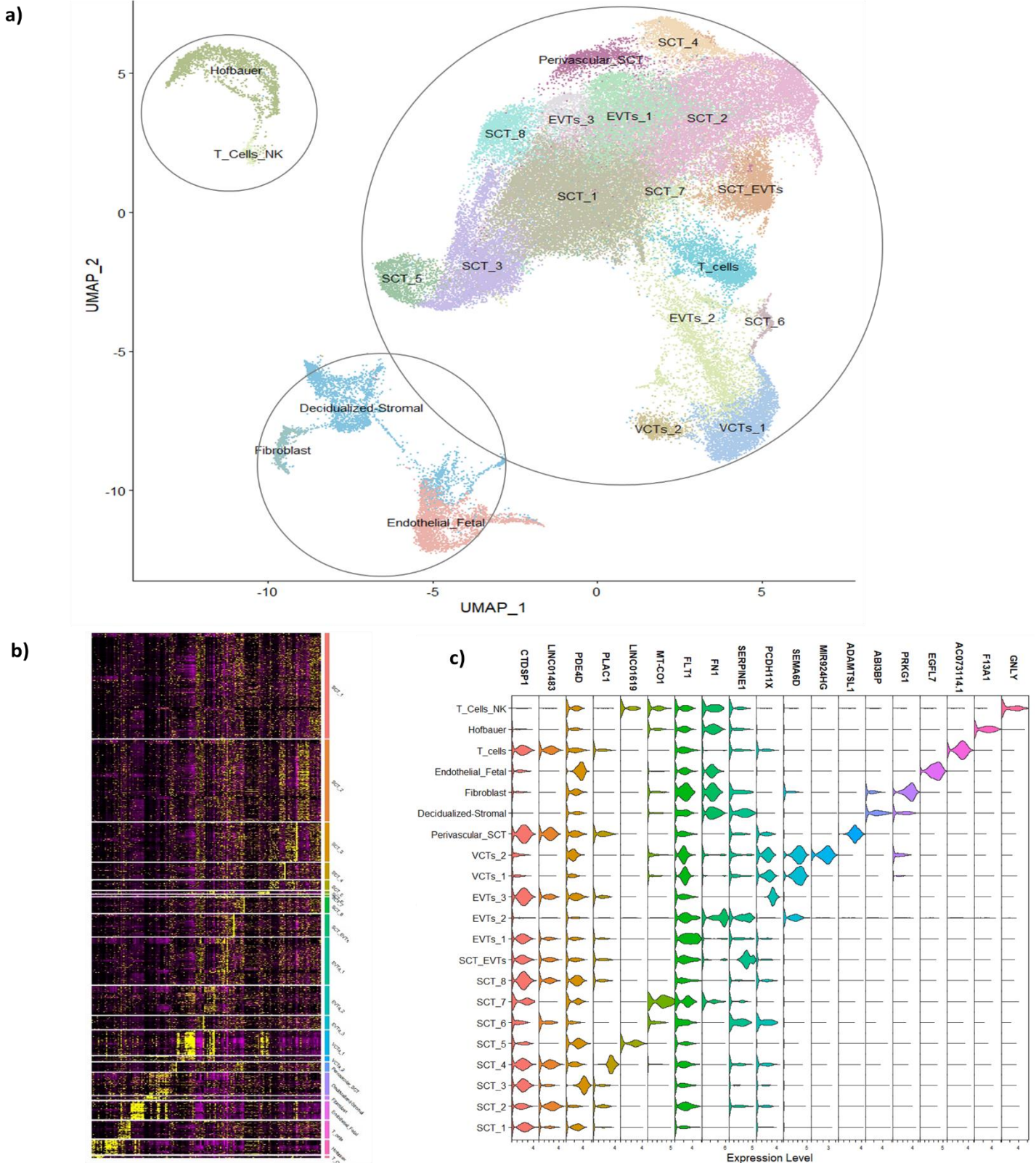


Figure 2.5: Identification of cell types in term placenta. **a)** Placental cell clusters from 10x Genomics snRNA-seq analysis visualized by UMAP with automated annotation. Top left: immune cell subsets composed of Hofbauer cells and other immune cells such as T Cells and NK cells; top right: trophoblast cell subsets composed of CTB, EVT and 7 distinct subclusters of SCT, the largest subpopulation captured. On the left bottom: structural cell subsets composed of decidualized stromal cells, fibroblasts and endothelial fetal cells. **b)** Heatmap of the top 10 markers per cluster **c)** Violin plots illustrating the signature genes of each cluster).



Figure 2.6: Heatmap of similarities between our clusters (Clusters) and the reference data from Tormo et al. 2017. The heatmap displays the scores for all nuclei (column) across all reference labels (line). Highest score is showed in bright yellow while lowest is dark blue (Scale on the top right).

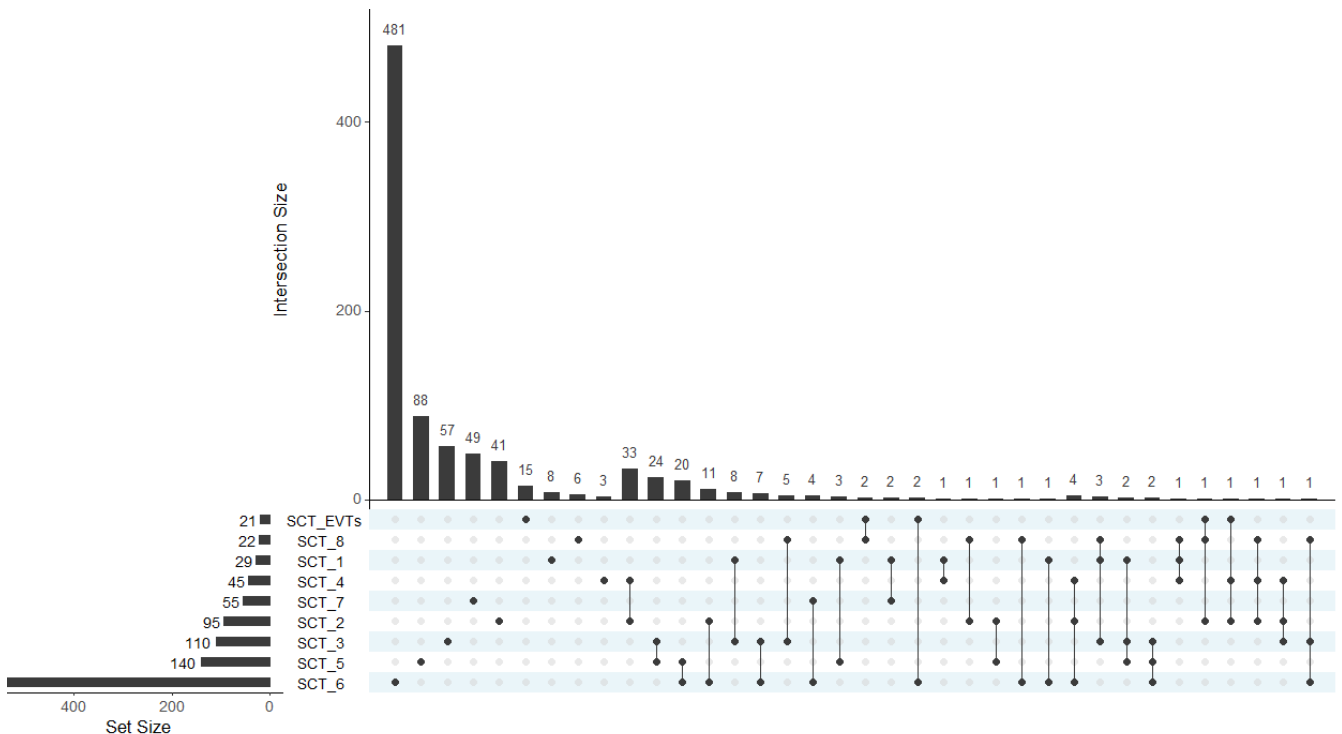


Figure 2.7: Upset plot of the syncytiotrophoblast clusters markers to determine common markers among clusters. Number of markers found in each cluster: SCT_1 (29 genes), SCT_2 (95 genes), SCT_3 (110 genes), SCT_4 (45 genes), SCT_5 (140 genes), SCT_6 (534 genes), SCT_7 (55 genes), SCT_EVTs (21 genes). As an example, if we look at SCT_6, the set size indicates the total of markers found for the cluster, the first dot indicates the markers found only in SCT_6 (482), the first intersection (the column 11) shows there are 20 markers in common between cluster SCT_6 and SCT_5, the following intersection shows there are 11 markers in common between SCT_6 and SCT_2.

Functional characterization of the SCT nuclei

Gene enrichment analysis was performed to determine the main pathways associated with each cluster's markers. The top cellular and molecular pathways per cluster are shown in **Figure 2.8**.

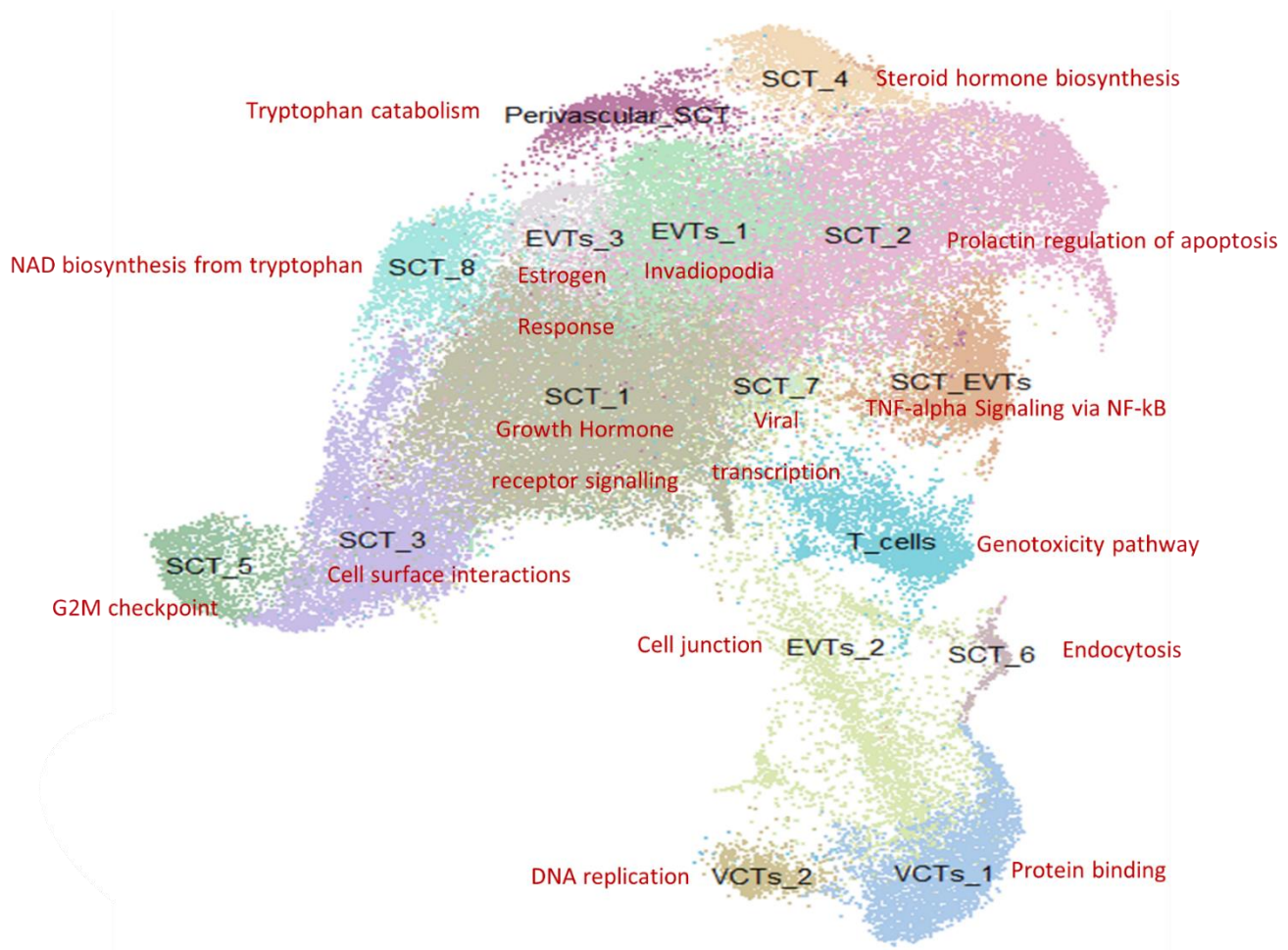


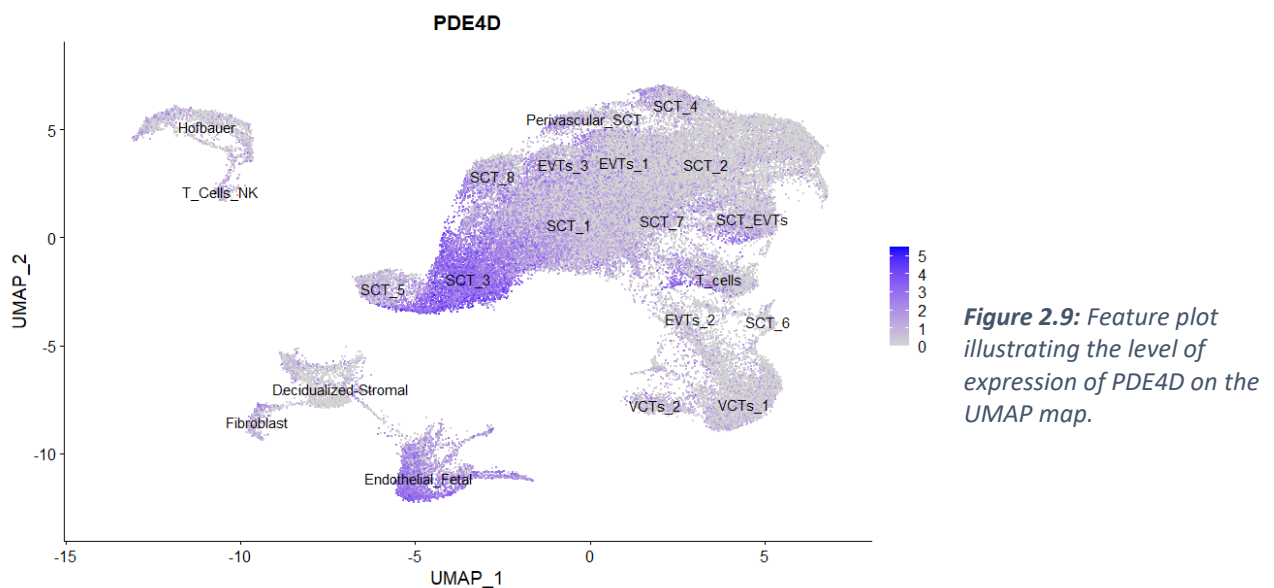
Figure 2.8: Top cellular functions (in red) enriched per cluster of cells (in black).

The largest SCT cluster, **SCT_1**, is composed of a total of 15,106 nuclei. A total of 29 markers were enriched in genes related to Neuroactive ligand-receptor interaction (KEGG 2021, p.val=0.038) and Growth Hormone Receptor synthesis and secretion (KEGG 2021 Human, p.val=0.0137). Some of the most known trophoblast lineages are highly expressed in this cluster: PAPP, CSH1, CSH2. These genes have been previously observed to be upregulated in the syncytiotrophoblast layer from 12 to 20 weeks of gestation, plateauing at term (Männik, Vaas, Rull, Teesalu, & Laan, 2012). Moreover, several pregnancy-specific glycoproteins (PSG6, PSG4, PSG1, PSG9) are observed to be enriched in

this cluster. These genes are early markers of syncytial differentiation and are implicated in immunoregulation, angiogenesis and antiplatelet functions (Camolotto et al., 2010).

SCT_2, the second largest syncytiotrophoblast cluster, is composed of 11,740 nuclei with a gene signature composed of 96 markers. The most enriched pathways are those related to prolactin induction of apoptosis (BioPlanet 2019, p.val=0.0247) and estrogen hormone biosynthesis (Reactome 2016, p.val=0.000225). Several studies have stated the importance of prolactin in trophoblast development. Prolactin is able to suppress cell death mechanisms induced by cytokine or hormone deprivation (Buckley & Buckley, 2000). In the placenta, prolactin is implicated in acting as a negative regulator of inflammatory pathways, leading to immunoregulatory activities under inflammatory scenarios (Olmos-Ortiz et al., 2019).

SCT_3, composed of 5,568 nuclei, has a total of 111 significant makers, but displays no significant enriched pathway. PDE4D is the main gene characterizing these cells (**Figure 2.9**). This gene is a ebay High levels of PDE4D activity may reduce fusion ability in trophoblast cells (Gerbaud, Taskén, & Pidoux, 2015).



SCT_4, composed of 2,368 nuclei, the 46 markers genes are enriched in Steroid hormone biosynthesis (KEGG 2021 Human, p.val = 0.02874), specifically estrogen (Reactome 2016, p.val=0.00005152) and estradiol biosynthesis (HumanCyc201, p.val=0.0000515). These cells are characterized by expressing **PLAC1** (**Figure 2.10**). PLAC-1 expression is increased in cytotrophoblast differentiating in syncytiotrophoblast and downregulated expression of this gene in primary cytotrophoblast attenuates spontaneous syncytialization (Chang et al., 2016).

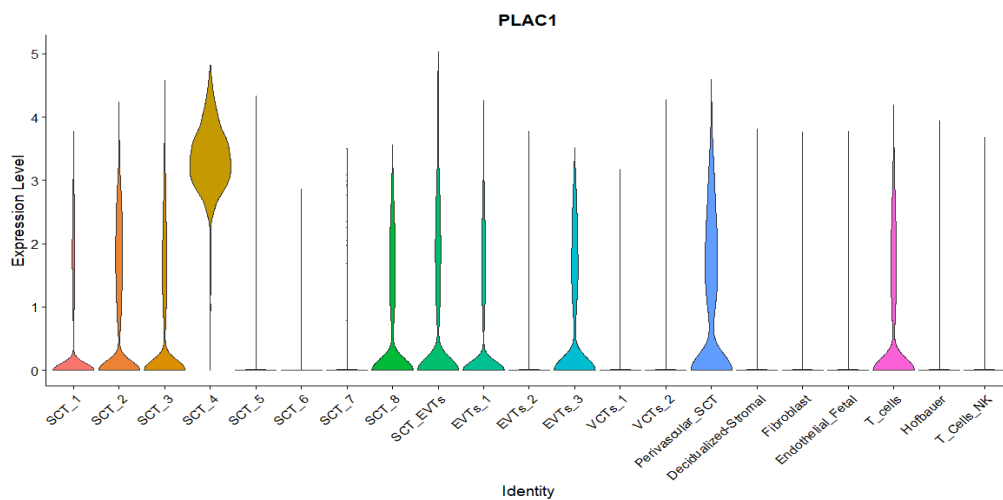


Figure 2.10: Violin plot illustrating the relative expression level of PLAC-1 per cluster.

SCT_5, formed by 1,360 nuclei, seems to be composed of damaged cells in which the G2M checkpoint has been activated (MSigDM Hallmark 2020, p.val=0.00001466). G2M checkpoint is an essential step in the progression of apoptosis, it blocks the proliferation and invasion of damaged cells to repair their DNA. These cells appear thus in a proapoptotic stage

SCT_6, composed of a total of 316 nuclei, has a total of 535 markers. The main enriched pathway observed in this cluster is endocytosis (KEGG 2021 Human, $p.val=4.612e-7$). Interestingly, although syncytin-1 (ERVW-1) is expressed in most of the placental cells, expression syncytin-2 (ERVFRD-1) appears restricted to this specific cluster (**Figure 2.11**). Syncytin-2 has a stronger role than syncytin-1 in trophoblast cell fusion, suggesting this cluster is formed by the immediate precursor cells that form the initiating syncytium (Vargas et al., 2009). These nuclei are still present in complete full cells and are the only syncytial cells found in single-cell RNAseq analysis (Roberts et

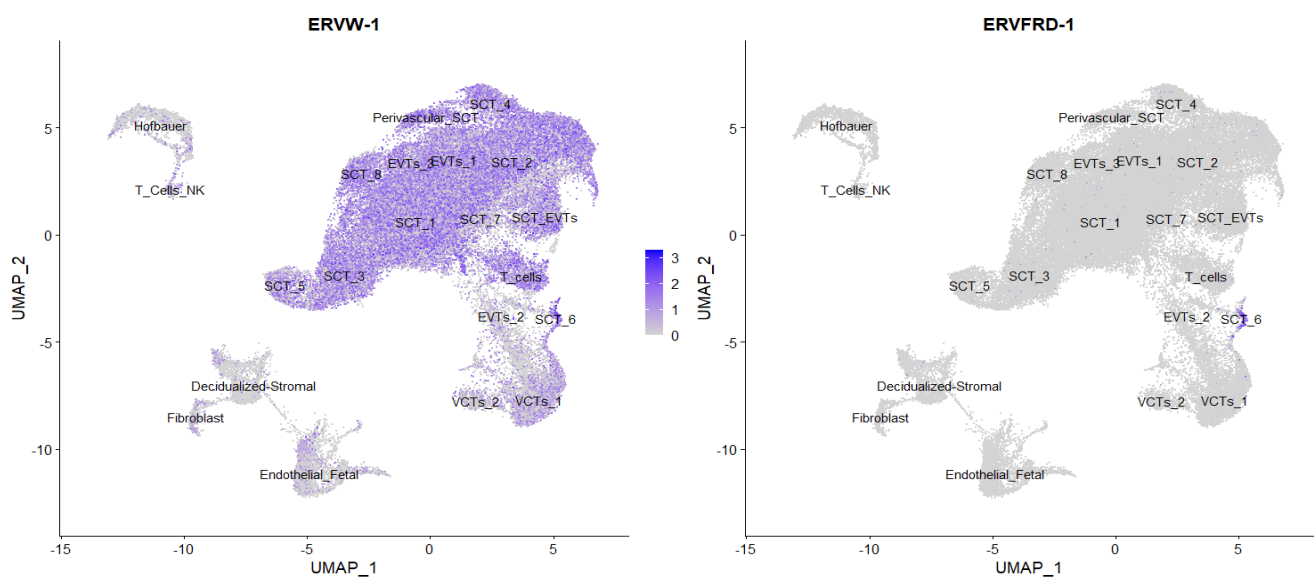


Figure 2.11: Feature plot illustrating the level of expression of Syncytin 1 (ERVW-1) and Syncytin 2 (ERVFRD-1) on the UMAP map

al., 2021).

SCT_7, composed of 230 nuclei, has 56 significant markers, enriched in genes related to ribosomal structure (KEGG 2021 Human, $p.val=2.623e-27$) and leukocyte transendothelial migration (KEGG 2021 Human, $p.val=0.00176$). More than 10 of these markers are mitochondrial genes, implicated in oxidoreductase activity and suggesting these cells are suffering oxidative phosphorylation.

SCT_8, composed of 2199 nuclei, displays 23 specific markers. This cluster shows cell signature of both SCT and Hofbauer cells, suggesting a mix of cells in the cluster. Enriched pathways are the ones of production of Nicotinamide adenine dinucleotide (NAD) using tryptophan (WikiPathway 2021 Human, p.val=0.00003221) and tryptophan metabolism (KEGG 2021 Human, p.val=0.0009683). Kynurenine 3-monooxygenase (KMO), kynureninase (KYNU), two enzymes necessary in the catabolism pathway of tryptophan, are markers of this subset of cells at a p.value of 5.84E-43 and 3.84E-76 respectively. Tryptophan catabolism is highly important in placenta development and trophoblast differentiation (Karahoda et al., 2020). Local depletion and the production of metabolites from tryptophan stimulate the creation of an immunosuppressive environment IDO (Munn et al., 1998).

SCT_EVTs is composed of 3,201 nuclei and described by a 21-gene signature. These markers are associated with TNF-alpha Signalling via NF-kB (MSigDB Hallmark 2020, p.value=0.000002181), suggesting this cluster is in a high inflammatory state. The main gene expressed in this subset is SERPINE-1 (**Figure 2.12**). SERPINE-1 or plasminogen activator inhibitor 1 (PAI1) is observed in the surface of the chorionic villi and the invasive front of the anchoring villi (Floridon et al., 2000). Therefore, this group of syncytial nuclei may be located at the tip of villi columns.

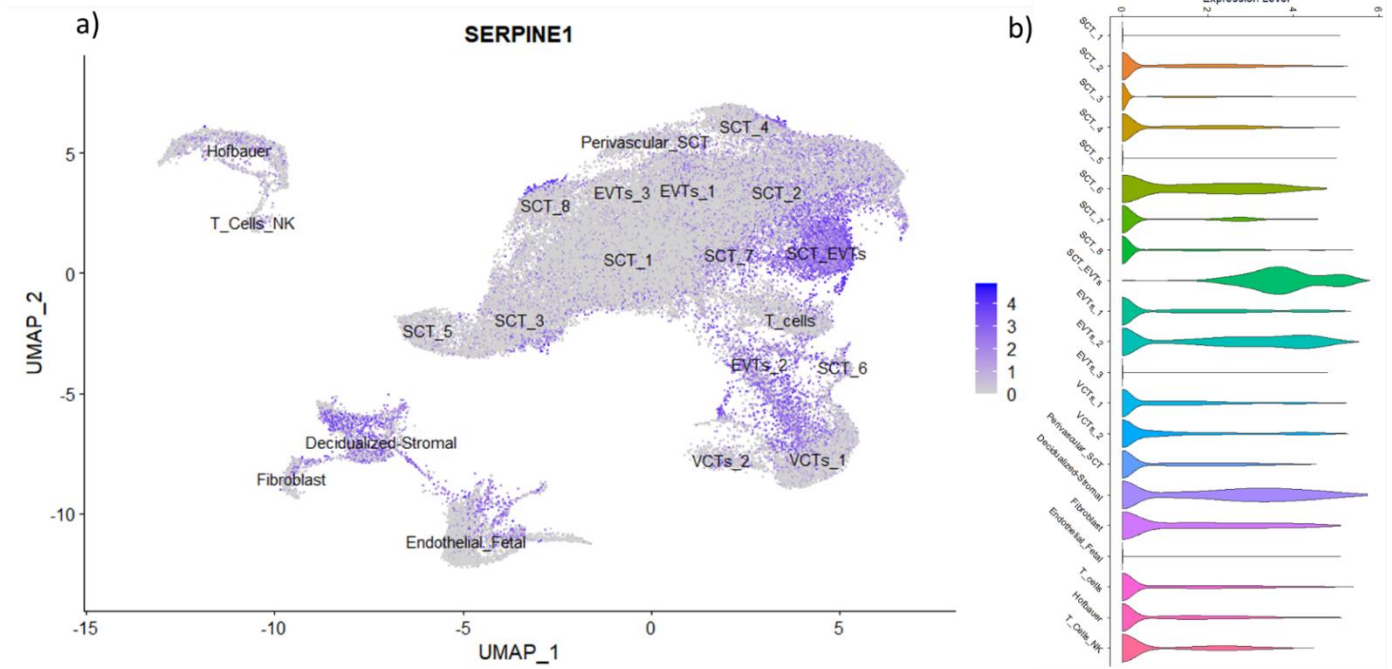


Figure 2.12: Localized expression of SERPINE-1 in the SCT_EVTs cluster. a) UMAP with an expression of SERPINE1. Purple (Gene expression=5), grey (Gene expression=0). **b)** Violin plot of the relative expression level of SERPINE1 per cluster

Analyses of the differences between Unaffected and PE-affected placentas

We have selected a UMAP resolution that gives a balanced distribution of nuclei across clusters. However, as mentioned in the methods section, we can regroup these clusters by specific populations — syncytiotrophoblasts, trophoblasts, stromal cells, endothelial cells, and macrophages — and compare their proportion between the healthy and the diseased placentas. As shown in **Figure 2.13**, and in **Annex 2.1**, the main cell type observed in the samples is syncytiotrophoblasts (60% of the total nuclei), followed by trophoblasts (20%), immune cells (10%), endothelial cells (10-5%) and stromal cells (2%). These proportions were very alike what we found with methylation analysis (see Chapter 1). Moreover, there are no significant difference in terms of population composition between the healthy and diseased placentas.

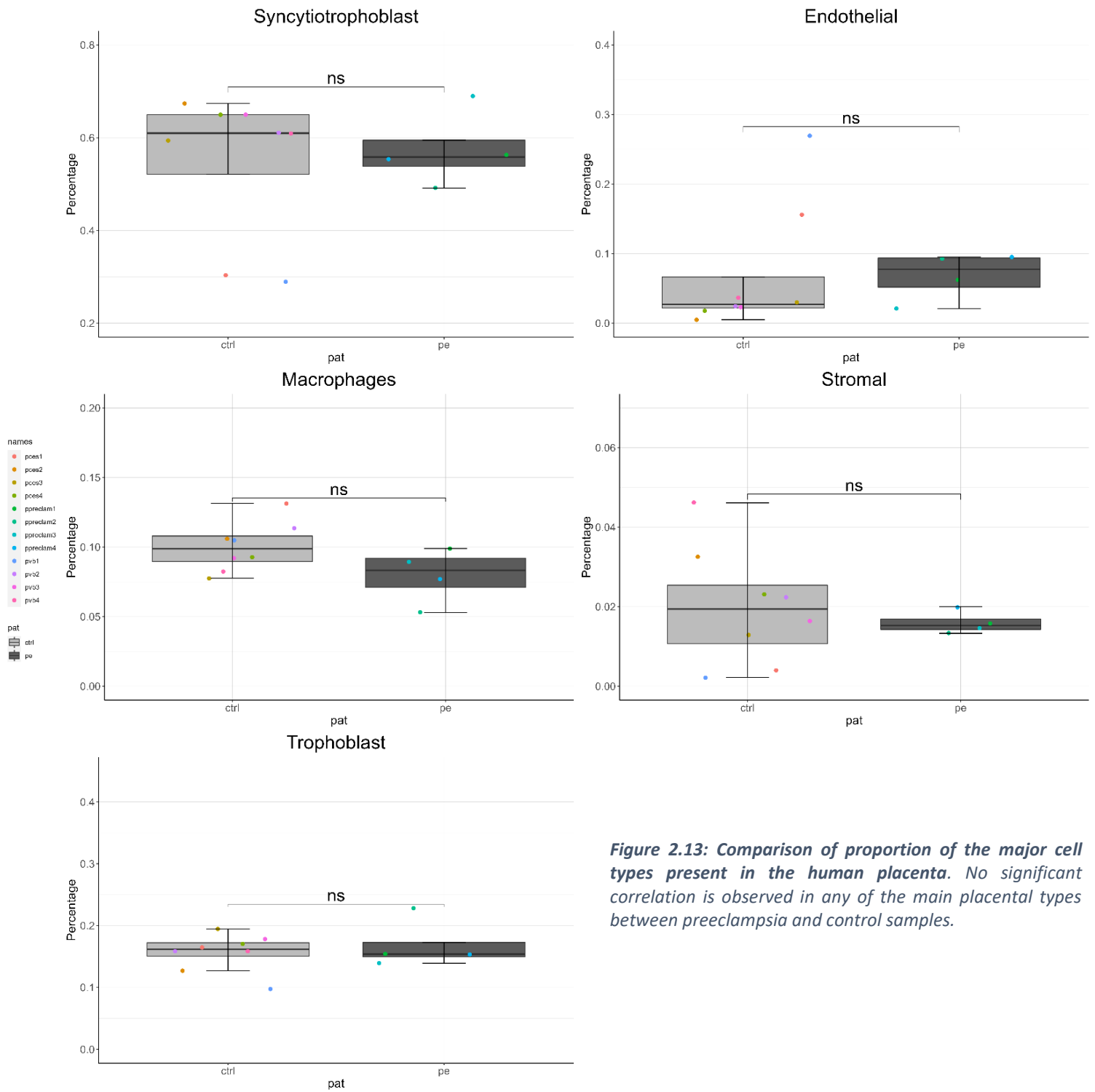


Figure 2.13: Comparison of proportion of the major cell types present in the human placenta. No significant correlation is observed in any of the main placental types between preeclampsia and control samples.

Differentially expressed genes between Unaffected and PE-affected placentas

One of the most interesting features of single nuclei/cell analysis is the ability to calculate differentially expressed genes (DEGs) in a cell-specific manner. When comparing Control vs PE placentas, we detected differentially expressed genes (DEGs) in all the cell clusters (**Figure 2.14**).

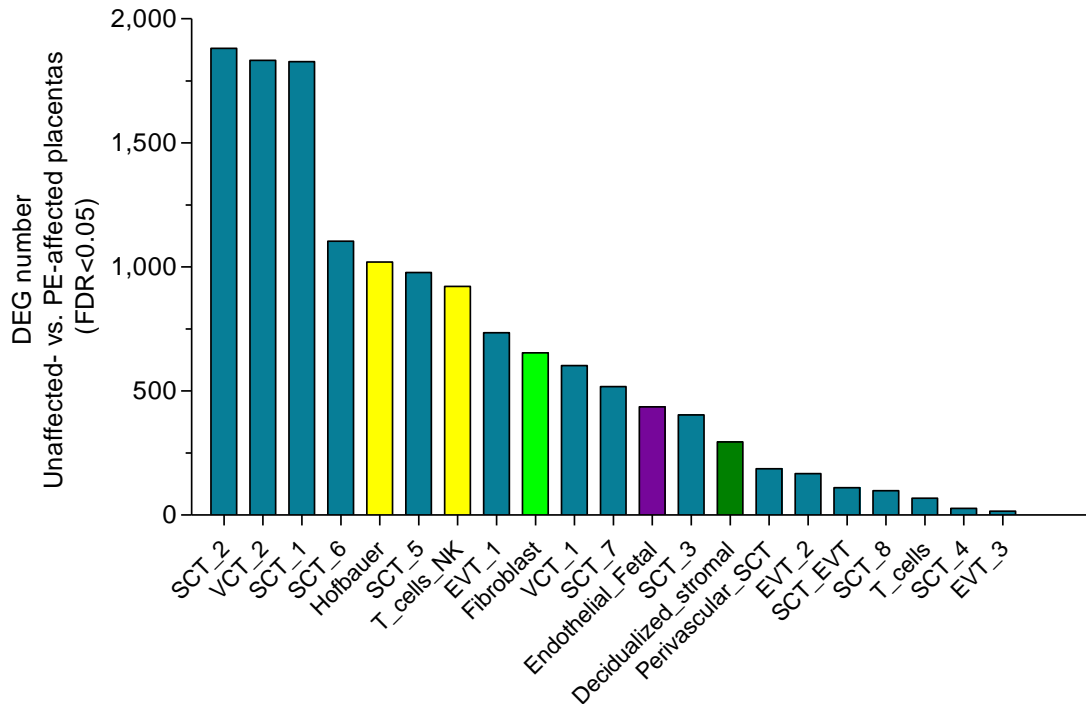


Figure 2.14: Barplot of the number of DEGs found in control vs PE by cell cluster. Trophoblast in blue, immune cells in yellow, stromal in green and endothelial in purple.

The cluster with the highest number of DEG is the SCTs_2, with 1,880 genes. These genes are enriched in pathways implicated in oxidative phosphorylation. The most significant DEGs in this cluster are two non-coding RNAs: AC079921.1 (logFC= -4.1088402 | p.adj.value= 7.1149E-55) and AC004160.1 (logFC= -2.98897069| p.adj.value= 2.926E-39), followed by an annotated gene DYNC2H1 (logFC= -3.03019722| p.adj.value= 5.0197E-31) and another lncRNA DIAPH2-AS1 (logFC= -3.03872301| p.adj.value=9.4108E-30) (**Annex 2.3**). DYNC2H1, 3-fold times upregulated in PE, is a central ATPase subunit of IFT dynein-2 complex and it is key in ciliogenesis and in the cytoplasmic the transport between the endoplasmic reticulum and the Golgi. Previous studies have observed a

defective cilium in preeclamptic trophoblastic cells, thus, failures in migration, invasion and tube formation are displayed under this pathology (Ritter et al., 2020).

The second cluster is VCTs_2, comprising 1,832 genes. This cluster is implicated in cell cycle and DNA replication (KEGG 2021 Human, $pval=2.529e-15$ and $2.141e-10$ respectively), suggesting these cells are implicated in either proliferation of VCTs or in the differentiation towards SCT. DEGs ontology analysis shows enrichment in oxidative phosphorylation and Reactive Oxygen Species pathways ($p.val= 0.000004659$ and 0.004108 respectively, MSigDM Hallmark 2020). The top most downregulated genes in PE-affected samples are STXBP6 ($\logFC= 7.54220211$ | $p.adj.value= 0.0001604$), HEG1 ($\logFC= 6.97550676$ | $p.adj.value= 0.00099647$), LAMA3 ($\logFC= 6.73865456$ | $p.adj.value= 0.00071521$) while the most upregulated are lncRNAs such as AC012050.1 ($\logFC=-8.08813991$ | $p.adj.value= 3.9227E-13$), AP000462.1 ($\logFC= -7.56878842$ | $p.adj.value= 2.0675E-12$) and SLC16A12-AS1 ($\logFC= -6.95692403$ | $p.adj.value= 1.6674E-12$) (**Annex 2.4**).

The third cluster is SCT_1, with a total of 1,828 DEGs, enriched in genes implicated in oxidative phosphorylation pathways (MSigDB Hallmark 2020, $p.val=1.591e-16$). The most significant DEG is DIAPH2-AS1 ($\logFC = -3.37433012$ | $p.val=3.059E-27$), which was also differentially expressed in SCT_2 with the pathology. This lncRNA has been previously described as a potential PE modulator in the trophoblast cell line HTR-8/SVneo, as part of a network involving HOXD8 and PAX3 (Feng et al., 2019). Increased expression of DIAPH2-AS1 affects the methylation state of PAX3, leading to its repression and the inhibition of the proliferative and invasive capacities of trophoblast cells. We could detect increased expression levels of DIAPH2-AS1 in PE. However, PAX3 or HOXD8 were not present in our dataset (**Figure 2.15**).

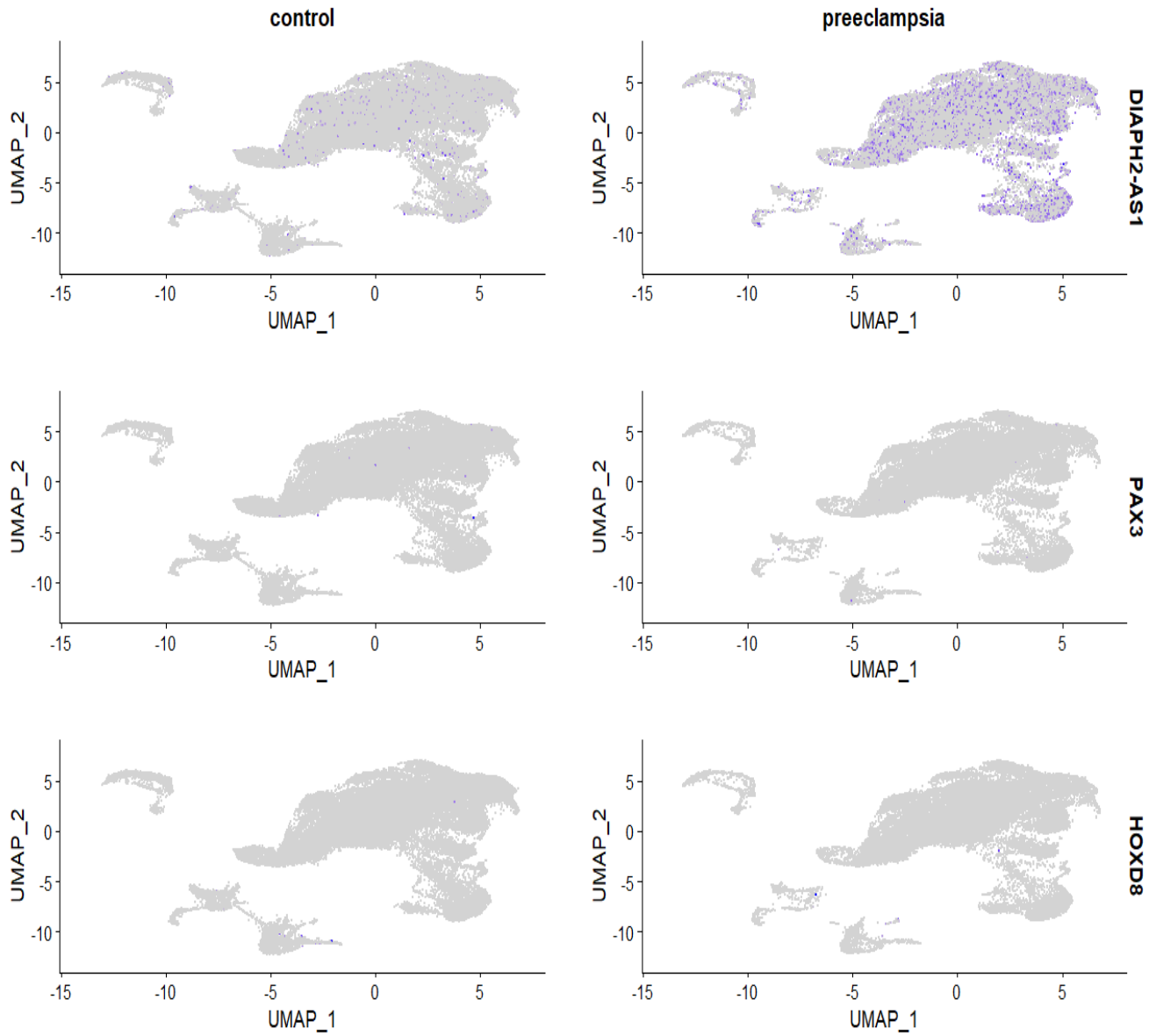


Figure 2.15: FeaturePlot of the expression of DIAPH2-AS1, PAX3 and HOXD8 in control and preeclampsia samples.

We next compared the lists of DEGs in these three clusters (**Figure 2.16**). DEGs common to the three clusters are enriched in genes involved in oxidative phosphorylation, Reactive Oxygen

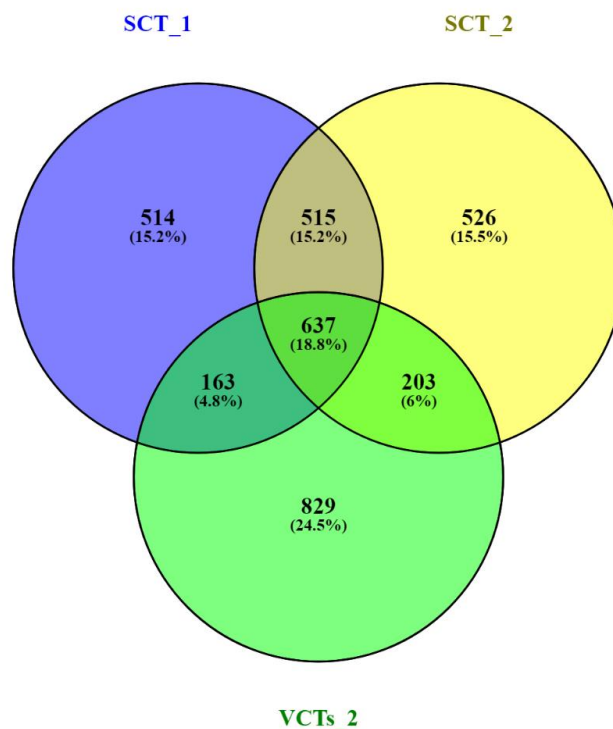


Figure 2.16: Venn diagram illustrating the common and unique DEGs in SCT_1, SCT_2 and VCT_2.

Species pathway and DNA repair (MSigDB Hallmark 2020, p.val= 2.593e-8, p.val= 0.0008640, p.val= 0.02199 respectively). VCT-specific DEG (829 genes) are enriched in genes involved in Angiotensin II signaling (Elsevier Pathway Collection, p.val=3.759e-7) and the MAPK cascade in angiogenesis (BioPlanet 2019, p.val=0.00005784). DEGs found only in SCT_2 (526 genes) showed no specific enrichment while DEGs found only in SCT_1 (514 genes) are enriched in oxidative stress (MSigDB Hallmark 2020, p.val=0.002) and ER associate protein degradation (Elsevier Pathway Collection, p.val=0.001). Gene enrichment analysis of every cell type is resumed in **Table 2.3**.

Table 2.3: Enriched pathways obtained after Muscat pseudobulk analysis on each individual cluster comparing all the control samples (C-section and Vaginal delivery) against PE.

Cell type	Enrichment Analysis on DEGs		
	Database	Enriched pathway	p-value
SCT_1	MSigDB Hallmark 2020	Oxidative phosphorylation	1.591e-16
SCT_2	MSigDB Hallmark 2020	Oxidative phosphorylation	8.793e-10
EVTs_1	Elsevier Pathway Collection	ER Associated Protein Degradation in Vesicular Transport	0.0004314
SCT_3	MSigDB Hallmark 2020	Unfolded Protein Response	0.02692
EVTs_2	MSigDB Hallmark 2020	Complement / mTORC1 Signalling	0.02586
VCTs_1	MSigDB Hallmark 2020	Myc Targets V1	0.0001219
SCT_ETVs	MSigDB Hallmark 2020	Unfolded Protein Response	0.003522
Decidualized_stromal	Elsevier Pathway Collection	Focal Junction Assembly	0.0009393
Endothelial_Fetal	MSigDB Hallmark 2020	P53	0.01262
T_cells	MSigDB Hallmark 2020	Mitotic spindle	0.0005816
SCT_4	KEGG 2021 Human	JAK-STAT signaling pathway	0.00005396
SCT_8	MSigDB Hallmark 2020	TGF-beta Signaling	0.02883
Hofbauer	MSigDB Hallmark 2020	Oxidative phosphorylation	0.00003217
EVTs_3	MSigDB Hallmark 2020	mTORC1 Signaling	0.008366
SCT_5	MSigDB Hallmark 2020	Oxidative Phosphorylation	0.000001704
Perivascular	MSigDB Hallmark 2020	Hypoxia	0.002727
VCTs_2	MSigDB Hallmark 2020	Oxidative Phosphorylation	0.000004659
Fibroblast	MSigDB Hallmark 2020	Protein Secretion	0.001162
T_cells_NK	MSigDB Hallmark 2020	Androgen Response	6.456e-7
SCT_6	MSigDB Hallmark 2020	TGF-beta Signaling	0.0006544
SCT_7	MSigDB Hallmark 2020	PI3K/AKT/mTOR Signaling	0.005968

The only common DEG to all 21 clusters is Tissue Factor Pathway Inhibitor 2 (TFPI-2). The level of TFPI-2 mRNA is increased 2-4-fold in samples affected by PE compared to unaffected samples (**Figure 2.17**). TFPI-2 or Placental Protein 5 (PP5) inhibits the degradation of the extracellular matrix by inhibiting plasmin, trypsin, chymotrypsin, cathepsin G, and plasma kallikrein. This gene has been implicated in the attenuation of trophoblast invasion and proliferation in PE-affected placentas (Karasz et al., 2019; Zheng et al., 2020)

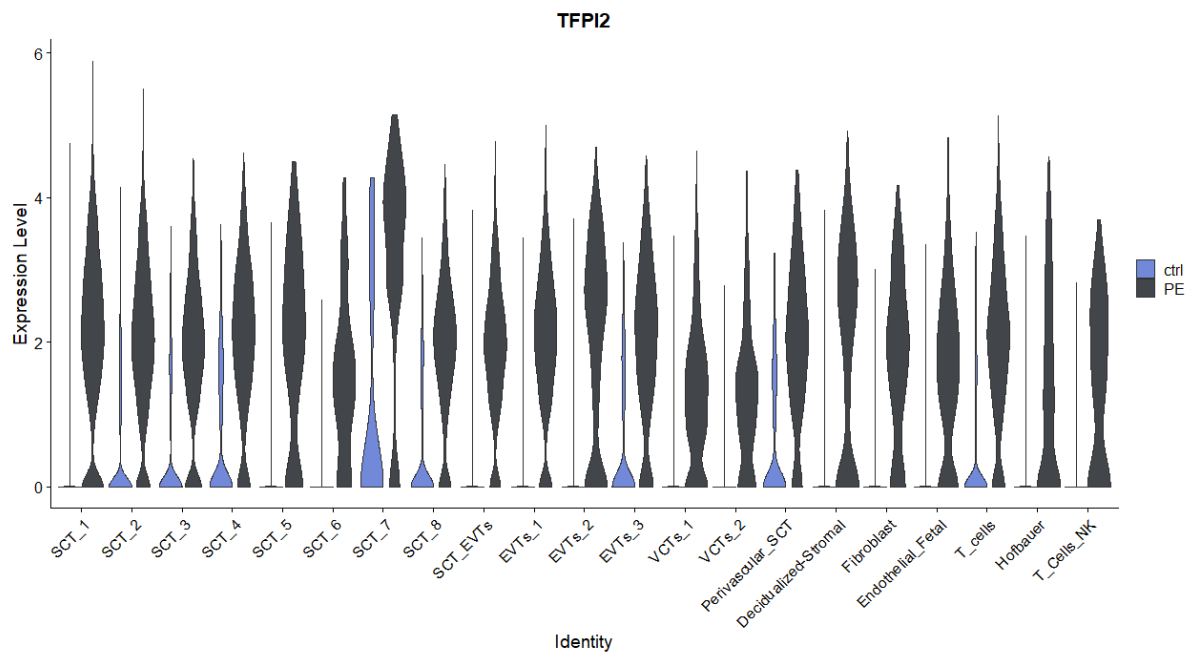


Figure 2.17: Expression of TFPI-2 by cell cluster in control (blue) and preeclampsia (grey) by cell cluster.

As a side note, expression of already known genes implicated in PE can be observed to be dysregulated in most of the cell types, such as the case of PAPP A2, FLT1 or KISS1. However, other well-known genes related to the pathology are differentially expressed in specific cellular subtypes, as observed in PGF expression limited to the SCT subtypes or the case of BMP7, limited to the villous cytotrophoblast (**Figure 2.18**).

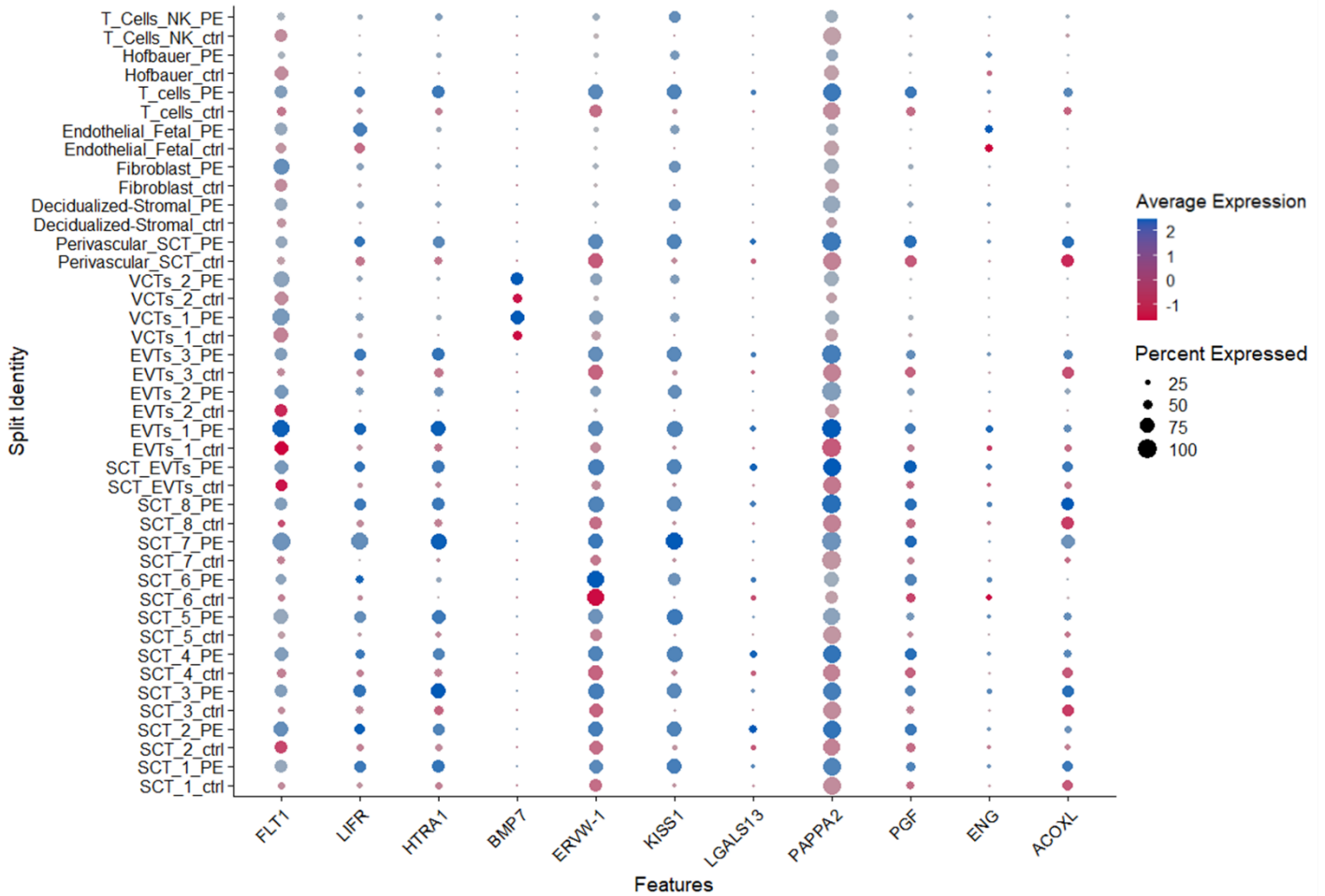


Figure 2.18: Common genes associated with PE are differentially expressed within the placental types. Average expression is calculated by the relative expression of the cells in each cluster against all the other cells. Diameter of the dot represents the percentage of nuclei within the cluster expressing the gene.

Transcriptomic Dynamics

We next performed RNA velocity using scVelo to produce vectors representing both the direction and speed of cellular dynamics (Bergen, Soldatov, Kharchenko, & Theis, 2021). We focussed our analysis on the trophoblasts, because they are the prevalent cell population and display the higher number of DEG. We first extracted and analysed separately the reads mapped on exonic and intronic regions. As expected, most of the captured mRNA in our snRNA-seq dataset are unspliced (72-74%) (**Figure 2.19**). Globally, no difference of spliced and unspliced proportions was observed between PE-affected and unaffected placentas.

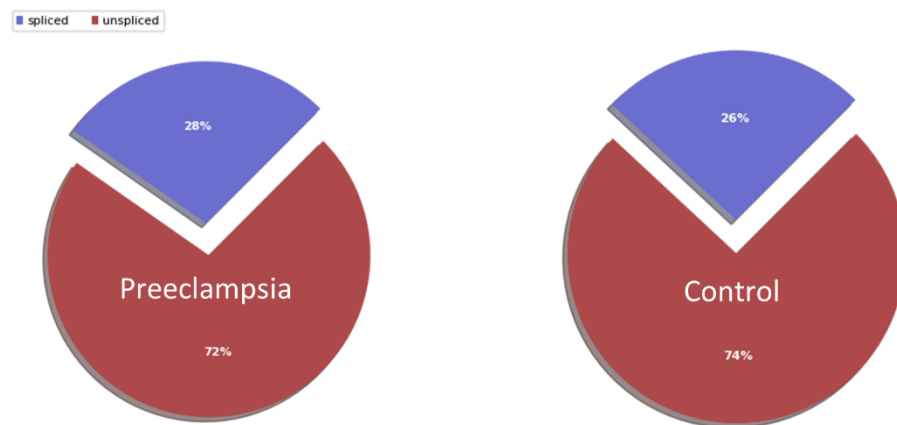


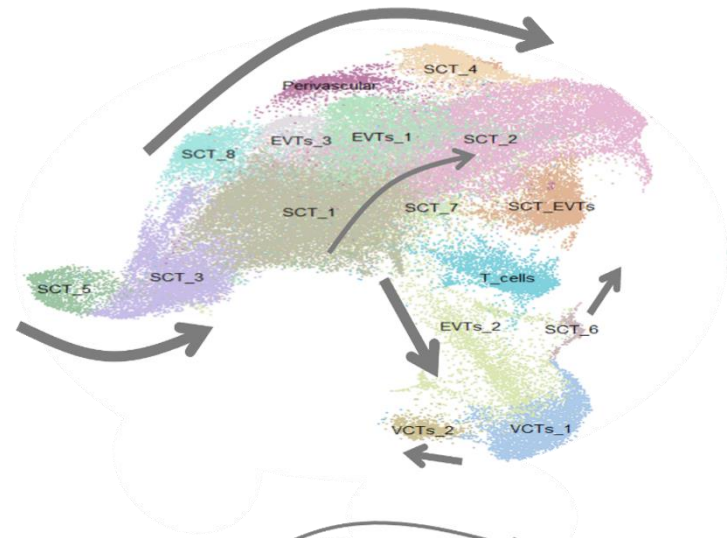
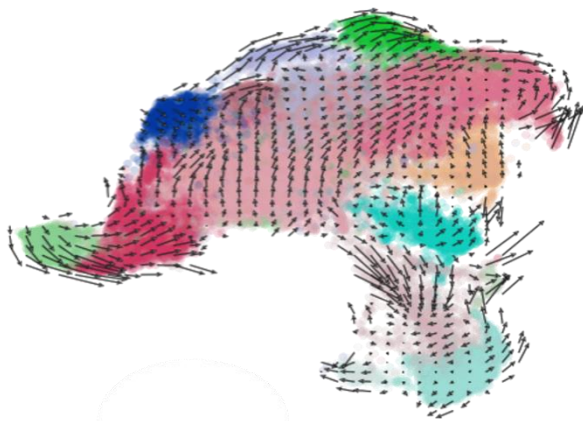
Figure 2.19: Proportions of splicing and unspliced mRNA in total (top). Preeclampsia on the left and Control on the right.

Different transcriptional dynamics in Unaffected vs. PE-affected placentas

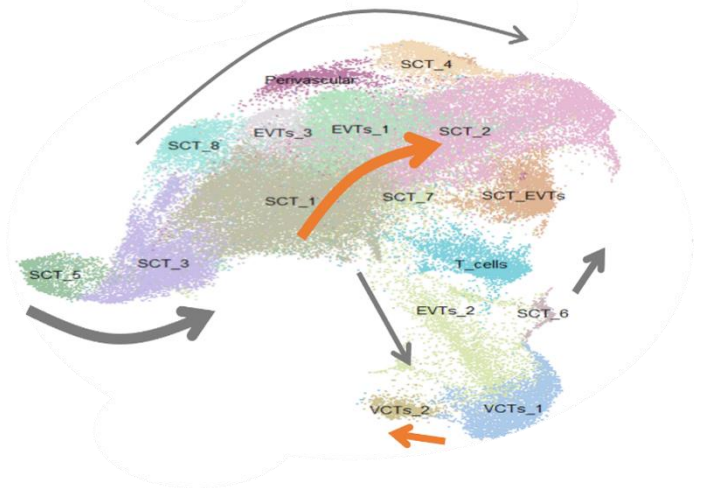
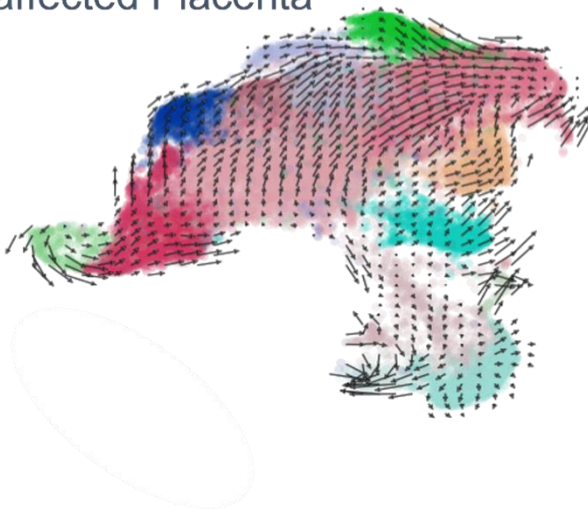
In the scVelo visualization, each nucleus is identified by an arrow representing the inferred direction and rate of cellular change projected in UMAP space. Length of the arrow represents the difference from an inferred steady-state ratio. Thus, long arrows correspond to high gene expression changes, meaning they are undergoing rapid differentiation. By contrast, short arrows can be intuitively associated with homeostasis.

In unaffected placentas, RNA velocity showed, in one hand, a strong directional flow from the edge toward the upper right and few moves in the centre, i.e., the largest SCT clusters (**Figure 2.20**). The SCT₅ and SCT₃ clusters also display strong RNA dynamics. In the other hand, in the lower right edge depicting VCT, velocity is higher in VCT₂ —i.e., the dividing VCT— and in SCT₆ —the fusing trophoblasts—, whereas VCT₁s are essentially homeostatic. In PE-affected placentas, RNA velocity increased in the largest SCT clusters and pointed toward the upper right, while the edges displayed shorter arrows as compared to unaffected-placenta. Also, velocity increased in VCTs, with a faster dynamic in the dividing VCTs and in a less extent, in the not dividing ones.

Control Placenta



PE-affected Placenta



To determine the root cells (progenitor cells) and the end points (differentiated cells), pseudo-time analysis was performed (**Figure 2.20**). Root cells (purple) in both unaffected and PE-affected placentas are located as expected, in the lower right edge of the map corresponding to VCTs (VCT_1 and VCT_2) and EVT_2. However, VCT_1 nuclei appear less mature in PE-affected than in unaffected placentas. Also, SCTs are mapped to earlier pseudotime in PE-affected than in unaffected placentas.

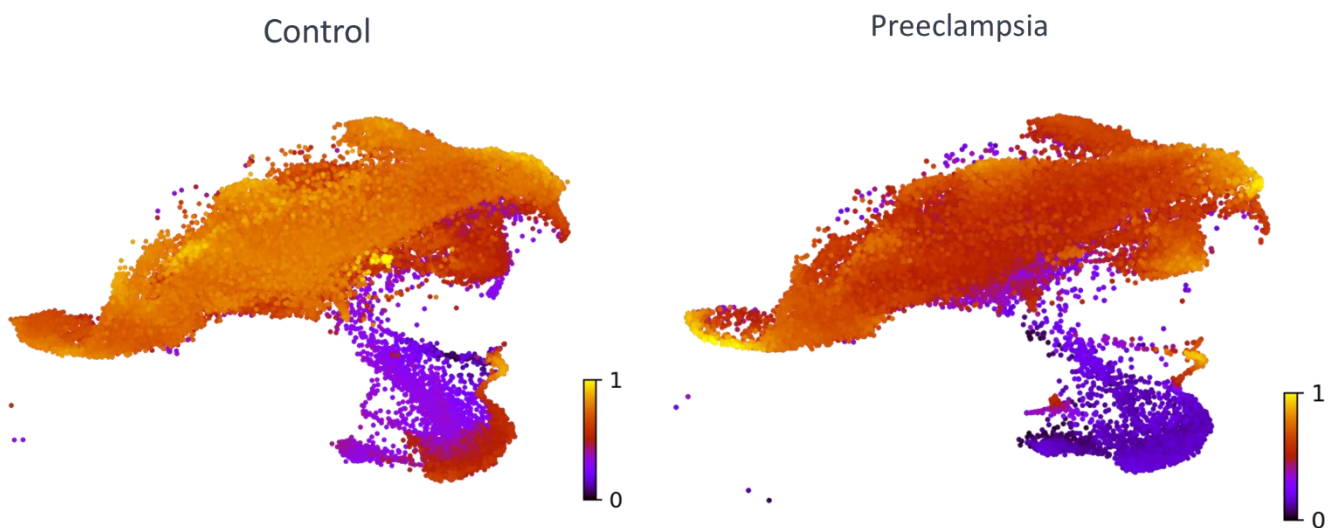


Figure 2.21: Latent time, from 0 to 1, 0 (purple) represents the root cell and 1 (yellow) represents to differentiated cells.

Discussion

In summary, preliminary analyses of our late-term placental snRNA-seq dataset revealed 1) distinct subpopulations of SCTs with specific functional identity, 2) that PE is associated with changes in transcriptional profiles linked to oxidative phosphorylation, mostly in SCTs and the subpopulation of dividing VCTs, and 3) that, globally, RNA dynamics are different in unaffected vs. PE-affected placentas.

To the best of our knowledge, the current study represents the most comprehensive single-cell analysis of human late-term placenta, to date. Transcriptional profile of 71k individual nuclei from 12 placentas were captured, while previous studies reported 19K and 20K individual captured cells from 7 and 6 late-term placentas, respectively (Pique-Regi et al., 2019; Tsang et al., 2017). Sixty percent of the total captured nuclei were labelled as syncytiotrophoblast, followed by 20% of nuclei identified as trophoblast, 10% as Macrophages, 10-5% as Endothelial cells and 2% as Stromal cells. These cell proportions are very similar to those predicted by the analysis of placental DNAm patterns (see Chapter 1), strongly supporting that SCT is the main cell type in late-term placentas. Stereological analyses of full-term placenta found that 90% of nuclei are located within the syncytium (Mayhew & Simpson, 1994; R. A. Simpson et al., 1992). Histological characterization of term placentas also described increased numbers of SCT and decreased numbers of VCT, while fetal capillaries increase in size and an increased oxygen diffusion capacity is observed as compared to earlier term (Turowski & Vogel, 2018).

With the resolution that best represents the overall topology of our dataset, 21 clusters were identified in the UMAP projection and nine of them were classified as SCTs. However, minimal gene marker signatures were shared across these 9 clusters, suggesting high diverse functionality across nuclei sharing the same cell identity. Gene enrichment analysis revealed that each cluster was committed to a specific function. Indeed, we were able to find SCT subclusters dedicated to steroidogenesis, prolactin pathways, tryptophan metabolism, invasion, and viral transcription among

others. These results raise several questions regarding the syncytial architecture and syncytial nuclei location within this layer. Two main architectures can be speculated: a) nuclear patches or compartments of nuclei with the same functionality or b) independency of each nucleus, stochastically embedded in the syncytial layer. Interestingly, a snRNA-seq study on syncytial skeletal muscle cells described the myonuclei transcriptional heterogeneity and their functional compartmentalisation along the myofiber, creating a regional transcription architecture (Kim et al., 2020). This opens the possibility that SCT nuclei exhibit the same behavior. To the best of our knowledge, no previous study has fully addressed the question of functional heterogeneity in the placental syncytial nuclei. One study has hypothesized transcriptional activity differences after observation of morphological nuclear variance between the young and the old damaged nuclei located in the syncytial knots (Fogarty, Ferguson-Smith, & Burton, 2013). Our results support the hypothesis that nuclei within placenta syncytium possess distinct transcriptional profiles that regulate placenta biology.

DEGs between unaffected and PE-affected samples were identified at the cell-type level. We observed a higher DEG number in SCTs and VCTs clusters than in the other cell types, suggesting these cell types are the most sensitive to the preeclamptic environment. Oxidative phosphorylation, inflammation and endoplasmic reticulum pathways are the most enriched pathways, illustrating the placental oxidative stress in PE-affected samples. The three clusters with the most abundant DEGs, i.e. SCT_1, SCT_2 and VCTs_2, share a total of 628 DEGs enriched genes involved in oxidative phosphorylation. These results are in line with previous studies showing that PE is associated with a dysfunctional placenta, characterized by increased oxidative stress and the trigger of the unfolded protein response (Burton & Jauniaux, 2004; Yung et al., 2019). Increased stress can, in turn, induce apoptosis in the syncytia and activate inflammatory pathways (Mukherjee et al., 2021). Off note, we also found numerous dysregulated non-coding RNAs in PE-affected placentas; this is in line with the data we reviewed in our publication in Annex 5 on the role of ncRNAs in placental development and pathology (Apicella, Ruano, Méhats, Miralles, & Vaiman, 2019).

Interestingly, a single gene — TFPI2 (Tissue Factor Placenta Inhibitor 2)— was identified as a DEG common to all clusters, with its expression increased 2-4 times in placentas affected by PE compared to unaffected samples. TFPI-2, a.k.a. Placental Protein (PP5) is a protease inhibitor. Its expression has been previously reported to be upregulated in serum and placenta of PE patients (Karaszi et al., 2019). Although the trophoblast is the main source of this protein, expression of TFPI-2 expression from perivascular and endothelial cells contribute to its expression in the maternal circulation (Karaszi et al., 2019). TFPI2 downregulation in the trophoblastic HTR8/Svneo cell line increased the cell invasion and the expression of MMP2 and MMP9, suggesting that TFPI2 might control trophoblast invasion (Zheng et al., 2020).

We also evaluated RNA velocity in trophoblasts to gain insight into future states of the cell. We found changes in the dynamics and the direction of gene expression between PE-affected and unaffected placentas. Here again, the two largest syncytiotrophoblast clusters (SCT_1 and SCT_2) and the dividing VCT_2 present the most striking differences, with higher dynamics in PE as compared to healthy placentas. Although the genes behind these differences have not yet been formally identified, we can speculate that these differences are driven by oxidative stress-related genes.

Developmental trajectory of each nucleus was also inferred from our snRNA-seq dataset by pseudotime analysis. According to our dataset, progenitor-like cells are clustered with the VCTs. The exact nature of these progenitor-like cells remains to be explored. In particular, their relation with Trophoblast Stem Cells (TSC) is unclear; TSCs have not been yet able to be isolated from third trimester placenta (Knöfler et al., 2019). However, PE-affected VCTs appear less mature than healthy VCTs, with higher abundance of progenitor-like cells. This data can be explained by two main hypotheses:

1. **Gestational Age differences:** PE-affected placentas analysed in our study are about 2 to 4 weeks younger than unaffected samples and the proliferative activity of VCT declines in full-term placentas.
2. **Syncytial dysregulation:** Some studies suggest a general immaturity of the syncytiotrophoblast layer in PE due to its decreased metabolic activity, decreased levels of hPL and the secretion by the pathological syncytia microvesicles with high content of glycogen (Redline & Patterson, 1995; Roland et al., 2016). Other studies pinpoint that placenta syncytiotrophoblast suffers premature ageing, with increased senescence and the shortening of telomere length (Devisme et al., 2013; Goldman-Wohl & Yagel, 2014; Sankar, Bhanu, Ramalingam, Kiran, & Ramakrishna, 2013). Also, placental pathologies such as IUGR are associated with distal villous immaturity (DVI), in which placentas show both mature and immature villi, collagenous villous stroma and a thickened later of VCTs with very few SCT membrane (Redline, 2012).

Limitations: RNA velocity Issues

RNA velocity is a computational method still under development and presents several pitfalls in its current form. Considering the mathematical model (Bergen et al., 2021):

- a. The accepted steady-state assumption used to estimate velocity vectors is deterministic while transcriptomics are dynamic processes acting in a heterogeneous population of cells. Assumptions accepted in the model cannot describe the transcriptomic dynamics, especially those genes which are upregulated or downregulated at the beginning or an end of a process and cannot reach a “steady-state”.
- b. It is based on accurate quantification abundances, however intronic reads on RNAseq are noisy approximations of nascent transcription.

Moreover, RNA velocity analysis was developed for single-cell RNA-seq, there are not yet studies comparing trajectory inference from nuclear data vs. cytoplasmic data, thus, precautions about our results regarding this part should be considered. Thus, although we see different transcriptomic dynamics between unaffected and PE-affected placentas, this should be taken cautiously and just as a grasp of potential molecular changes in the placenta. Further analysis on specific genes implicated in the lineage switch might also be performed to determine the topmost dynamical genes in the differentiation process from VCT towards EVT_s and SCT_s.

In conclusion, our snRNA-seq analysis revealed the transcriptomic heterogeneity of the syncytiotrophoblast layer in healthy and pathological placentas. Although these results are compelling, experimental validation, such as immunohistochemistry or RNA in situ hybridization (FISH) experiments are needed to better understand the full SCT transcriptomic heterogeneity and spatiality in the placenta. These experiments will allow the determination of specific nuclei location within the placenta villi and the organ architecture. Further studies will also help to clarify the mechanisms that lead to assignment of certain nuclei to specialized compartments within a shared placenta cytoplasm.

CHAPTER 3: Alternative Splicing Dysregulation in Placental Pathologies

Alternative splicing is defined as a post-transcriptional process in which unmaturation messenger RNA (pre-mRNA) undergoes the removal of specific alternative exons to produce different transcripts from one genomic locus (Chen & Manley, 2009).

In the context of placental pathologies, one of the earliest markers of PE is an excessive increase of the soluble form of the VEGF receptor (sFLT1) in maternal circulation (Maynard et al., 2003; Nevo et al., 2006; Souders et al., 2015). FLT1 is a membrane receptor expressed in the placenta with implications in angiogenesis, vasodilation, and novo-vascularization. Its soluble form, sFLT1 acts as a trap, binding to VEGF and Placental Growth Factor (PlGF) decreasing its bioavailability for the membrane receptor. Reduced circulating levels of VEGF and PlGF induce endothelial dysfunction and hypertension (Luttun & Carmeliet, 2003). It is classically assumed that sFLT1 production is generated by an alternative exon splicing event, hypothesizing the role of alternative splicing in the development of placental pathologies (He et al., 1999; Maynard et al., 2003).

Although alternative splicing seems to have a major role in the development of PE, no study, to the best of our knowledge, has assessed global splicing dysregulations in pathological placentas. Thus, we aimed to determine the global effect of alternative splicing in pathological placentas in our work “Alternative splicing in normal and pathological human placentas is correlated to genetic variants”. The full publication can be found in Annex 3.

To achieve this, two placental sample series were studied, one series collected at the Hospital Cochin, Paris (PE = 7 and control (low-risk pregnancy) = 9) and the other series collected at the Hospital of Angers (IUGR = 13 and control = 8). Transcriptomic data from both cohorts was assessed by Affymetrix Clariom D microarray, in which transcripts are interrogated at the exon level, making possible the study of alternative splicing events of coding and long non-coding (lncRNA).

We first studied transcriptomic variations driven by the effect of experimental batches and/or gestational age. Since placental transcriptome vary as pregnancy progresses and pathological placentas are often collected at earlier gestational age than control placentas (as discussed in Chapter 1). We observed only a small percentage (6-12%) of the Differentially Expressed Genes (DEGs) between diseased and control placentas were associated with gestational age, birth weight, and sex. Considering this, we assumed that the effects linked to these covariates are meek compared to the ones associated with the disease per se.

To further elucidate the complexity of the alternative splicing issue in pathological placentas, we ranked the genes according to their alternative splicing index, a measure provided by the Affymetrix Transcriptomic Analysis Console to explore coding and non-coding RNA and interpret complex alternative splicing events. A total of 1071 genes were differentially spliced between Ctrl and PE, 575 genes between Ctrl and IUGR with a significant threshold of p-value < 0.001. 176 genes were found to be in common between PE and IUGR. To note, splicing index alterations were not generally correlated to changes at the gene expression level, increasing the complexity of the alternative splicing issue in placental pathologies. As an example, BAIAP2, FNDC3B or PSG4 which are not DEGs show extremely high splicing indexes.

Gene enrichment analysis was performed in these highly spliced genes, showing that alternative splicing does not occur in random genes along the genome. The 176 genes found to be in common in both pathologies are highly enriched of genes related to fetal diseases, hypoxia, and cancer pathways and, in terms of biological function, the most enriched terms were secretion, vesicle metabolisms and exocytosis. However, specific clustering is observed when studying each disease separately. Spliced genes in PE are enriched in genes related to extracellular matrix, circulatory system development, and neuronal physiology while IUGR spliced genes are enriched in genes involved in steroidogenesis, hormone metabolisms and anion transport.

We validated some of these results by a targeted approach based upon exon-specific primers and RT-qPCR. We selected genes based on their implication in PE/IUGR and/or their high splicing index: FLT1, CLDN1, LEP3, FSTL3, TXK, CAP2, CA10, TNFRSF1B, ACOXL, TIE1, LAGLS14 and CPXM2. As an example, concerning FLT1, upregulation of the exon 1 (E1) is observed in pathological placentas (PE, PE+IUGR and IUGR) compared with control placentas, but E12, E14 and E15-E17 are not differentially expressed in PE and IUGR as compared to control samples (**Figure 3.1**). This result is in line with previous observations on short isoform overexpression observed in preeclampsia (Rajakumar et al., 2009).

FLT1

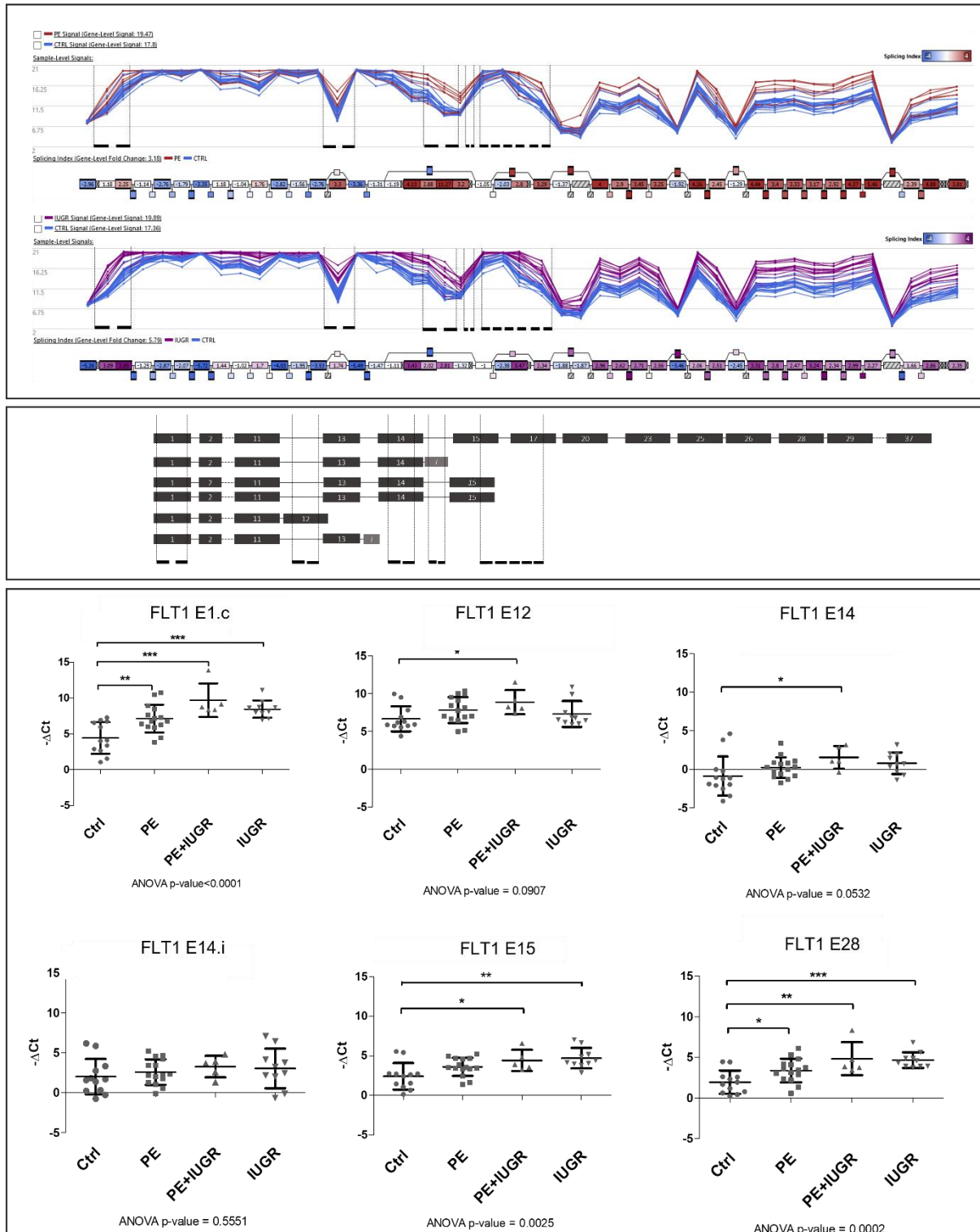


Figure 3.1: Locus-specific RT-qPCR analysis of FLT1. The top graph represents the splicing profile of the gene, in the middle, the position of the primer couples selected to assess the specific locus and, on the bottom, comparisons of the $-\Delta Ct$ between the groups among the exons studied.

We further studied the effect that a single genetic variant may have on the level of splicing in the placenta by identifying splicing Quantitative Trait Loci (sQTLs). Variations in a single nucleotide or so-called SNP can be located in splicing relevant sites such as canonical splice site consensus sequences, in exonic and intronic splice enhancers or silencers, affecting the splice site strength and/or modifying the splicing behaviour of the gene. The 48 genes with the highest splicing index were correlated towards a total of 331,204 SNPs using gestational age and sex of the fetus as covariates. A total of 52 cis-QTLs and 52 trans-QTLs with an $FDR < 0.05$ were identified with this strategy.

In retrospect, this paper can only be considered as exploratory on the effect of genetic variation on alterations in splicing given the small sample size, which limits the statistical power of the results. As mentioned in the paper, we were aware of this limitation, and we were very stringent on the number of SNPs selected and on the significance threshold. To counter back this flaw, we performed a Monte-Carlo approach to determine the scope of our results. By these randomization tests, we observed that, indeed, the organization SNP-gene couple along the genome is not random.

Another point to be made is the role of ethnicity in genetic studies. In our paper, we did not consider the ethnicity of our samples, which should be added as a covariate to adjust for population stratification and avoid bias. Different ethnicities show different Linkage Disequilibrium (LD) patterns due to the evolutionary process. These LD patterns are blocks of alleles that are transmitted to the next generation due to the low rate of genetic recombination that occurs within these genomic locations. African populations show much smaller blocks of LD than European populations. For this reason, African ancestry is characterized by a higher number of haplotypes for any given region of the genome than other populations. In smaller populations, such as Europeans, this difference can still be observed in different European subpopulations. These genetic differences can be observed when performing PCA analysis in the genotyping data of the samples, being able to group the samples by their ancestry. These PC axes represent features of genomic ancestry that capture

population stratification. Since the adjustment of each single nucleotide polymorphism (SNP) varies along each axis of ancestry, PCA corrects not only for false positives but also for false negatives. Therefore, on wide-genome analysis, the first 10 PCs should be used as a covariate to remove this population stratification difference.

Overall, our approach led to the confirmation of placental overexpression of well-known markers of PE, the discovery of new genes involved in PE and IUGR pathologies and raised attention to the necessity of systematic exploration of genetic approaches to assess global alternative splicing in both normal and pathological placentas.



Alternative splicing in normal and pathological human placentas is correlated to genetic variants

Camino S. M. Ruano¹ · Clara Apicella¹ · Sébastien Jacques¹ · Géraldine Gascoin^{2,3} · Cassandra Gaspar⁴ · Francisco Miralles¹ · Céline Méhats¹ · Daniel Vaiman¹

Received: 6 October 2020 / Accepted: 14 December 2020 / Published online: 12 January 2021
© The Author(s) 2021

Abstract

Two major obstetric diseases, preeclampsia (PE), a pregnancy-induced endothelial dysfunction leading to hypertension and proteinuria, and intra-uterine growth-restriction (IUGR), a failure of the fetus to acquire its normal growth, are generally triggered by placental dysfunction. Many studies have evaluated gene expression deregulations in these diseases, but none has tackled systematically the role of alternative splicing. In the present study, we show that alternative splicing is an essential feature of placental diseases, affecting 1060 and 1409 genes in PE vs controls and IUGR vs controls, respectively, many of those involved in placental function. While in IUGR placentas, alternative splicing affects genes specifically related to pregnancy, in preeclamptic placentas, it impacts a mix of genes related to pregnancy and brain diseases. Also, alternative splicing variations can be detected at the individual level as sharp splicing differences between different placentas. We correlate these variations with genetic variants to define splicing Quantitative Trait Loci (sQTL) in the subset of the 48 genes the most strongly alternatively spliced in placental diseases. We show that alternative splicing is at least partly piloted by genetic variants located either in cis (52 QTL identified) or in trans (52 QTL identified). In particular, we found four chromosomal regions that impact the splicing of genes in the placenta. The present work provides a new vision of placental gene expression regulation that warrants further studies.

Camino S. M. Ruano and Clara Apicella contributed equally to this study.

Céline Méhats and Daniel Vaiman supervised this work equally.

Supplementary Information The online version contains supplementary material available at <https://doi.org/10.1007/s00439-020-02248-x>.

✉ Daniel Vaiman
daniel.vaiman@inserm.fr

¹ Université de Paris, Institut Cochin, Inserm U1016, CNRS, 24 rue du Faubourg St Jacques, 75014 Paris, France

² Unité Mixte de Recherche MITOVASC, Équipe Mitolab, CNRS 6015, INSERM U1083, Université d'Angers, Angers, France

³ Réanimation et Médecine Néonatales, Centre Hospitalier Universitaire, Angers, France

⁴ Sorbonne Université, Inserm, UMS Production et Analyse des Données en Sciences de la vie et en Santé, PASS, Plateforme Post-génomique de la Pitié-Salpêtrière, P3S, 75013 Paris, France

Introduction

Preeclampsia (PE) is a major disease of pregnancy, marked by hypertension, proteinuria, and a generalized endothelial maternal disorder (Sibai et al. 2005; Rana et al. 2019). PE induces 70,000 maternal deaths and ~1,000,000 fetal deaths worldwide (1.5–10% of pregnancies according to the country, with a high prevalence in sub-Saharan Africa). IUGR, a failure of the fetus to reach its normal growth potential, affects up to 10% of the fetuses, and is a major cause of the birth of small babies, that are at risk for acute diseases of the retina (Gupta et al. 2008), the lung (Arroyas et al. 2020; Fandino et al. 2019; Zana-Taieb et al. 2015), the heart (Crispi et al. 2008) (in the most severe cases) and long term increased risk of cardiovascular diseases (less severe cases) (Jansson and Powell 2007; Savage et al. 2020). These two gestational pathologies are strongly connected since one third of the preeclampsia cases results in IUGR. PE and IUGR are accompanied by epigenetic alterations at the placental level and have been strongly associated with an imbalance of the oxidative and nitrosative stresses (Myatt 2010; Aouache and Biquard 2018; Doridot et al. 2014). One of the

Springer

Content courtesy of Springer Nature, terms of use apply. Rights reserved.

earliest markers of preeclampsia is an excessive increase of the soluble form of the VEGF receptor, sFLT1, in the maternal plasma (Souders et al. 2015). This form is generated by an alternative exon splicing event that will generate a protein encoded by the first 13–15 exons of the FLT1 gene (Szalai et al. 2015).

This soluble receptor is classically thought to perform as a trap for the VEGF and PGF angiogenesis factors (Phipps et al. 2019). Thus, it is classically assumed that an exon-splicing event of FLT1 is a major causative factor in the onset of PE. The idea that alternative splicing mechanisms are more general in the pathophysiology of pregnancy, including IUGR, has not been systematically analyzed so far.

Exon splicing events on a global scale are currently theoretically measurable by two technical approaches: exon-specific microarrays and RNA sequencing. Nevertheless, splicing events are rarely mentioned in the RNA-seq experiments carried out in normal and pathological placental samples, with a recent exception (Majewska et al. 2019). To address alternative splicing, RNA-seq need very high depth of reads (60–100X), and paired-end reads. These requirements are seldom achieved and studies using RNA-seq approaches on preeclamptic placental or decidual samples do not dive into details on splicing profile (Tong et al. 2018; Sober et al. 2015). This is also true for other defective pregnancy outcomes, such as recurrent miscarriage (Sober et al. 2016). Notwithstanding, genes involved in splicing and mRNA processing are highly expressed both in normal and pathological placentas (Aouache and Biquard 2018).

In the present study, we decided to thoroughly analyze alternative splicing events in the placenta in the context of pathological pregnancies. We profiled placental RNA levels from controls, preeclamptic patients and IUGR patients at the exon level using exon-microarrays. In parallel, the same patients and controls were genotyped using SNP-microarray technology. This design allowed us to discover extensive alterations of splicing throughout the placental genome in pathological situations. In addition, we identified genetic variants that are associated to splicing modifications, located in *cis* and *trans*, with or without connection with the disease status. These splicing Quantitative Trait Loci (sQTLs) may thus reflect individual-specific regulations of placental functions.

Results

A genomic search for alternative splicing in the human placenta

Placental alternative splicing is a prominent feature of gestational diseases

To determine whether there are differences in mature transcripts for a given gene between healthy and diseased placentas, gene expression at the exon level was measured in placentas from two distinct cohorts of patients: a cohort of PE-affected women and matched controls (Institut Cochin-PE cohort, $n=7$ and 9 , respectively) and another of IUGR-affected women and matched controls (Angers Hospital-IUGR cohort, $n=13$ and 8 , respectively). Patient characteristics are presented in Supplementary Table S1. As expected, both gestational age and birth weight are significantly different between disease and control groups. This difference is a recurrent and expected feature of transcriptome analysis comparing normal and pathological placentas. In this case, since most of the samples (including the pathological ones) are from third-trimester placentas, the effects linked to placental age are probably meek compared to the ones associated with the disease per se. To more thoroughly ascertain this, we proceeded to identify and estimate surrogate variables for known and unknown sources of variation in our dataset using the SVA package (Leek et al. 2012). In the IUGR vs CTRL comparison, 6.5% of the probes differentially expressed according to disease, were also associated to gestational age, 12.5% to birth weight, and 10.9% to sex. In the PE vs CTRL comparison, 7.5% of the genes significantly changed due to PE effects were significantly associated to gestational age, 6.8% to birthweight and 10% to the sex of the baby. Considering these data, we assumed that the gene expression and splicing alterations detected are strongly influenced by the disease status. These data are summarized as Supplemental Table S2a, S2b and S2c for the comparison between CTLs on the one hand, vs IUGRs, all PEs, and isolated PEs, respectively.

The comparison of gene expression at the exon level was carried out using Affymetrix ClariomD microarray, an attractive solution for tackling the complex question of alternative splicing regulation, compared to other more computation-intensive approaches depending upon RNA-seq. Analyses through the Affymetrix Transcriptome Analysis Console software lead to the definition of a splicing index associated with a relative p value for each gene and each comparison (Gardina et al. 2006), allowing to rank the genes from the most differentially spliced, to the least. The complete dataset is available with the accession number E-MTAB-9416 (EMBL-EBI ArrayExpress).

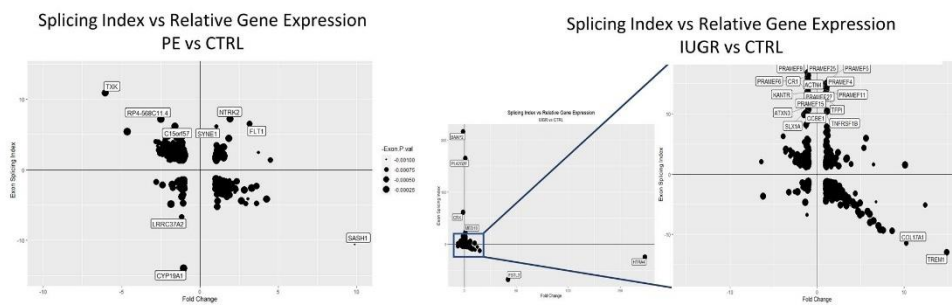
When using a p value threshold of 0.001, 1060 and 1409 genes had a significant splicing index value in PE vs controls and IUGR vs controls, respectively. Splicing index alterations were not correlated with gene expression deregulation between preeclamptic and control samples (Fig. 1a).

For instance, *CYP19A1* or *BALAP2* were not strongly modified at the expression levels in PE placental samples and IUGR samples, respectively, while the splicing index alteration in these genes was amongst the highest (Table 1).

Alternative splicing concerns specific gene categories in PE and IUGR

Since p value allows to pinpoint significant but also small variations in splicing (that may not be relevant), we decided to focus on transcripts with $SI > 3$, a list marginally different from the one given with the $p < 0.001$ threshold. We identified a list of 1456 transcripts in PE vs control placentas, and 725 transcripts in IUGR vs control placentas at the same threshold. Among those, 1071 and 575 have an official gene symbol (Supplementary Tables S3 and S4) and 176 were found alternatively spliced in both diseases (Fig. 1b). These

A



B

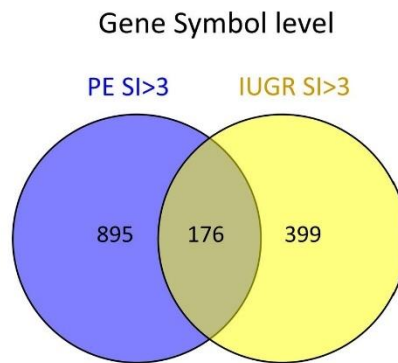


Fig. 1 a Splicing index represented in function of the fold change of gene expression in PE vs CTRL (left) or IUGR vs CTRL, right. A zoom of the cloud in the blue square is presented. For preeclampsia, gene labels are shown for genes with $SI > 16$ and for IUGR > 110 .

Overall, there was no marked correlation between splicing and gene expression level (see text). **b** A part of the genes only is found both in preeclampsia and IUGR

Table 1. 48 genes sorted by Splicing Index as modified in pregnancy diseases

Gene	Max SI PE	Max SI PE+IUIGR	Max SI IUIGR	RT-qPCR validation	Institut Cochin Cohort		Anger Hospital Cohort		Expression 3rd trimester (Pique-Regi et al. 2020)
					Ctrl expression	PE expression	Ctrl expression	PE+IUIGR expression	
BALAP2	51.89	35.61	215.91	No	6.87	6.6	6.78	6.73	STB
PLA2G2F	29.19	22.57	164.47	No	6.1	5.86	6.14	6.15	
FNDC3B	19.23	18.27	1.69	No	19.31	19.31	19.16	19.15	EVT
RP11-113122.1	18.85	16.99	-1.46	No	4.3	4.22	4.38	4.26	
CLDN1	15.51	9.17	4.25	Yes	15.54	11.55	15.67	13.4	Endometrial
HMHA1	11.65	4.31	7.84	No	3.46	3.61	3.45	3.58	
FLT1	11.27	5.43	-6.24	Yes	17.8	19.47	17.36	19.89	EVT
TXK	10.9	16.7	4.67	Yes	11.17	8.57	11.54	10.24	
CA10	10.84	7.1	3.14	Yes	3.88	3.7	10.3	8.94	
CPXM2	10.64	10.81	4.11	Yes	12.48	9.7	12.13	10.82	
CDY7P	9.14	-1.64	-1.07	No	4.27	4.32	4.17	4.03	
FLT4	9.05	8.72	6.42	No	10.09	9.27	9.83	10.16	LED (Lymphoid Endothelial Decidual cells)
AGER3	8.51	-9.21	5.99	No	13.58	14	13.3	14.01	
STAT4	8.37	6.48	2.63	No	7.37	6.34	7.46	6.79	
PSMD13	8.35	3.39	3.31	No	12.96	12.96	12.81	12.6	
FAM47E; STBD1; STBD1	8	7.05	1.86	No	5.56	5.14	5.56	5.43	
SPX	8	-7.01	7.15	No	8.14	5.92	8.16	5.52	
NCKAP1	7.86	2.85	-2.5	No	13.81	13.63	13.37	13.5	EVT
NTRK2	7.26	4.1	-4.44	Yes	5.14	6.06	4.62	6.3	
SPP1	7.16	2.19	-3.48	No	15.54	13.15	15.86	15.22	Macrophage
TNFRSF1B; MIR4632; MIR7846	7.03	5.39	10.42	Yes	8.37	8.83	8.96	9.14	
EIF1AY	6.93	-11.93	5.64	No	8.16	6.46	8.05	7.35	VCT
CYP19A1	-68.93	-5.02	3.56	No	14.08	13.08	19.92	19.92	CTB
PSG4	-31.84	-28.56	3.8	No	19.91	19.85	19.89	19.93	STB
XIST	-24.17	298.39	-24.55	No	13.95	16.16	12.71	17.02	
FSTL3	-21.76	-16.73	-67.97	No	8.03	11.87	7.06	12.45	EVT



Content courtesy of Springer Nature, terms of use apply. Rights reserved.

Table 1. (continued)

Gene	Max SI PE	Max SI PE+IUGR	Max SI IUGR	RT-qPCR validation	Institut Cochin Cohort		Anger Hospital Cohort		Expression 3rd trimester (Pique-Regi et al. 2020)
					Ctrl expression	PE expression	Ctrl expression	IUGR expression	
RPSA; SNORA62; SNORA6	-20.35	2.81	-1.67	No	15.46	15.39	15.19	15.33	npICTB (non-proliferative interstitial cytotrophoblast) CTB
GABRE; MIR224; MIR452	-20.35	-2.44	-8.66	No	16.08	15.37	16.49	15.99	
SH3BP5	-14.23	-2.01	-4.91	No	8.95	8.88	8.09	10.15	EVT
PDXDC2P	-13.05	-5.63	2.27	No	12.29	11.82	13.08	12.76	
BIN2	-10.91	-11.55	-8.01	No	6.42	7.17	8.84	11.45	
SASH1	-10.59	-16.6	-9.28	No	7.96	11.27	8.01	10.93	LED
LGALS8	-9.52	-5.48	2.31	No	14.39	13.58	14.77	14.47	
ST18	-9.36	3.05	-3.69	No	3.37	3.47	3.25	3.19	
HTRA4	-9.29	-12.66	-24.88	No	10.91	15.72	10.23	17.67	EVT
ATG2B	-9.11	-2.92	1.87	No	8.33	8.06	8.34	8.39	
DDX17	-8.9	-1.77	2.02	No	16.78	16.58	16.82	16.84	EVT
CAP2	-8.58	-5.82	1.92	No	14.36	13.62	14.59	14.14	STB
BCAP29	-6.6	-2.59	2.67	No	13.53	13.4	12.98	13.38	LED
ORC4	-6.17	-3.95	1.62	No	11.53	10.81	11.13	11.14	
SLC6A10P	-6.11	-4.13	-8.59	No	8.96	11.13	8.56	11.39	EVT
P4HA1	-6.08	-6.88	-4.86	No	8.83	10.65	8.79	10.47	
LYRM5	-6.06	-7.47	-1.84	No	8.5	8.26	6.13	5.02	
DPP4	-5.94	1	-1.01	No	5.95	6.37	6.42	6.42	CTB
ACOXL	4.46	6.24	3.64	Yes	9.12	7.47	9.35	8.1	
TIE1	4.01	5.13	-1.66	Yes	6.19	6.49	6.08	6.29	LED
LGALS14	-2.22	-2.42	-2.02	Yes	19.9	19.7	19.92	19.58	STB
LEP	-1.91	-2.54	-1.56	Yes	11.85	12.79	7.42	15.28	STB



Content courtesy of Springer Nature, terms of use apply. Rights reserved.

latter 176 genes encoded proteins that constituted a network of Protein–Protein Interactions ($p=0.00097$, Supplemental figure S1, String database, <https://string-db.org/cgi> (Szklarczyk et al. 2019)), showing that the splicing alteration does not occur randomly in the placental genome in pathological situations. We then performed an over-representation analysis using WebGestalt (Wang et al. 2017; Liao et al. 2019) on the 176 genes found alternatively spliced in both disease conditions. We compared our gene list with the GLAD4U database (Jourquin et al. 2012), that collects gene sets associated with diseases. We found a significant enrichment for Pregnancy complications, fetal diseases, gestational hypertension, hypoxia and several cancer pathways (Fig. 2a). The exhaustive values and genes involved are presented as Fig. 2b for ‘Gestational Hypertension’, ‘Pregnancy complications’, ‘Anoxia’, and ‘Pregnancy’.

Functional clustering of alternatively spliced genes partly differs between PE and IUGR

Then we proceed to separately analyze the genes spliced in either IUGR or PE. We found that while the two pathologies shared biological processes related to secretion, exocytosis and vesicle metabolism, substantial clustering differences were observed.

In IUGR (Table 2), KEGG and Reactome pathways related to hypoxia, steroidogenesis, hormone metabolism and anion transport were enriched. Against disease database (GLAD4U and OMIM), the alternatively spliced genes in IUGR were widely associated to ‘pregnancy complications’, ‘Nitric Oxide metabolism’ (known as intimately linked to placental pathology) (Aouache and Biquard 2018; Motta-Mejia et al. 2017; Dymara-Konopka and Laskowska 2019), ‘preeclampsia’ and ‘eclampsia’, but also to autoimmune diseases, especially ‘lupus erythematosus’ (SLE), which is consistent with the increased risk of IUGR and other defective pregnancy outcomes documented in autoimmune patients, especially those affected by SLE (Do and Druzin 2019).

The same type of analysis applied to the PE-alternatively spliced genes yielded quite different results (Table 3). In terms of Biological processes, extracellular matrix, circulatory system and several neuron/axon ontology terms were found enriched specifically in PE. KEGG and Reactome pathways consistently pointed out to extracellular matrix organization pathways. In terms of diseases databases (GLAD4U and OMIM), ‘pregnancy’ and ‘pregnancy complications’ appeared enriched, but also, interestingly, numerous pathological pathways implicated in neurodevelopmental diseases emerged with GLAD4U (‘Brain diseases’, ‘CNS diseases’, ‘Dementia’, ‘Cri-du-Chat syndrome’), while OMIM pointed out to SLE (Qing et al. 2011) and Malaria susceptibility, consistently with the IUGR OMIM terms. In this case, nevertheless, an enrichment in genes involved in

Alzheimer’s disease was also found, consistently with the GLAD4U keywords.

In summary, this comprehensive description of abnormal splicing in IUGR and PE reveals quite different enrichment of alternatively spliced genes between two important placental diseases and normal placentas. Notably, a connection with neurological disease genes was exclusive to PE. Comparing our sQTLs results, with placental eQTLs identified in previous studies (Peng et al. 2017), we found four genes in common amongst the cis-eQTLs (ACER3, CLDN1, PSG4, LGALS8). A contingency chi2 revealed a marginally significant enrichment (12.8% expected versus 33% observed, $p=0.034$).

Individual validation of alternative splicing on an enlarged collection of placental samples

We next validated some of these alterations through a targeted approach, based upon exon-specific primers and RT-qPCR. For this validation, we selected 12 genes based upon their known involvement in preeclampsia and/or their very high splicing index differences between healthy and preeclamptic placentas: FLT1, CLDN1, LEP, FSTL3, TXK, CAP2, CA10, TNFRSF1B, ACOXL, TIE1, LAGLS14, CPXM2. Maximal splicing indexes (p values) were respectively: FLT1 11.27 ($p=0.0016$), CLDN1 15.51 ($p=0.0063$), LEP 2 (0.2957), FSTL3 – 21.76 ($p=0.005$), TXK 10.9 ($p=8.55E^{-05}$), CAP2 – 8.58 ($p=0.0331$), CA10 10.84 ($p=0.0557$), TNFRSF1B 7.03 ($p=0.0035$), ACOXL 4.46 (0.0241), TIE1 4.01 ($p=0.0034$), LGALS14 – 2.22 ($p=0.5275$), CPXM2 10.64 ($p=0.0301$). Additional new samples were included along with the samples used in the microarray analysis, for a final total of 13 controls, 15 isolated PE, 5 PE + IUGR and 10 isolated IUGR samples. Overall, we confirmed splicing alterations in diseased placentas for 10 out of 12 genes (except LGALS14 and CPXM2). An example of analysis is given for five genes (FLT1, CLDN1, LEP, FSTL3 and TXK) in Fig. 3, and the remaining genes are presented as Supplementary figures S2.

Genetic regulation of alternative splicing in the human placenta—determination of sQTLs

We next analyzed the genetic basis of splicing alterations in the different individual placentas, focusing upon a sample of 48 genes with the most differential splicing index between normal and preeclamptic placentas (Table 1). Several of these genes are well known from the literature to be modified at the expression level between PE and normal placentas such as FLT1, LEP, PAPP2, HTRA4 (Vaiman et al. 2013). Nineteen out of the 48 genes were also significantly modified at the expression level between controls and IUGR, as assessed by the analysis of the Angers Hospital-IUGR

cohort. By PCA analysis, we could show that there was no major effect of the batch (Supplementary Figure S3).

Splicing is influenced by variants located in the vicinity of genes (cis-sQTL) and at far locations (trans-sQTL)

Each placental DNA was genotyped using a SNP genotyping array that encompasses ~ 710,000 SNPs and *MatrixeQTL* R package was used to investigate the impact of SNP variants on individual splicing indexes (Shabalin 2012). Placental Individual Splicing Indexes (ISIs) were computed along with the genotype data. A QQ-plot (Fig. 4) was obtained and allowed the identification of 180 cis-sQTLs (1 Mb around the gene under scrutiny) with $p < 0.01$ and 52 with $FDR < 0.05$ and 199,884 trans-sQTLs (> 1 Mb) with $p < 0.01$ and 52 with $FDR < 0.05$. The detailed list of cis-sQTLs identified is given as Supplementary Table S5. To add stringency to the approach, we re-ran the program focusing only on the control samples (Tong et al. 2018). Despite the loss of power due to this reduced size, we were still able to detect 5 cis-sQTL with a $FDR < 0.05$ that are all common to the complete list and presented in bold in Table S5.

Cis-sQTLs have additive effects on splicing

A selection of highly significant cis-sQTLs are presented in Fig. 5. It is interesting to note that in these cases, the splicing effect is overall linear in function of the occurrence of one of the alleles (additive effect). For instance, in the first example (CYP19A1-rs12907866), the splicing index is the lowest in AA genotypes, intermediate in AB and higher in BB. The same type of profile is visible in the other examples presented. These influences on SI do not appear to be strictly connected to the disease status. Cis-sQTLs may induce alternative splicing by influencing the binding of splicing factors, by modifying the secondary structure of mRNAs, or any other local influence. However, they are not giving an image of the alternative splicing regulation at the genome level. Thus, to identify variants that influence splicing distantly from their location, we studied in more detail trans-sQTLs.

Trans s-QTL analysis reveals major loci associated to splicing in the placenta

The conventional significance threshold for a genome-wide analysis ($p < 10^{-8}$) identified 52 significant SNP-gene couples for trans-sQTL (Supplementary Table S6). At $p < 0.001$, 24,867 QTLs were found, while 3,639 QTLs passed the $p < 0.0001$ threshold. As reported in many studies, keeping an $FDR < 0.05$ or a $p < 10^{-8}$ will miss QTL with biological relevance (Morrow et al. 2018). Therefore, we developed a novel approach not to lose this relevant biological information; in particular, we were interested in identifying

bandmaster loci that would control the splicing of a large part of the 48 genes that we identified as the most strongly spliced.

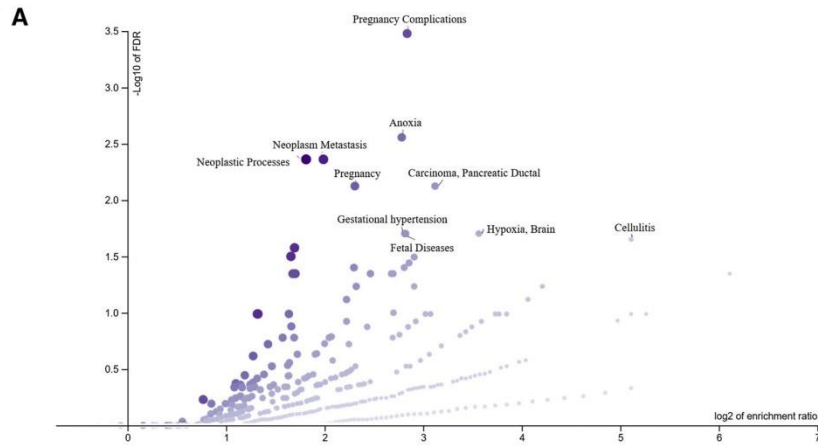
To perform this, we organized the dataset by sorting the SNPs along the chromosomes to find isolated SNPs (or windows of SNPs separated by less than 2000 bp—a distance in the range of minimal chromosomal block sizes of markers in linkage disequilibrium (Pritchard and Przeworski 2001)) that were significantly associated to alternative splicing of more than one gene.

A Monte-Carlo statistical analysis was performed to evaluate the longest possible windows of consecutive SNP-gene couples obtained from a random organization of the SNPs (simulated windows). At a threshold of 0.001, the maximal window length was of 19 consecutive gene-SNP couples, while random cases lead to a maximal size of 10 gene-SNP couples. Performing the same operation at the 0.0001 threshold we identified a maximum window size of 6 in the randomized dataset (one occurrence), while nine windows of more than 6 consecutive SNP-gene couples (Fig. 6a) were identified from the real dataset. The nine windows identified are located on chromosomes 2, 5, 7, 8, 10, 13, 14 (at two locations) and 21. To note, four of these windows were also detected at the threshold of 0.001: on chromosomes 5, 7, 8, and the second region on chromosome 14. Also, two of these windows (on chromosome 2 and 14) encompassed gene-SNP couples that were significant at a genome-wide threshold ($p < 10^{-8}$, rs13006826-SLC6A10P and rs9323491-CYP19A1). We decided to focus on these four regions, presented in Fig. 6b as the blue, green, orange and purple fountains of a circus Plot (Gu et al. 2014).

The Chromosome 5 region contains two SNPs separated by 702 bp, rs13185255 and rs12520828. These SNPs are located inside the ARHGAP26 gene, or its antisense and are associated with increased splicing alterations for FLT4, CLDN1, PLA2G2F, SH3BP5, P4HA1 and SLC6A10P.

The Chromosome 7 region spans 314 base pairs and encompasses 2 SNPs (rs6964915 and rs6965391). These SNPs are located inside the LOC105375161 non-coding RNA, which harbors the highest level of expression in the placenta (<https://www.ncbi.nlm.nih.gov/gene/105375161>) and (Fagerberg et al. 2014). RT-qPCR results interrogating two distinct regions of LOC105375161 showed no difference in expression between the sample groups (Supplementary Fig. S5). The splicing alterations of 3 genes were found associated with variants in this Chr7 region (FLT1, TXK and NTRK2).

The Chromosome 8 region encompasses a unique SNP (rs1431647) located inside the non-coding RNA LOC105375897, which is expressed at a low level in the placenta. Eight genes were potentially affected by this variant at the splicing level (FSTL3, FLT1, P4HA1, NTRK2, FLT4, BAIAP2, CLDN1, ST18). By RT-qPCR, we could



B

Select an enriched gene set...
PA165108364: Gestational hypertension

Gene set: PA165108364 Gestational hypertension

FDR: 0.021387, P Value: 0.00005911, 4

Gene Set Size: 171, Expected Value: 0.38174, Overlap: 7, Enrichment Ratio: 7.1302

User ID	Gene Symbol	Gene Name	Entrez Gene ID
DDAH1	DDAH1	dimethylarginine dimethylaminohydrolase 1	23576
FLT1	FLT1	fms related tyrosine kinase 1	2321
FSTL3	FSTL3	folliculin like 3	10272
HTRA4	HTRA4	HtrA serine peptidase 4	203100
PAPPA2	PAPPA2	pappalysin 2	60676
PLAC1	PLAC1	placenta specific 1	10761
PLAC3	PLAC3	placenta specific 3	51316

Select an enriched gene set...
PA445403: Pregnancy Complications

Gene set: PA445403 Pregnancy Complications

FDR: 0.0024792, P Value: 9.1182e-7

Gene Set Size: 290, Expected Value: 1.6649, Overlap: 11, Enrichment Ratio: 6.6069

User ID	Gene Symbol	Gene Name	Entrez Gene ID
CCBE1	CCBE1	collagen and calcium binding EGF domains 1	147372
DIS3L2	DIS3L2	DIS3 like 3'-5' nonBromodomain 2	129563
FLT1	FLT1	fms related tyrosine kinase 1	2321
FLT4	FLT4	fms related tyrosine kinase 4	2324
FRMD4A	FRMD4A	FERM domain containing 4A	55691
FSTL3	FSTL3	folliculin like 3	10272
HTRA4	HTRA4	HtrA serine peptidase 4	203100
IL1R2	IL1R2	interleukin 1 receptor type 2	7850
PAPPA2	PAPPA2	pappalysin 2	60676
PLAC1	PLAC1	placenta specific 1	10761

Select an enriched gene set...
PA443382: Anoxia

Gene set: PA443382 Anoxia

FDR: 0.0025609, P Value: 0.00000188, 37

Gene Set Size: 251, Expected Value: 1.4410, Overlap: 10, Enrichment Ratio: 6.9395

User ID	Gene Symbol	Gene Name	Entrez Gene ID
BHLHE40	BHLHE40	basic helix-loop-helix family member e40	8553
ERD1A	ERD1A	endoplasmic reticulum oxidoreductase 1 alpha	30001
ESRRG	ESRRG	estrogen related receptor gamma	2104
FLT1	FLT1	fms related tyrosine kinase 1	2321
LDHA	LDHA	lactate dehydrogenase A	9939
NDRG1	NDRG1	N-myc downstream regulated 1	10397
P4HA1	P4HA1	prolyl 4-hydroxylase subunit alpha 1	5033
PKM	PKM	pyruvate kinase M1/2	5315
FLOD2	FLOD2	procollagen-lysine-2-oxoglutarate 5-dioxygenase 2	5352
THBS1	THBS1	thrombospondin 1	7057

Select an enriched gene set...
PA16608714: Pregnancy

Gene set: PA16608714 Pregnancy

FDR: 0.021691, P Value: 0.00007462, 4

Gene Set Size: 384, Expected Value: 2.2046, Overlap: 10, Enrichment Ratio: 4.5360

User ID	Gene Symbol	Gene Name	Entrez Gene ID
FLT1	FLT1	fms related tyrosine kinase 1	2321
FRMD4A	FRMD4A	FERM domain containing 4A	55691
FSTL3	FSTL3	folliculin like 3	10272
HTRA4	HTRA4	HtrA serine peptidase 4	203100
IL1R2	IL1R2	interleukin 1 receptor type 2	7850
PAPPA2	PAPPA2	pappalysin 2	60676
PLAC1	PLAC1	placenta specific 1	10761
PRG2	PRG2	proteoglycan 2, pro-α2(I) major basic protein	5553
PSGA	PSGA	pregnancy specific beta-1-glycoprotein 4	5672
PSG7	PSG7	pregnancy specific beta-1-glycoprotein 7 (gene/pseudogene)	5476

Fig. 2 WebGestalt analysis of the genes that are alternatively spliced in common in the two diseases under scrutiny, in comparison with the disease database GLAD_4U. The database recognized 116 genes among the 176 submitted. **a** The enrichment in genes in the group is represented on the X-axis, while the FDR is represented on the Y-axis. The most significant pathways (with $FDR < 0.05$) are identified. **b** Highly relevant gene sets are represented. As an example of how to read the figure, the first on the upper left means that 178 genes are in the geneset 'Gestational Hypertension', 7 of which are in common with the 116 that constitute the input (the 116 that were identified out of the initial input of 176). This enrichment is highly significant (7.1 more genes that expected, $FDR = 0.0214$)

show that LOC105375897 is expressed at similar levels between control and preeclamptic placentas, while is over-expressed significantly in IUGR ~ 30 fold (p value < 0.01) (Supplementary Fig. S5).

The Chromosome 14 region spans 828 bp and encompasses two SNPs, rs7145295 and rs7151086 that are located inside the GPHN gene (harboring the non-coding RNA LOC105370538, which was not detectable in our samples by RT-qPCR). Six genes were potentially affected at the splicing level: CYP19A1, FLT1, P4HA1, FLT4, SH3BP5, and NTRK2).

The association between these SNPs and splicing levels is represented in Fig. 7. The two SNPs identified for chromosome 5 as well as for chromosome 7 had the same profile, and thus only one SNP of each region was represented. For rs13185255 it was the heterozygous genotype that was different from the homozygous genotypes (Fig. 7a). There were no obvious association between the levels of splicing, the genotypes of the QTL and the status of the patient. For rs6965391 the AA genotype was characterized by a higher splicing index for the three target genes (Fig. 7b), with a possible association with preeclampsia but that should be confirmed on a larger sample since the AA genotype was the rarest. For rs1431647, it was also the heterozygous genotype that was different from the others, without obvious connections with the disease status (Fig. 7c). In Fig. 7d are represented the two SNPs characterizing the fourth region studied. One of the SNPs (rs7145295) presents an additive behavior in terms of splicing levels for CYP19A1 ($r = 0.85$, $p < 10^{-4}$). AA was marginally associated with preeclampsia (Chi-Square, $p = 0.022$, Log-Likelihood, $p = 0.029$), and the data are consistent with the second SNP nearby rs7151086. In both cases, a higher splicing index characterizes the BB genotype.

Methods

Ethical statements and sample collection

The placenta collections have already been described elsewhere (Gascoin-Lachambre et al. 2010; Ducat et al. 2019).

Cochin Hospital cohort: placentas were collected from two maternity wards (Hôpital Cochin and Institut de Puériculture, Paris, France). This study was approved by the Ethics Committee and CCPPRB (Comité Consultatif de Protection des Personnes dans la Recherche Biomédicale) of Paris Cochin. Placentas were obtained from cesarean sections before the onset of labor. Exclusion criteria were diabetes, chromosomal and fetal malformations, maternal infections, and addictions. The inclusion criteria used for pre-eclampsia were systolic pressure above 140 mmHg, diastolic pressure above 90 mmHg and proteinuria above 0.3 g per day. Women who underwent a cesarean section without disease during pregnancy formed the control group. All patients gave their written consent for the use of their placenta and blood samples.

Angers University Hospital cohort: collection and use for research purpose (including genetic analyses) of placentas from pregnancies complicated with IUGR or healthy pregnancy have been approved by the Ethics Committee of Angers. The inclusion criteria used for IUGR was weight at birth < 10 th percentile. Vascular IUGR was defined by a reduction of fetal growth during gestation, with a notch observed by Echo-Doppler in at least one uterine artery and with Doppler abnormalities on umbilical Doppler and/or cerebral Doppler and/or ductus venosus, and with a birth weight below the 10th percentile according to Audipog growth curves. As for the Cochin cohort, women who exhibited any of the following criteria were excluded from the study: diabetes, pre-eclampsia, chromosomal and fetal malformations, maternal infections, aspirin treatment, and addictions (such as tobacco or drug usage). This collection is registered to the French Ministry of Research under number DC-2011-1467. The processing of personal data implemented as part of the project has been authorized by the French Data Protection Authority (CNIL, no. pWP03752UL). All participants provided written informed consent prior to inclusion. The study was conducted in accordance with the declaration of Helsinki (Chabrun et al. 2019).

The placental sampling was systematically done in placental regions that appeared visually normal.

RNA and DNA extraction from human placentas

RNA isolation followed classical protocols. The placentas were processed in the 30 min post cesarean section. The fetal membranes were discarded, and then, from two cotyledons to three cotyledons, villous trees were washed thoroughly in PBS and placed in TriZol™. Then the tissue was ground with a metal bead in a tissue grinder in 1.5 ml tubes. Then, 200 μ l of chloroform were added, the tubes were centrifuged at 10,000g RT, and the supernatant collected, reprecipitated in isopropanol by centrifugation. The pellet was then washed in 70% ethanol, dried under a fume hood, and resuspended

Table 2 Enrichment analysis of genes differentially spliced in IUGR

Gene set	Description	Expect	Ratio	<i>p</i> value	FDR
Gene ontology biological processes					
GO: 0,046,903	Secretion	33.803	1.8638	8.58E-07	0.006826
GO: 0,009,628	Response to abiotic stimulus	23.651	2.0295	2.16E-06	0.006826
GO: 0,032,940	Secretion by cell	31.002	1.8709	2.25E-06	0.006826
GO: 0,045,055	Regulated exocytosis	16.491	2.1831	9.5E-06	0.017593
GO: 0,071,363	Cellular response to growth factor stimulus	13.9	2.3021	1.07E-05	0.017593
GO: 0,009,719	Response to endogenous stimulus	33.592	1.7564	1.28E-05	0.017593
GO: 0,009,725	Response to hormone	20.261	2.0236	1.37E-05	0.017593
GO: 0,002,576	Platelet degranulation	2.6747	4.4864	1.55E-05	0.017593
GO: 0,006,820	Anion transport	12.321	2.3538	1.86E-05	0.018812
GO: 0,070,848	Response to growth factor	14.532	2.202	2.57E-05	0.023392
KEGG pathways					
hsa04913	Ovarian steroidogenesis	1.1546	6.9286	1.6E-05	0.003405
hsa04066	HIF-1 signaling pathway	2.3564	4.6681	2.09E-05	0.003405
hsa04923	Regulation of lipolysis in adipocytes	1.2725	5.5012	0.000249	0.027062
hsa04014	Ras signaling pathway	5.4669	2.7438	0.000359	0.029234
Reactome pathways					
R-HSA-114608	Platelet degranulation	3.1046	3.8652	6.28E-05	0.048135
R-HSA-76005	Response to elevated platelet cytosolic Ca ²⁺	3.2249	3.721	9.1E-05	0.048135
R-HSA-202733	Cell surface interactions at the vascular wall	3.2971	3.6395	0.000113	0.048135
R-HSA-879518	Transport of organic anions	0.2888	13.85	0.000139	0.048135
R-HSA-209822	Glycoprotein hormones	0.2888	13.85	0.000139	0.048135
Disease_GLAD4U					
PA445403	Pregnancy complications	5.0666	5.5264	2.53E-13	3.80E-10
PA166048714	Pregnancy	6.7088	4.7698	2.79E-13	3.80E-10
PA165108364	Gestational hypertension	2.9875	6.3598	1.73E-10	1.57E-07
PA445398	Pre-Eclampsia	2.8128	5.6882	2.44E-08	1.45E-05
PA443984	Eclampsia	2.8303	5.6531	2.67E-08	1.45E-05
PA445058	Neoplasm metastasis	11.409	2.8049	1.67E-07	7.58E-05
PA166048749	Pregnancy third trimester	1.1531	8.6724	2.07E-07	8.02E-05
PA165108943	Retained placenta NOS	0.47171	14.839	3.08E-07	0.000105
PA446021	Vascular diseases	8.5782	3.0309	5.96E-07	0.00018
PA166048848	Menopause	2.7429	5.104	7.00E-07	0.00019
Disease_OMIM					
611,162	Malaria, susceptibility to malaria, resistance to, included	0.076176	52.51	6.48E-07	4.28E-05
152,700	Systemic lupus erythematosus	0.035848	55.792	0.000523	0.017249
609,423	Human immunodeficiency virus type 1, susceptibility to	0.067214	29.756	0.001924	0.028948
601,665	Obesity, leanness included	0.067214	29.756	0.001924	0.028948
415,000	Spermatogenic failure, y-linked, 2	0.071695	27.896	0.002193	0.028948

in RNase-free water. The quality of the RNA was evaluated by 2100 bioanalyzer (Agilent). Samples with RIN > 7 were used for microarray analysis and RT-qPCR. DNA was prepared from the same sample by standard lysing protocols (Proteinase K treatment overnight at 55 °C), spooling of the DNA, washing with ethanol 70%, resuspension I TE (1–0.1) at ~200 ng/μl.

Transcriptomics and genotype datasets

One hundred ng of RNA from each placental sample were analyzed by ClariomD (Affymetrix) microarray assay. This tool interrogates 134,748 probes, including coding genes (18,858), non-coding genes (66,845) and genes deduced by bioinformatics analysis (10,001), in addition to pseudo-genes, small RNA and ribosomal RNAs. Overall, more than 540,000 transcripts are analyzed with this tool. With the

Table 3 Enrichment analysis of genes differentially spliced in PE

Gene Set	Description	Expect	Ratio	p value	FDR
Gene ontology biological processes					
GO: 0,016,192	Vesicle-mediated transport	70.148	1.6394	4.34E-08	0.000199
GO: 0,030,198	Extracellular matrix organization	12.534	2.7924	4.37E-08	0.000199
GO: 0,043,062	Extracellular structure organization	14.449	2.4916	4.80E-07	0.001455
GO: 0,006,887	Exocytosis	32.293	1.889	1.25E-06	0.002845
GO: 0,072,359	Circulatory system development	37.061	1.8078	1.7E-06	0.003095
GO: 0,031,102	Neuron projection regeneration	1.8783	5.3239	1.41E-05	0.021369
GO: 0,031,103	Axon regeneration	1.5532	5.7944	1.85E-05	0.024045
GO: 0,048,678	Response to axon injury	2.4201	4.5452	2.55E-05	0.028951
GO:0,035,295	Tube development	35.832	1.7024	3.19E-05	0.030548
GO: 0,045,055	Regulated exocytosis	28.283	1.8032	3.38E-05	0.030548
KEGG pathways					
hsa04510	Focal adhesion	7.8332	2.6809	3.33E-05	0.010845
hsa04512	ECM-receptor interaction	3.2277	3.408	0.000337	0.05495
hsa04960	Aldosterone-regulated sodium reabsorption	1.4564	4.8063	0.000507	0.055129
Reactome pathways					
R-HSA-1474244	Extracellular matrix organization	11.893	2.8589	2.91E-08	5.03E-05
R-HSA-216083	Integrin cell surface interactions	3.3584	4.7641	1.70E-07	0.000147
R-HSA-114608	Platelet degranulation	5.0969	2.9429	0.000168	0.078328
Disease_GLAD4U					
PA443275	Adhesion	22.33	2.4183	2.04E-09	5.55E-06
PA443553	Brain diseases	16.179	2.2251	7.22E-06	0.008322
PA166048714	Pregnancy	11.194	2.5013	9.18E-06	0.008322
PA443657	Central nervous system diseases	16.674	2.159	1.39E-05	0.009476
PA444447	Carcinoma, hepatocellular	11.077	2.4374	2.1E-05	0.011403
PA443853	Dementia	8.1915	2.6857	2.83E-05	0.012844
PA445403	Pregnancy complications	8.4538	2.6024	4.57E-05	0.016622
PA166123006	interstitial fibrosis	2.128	4.6992	4.89E-05	0.016622
PA443812	Cri-du-chat syndrome	0.46642	10.72	6.92E-05	0.020562
PA445080	Neovascularization, pathologic	6.3841	2.8195	8E-05	0.020562
Disease_OMIM					
146,110	Hypogonadotropic hypogonadism 7 with or without anosmia	0.11153	35.866	3.14E-06	0.000207
611,162	Malaria, susceptibility to malaria, resistance to, included	0.13542	29.537	7.35E-06	0.000242
152,700	Systemic lupus erythematosus	0.063729	31.383	0.001671	0.036762
104,300	Alzheimer disease	0.087628	22.824	0.003234	0.053355

TAC tool, a splicing index can be calculated and a statistical value associated to it. The splicing index was calculated by the Transcriptome Analysis Console (TAC) from Affymetrix, using the following formula:

$$\text{Log2} \left[\frac{\left(\frac{\text{probeset1 intensity}}{\text{Gene1 intensity}} \right)}{\left(\frac{\text{probeset1 control intensity}}{\text{Gene1 control intensity}} \right)} \right] \quad (1)$$

The probeset is defined by the fluorescence of a given probe (either a junction probe, or an exon-specific probe),

present in the array. More details can be obtained in (Jimeno-Gonzalez et al. 2015).

To be able to evaluate the splicing variation on an individual basis, we first defined an individual splicing index for each sample (Individual splicing index—ISI). Inside a given gene and for a given placental sample, we obtained the different fluorescent measures for each of the probes spanning the gene. We then selected the probe with the highest splicing index and divided its fluorescent signal level by the geometric mean of the complete group of probes. For a given placental sample, the relative splicing index for Gene A is therefore given by

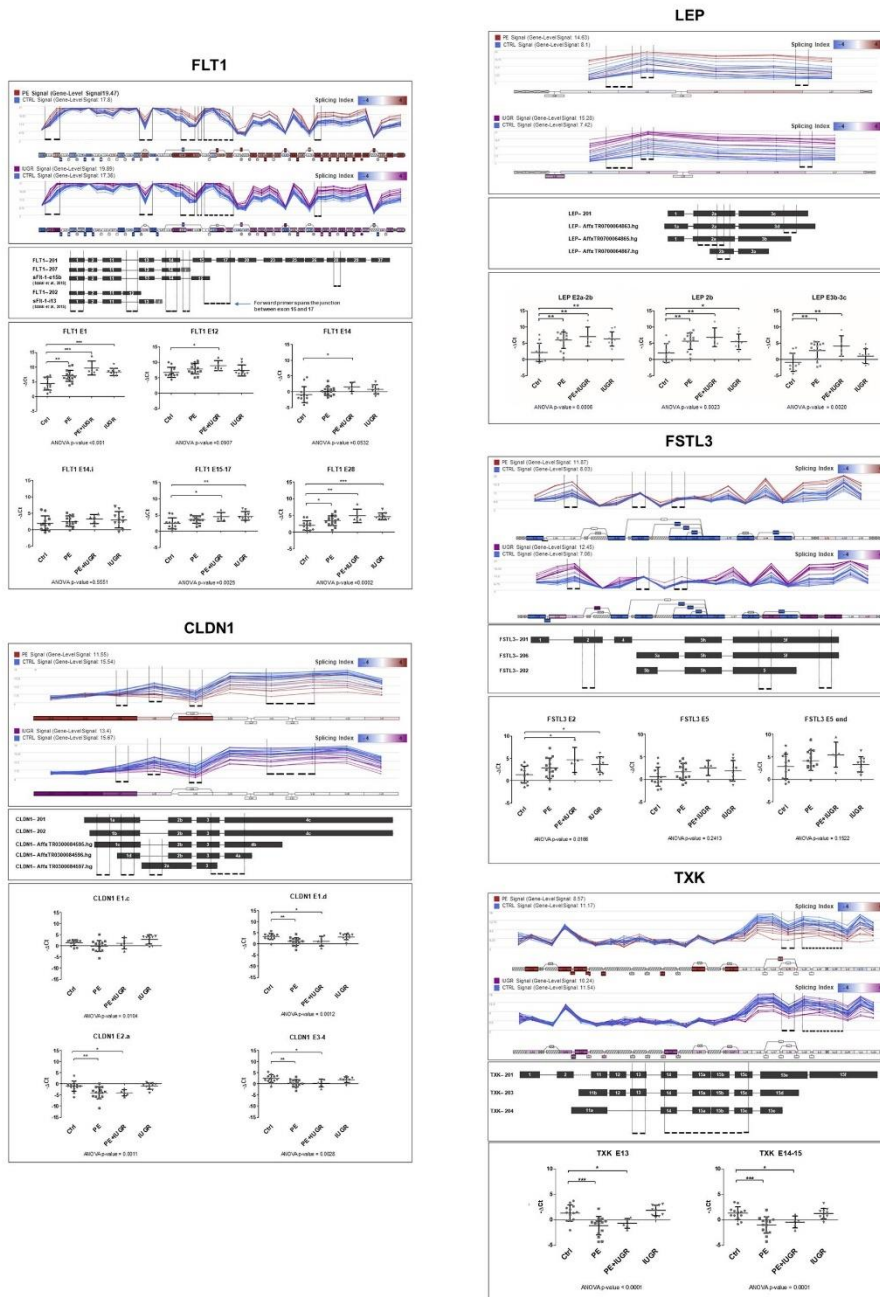


Fig. 3 Locus-specific RT-qPCR analysis of genes that were found modified in pathological placentas. Each panel represents the splicing profile of a gene. For instance, for *FSTL3* there is an increased splicing index in the 5' and 3' regions of the gene, in preeclampsia versus controls and IUGR vs controls (two upper graphs), drawn with the positions of the primer couples that were used for the RT-qPCR. Significant alterations are in this case essentially detected in the E2 tested region, while the others are not significant, consistently with the microarray graph

$$\frac{\text{MAX}(\text{FprobeGAI}_i)}{\sqrt[n]{\prod_1^n \text{FprobeGAI}_i}} \tag{2}$$

where 'FprobeGAI' refers to the log2(fluorescence level) of a given *i* probe in gene A. An example of the calculation is given as Supplementary Fig. S4. In this example, for the long non-coding RNA RP11-113122.1, the strongest splicing index is given for the probe PSR0500147825.hg.1. It appears that the abnormal splicing compared to the rest of the probes occurs clearly for some placentas but not for all.

Library preparation, hybridization and data acquisition were performed by GENOMIC platform according to manufacturer's instructions. ClariomD microarray data were extracted using the Transcriptomic Analysis Console provided by Affymetrix. The data from the control subjects of the two cohorts were merged to generate the control group data. When compared against the PE or the IUGR data, a batch correction was applied using the built-in *Batch* parameter in TAC.

Genomic DNA samples were genotyped using the Infinium OmniExpress-24 kit (Illumina) array, in collaboration with Plateforme P3S, Sorbonne Université – site Pitié Salpêtrière, Paris, France. Data were extracted using Genomestudio 2.0.

Real time-qPCR

Four µg of RNAs from each placental sample were pre-treated with DNase-I to remove genomic DNA contamination with RQ1 RNase Free DNase (Promega) according to manufacturer's instructions. The DNase-I treated RNA samples were then retrotranscribed to cDNA, using the M-MLV kit (Invitrogen) according to manufacturer's instructions. Placental cDNAs were analyzed by RT-qPCR with SensiFAST SYBR No-ROX One-Step Kit (Bioline). To calculate probe expression levels, -ΔCt was calculated by normalizing individual Ct values for each probe of interest, to house-keeping gene (*SDHA*) Ct. Primers are listed Supplemental Table S7.

Statistical analyses and computational details

Institut Cochin Cohort full cohort and Angers Control Samples were used for sQTL interrogation. SNPs whose three genotypes (AA, AB, BB) were not represented in at least two samples were discarded (corresponding to Minor Allele Frequency > 20%). A total of 331,204 SNPs was assessed against 48 individual splicing indexes using *MatruxeQTL* (R package) under the ANOVA model and accounting for gestational age and sample sex as covariates. This means that a full genotypic model was used, surmising independent effects of the three possible genotypes, and not always additive effects of one given allele.

MatruxeQTL generates a matrix correlating gene expression and SNP variants using an accelerated bioinformatics procedure basically dividing the initial matrix in smaller blocks. For cis-sQTL, the distance parameter was fixed to 1 Mb while for trans-sQTL all the genome was interrogated. Only cis-sQTLs and trans-sQTLs with an FDR < 0.05 were used for downstream analyses.

For the surrogate variable analyses (SVA), we used the SVA package available in R (Leek et al. 2012) on R version 3.6.3 (2020-02-29), to estimate latent sources of variations (surrogate variables) in our datasets. We considered three different subsets of samples: (1) CTRL + PEall (PE only + PE_IUGR), (2) CTRL + PEonly, and (3) CTRL + IUGR. The analysis was performed stratified by cases and controls thanks to the inclusion of the disease status variable, which described whether the sample had disease (= 1) or if it was a control sample (= 0). The *mod* and *mod0* parameters in the SVA package allow to build a linear model that describes the gene expression dataset according to the included variables with the function *model.matrix*. The two models were built as follow, in this case disease status is the Variable of Interest:

```
mod = model.matrix (Disease.status + Gestational.age + Birth.weight + Sex)
mod0 = model.matrix (Gestational.age + Birth.weight + Sex)
```

Then the *num.sv* function was used to see whether differences between the two linear models can be explained only by the presence of the variable of interest (disease status) or if any other surrogate variables can be identified, followed by the *sva* function to test whether these surrogate variables are significant:

```
n.sv = num.sv(edata,mod,method="leek")
svobj = sva(edata,mod,mod0, n.sv=n.sv)
```

No additional surrogate variables were found to play a role on gene expression differences in any of the three



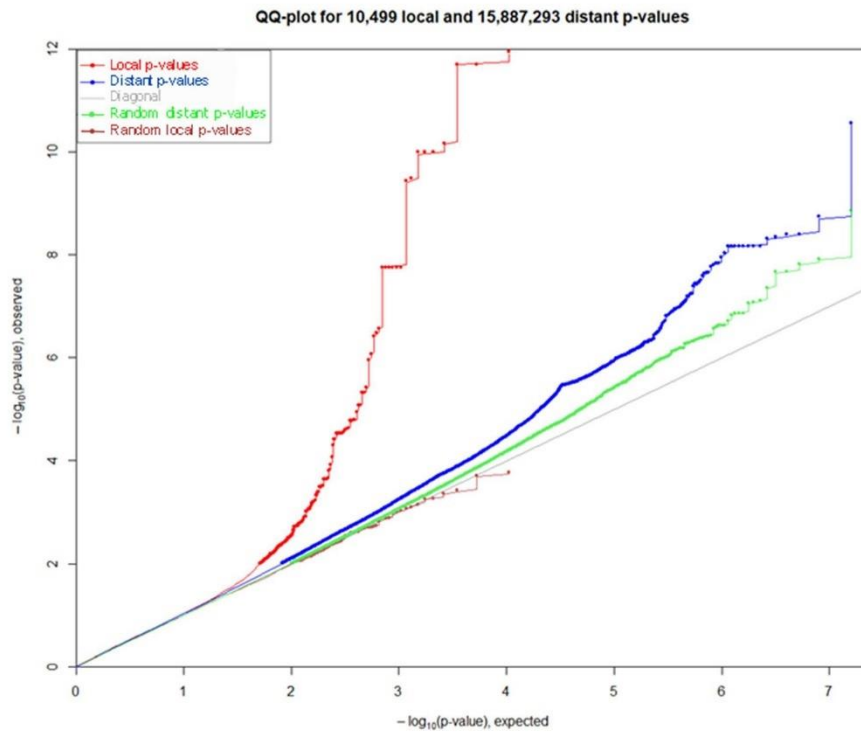


Fig. 4 QQ-plot measuring the discrepancy between real data and expected data from random (grey line)

datasets analyzed. At this stage we wanted to identify genes that could be significantly associated with either of the variables: disease status, gestational age, birth weight, Sex. In order to do so the, Variable Of Interest was assigned in turn to each of the variables i.e. disease status, gestational age, birth weight, sex, followed by *p value* function that performs a F-statistic test to assign *p-value* to each gene in relation to the influence of the Variable of Interest under scrutiny (significance threshold at *p val* < 0.05). For example, to identify genes potentially influenced by “gestational age” the following code was used:

```
#Creating the full model
mod= model.matrix (~as.factor(Disease.status)
+Gestational.age+Birth.weight
+Sex, data=pheno)

#Creating the null model (mod)
- only adjustment variables
mod0= model.matrix (~as.factor(Disease.status)
+Birth.weight+Sex, data=pheno)

#identifying latent factors – no factors identified
n.sv = num.sv(edata,mod,method="leek")
svobj = sva(edata,mod,mod0, n.sv=n.sv)

#Testing for significant association between
Variable of Interest and genes
pValues = f.pvalue(edata,mod,mod0)
```

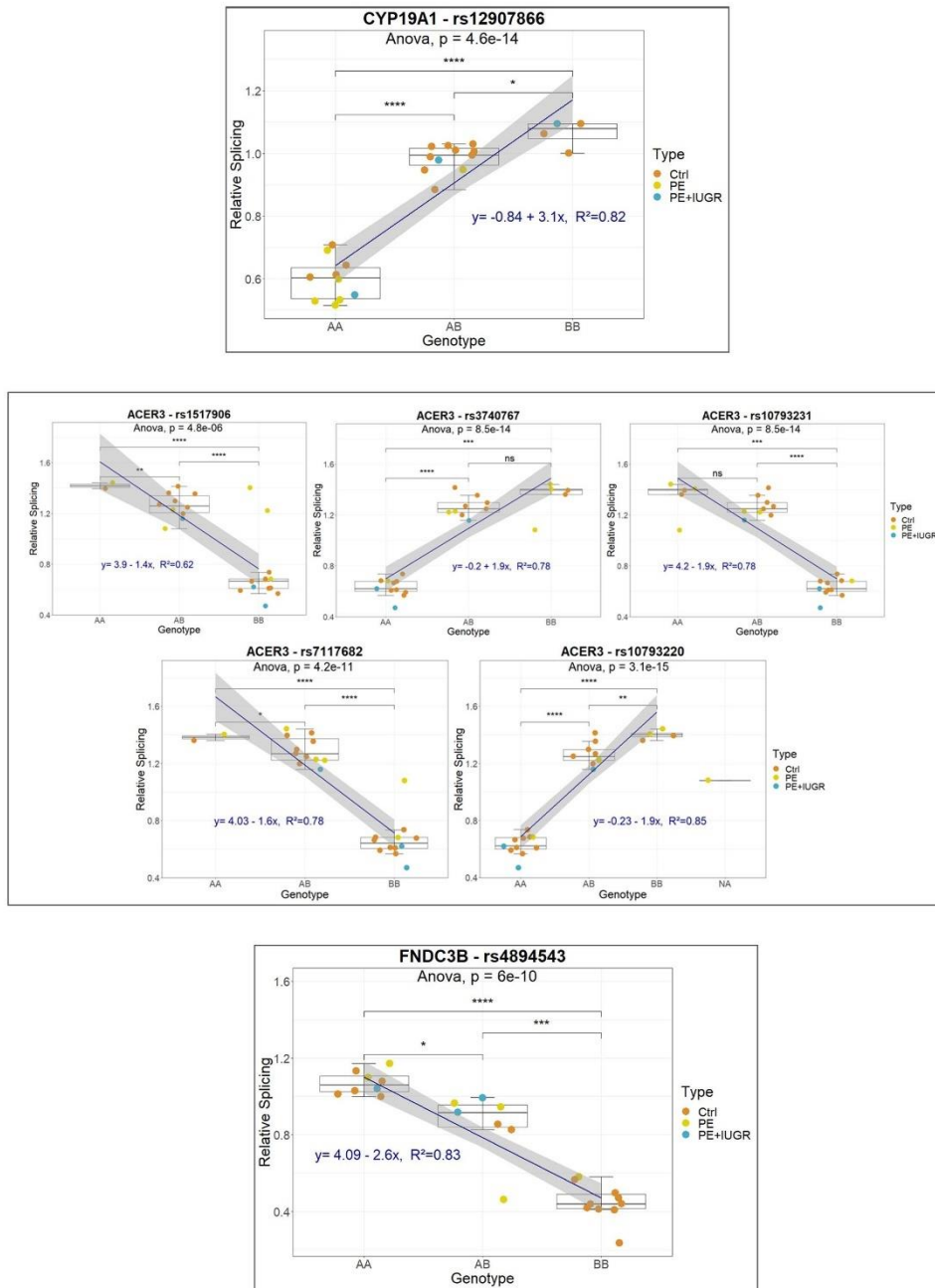



Fig. 5 Analysis of genotype versus splicing at the individual level for cis sQTLs in the placenta



Content courtesy of Springer Nature, terms of use apply. Rights reserved.

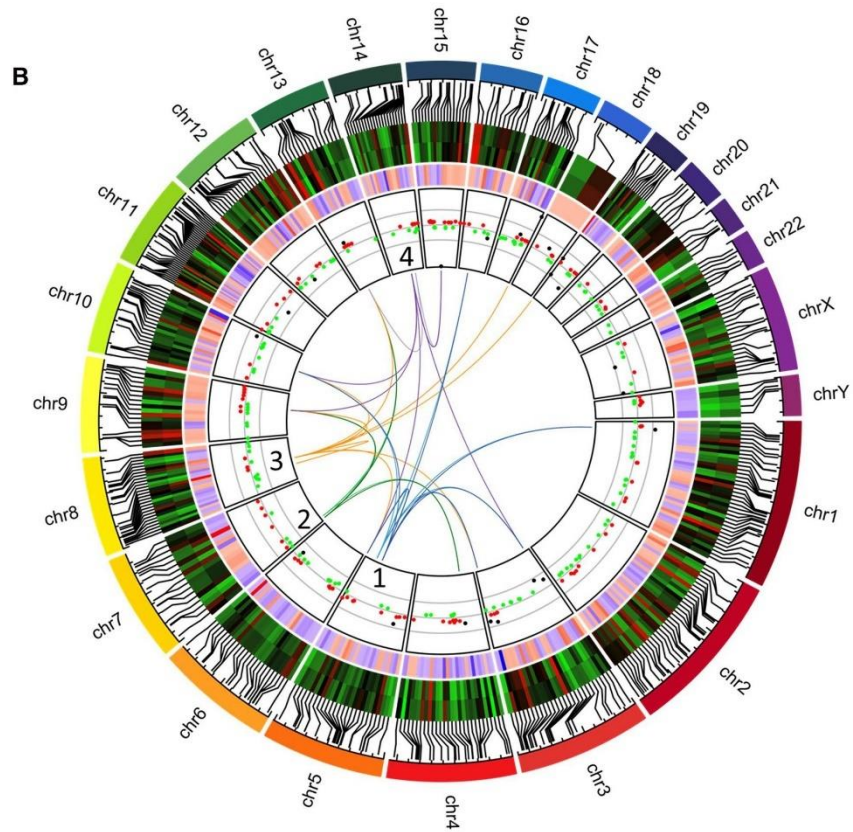
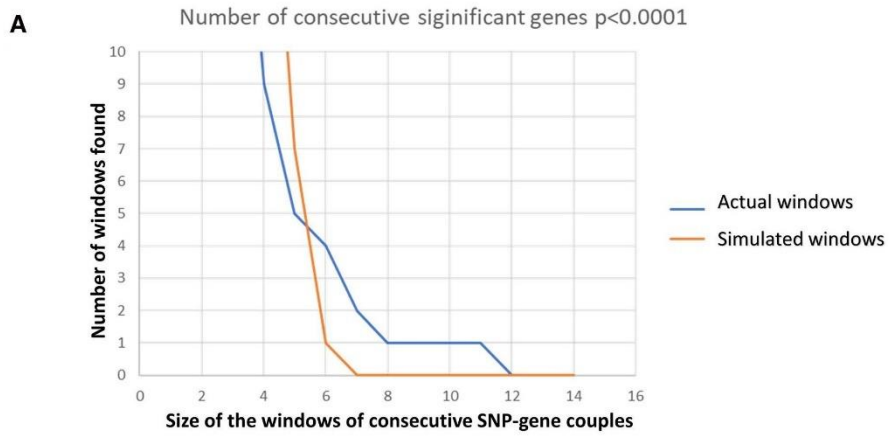


Fig. 6 Presentation of trans-sQTL. **a** Monte-Carlo analysis of windows of consecutive trans sQTL in the placentas. Trans sQTL were defined at a threshold of $p < 0.0001$ (see text). In the windows computed from the actual dataset (blue line) the longest found was of 11 consecutive SNP-genes. In the simulated windows, the longest found was composed of 6 consecutive SNP-genes (4 such in the actual dataset). Overall, while one > 5 window was found in the simulated data, 9 were found in the actual dataset. **b** circus-plot presenting the four trans-sQTL regions analyzed further in the study. Tracks are numbered from the outer to the inner part of the plot. 1st track: representation of each chromosome. 2nd track: location of the 467 genes used in the 3rd track. 3rd track: heatmap of the splicing indexes in PE and Ctrl samples for the 467 genes presenting a standard deviation equal or higher than 0.5: (Red = 19.42, Green = 3.82). 4th track: ratio of downregulation/upregulation of the 467 genes between PE and Ctrl (Red: > 3 (increased in PE), Blue < -3 (increased in controls). 5th track: Splicing index of the 286 most differentially spliced genes observed in TAC comparing Ctrl vs PE (red dots = gene with SI between 10 and 3.99, green dots = genes with SI between -3.99 and -10, black dots = genes with SI higher than 10 or lower than -10). 6th track: constant trans-eQTLs. Blue (1) SNPs located in ARHGAP26/AS; Green (2) SNPs located in LOC105375161; Orange (3) SNPs located in LOC105375897; Purple (4) SNPs located in GPHN/LOC105370538. The other side of the line marks the location of the gene in which the relative splicing index is affected by the corresponding SNP

In the boxplots, correlation of Individual Splicing Index (ISI) of the gene with the locus genotype was assessed by one-way ANOVA. Group–group comparison of means was executed by *T* test ($*p = 0.05$, $**p = 0.01$, $***p = 0.001$, $****p = 0.0001$). Linear regression was performed to determine the effect of genotype on ISI in each cis-QTL represented.

Gene enrichment analysis was performed using the Gene Set Enrichment Analysis module available in WebGestalt. The principle of enrichment relative to any database used as reference is the following. The list of ranked genes of the study is compared to a given set of genes specific of a biological function, a gene ontology term, or a given disease, for instance. The rank of occurrence of each gene is recorded and compared to the average expected density (for instance 100 genes out of 10,000 are expected to occur at a frequency of one every 100 genes. When the density is higher than expected, the enrichment score increases. It will reach a maximum or a minimum that will be compared with 1000 random rankings, and the actual value obtained will be compared with the random values yielding a p-value and an enrichment score. The reference databases analyzed are KEGG (<https://www.genome.jp/kegg/>), Reactome (<https://reactome.org/>), OMIM (omim.org), GO (<http://geneontology.org/>).

For RT-qPCR analyses, statistical significance of differences in expression levels of each tested region was assessed by analyzing the $-\Delta\text{Ct}$ distributions between groups (Ctrl ($n = 13$), PE ($n = 15$), PE + IUGR ($n = 5$) and IUGR ($n = 10$)) by 1-way ANOVA followed by Dunnett's

multiple comparison test between diseased groups and control ($*p < 0.05$; $**p < 0.01$; $***p < 0.001$).

The Monte-Carlo analysis was carried out using a homemade program in VisualBasic accompanying an Excel sheet entitled trans_sQTL_Relative splicing ANOVA, provided as a supplementary material.

The circus plot graph was generated according to the following documentation: https://jokergoo.github.io/circulize_book/book/.

Discussion

In this study, we present for the first time, to the best of our knowledge, a systematic analysis of alternative splicing alterations in the pathological human placenta. After describing splicing in IUGR and PE compared to control placentas, we validated the finding at the exon level through targeted quantitative RT-qPCR. The splicing index alterations that we observed may be a consequence of the disease, or maybe driving the disease (although in some cases, they can be indirectly triggered by birth weight or shorter gestational age). In fact, the two mechanisms can be operative differently for some specific genes. The large published GWAS analysis of preeclampsia (McGinnis et al. 2017), revealed a SNP in the vicinity of the gene FLT1 (rs4769613), not in the coding region, possibly influencing splicing, that we did not find significant in our study probably due to the limited size of our sample. Indeed, our current sample size qualify our study as exploratory; with a larger sample size, other sQTL with milder effects could be found. In the specific case of sFLT1, one can imagine that a variant may influence splicing and result in being disease-prone. Currently, the cause or consequence question cannot be resolved directly in our study, but is an interesting open question that could be addressed in cell and animal models.

Another interesting question is the relation between placenta eQTL (Peng et al. 2017; Kikas et al. 2019) and the splicing QTL that we identified here. Peng and coworkers surmised that the genes affected in the placenta may mark future risks for the patients (cardiovascular, neurologic). We compared our list of 48 top cisQTL corresponding to 12 different genes with the cis eQTL (3218 cis eQTL were found as associated to SNP variant at the expression level). Four genes were in common between the two lists (33%). A contingency Chi-square calculated between the two datasets revealed a marginally significant enrichment ($p = 0.034$), while none was detected for the trans eQTL. This suggests that there may be a link between expression and splicing regulation in the placenta.

Amongst the genes that we found alternatively spliced in disease, FLT1 was identified amongst the genes that are up-regulated as well as highly differentially spliced in both

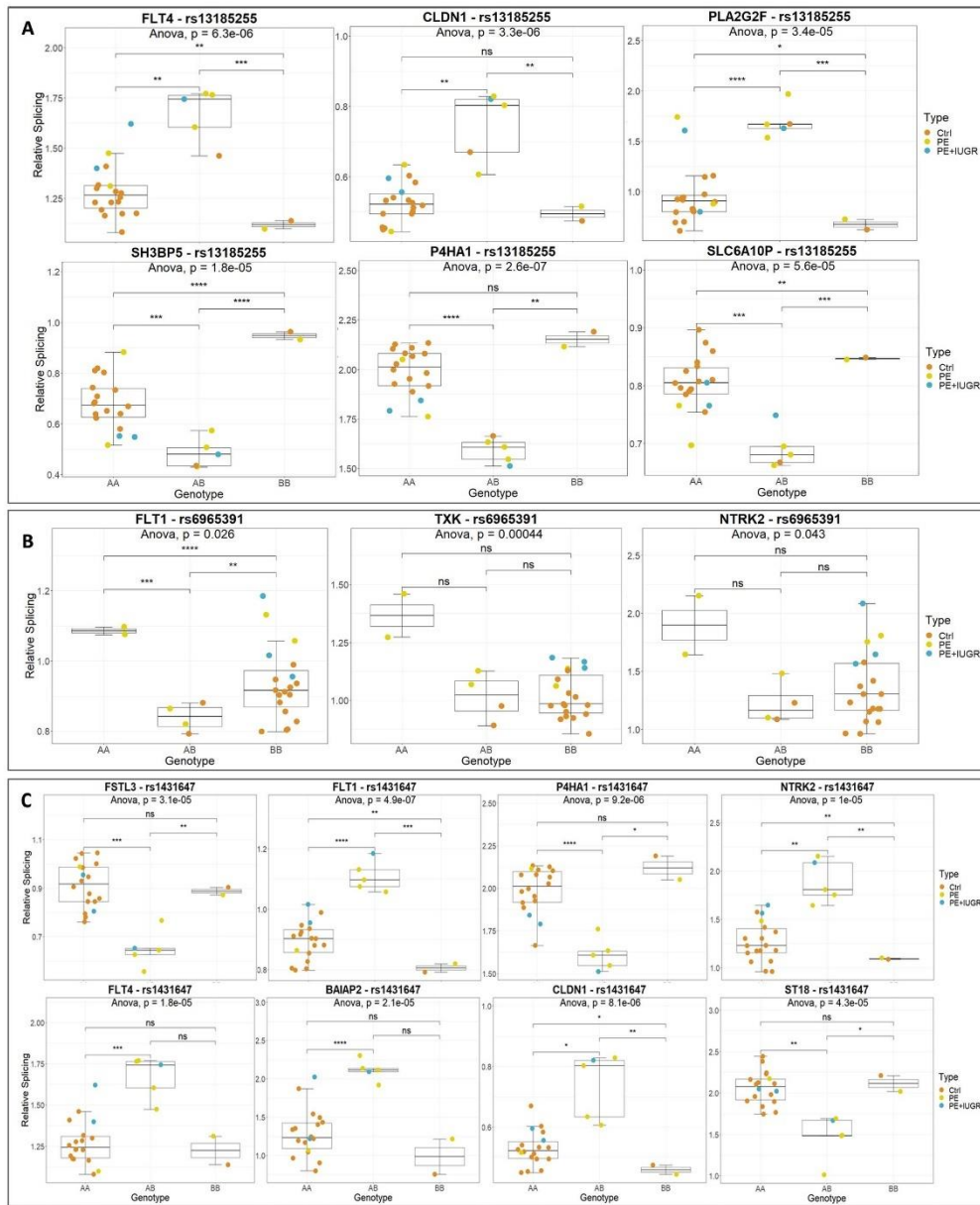


Fig. 7 Presentation of trans-sQTLs data for three SNPs found in the regions presented in Fig. 6. **a** rs13185255 from the chromosome 5 trans-sQTLs, **b** rs6965391 from the chromosome 7 trans-sQTLs, **c** rs1431647 from chromosome 8. **d** rs7145295 and rs7151086 from chromosome 14

pathological states, which is a good confirmation of the approach, given the abundant literature positing FLT1 alternative splicing as a hallmark of preeclampsia. The quantitative analysis at the exon level revealed large heterogeneities along the mRNA molecules. We chose primer pairs located in the 1st exon, the 12th exon, the 14th exon, the 28th and between the 15th and the 17th exon. There were significant differences in expression in the first exon that is common to the different isoforms, confirming the well-known induction of this gene in the disease state. The significance weakened for exon 12 and 14, indicating that this increase in expression was untrue for this part of the gene, suggesting a relative decrease of long isoforms encompassing exons 12 and 14 in pathological placentas. When the farthest exon was analyzed (E28), the difference is also significant but to a lesser extent than for Exon 1. The induction ratio in disease compared to control was ~11-fold in exon 1, and ~fivefold in exon 28. This indicates that short isoforms are increased in the pathological state. The data are consistent with an overall induction of the gene in disease, with a more pronounced overexpression of the shorter isoforms.

CLDN1 profile was opposite to FLT1, with a trend towards decrease in pathological state in the 3' region of the gene. The differential expression does not concern the region located in the 5' region of the first exon (E1c). However, at the 3' region of the same exon (E1d), a decreased expression in PE, but not in IUGR is observed. The same trend applies to the two more 3' regions of exon 2, 3 and 4. The amount of the protein coded by CLDN1 is significantly reduced in PE placentas (Lievano et al. 2006). Here, we show that the two CLDN1 shortest transcripts are differentially expressed in PE, but not the longest one.

Another example of a gene where differentially expressed transcripts can be identified in disease is the one coding for leptin (LEP). As expected, LEP was highly upregulated at the gene level in disease compared to control, confirming numerous previous observations, including from our group (Madeleneau et al. 2015; Biesiada et al. 2019). The alternative splicing profile of LEP showed that the first part of the gene (exons 1–2a) has a higher expression in diseased placentas as compared to controls. We designed primers to interrogate the expression of exon 2a, found only in three out of the four isoforms putatively expressed in the tissue (LEP-201, LEP—Affx TR0700064863.hg, LEP—AffxTR0700064865.hg), exon 2b common to all isoforms, and finally of the boundaries between Exons 3b and 3c (encompassed in LEP-201 and LEP—Affx TR0700064863.hg). The RT-qPCR results showed a significant upregulation of all three tested regions in PE compared to control, whilst only the 2a-2b region showed a higher expression in IUGR samples. Our results clearly indicate that IUGR and PE have different repertoires of LEP isoforms.

FSTL3 is also known as increased in preeclampsia (Founds et al. 2009; Gormley 2017). In this case, the increase of the gene was observable all along the molecule, but only significantly in 5' exons. In summary, the middle region of the gene is not deregulated while there is an increase in isoforms were this section could be spliced out. We also present the profile of TXK kinase. While the 5' part of the gene was not different according to the microarray data, the 3' appeared selectively deregulated in PE with or without IUGR. This deregulation was confirmed by RT-qPCR as shown by analysis of exons 13 and 14–15 that behave very similarly. This tyrosine kinase has not previously been associated with preeclampsia in the literature, but the mRNA is highly expressed in the placenta (trophoblast and endothelial cells), and the protein participates in immune regulation.

Pathology-driven alterations of alternative splicing require specific mechanisms and a specific molecular machinery, incorporating in particular small nuclear ribonucleoproteins, such as U1, U2, U4, U5 and U6, and spliceosome proteins, as nicely reviewed in (Scotti and Swanson 2016). To date, alternative splicing in complex diseases has essentially been considered in neurological and neuromuscular disorders, such as the abnormal splicing of Tau proteins encoding genes responsible for tauopathies (Bartsch et al. 2016). A paradigmatic example of alternative splicing in disease is the LaminA gene (*LMNA*), whose different dominant mutations induce respectively, and independently, muscular dystrophy, progeria, or dilated cardiomyopathy. In these cases, a monogenic variant induces a complex disease. However, understanding altered splicing in the context of polygenic and highly multifactorial diseases and processes is trickier, but starts to be addressed. For instance, in the aging brain, alternative splicing was recently studied in 44 mouse brain areas (Li et al. 2019). Interestingly, premature aging of the placenta is thought as a putative general feature of preeclampsia (Manna et al. 2019).

Any evaluation of the splicing species for complex diseases or conditions requires an accurate description of the spliced species found in the relevant organ. In obstetric diseases, this pivotal organ is the placenta. Therefore, a first effort should be carried out to evaluate the diseased placenta, which is the exact purpose of the present article. Here, we demonstrate that genes that harbor differential splicing are indeed a component in the pathogenesis of PE and IUGR. These associations with splicing are not systematically associated with a difference in the overall level change of a given mRNA, and are partly piloted by genomic variants.

Our sample size is relatively small, and our results have to be considered as a proof-of-concept warranting other targeted studies. Nevertheless, the simulation data presented in (Huang et al. 2018), indicate that a QTL with an effect of > 1 Standard Deviation is detected with sample of the size

of ours, if the Minor Allele Frequency is above 0.2 (which is the case here, since we selected SNPs for which each genotype was carried by at least two individual samples). Also for individual probes, we have a QTL effect > 1 SD in many cases, due to our stringent selection of the largest splicing indexes. Independently of variations in the expression level, we found that the subset of genes that are alternatively spliced have a disease-specific profile, with marked differences between preeclampsia and IUGR, showing in particular that the first condition but not the second, correlates with brain diseases. This fascinating observation is in accordance with many recent studies showing strong links between preeclampsia and brain vascular diseases (Andolf et al. 2020; Patel et al. 2020; Miller 2019; Basit et al. 2018; Cheng and Sharma 2016). For example, deregulation of alternative splicing of the gene *STOX1*, involved in preeclampsia and Alzheimer's disease (Dijk et al. 2005, 2010) induces a disequilibrium of its two isoforms and increases the risk of disease (Vaiman and Miralles 2016; Ducat 2020).

Focusing our work on 48 genes that were found strongly alternatively spliced between healthy samples and disease, we showed that genetic variants (SNP) impact these splicing differences. On the one hand, the cis-sQTLs had an additive effect, which is consistent with an impact of the genetic variant either on the mRNA tridimensional structure, or on the binding of splicing factors, that would affect the splicing of the RNA molecule carrying the variant. On the other hand, trans-sQTLs could give insights on how specific loci act on splicing at various genome locations. After a stringent screen, we show an allele-specific impact of four trans sQTL loci on splicing.

The influence of the cis and trans-sQTL on splicing was generally disconnected from the disease state. This issue is not surprising since, albeit we initially restrict our genes of interest to genes that are alternatively spliced in disease, this screen was preferably used to detect genes that are highly splicing-prone. The genetic determination of the splicing is driven by specific sQTLs that may not be a strong determinant of the disease status, compared to other regulators modulating, for instance, gene expression levels. One exception could be rs1431647. This SNP located in the long non-coding RNA LOC105375897 is systematically associated with the disease when the SNP is heterozygous, associated systematically in this case to divergent splicing for *FLT1*, *FSTL3*, *P4HA1*, *NTRK2*, *FLT4*, *BAIAP2*, *CLDN1* and *ST18*. The ways these variants play their function remains an open mechanistic question.

Splicing in the placenta was observed previously for collagen 1 (Type XIII collagen) in the early human placenta (Juvonen et al. 1993). A more systematic approach was used by Kim and coworkers (Miyagawa et al. 2012), revealing that compared to other tissues, the splicing in the placenta presents specific aspects; interestingly, they found

that enrichment of genes involved in placental anomalies and pre-term birth are selectively enriched in the set of placental alternatively spliced genes. One of the most studied gene in terms of pathological alternative splicing is *FLT1*, recently shown to be alternatively spliced through the action of U2AF65 and JMJD6 (Eddy et al. 2020).

In summary, these analyses de novo re-identified a known factor of preeclampsia and IUGR, alternative splicing of *FLT1*, which validates the approach, and found hundreds of other disease-associated genes that are affected by splicing. We also show that these alterations are potentially genetically based. This present study paves the way towards a systematic exploration of the mechanisms and consequences of alternative splicing in normal and pathological placental function.

Acknowledgements We thank the genomic platform of Cochin Institute (Paris) and the Post-Genomic Platform of Sorbonne University (Paris), where the genomic data were generated. The PhD projects of CRSM and CA is funded by the European Union's Horizon 2020 research and innovation program under Marie Skłodowska-Curie Actions Innovative Training Network (H2020-MSCA-ITN 2017), Grant No. 765274, acronym iPLACENTA (<http://www.iplacenta.eu>). We thank Dr Odile Blanchet and the Centre for Biological Resources (CHU Angers, France) for the provision of biological samples from the Angers University Hospital Cohort.

Author contributions All the authors made a significant contribution to the present work.

Funding The PhD projects of CRSM and CA is funded by the European Union's Horizon 2020 research and innovation program under Marie Skłodowska-Curie Actions Innovative Training Network (H2020-MSCA-ITN 2017), Grant No. 765274, acronym iPLACENTA (<http://www.iplacenta.eu>); in addition, recurrent funding was obtained from INSERM. The Angers University Hospital Cohort was funded by a grant from the Angers University Hospital, France.

Availability of the data The datasets supporting the conclusions of this article are available in the EMBL-EBI repository, E-MTAB-9416.

Code availability Monte-Carlo program associated to an Excel file provided as supplementary material).

Compliance with ethical standards

Conflict of interest On behalf of all authors, the corresponding author states that there is no conflict of interest.

Ethics approval Listed in Material and methods section.

Consent to participate Listed in Material and methods section.

Consent for publication All the authors validated the document.

Open Access This article is licensed under a Creative Commons Attribution 4.0 International License, which permits use, sharing, adaptation, distribution and reproduction in any medium or format, as long as you give appropriate credit to the original author(s) and the source,

provide a link to the Creative Commons licence, and indicate if changes were made. The images or other third party material in this article are included in the article's Creative Commons licence, unless indicated otherwise in a credit line to the material. If material is not included in the article's Creative Commons licence and your intended use is not permitted by statutory regulation or exceeds the permitted use, you will need to obtain permission directly from the copyright holder. To view a copy of this licence, visit <http://creativecommons.org/licenses/by/4.0/>.

References

- Andolf E, Bladh M, Moller L, Sydsjo G (2020) Prior placental bed disorders and later dementia: a retrospective Swedish register-based cohort study. *BJOG* 127:1090
- Aouache R, Biquard L, Vaiman D, Miralles F (2018) Oxidative stress in preeclampsia and placental diseases. *Int J Mol Sci* 19:1496
- Arroyas M, Calvo C, Rueda S, Esquivias M, Gonzalez-Menchen C, Gonzalez-Carrasco E, Garcia-Garcia ML (2020) Asthma prevalence, lung and cardiovascular function in adolescents born preterm. *Sci Rep* 10:19616
- Bartsch E, Medcalf KE, Park AL, Ray JG (2016) Clinical risk factors for pre-eclampsia determined in early pregnancy: systematic review and meta-analysis of large cohort studies. *BMJ* 353:i1753
- Basit S, Wohlfahrt J, Boyd HA (2018) Pre-eclampsia and risk of dementia later in life: nationwide cohort study. *BMJ* 363:k4109
- Biesiada L, Sakowicz A, Grzesiak M, Borowiec M, Lisowska M, Pietrucha T, von Kaisenberg C, Lewandowski K (2019) Identification of placental genes linked to selective intrauterine growth restriction (IUGR) in dichorionic twin pregnancies: gene expression profiling study. *Hum Genet* 138:649–659
- Chabrun F, Huetz N, Dieu X, Rousseau G, Bouzillé G, Chao JM, de la Barca V, Procaccio GL, Blanchet O, Legendre G, Mirebeau-Prunier D, Cuggia M, Guardiola P, Reynier P, Gascoin G (2019) Data-mining approach on transcriptomics and methylomics placental analysis highlights genes in fetal growth restriction. *Front Genet*. 10:1292
- Cheng SB, Sharma S (2016) Preeclampsia and health risks later in life: an immunological link. *Semin Immunopathol* 38:699–708
- Crispi F, Hernandez-Andrade E, Pelsers MM, Plasencia W, Benavides-Serralde JA, Eixarch E, Le Noble F, Ahmed A, Glatz JF, Nicolaidis KH, Gratacos E (2008) Cardiac dysfunction and cell damage across clinical stages of severity in growth-restricted fetuses. *Am J Obstet Gynecol* 199(254):e251–258
- Do SC, Druzin ML (2019) Systemic lupus erythematosus in pregnancy: high risk, high reward. *Curr Opin Obstet Gynecol* 31:120–126
- Doridot L, Chatre L, Ducat A, Vilotte JL, Lombes A, Mehats C, Barbaux S, Calicchio R, Ricchetti M, Vaiman D (2014) Nitroso-redox balance and mitochondrial homeostasis are regulated by STOX1, a pre-eclampsia-associated gene. *Antioxid Redox Signal* 21:819–834
- Ducat A, Vargas A, Doridot L, Bagattin A, Lerner J, Vilotte JL, Buffat C, Pontoglio M, Miralles F, Vaiman D (2019) Low-dose aspirin protective effects are correlated with deregulation of HNF factor expression in the preeclamptic placentas from mice and humans. *Cell Death Discov* 5:94
- Ducat A, Couderc B, Bouter A, Biquard L, Aouache R, Passet B, Doridot L, Cohen MB, Ribaux P, Apicella C et al (2020) Molecular mechanisms of trophoblast dysfunction mediated by imbalance between STOX1 isoforms. *iScience* 23:101086
- Dymara-Konopka W, Laskowska M (2019) The role of nitric oxide, ADMA, and homocysteine in the etiopathogenesis of preeclampsia-review. *Int J Mol Sci* 20:2757
- Eddy AC, Chapman H, Brown DT, George EM (2020) Differential regulation of sFlt-1 splicing by U2AF65 and JMJD6 in placental-derived and endothelial cells. *Biosci Rep* 40:20193252
- Fagerberg L, Hallstrom BM, Oksvold P, Kampf C, Djureinovic D, Odeberg J, Habuka M, Tahmassebpour S, Danielsson A, Edlund K et al (2014) Analysis of the human tissue-specific expression by genome-wide integration of transcriptomics and antibody-based proteomics. *Mol Cell Proteomics* 13:397–406
- Fandino J, Toba L, Gonzalez-Matias LC, Diz-Chaves Y, Mallo F (2019) Perinatal under nutrition, metabolic hormones, and lung development. *Nutrients* 11:2870
- Foundas SA, Conley YP, Lyons-Weiler JF, Jeyabalan A, Hogge WA, Conrad KP (2009) Altered global gene expression in first trimester placentas of women destined to develop preeclampsia. *Placenta* 30:15–24
- Gardina PJ, Clark TA, Shimada B, Staples MK, Yang Q, Veitch J, Schweitzer A, Awad T, Sugnet C, Dee S et al (2006) Alternative splicing and differential gene expression in colon cancer detected by a whole genome exon array. *BMC Genomics* 7:325
- Gascoin-Lachambre G, Buffat C, Rebouret R, Chelbi ST, Rigourd V, Mondon F, Mignot TM, Legras E, Simeoni U, Vaiman D, Barbaux S (2010) Cullins in human intra-uterine growth restriction: expression and epigenetic alterations. *Placenta* 31:151–157
- Gormley M, Ona K, Kapidzic M, Garrido-Gomez T, Zdravkovic T, Fisher SJ (2017) Preeclampsia: novel insights from global RNA profiling of trophoblast subpopulations. *Am J Obstet Gynecol* 217(200):e201–200.e217
- Gu Z, Gu L, Eils R, Schlesner M, Brors B (2014) circlize: Implementations and enhances circular visualization in R. *Bioinformatics* 30:2811–2812
- Gupta A, Kaliaperumal S, Setia S, Suchi ST, Rao VA (2008) Retinopathy in preeclampsia: association with birth weight and uric acid level. *Retina* 28:1104–1110
- Huang QQ, Ritchie SC, Brozynska M, Inouye M (2018) Power, false discovery rate and Winner's Curse in eQTL studies. *Nucleic Acids Res* 46:e133
- Jansson T, Powell TL (2007) Role of the placenta in fetal programming: underlying mechanisms and potential interventional approaches. *Clin Sci (Lond)* 113:1–13
- Jimeno-Gonzalez S, Payan-Bravo L, Munoz-Cabello AM, Guijo M, Gutierrez G, Prado F, Reyes JC (2015) Defective histone supply causes changes in RNA polymerase II elongation rate and cotranscriptional pre-mRNA splicing. *Proc Natl Acad Sci USA* 112:14840–14845
- Jourquin J, Duncan D, Shi Z, Zhang B (2012) GLAD4U: deriving and prioritizing gene lists from PubMed literature. *BMC Genomics* 13(Suppl 8):S20
- Juvonen M, Pihlajaniemi T, Autio-Harmanen H (1993) Location and alternative splicing of type XIII collagen RNA in the early human placenta. *Lab Invest* 69:541–551
- Kikas T, Rull K, Beaumont RN, Freathy RM, Laan M (2019) The effect of genetic variation on the placental transcriptome in humans. *Front Genet* 10:550
- Leek JT, Johnson WE, Parker HS, Jaffe AE, Storey JD (2012) The sva package for removing batch effects and other unwanted variation in high-throughput experiments. *Bioinformatics* 28:882–883
- Li ML, Wu SH, Zhang JJ, Tian HY, Shao Y, Wang ZB, Irwin DM, Li JL, Hu XT, Wu DD (2019) 547 transcriptomes from 44 brain areas reveal features of the aging brain in non-human primates. *Genome Biol* 20:258
- Liao Y, Wang J, Jaehnig EJ, Shi Z, Zhang B (2019) WebGestalt 2019: gene set analysis toolkit with revamped UIs and APIs. *Nucleic Acids Res* 47:W199–W205
- Lievano S, Alarcon L, Chavez-Munguia B, Gonzalez-Mariscal L (2006) Endothelia of term human placenta display diminished

- expression of tight junction proteins during preeclampsia. *Cell Tissue Res* 324:433–448
- Madelencau D, Buffat C, Mondon F, Grimault H, Rigourd V, Tsatsaris V, Letourneur F, Vaiman D, Barbaux S, Gascoin G (2015) Transcriptomic analysis of human placenta in intrauterine growth restriction. *Pediatr Res* 77:799–807
- Majewska M, Lipka A, Pauksztó L, Jastrzebski JP, Szeszko K, Gowkielewicz M, Lepiarczyk E, Jozwik M, Majewski MK (2019) Placenta transcriptome profiling in intrauterine growth restriction (IUGR). *Int J Mol Sci* 20:1510
- Manna S, McCarthy C, McCarthy FP (2019) Placental ageing in adverse pregnancy outcomes: telomere shortening, cell senescence, and mitochondrial dysfunction. *Oxid Med Cell Longev* 2019:3095383
- McGinnis R, Steinhilber V, Williams NO, Thorleifsson G, Shooter S, Hjartardottir S, Bumpstead S, Stefansdottir L, Hildyard L, Sigurdsson JK et al (2017) Variants in the fetal genome near FLT1 are associated with risk of preeclampsia. *Nat Genet* 49:1255
- Miller EC (2019) Preeclampsia and cerebrovascular disease. *Hypertension* 74:5–13
- Miyagawa R, Tano K, Mizuno R, Nakamura Y, Ijiri K, Rakwal R, Shibato J, Masuo Y, Mayeda A, Hirose T, Akimitsu N (2012) Identification of cis- and trans-acting factors involved in the localization of MALAT-1 noncoding RNA to nuclear speckles. *RNA* 18:738–751
- Morrow JD, Cho MH, Platig J, Zhou X, DeMeo DL, Qiu W, Celli B, Marchetti N, Criner GJ, Bueno R et al (2018) Ensemble genomic analysis in human lung tissue identifies novel genes for chronic obstructive pulmonary disease. *Hum Genomics* 12:1
- Motta-Mejia C, Kandzija N, Zhang W, Mhlomi V, Cerdeira AS, Burdujan A, Tannetta D, Dragovic R, Sargent IL, Redman CW et al (2017) Placental Vesicles Carry Active Endothelial Nitric Oxide Synthase and Their Activity is Reduced in Preeclampsia. *Hypertension* 70:372–381
- Myatt L (2010) Review: Reactive oxygen and nitrogen species and functional adaptation of the placenta. *Placenta* 31(Suppl):S66–69
- Patel H, Aggarwal NT, Rao A, Bryant E, Sanghani RM, Byrnes M, Kalra D, Dairaghi L, Braun L, Gabriel S, Volgman AS (2020) Microvascular disease and small-vessel disease: the nexus of multiple diseases of women. *J Womens Health (Larchmt)* 29:770–779
- Peng S, Deysenroth MA, Di Narzo AF, Lambertini L, Marsit CJ, Chen J, Hao K (2017) Expression quantitative trait loci (eQTLs) in human placentas suggest developmental origins of complex diseases. *Hum Mol Genet* 26:3432–3441
- Phipps EA, Thadhani R, Benzing T, Karumanchi SA (2019) Preeclampsia: pathogenesis, novel diagnostics and therapies. *Nat Rev Nephrol* 15:275–289
- Pique-Regi R, Romero R, Tarca AL, Luca F, Xu Y, Alazizi A, Leng Y, Hsu CD, Gomez-Lopez N (2020) Does the human placenta express the canonical cell entry mediators for SARS-CoV-2? *Elife* 9:58716
- Pritchard JK, Przeworski M (2001) Linkage disequilibrium in humans: models and data. *Am J Hum Genet* 69:1–14
- Qing X, Redecha PB, Burmeister MA, Tomlinson S, D'Agati VD, Davison RL, Salmon JE (2011) Targeted inhibition of complement activation prevents features of preeclampsia in mice. *Kidney Int* 79:331–339
- Rana S, Lemoine E, Granger JP, Karumanchi SA (2019) Preeclampsia: pathophysiology, challenges, and perspectives. *Circ Res* 124:1094–1112
- Savage M, Steitieh D, Amin N, Malha L, Chasen S (2020) Obstetrical complications and long-term cardiovascular outcomes. *Curr Hypertens Rep* 22:92
- Scotti MM, Swanson MS (2016) RNA mis-splicing in disease. *Nat Rev Genet* 17:19–32
- Shabalina AA (2012) Matrix eQTL: ultra fast eQTL analysis via large matrix operations. *Bioinformatics* 28:1353–1358
- Sibai B, Dekker G, Kupferminc M (2005) Pre-eclampsia. *Lancet* 365:785–799
- Sober S, Reiman M, Kikas T, Rull K, Inno R, Vaas P, Teesalu P, Marti JML, Mattila P, Laan M (2015) Extensive shift in placental transcriptome profile in preeclampsia and placental origin of adverse pregnancy outcomes. *Sci Rep* 5:13336
- Sober S, Rull K, Reiman M, Ilisson P, Mattila P, Laan M (2016) RNA sequencing of chorionic villi from recurrent pregnancy loss patients reveals impaired function of basic nuclear and cellular machinery. *Sci Rep* 6:38439
- Souders CA, Maynard SE, Yan J, Wang Y, Boatright NK, Sedan J, Balyozian D, Cheslock PS, Molrine DC, Simas TA (2015) Circulating levels of sFlt1 splice variants as predictive markers for the development of preeclampsia. *Int J Mol Sci* 16:12436–12453
- Szalai G, Romero R, Chaiworapongsa T, Xu Y, Wang B, Ahn H, Xu Z, Chiang PJ, Sundell B, Wang R et al (2015) Full-length human placental sFlt-1-e15a isoform induces distinct maternal phenotypes of preeclampsia in mice. *PLoS ONE* 10:e0119547
- Szklarczyk D, Gable AL, Lyon D, Junge A, Wyder S, Huerta-Cepas J, Simonovic M, Doncheva NT, Morris JH, Bork P et al (2019) STRING v11: protein-protein association networks with increased coverage, supporting functional discovery in genome-wide experimental datasets. *Nucleic Acids Res* 47:D607–D613
- Tong J, Zhao W, Lv H, Li WP, Chen ZJ, Zhang C (2018) Transcriptomic Profiling In Human Decidua Of Severe Preeclampsia Detected by RNA sequencing. *J Cell Biochem* 119:607–615
- Vaiman D, Miralles F (2016) Targeting STOX1 in the therapy of preeclampsia. *Expert Opin Ther Targets* 20:1433–1443
- Vaiman D, Calicchio R, Miralles F (2013) Landscape of transcriptional deregulations in the preeclamptic placenta. *PLoS ONE* 8:e65498
- van Dijk M, Mulders J, Poutsma A, Konst AA, Lachmeijer AM, Dekker GA, Blankenstein MA, Oudejans CB (2005) Maternal segregation of the Dutch preeclampsia locus at 10q22 with a new member of the winged helix gene family. *Nat Genet* 37:514–519
- van Dijk M, van Bezu J, Poutsma A, Veerhuis R, Rozemuller AJ, Scheper W, Blankenstein MA, Oudejans CB (2010) The preeclampsia gene STOX1 controls a conserved pathway in placenta and brain upregulated in late-onset Alzheimer's disease. *J Alzheimers Dis* 19:673–679
- Wang J, Vasaikar S, Shi Z, Greer M, Zhang B (2017) WebGestalt 2017: a more comprehensive, powerful, flexible and interactive gene set enrichment analysis toolkit. *Nucleic Acids Res* 45:W130–W137
- Zana-Taieb E, Pham H, Franco-Montoya ML, Jacques S, Letourneur F, Baud O, Jarreau PH, Vaiman D (2015) Impaired alveolarization and intra-uterine growth restriction in rats: a postnatal genome-wide analysis. *J Pathol* 235:420–430

Publisher's Note Springer Nature remains neutral with regard to jurisdictional claims in published maps and institutional affiliations.

Terms and Conditions

Springer Nature journal content, brought to you courtesy of Springer Nature Customer Service Center GmbH (“Springer Nature”).

Springer Nature supports a reasonable amount of sharing of research papers by authors, subscribers and authorised users (“Users”), for small-scale personal, non-commercial use provided that all copyright, trade and service marks and other proprietary notices are maintained. By accessing, sharing, receiving or otherwise using the Springer Nature journal content you agree to these terms of use (“Terms”). For these purposes, Springer Nature considers academic use (by researchers and students) to be non-commercial.

These Terms are supplementary and will apply in addition to any applicable website terms and conditions, a relevant site licence or a personal subscription. These Terms will prevail over any conflict or ambiguity with regards to the relevant terms, a site licence or a personal subscription (to the extent of the conflict or ambiguity only). For Creative Commons-licensed articles, the terms of the Creative Commons license used will apply.

We collect and use personal data to provide access to the Springer Nature journal content. We may also use these personal data internally within ResearchGate and Springer Nature and as agreed share it, in an anonymised way, for purposes of tracking, analysis and reporting. We will not otherwise disclose your personal data outside the ResearchGate or the Springer Nature group of companies unless we have your permission as detailed in the Privacy Policy.

While Users may use the Springer Nature journal content for small scale, personal non-commercial use, it is important to note that Users may not:

1. use such content for the purpose of providing other users with access on a regular or large scale basis or as a means to circumvent access control;
2. use such content where to do so would be considered a criminal or statutory offence in any jurisdiction, or gives rise to civil liability, or is otherwise unlawful;
3. falsely or misleadingly imply or suggest endorsement, approval, sponsorship, or association unless explicitly agreed to by Springer Nature in writing;
4. use bots or other automated methods to access the content or redirect messages
5. override any security feature or exclusionary protocol; or
6. share the content in order to create substitute for Springer Nature products or services or a systematic database of Springer Nature journal content.

In line with the restriction against commercial use, Springer Nature does not permit the creation of a product or service that creates revenue, royalties, rent or income from our content or its inclusion as part of a paid for service or for other commercial gain. Springer Nature journal content cannot be used for inter-library loans and librarians may not upload Springer Nature journal content on a large scale into their, or any other, institutional repository.

These terms of use are reviewed regularly and may be amended at any time. Springer Nature is not obligated to publish any information or content on this website and may remove it or features or functionality at our sole discretion, at any time with or without notice. Springer Nature may revoke this licence to you at any time and remove access to any copies of the Springer Nature journal content which have been saved.

To the fullest extent permitted by law, Springer Nature makes no warranties, representations or guarantees to Users, either express or implied with respect to the Springer Nature journal content and all parties disclaim and waive any implied warranties or warranties imposed by law, including merchantability or fitness for any particular purpose.

Please note that these rights do not automatically extend to content, data or other material published by Springer Nature that may be licensed from third parties.

If you would like to use or distribute our Springer Nature journal content to a wider audience or on a regular basis or in any other manner not expressly permitted by these Terms, please contact Springer Nature at

onlineservice@springernature.com

CHAPTER 4: The Role of Non-coding RNAs in Trophoblast Fusion and Placental Pathologies

Non-coding RNAs (ncRNAs) are RNA molecules that do not translate into proteins. This RNA category includes transfer RNAs (tRNAs), ribosomal RNAs (rRNAs), small RNAs (sRNA, miRNAs, siRNAs, piRNAs, snoRNAs, and scaRNAs), and long ncRNAs). Despite not encoding proteins, these molecules can regulate a wide variety of important cellular processes, such as gene transcription, chromosome remodelling, mRNA maturation and protein post-transcriptional modifications.

In our review on epigenetic mechanisms involved in placenta development (see **Annex 3**), we reported studies supporting the role of ncRNAs in the placental physiology and pathophysiology. For example, a cluster on chromosome 19 includes 46 intronic miRNAs genes and 58 miRNA species, which have been found to be expressed in the placenta in early pregnancy. Their expression increases as pregnancy progresses. These miRNAs are implicated in cell proliferation and differentiation and can be also found in exosomes, transducing placental signals to the maternal and fetal tissues (Donker et al., 2012; Sadovsky, Mouillet, Ouyang, Bayer, & Coyne, 2015; Xie et al., 2014).

We also identified two ncRNAs implicated in trophoblast fusion and whose expression is deregulated in pathological placentas. The full manuscript: “Urothelial Cancer-Associated 1 (UCA1) and miR-193 Are Two Non-coding RNAs Involved in Trophoblast Fusion and Placental Diseases”

To sum up, we used the BeWo trophoblast cell line to study trophoblast fusion. This carcinogenic trophoblast-like cell model can be used as a proxy of human CTBs, as they can fuse and create a syncytium upon forskolin (FSK) treatment. We stimulated BeWo cells with FSK for 72h, extracted the RNAs and hybridized them on Affymetrix ClariomD microarrays. Differentially expression analysis identified a total of 800 upregulated genes and 1,281 downregulated genes after the FSK treatment. Gene enrichment analysis of the DEGs showed upregulation of genes involved in

inflammation and hypoxia, while downregulated genes were enriched in genes involved in cell cycle and nutrient-sensing pathways linked to mTORC1.

Among the 2,081 DEGs, 307 belong to the ncRNAs class, including lncRNAs, RNA antisense, miRNAs, circRNAs, etc. Different databases were interrogated to determine the targets of these dysregulated ncRNAs. Ontology analysis of the targets revealed enrichment in genes involved in cell cycle progression, TNF-signalling, and hypoxia. The list of 307 ncRNAs was compared to published lists of deregulated ncRNAs in PE and IUGR. Eight miRNAs (miR-193b, miR-365a, miR-936; miR-6886; miR-7110; miR-518A1; miR-4454, and miR-1283-2) and one lncRNA (UCA1) were found in common.

We focused our attention on the lncRNA UCA1 because a) it is upregulated in SCTs in PE and IUGR-affected placentas as compared to unaffected placentas; b) it shows a specific compartmentalized expression in the SCT vs. the CTB and c) it is upregulated in primary cultures of human SCTs exposed for 24 h to 1% oxygen as compared to the same cells exposed to 20% oxygen. To further investigate the role of UCA1 in fusion, we knocked-down (KD) UCA1 expression using small interfering RNA (siRNA) and tested by RT-qPCR the expression of genes involved in cell proliferation, oxidative stress, trophoblast fusion, endocrine differentiation of trophoblast, SCT stabilization, cell migration, oxygen sensing, and apoptosis. Globally, the KD of UCA1 reduced the differences between FSK-treated cells and control group. This suggests that UCA1 KD impaired syncytialization.

Previous work in our group showed that STOX1A overexpression in a murine model induces the development of a PE-like phenotype (Doridot et al., 2013) and that is a major actor in the syncytialization process in the BeWo model (Ducat et al., 2020). STOX1 has two isoforms, STOX1A and STOX1B. In Bewo cells, overexpression of STOX1B (BeWo-B cells), the shorter form, blocks cell fusion in BeWo while overexpression of the long form STOX1A (BeWo-A cells) stimulates syncytialization. When STOX1B is abundant, the effects of UCA1 down-regulation on FSK response are alleviated.



Urothelial Cancer Associated 1 (UCA1) and miR-193 Are Two Non-coding RNAs Involved in Trophoblast Fusion and Placental Diseases

Clara Apicella^{1†}, Camino S. M. Ruano^{1†}, Sébastien Jacques¹, Géraldine Gascoin^{2,3}, Céline Méhats¹, Daniel Vaiman^{1*†} and Francisco Miralles^{1†}

OPEN ACCESS

Edited by:

Tang Zhonglin,
Agricultural Genomics Institute
at Shenzhen, Chinese Academy
of Agricultural Sciences, China

Reviewed by:

Marie Van Dijk,
Amsterdam University Medical
Centers, Netherlands
Stephen Lye,
Lunenfeld-Tanenbaum Research
Institute, Canada

*Correspondence:

Daniel Vaiman
daniel.vaiman@inserm.fr

[†]These authors have contributed
equally to this work

Specialty section:

This article was submitted to
Cell Growth and Division,
a section of the journal
Frontiers in Cell and Developmental
Biology

Received: 26 November 2020

Accepted: 19 April 2021

Published: 13 May 2021

Citation:

Apicella C, Ruano CSM,
Jacques S, Gascoin G, Méhats C,
Vaiman D and Miralles F (2021)
Urothelial Cancer Associated 1
(UCA1) and miR-193 Are Two
Non-coding RNAs Involved
in Trophoblast Fusion and Placental
Diseases.
Front. Cell Dev. Biol. 9:633937.
doi: 10.3389/fcell.2021.633937

¹Institut Cochin, Université de Paris, U1016 INSERM, UMR 8104, CNRS, Paris, France, ²Unité Mixte de Recherche MITOVASC, Équipe Mitolab, CNRS 6015, INSERM U1083, Université d'Angers, Angers, France, ³Réanimation et Médecine Néonatales, Centre Hospitalier Universitaire, Angers, France

A bioinformatics screen for non-coding genes was performed from microarrays analyzing on the one hand trophoblast fusion in the BeWo cell model, and on the other hand, placental diseases (preeclampsia and Intra-Uterine Growth Restriction). Intersecting the deregulated genes allowed to identify two miRNA (mir193b and miR365a) and one long non-coding RNA (UCA1) that are pivotal for trophoblast fusion, and deregulated in placental diseases. We show that miR-193b is a hub for the down-regulation of 135 cell targets mainly involved in cell cycle progression and energy usage/nutrient transport. UCA1 was explored by siRNA knock-down in the BeWo cell model. We show that its down-regulation is associated with the deregulation of important trophoblast physiology genes, involved in differentiation, proliferation, oxidative stress, vacuolization, membrane repair and endocrine production. Overall, UCA1 knockdown leads to an incomplete gene expression profile modification of trophoblast cells when they are induced to fuse into syncytiotrophoblast. Then we performed the same type of analysis in cells overexpressing one of the two major isoforms of the STOX1 transcription factor, STOX1A and STOX1B (associated previously to impaired trophoblast fusion). We could show that when STOX1B is abundant, the effects of UCA1 down-regulation on forskolin response are alleviated.

Keywords: trophoblast, placenta, preeclampsia, intra uterine growth restriction, syncytialisation, non-coding RNAs

INTRODUCTION

In humans, abnormal placental development is associated with two major pregnancy diseases: preeclampsia (PE) and intrauterine growth restriction (IUGR).

PE occurs in a range of 2–5% pregnancies, and it is characterized by hypertension and proteinuria, surging from the mid-gestation at the earliest (Steegers et al., 2010). Despite a certain degree of heterogeneity in its pathogenesis, a consensus exists that abnormal placentation or placenta development could be at the origin of the disease. Notably, placental ischemia would

cause intermittent hypoxia, oxidative stress, cell death, and the release to the maternal circulation of anti-angiogenic factors and debris that promote inflammation and a systemic endothelial dysfunction (Rana et al., 2019). In some cases, the disease poses a real threat to the survival of the mother requiring the delivery of the fetoplacental unit. Thus, PE is one of the major causes of premature births (before 37 completed weeks of pregnancy), with their cortege of neonate complications (Goldenberg et al., 2008). The symptoms of the disease disappear after delivery. However, epidemiological studies have shown that the women who have suffered a preeclamptic pregnancy have an increased risk of developing a cardiovascular disease (CVD) later in life (Newstead et al., 2007; Brouwers et al., 2018), as well as other diseases affecting strongly vascularized tissues, such as the brain (Basit et al., 2018).

IUGR refers to a somehow loosely defined condition in which the unborn baby is smaller than expected for his or her gestational age (Nardoza et al., 2017). IUGR babies typically have an estimated weight that falls below that of 90% of unborn babies of the same gestational age. In addition, IUGR babies are sometimes born prematurely. Babies with IUGR are at increased risk of health problems before, and after birth. These problems include low oxygen levels while in the womb and high levels of distress during labor and delivery. In the long term, IUGR increases the risk of developing a metabolic disease such as type 2 diabetes and CVD (Darendeliler, 2019).

In about one third of the cases, PE is complicated with IUGR, suggesting that there could be an overlap in the etiology of both diseases. The considerable similarity in histopathology and gene expression in the placentas has been recently reported between both diseases (Awamleh et al., 2019; Gibbs et al., 2019; Medina-Bastidas et al., 2020).

In the human placenta, the maternal blood is in direct contact with a continuous multinucleated layer, the syncytiotrophoblast (STB). This polarized interface releases hormones and mediates the exchange of nutrients, gases and waste between mother and the developing fetus (Turco and Moffett, 2019). The STB is mitotically inactive, formation and constant renewal of the syncytium depends on the underlying mononuclear cytotrophoblasts (CTB). Throughout gestation, CTBs proliferate, differentiate and eventually fuse with the STB via cell-syncytial fusion. This process is balanced by a concomitant release of apoptotic material as syncytial knots from the STB to the maternal circulation. Hence, the process of syncytialization is critical to the integrity of the STB and in maintaining the essential functions of the placenta. Several *in vitro* and *in vivo* studies have demonstrated a close, if not a causal, relationship between structural/functional deficiency of the syncytium and the development of PE and IUGR (Guller et al., 2008; Roland et al., 2016; Costa, 2016).

Genome-wide transcriptomic and epigenomic studies have greatly contributed to the understanding of the molecular mechanisms involved in either normal or pathological placenta development. Thus, numerous studies have revealed altered placental expression of various genes in PE and IUGR (Cox et al., 2015; Deyssenroth et al., 2017; Chabrun et al., 2019; Majewska et al., 2019; Benny et al., 2020). A particular category concerns

those genes encoding for non-protein coding RNAs (ncRNAs). Classes of ncRNAs include transfer RNAs (tRNAs), ribosomal RNAs (rRNAs), small RNAs, such as microRNAs (miRNAs), siRNAs, piRNAs, snoRNAs, snRNAs, exRNAs, scaRNAs and the long ncRNAs (Hombach and Kretz, 2016). The ncRNAs display a great variety of mechanisms of action including: post-transcriptional gene regulation through controlling processes like protein synthesis, RNA maturation, transport and decay, but also, transcriptional gene regulation through the modification of chromatin structure (Fernandes et al., 2019). They are an important basis of epigenetic regulation in the human placenta, in normal and pathological situations (Hayder et al., 2018; Apicella et al., 2019). Structurally different ncRNAs engage diverse mechanisms that lead to different regulatory outcomes. The discovery of the diversity of functions played by the ncRNAs in the cell physiology has boosted the exploration of their role in placental development, physiology and pathology.

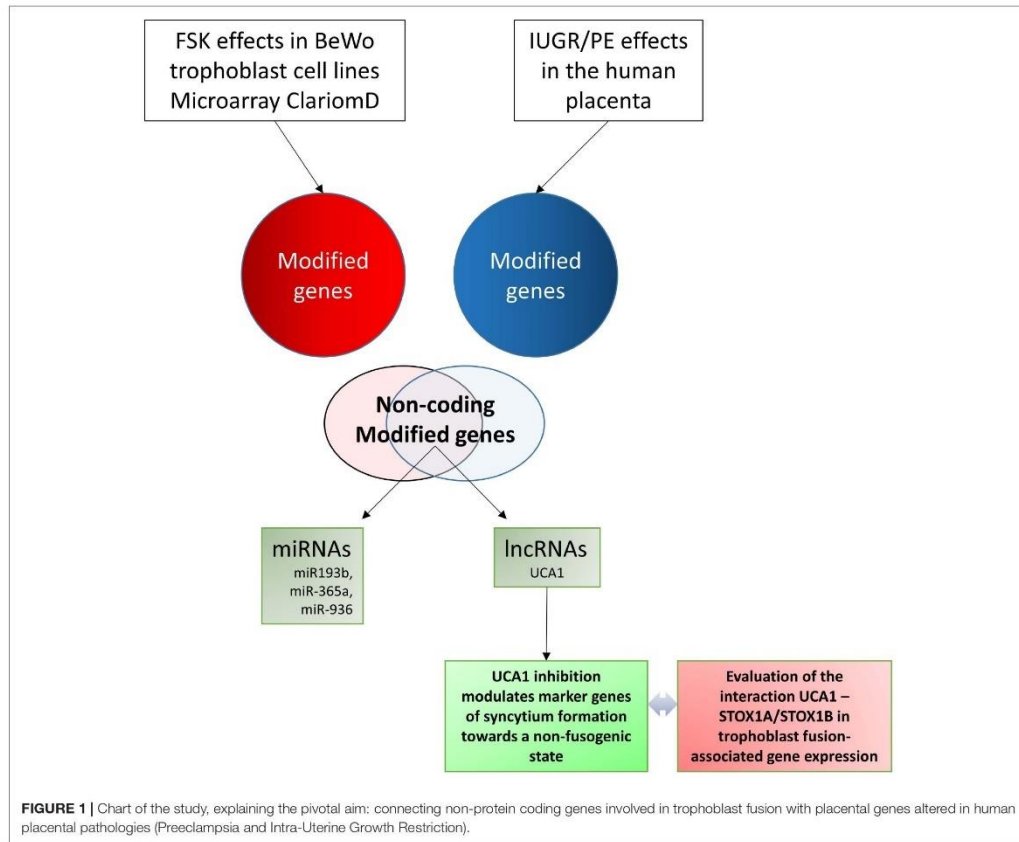
The central role of the STB in the physiology of the placenta, suggests that deregulation of ncRNAs specifically required for its formation and/or maintenance could be potentially involved in placental diseases. Here we combined two microarray analyses, one carried out on the classical fusogenic trophoblast model BeWo (under the accession number GSE148088) (Kudo et al., 2004; Ramos et al., 2008; Orendi et al., 2010; Shankar et al., 2015; Zheng et al., 2016), and one carried out on total human placentas with normal controls, PE and IUGR placentas (under the accession number E-MTAB-9416). A cross-analysis was carried out with a drastic filtering in order to identify ncRNA that are associated to disease (in the placentas) and to fusion (induced by forskolin treatment in the BeWo cells), in parallel.

This cross-analysis allowed the identification of a small subset of ncRNAs which are consistently modified both during fusion of trophoblast cells, and in the pathological placentas. We then carried on our analysis focusing upon the miRNA miR-193b (by a bioinformatic approach) and the lncRNA UCA1 (through knock-down (KD) experiments). In addition, we analyzed the effects of this KD in BeWo cells, overexpressing specifically one of the two major isoforms of the STOX1 transcription factor (STOX1A and STOX1B), previously identified as a key player in preeclampsia (George and Bidwell, 2013), and recently shown to modulate fusion through a specific equilibrium between its two isoforms (Vaiman and Miralles, 2016; Ducat et al., 2020). The chart of the present study is shown as **Figure 1**.

RESULTS

Transcriptional Modifications in BeWo Cells Following Forskolin Treatment

BeWo cells were cultured in the presence of 20 μ M forskolin to induce cell fusion (BeWo-FSK). Control cells were grown with the vehicle, DMSO (BeWo-CO). After 72 h, the total RNA was extracted, and global gene-expression profiles were analyzed with microarrays. Comparison of BeWo-FSK relative to BeWo-CO detected 2109 genes differentially expressed (DEGs) with a fold change (FC) either ≤ -2 or ≥ 2 , and

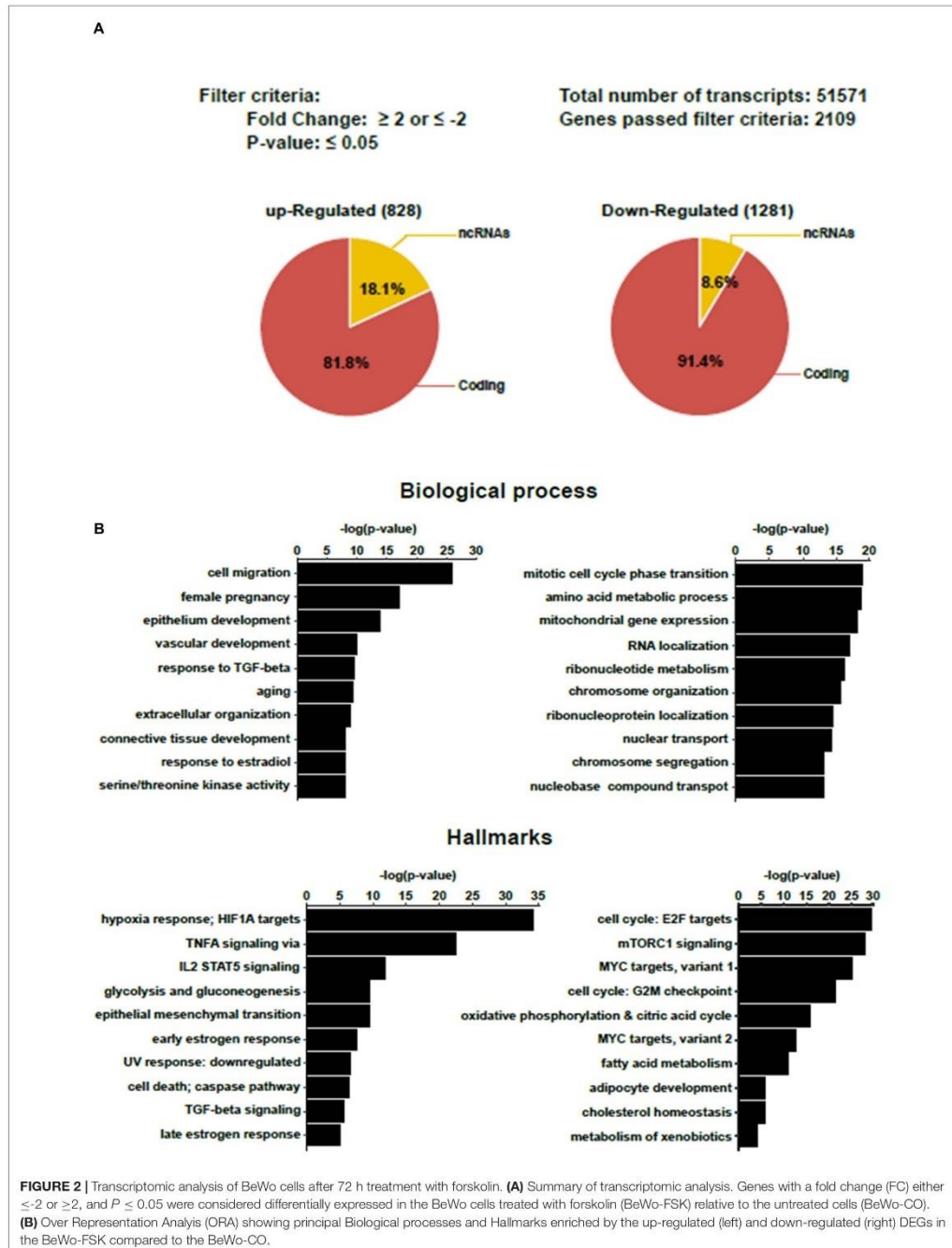


P -value ≤ 0.05 (Figure 2A and Supplementary Table 1). Of these, 828 genes were up-regulated and 1,281 down-regulated (Supplementary Table 1). Gene set enrichment analysis (GSEA), and over representation analysis (ORA) confirmed that our results were accurately consistent with previous reports having analyzed transcriptomic changes in BeWo cells after forskolin treatment (Supplementary Figure 1). In the BeWo-FSK we detected substantially increased expression of key markers of syncytialization such as CGA ($FC = 10.1$; $P = 2.1 \times 10^{-11}$), CGB1 ($FC = 20.5$; $P = 2.81 \times 10^{-12}$) or ERVFRD-1 (aka Syncytin2, $FC = 10.6$; $P = 6.23 \times 10^{-12}$). Up-regulated DEGs were associated with biological processes such as cell migration, vascular development, response to TGF-Beta and response to hypoxia. Down-regulated DEGs are mainly involved in cell cycle progression, amino-acid metabolism, and mitochondrial gene expression (Figure 2B). In terms of hallmarks present in the GSEA Broad database, inflammation and hypoxia pathways were particularly enriched in up-regulated genes, while cell cycle, nutrient sensing via mTORC1 pathway, were strongly enriched

in down-regulated genes, suggesting a whole silencing of basic pathways of cell physiology and energy expenditure slow down, accompanying the differentiation of the trophoblast cells into a syncytial structure.

Differentially Expressed Non-coding RNAs in Forskolin-Treated BeWo Cells

Three hundred and seven (307) of the DEGs detected in the BeWo-FSK relative to BeWo-CO, encode annotated ncRNAs. They belong to different categories including: sense-intronic RNA, antisense RNA, long non-coding RNA (lncRNA), circular (circRNA), microRNA (miRNA) and housekeeping ncRNAs (Y-RNAs, ribosomal RNAs, Small nucleolar RNAs and transfer RNAs) (Figure 3). The category of housekeeping ncRNAs was the most represented (111 genes). Nonetheless, we focused our study on the categories corresponding to regulatory ncRNAs. A selection of the most significantly modified regulatory ncRNAs detected



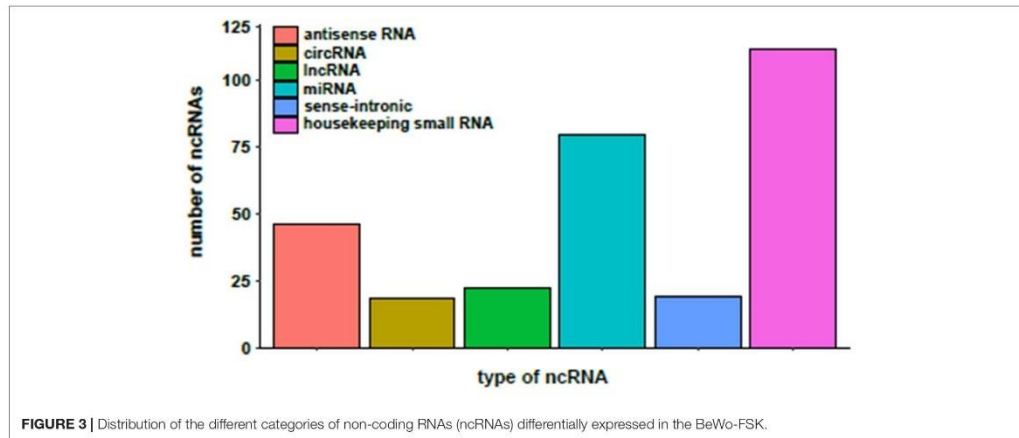


FIGURE 3 | Distribution of the different categories of non-coding RNAs (ncRNAs) differentially expressed in the BeWo-FSK.

TABLE 1 | Top 25 differentially expressed regulatory ncRNAs in the BeWo cells after 72 h of forskolin treatment.

Gene symbol	ncRNA class	Fold change	P-value	FDR P-value
hsa-miR-147b	miRNA	28.94	8.33E-11	3.53E-07
LINC01511	lncRNA	14.88	8.43E-13	1.63E-08
hsa-miR-4632	miRNA	8.93	6.38E-09	7.80E-06
RP11-420L9.5	antisenseRNA	7.6	1.61E-08	1.48E-05
LINC01237	lncRNA	4.45	2.70E-07	1.00E-04
MYCNUT	lncRNA	4.31	3.72E-09	5.15E-06
LINC01164	lncRNA	3.98	1.37E-07	8.14E-05
UCA1	lncRNA	3.76	2.19E-06	7.00E-04
CTB-60B18.12	antisenseRNA	3.46	2.06E-06	7.00E-04
hsa-miR-6810	miRNA	3.36	3.13E-06	9.00E-04
hsa-miR-936	miRNA	3.35	5.99E-06	1.50E-03
SLC2A1-AS1	antisenseRNA	3.23	6.17E-06	1.50E-03
IL10RB-AS1	antisenseRNA	3.14	5.32E-06	1.30E-03
hsa-miR-193b	miRNA	2.91	8.00E-04	4.54E-02
hsa-miR-365a	miRNA	2.73	3.90E-06	1.10E-03
hsa-miR-6888	miRNA	2.54	8.24E-05	9.80E-03
hsa-miR-3941	miRNA	2.16	3.18E-05	5.10E-03
Hsa-miR-636	miRNA	-2.16	4.69E-05	6.70E-03
hsa-miR-301a	miRNA	-2.27	2.92E-05	4.90E-03
RP11-884K10.7	antisenseRNA	-2.84	4.00E-04	2.68E-02
COX10-AS1	antisenseRNA	-3.12	5.63E-05	7.60E-03
OLMALINC	lncRNA	-3.33	9.98E-05	1.12E-02
hsa-miR-1908	miRNA	-3.45	6.12E-07	3.00E-04
DLEU2	lncRNA	-3.75	8.74E-05	1.03E-02
hsa-miR-6758	miRNA	-4.31	8.16E-07	3.00E-04

following forskolin treatment in the BeWo cells is shown in **Table 1**. These include the lncRNAs, antisenseRNAs and miRNAs. The list of the totality of ncRNAs (classified by category) detected as differentially expressed is provided as **Supplementary Table 2**.

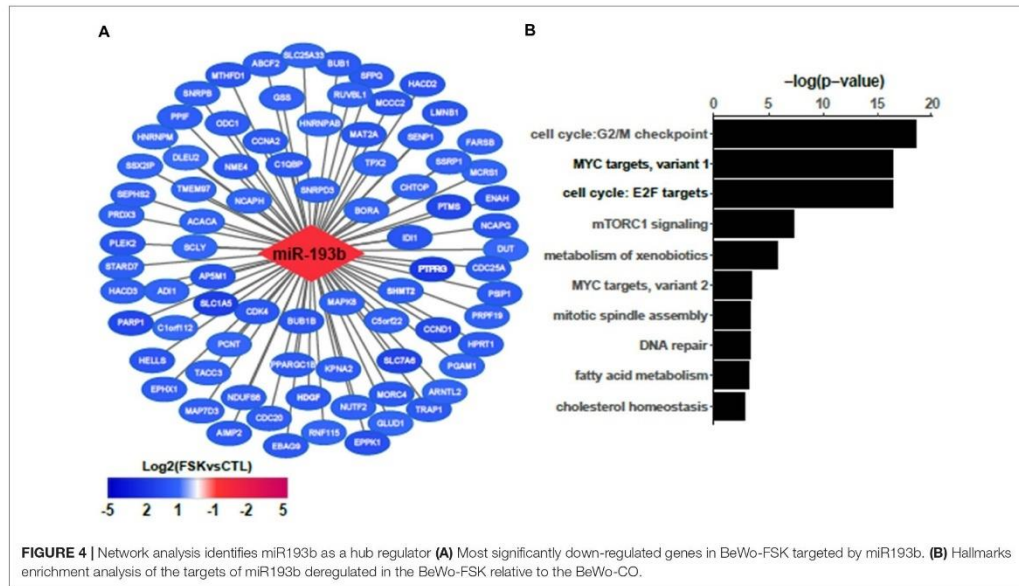
Identification of Regulatory ncRNAs Targets Reveals Their Potential Roles in Syncytialization

To investigate the role of these ncRNAs in the process of BeWo fusion we identified their putative targets (when known) using appropriate databases (miRBase, starBase v2.0. and DianaTools LncBase v.2). Since miRbase tends to provide a more limited list of putative target genes (~10% of the others) for a given miRNA, and since these were generally largely covered in the other databases, this constituted the major basis for the establishment of our lists of targets. Next, we selected among these targets those which are indeed detected as DEGs in the BeWo-FSK relative to the BeWo-CO cells. These resulted in a list of 278 up-regulated and 572 down-regulated DEGs. Out of the deregulated DEG list (**Supplementary Table 1**), this represents 33.6% for the up-regulated and 44.6% for the down-regulated DEGs. Assuming a total of 50,000 genes including the non-protein coding ones, the expected proportions are 1.6 and 1.1%, respectively, thus we observed a significant enrichment of putative targets in both cases (χ^2 contingency test, $p < 10^{-20}$).

Hallmark enrichment analysis using the ncRNAs targeted-DEGs revealed that the most significantly impacted functions are related to the cell cycle progression for the down-regulated DEGs, while TNF-signaling and hypoxia response are the most enriched processes for the up-regulated DEGs. Strikingly, these enriched pathways are quite similar to those obtained with the total DEG gene set, suggesting that many DEGs contributing to the definition of the hallmarks are targeted by the ncRNAs.

Network Analysis of ncRNAs and Their Targets Identifies miR-193b as a Hub

To further analyze the role of the differentially expressed ncRNAs in the process of BeWo fusion we used the Cytoscape tool to construct a regulatory network integrating these ncRNAs and their targets. This resulted in a network composed of



985 nodes (representing ncRNAs and targets) and 1,775 edges (representing interactions). Next, we submitted our network to topological analysis. MiR-193b was identified as the principal hub of our network, with 135 predicted targets (Figure 4A). Other lesser hubs corresponding to miR-16, miR-455, and miR-365 are presented as Supplementary Figure 2. Most of the targets of miR-193b were down-regulated (108 out of 135) in the BeWo-FSK relative to BeWo-CO, while miR-193b was significantly up-regulated ($FC = 2.91$; $P = 0.0008$). Hallmarks enrichment analysis shows that the down-regulated genes targeted by miR-193b are mainly involved in the control of cell cycle progression and energy usage/nutrient metabolism (Figure 4B).

A Small Subset of ncRNAs Involved in Syncytialization Is Also Associated With Preeclampsia and Intrauterine Growth Restriction

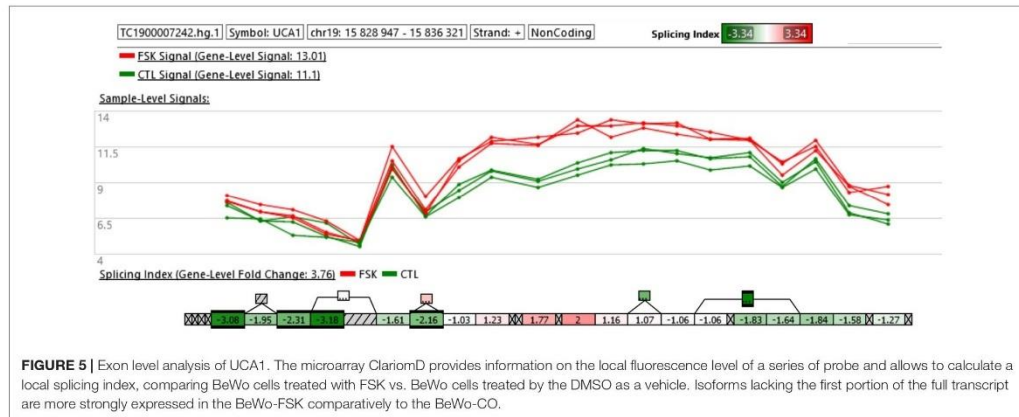
To identify ncRNAs associated with syncytialization in BeWo which could be also involved in PE and/or IUGR we compared the list of ncRNAs identified in BeWo with those identified in a list from our study on total human placentas with normal controls, PE and IUGR placentas (E-MTAB-9416) and other published datasets (GSE114349, GSE114691, GSE75010, GSE93839, and GSE66273). Comparison of all differentially expressed ncRNAs, revealed that two miRNAs (miR-193b and miR-365a) and one lncRNA (UCA1) were found most consistently up-regulated in both PE and IUGR. Therefore, miR-193b is associated to trophoblast fusion, together with pathological placentation, suggesting its overall implication in

normal placental function. A few additional miRNAs were also found simultaneously differentially expressed in preeclamptic placentas and in the BeWo-FSK (miR-936; miR-6886; miR-7110; miR-518A1; miR-4454, and miR-1283-2), but those were not studied further in the present paper.

We next focused our attention on the lncRNA UCA1. This was justified by the following: (i) UCA1 is up-regulated in PE and IUGR but also in primary cultures of human syncytiotrophoblasts exposed for 24 h to 1% oxygen as compared to the same cells exposed to 20% oxygen (Table 2), (ii) also, a study coupling laser microdissection to isolate specific trophoblast subpopulations and microarray analysis, identified UCA1 as the most differentially expressed ncRNA in STBs isolated from the placentas of pregnancies with severe PE relative to controls (Gormley et al., 2017), (iii) *in situ* hybridization confirmed up-regulation of UCA1 in the STBs compartment of the placenta. Alternative splicing isoforms have been described for UCA1 (Xue et al., 2016). We found that UCA1 was increased

TABLE 2 | Genome-wide transcriptomic studies showing up-regulation of UCA1 either in preeclampsia or intrauterine growth retardation.

Data set	Study	Fold change	P-value
E-MTAB-9416	IUGR vs. CO	8.91	3.20×10^{-03}
GSE75010	PE vs. CO	2.04	2.81×10^{-10}
GSE93839	PE STB vs. CO STB	5.93	1.55×10^{-03}
GSE66273	PE vs. CO	6.19	3.33×10^{-04}
GSE147776	IUGR vs. CO	2.01	3.58×10^{-02}
GSE41331	CTB 1%O2 vs. 20%O2	1.86	1.61×10^{-02}



in expression by 3.76-fold following FSK treatment. Exon level analysis of UCA1 (accessible through the ClariomD array used in this study) shows that probes located in the terminal part of the gene have a higher level of fluorescence in the forskolin-treated compared to the control cells (Figure 5). Thus, it shows that in the BeWo-FSK there is a specific increase in the production of the shorter isoforms (ENST00000600160.2, ENST00000589333.2) of UCA1, while the level of expression of the most complete isoform (ENST00000397381.4) is apparently unaffected.

UCA1 siRNA Knockdown Lead to Altered Regulation of Genes Involved in Fusion Mechanisms in BeWo Cells

The effect of the si-RNAs was evaluated by qRT-PCR. UCA1 levels were drastically affected (reduction ranging from 90 to 98% compared to the si-SCR, according to the experiment, Figure 6A). In a first characterization, we analyzed in BeWoC cells the expression of genes involved in cell proliferation (*ki67*, *ITIH5*), oxidative stress (*NOS3*, *GCLM* and *CAVI*-also involved in exosome physiology), membrane repair (*ANXA1*, *ANXA2*, *CAVI*), trophoblast fusion (*Syncytin1*, *Syncytin2*), endocrine differentiation of trophoblast (*CGA/CGB*), syncytiotrophoblast stabilization (*TGM2*) cell migration (*MMP9*), oxygen sensing (*INHA*), and apoptosis (*BAX*, *BCL2*, *DAPK1* and *BAD*). The KD of UCA1 led to significant alterations of almost all the genes involved in these pathways (Figure 6). A principal component analysis was carried out on the qPCR data and showed a clear separation of the cell replicates (Figure 7). The first axis (79% of the variation) is driven by the FSK treatment, while the second axis (10%) contrasts markers of differentiation vs. markers of proliferation. The analysis reveals that in terms of gene expression, the KD of UCA1 reduced the differences between FSK treated cells and control group in the center of the graph. This means that when levels of UCA1 are strongly reduced, the expression profile remains closer to that of untreated control cells. These

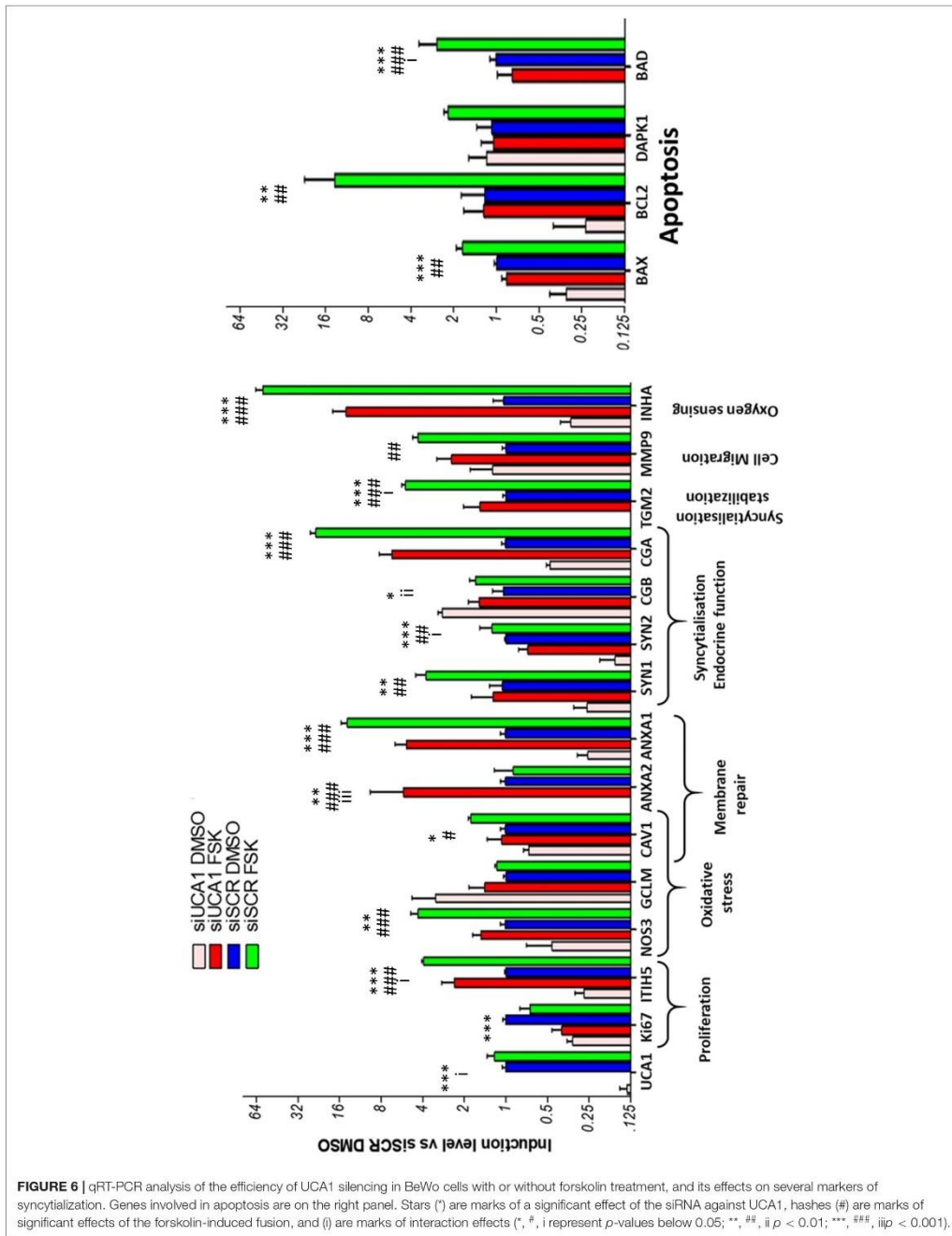
observations suggest that UCA1 is important for a successful syncytialisation process.

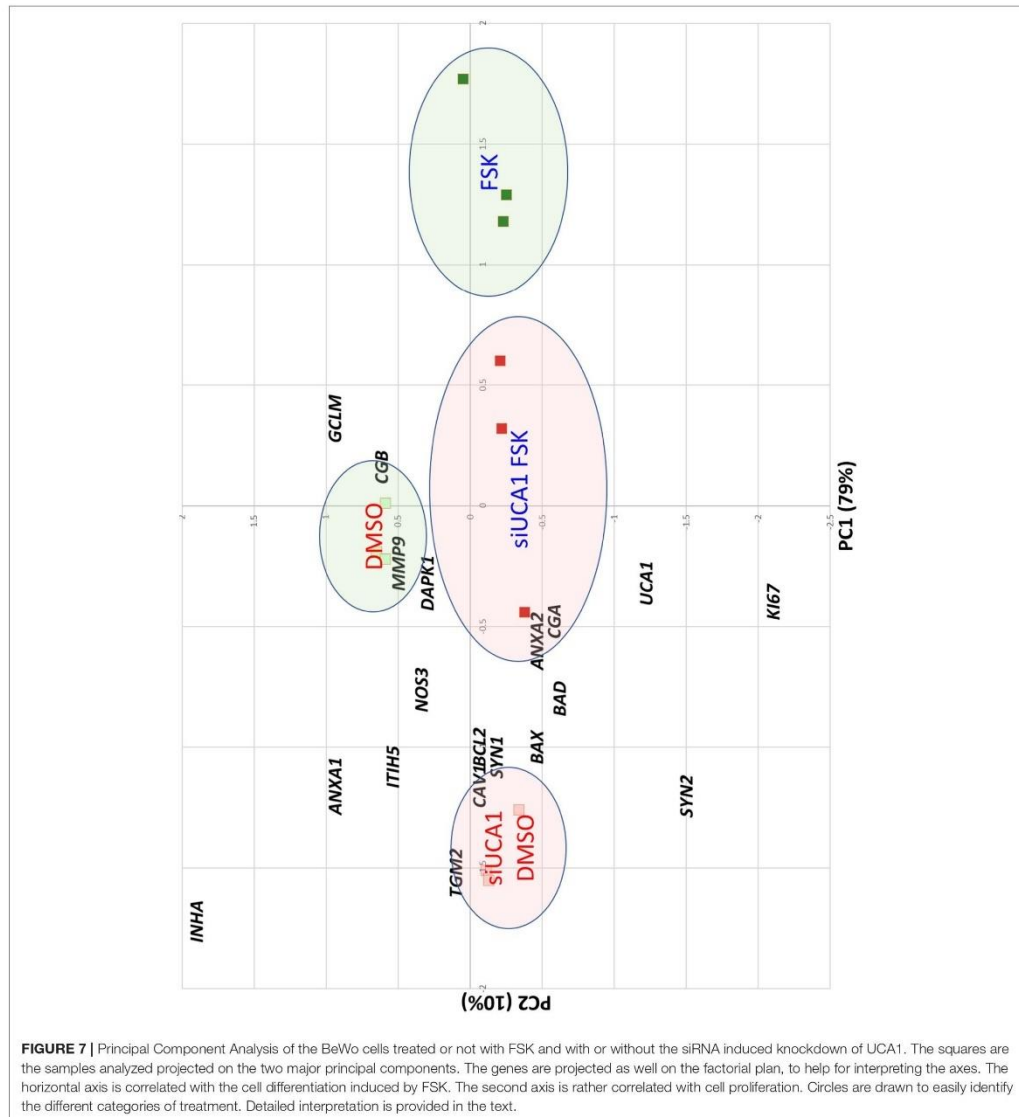
A statistical test by two-ways ANOVA revealed significant modifications for most genes except *GCLM* and *DAPK1* (Table 3 and Figure 6). The knockdown of UCA1 by itself affected all the genes, but *MMP9*. The FSK effect was significant in all the genes except UCA1, *CGB*, *KI67* (in addition to *GCLM* and *DAPK1*). Finally, there was a significant interaction effect between the FSK treatment and the UCA1 KD in the case of UCA1, *CGB*, *SYNCYTIN2*, *TGM2*, *ANXA2*, *ITIH5*, and *BAD*. These interaction effects indicate a differential effect of the UCA1 KD according to the FSK treatment leading to cell fusion.

Interference Between UCA1 and the Trophoblast Differentiation Factor STOX1 in BeWo Cells

Previously, we have identified *STOX1* as a major actor of the syncytialisation process in BeWo cells. More specifically, we showed that the short isoform of *STOX1*, *STOX1B*, antagonizes cell fusion when overexpressed and that disturbing the *STOX1A/B* balance mimics specific gene perturbations seen in PE CTBs in three well-characterized cell lines BeWoA, BeWoB and BeWoC, the first two overexpressing *STOX1A* and *STOX1B*, 20–30- and 6-fold, respectively (Ducat et al., 2020). In the present paper, analyzing exon-level microarrays, we show now for the first time that *STOX1* isoforms are differentially spliced when the BeWo cells fuse under forskolin (Supplementary Figure 3), strengthening the idea that the two isoforms are associated with different pivotal stages of trophoblast differentiation.

To explore the putative role of UCA1 in the syncytialization in normal and pathological conditions, we silenced this lncRNA using a specific small interfering RNA (si-RNA) in BeWo cells lines permanently transfected either with an empty plasmid (encoding G418 resistance), or with the same plasmid encoding for the expression of either *STOX1A* or *STOX1B* (These cells are





called BeWoC, BeWoA or BeWoB, respectively). The cells were transfected with the si-UCA1 or a scrambled siRNA, si-SCR, used as control. We analyzed by qPCR a panel of 8 genes (including UCA1). The choice of these 8 genes was motivated by the fact that strong correlations exist between the 19 genes analyzed in the first experiment. The chosen genes are representative of the different pathways analyzed (proliferation-KI67, oxidative

stress-INHA, trophoblast differentiation-SYN1, apoptosis-BCL2, BAX, invasion-MMP9, endocrine differentiation-CGA). The results are presented as a histogram (Figure 8A), with statistical values presented in Supplementary Table 3 (ANOVA), and as a PCA analysis, where the two first axes account for 40 and 19.5% of the variance (Figure 8B). BeWoC cells (represented by squares) harbor the same profile with the 8 genes from the

TABLE 3 | Statistical analyses of individual gene effects following UCA1 knock-down ± FSK treatment (significant values are in red fonts).

Overall tests of univariate models			Tests of univariate effects		
Y variable	F	Prob.	Source	F	Prob.
UCA1	22.504	0.00029659	Si treatment	56.948	6.6307 × 10 ⁻⁰⁵
			Fusion	4.288	0.07213567
			Si treatment*Fusion	6.275	0.03665572
CGB	8.208	0.00797657	Si treatment	10.373	0.01222583
			Fusion	0.283	0.60936093
			Si treatment*Fusion	13.967	0.00572781
CGA	127.930	4.243 × 10 ⁻⁰⁷	Si treatment	43.849	0.00016558
			Fusion	336.346	8.0411 × 10 ⁻⁰⁸
			Si treatment*Fusion	3.596	0.09452054
GCLM	2.521	0.13152052	Si treatment	4.143	0.07620217
			Fusion	0.975	0.3524659
			Si treatment*Fusion	2.445	0.15650114
NOS3	14.589	0.00131394	Si treatment	15.149	0.0045949
			Fusion	28.613	0.0006866
			Si treatment*Fusion	0.004	0.95003544
CAV1	5.155	0.02833346	Si treatment	7.939	0.02257829
			Fusion	7.147	0.02821257
			Si treatment*Fusion	0.379	0.55505375
KI67	13.163	0.00184323	Si treatment	34.327	0.00037894
			Fusion	0.891	0.37283458
			Si treatment*Fusion	4.272	0.07257943
SYN2	23.107	0.00027009	Si treatment	39.848	0.00022968
			Fusion	18.244	0.00271954
			Si treatment*Fusion	11.229	0.01006638
TGM2	51.718	1.3944 × 10 ⁻⁰⁵	Si treatment	63.473	4.4987 × 10 ⁻⁰⁵
			Fusion	84.869	1.5606 × 10 ⁻⁰⁵
			Si treatment*Fusion	6.811	0.0311362
ANXA2	39.218	3.939 × 10 ⁻⁰⁵	Si treatment	23.397	0.00129298
			Fusion	43.573	0.00016922
			Si treatment*Fusion	50.685	0.00010006
ITIHS	56.208	1.0168 × 10 ⁻⁰⁵	Si treatment	37.157	0.00029085
			Fusion	125.667	3.5958 × 10 ⁻⁰⁶
			Si treatment*Fusion	5.801	0.04260521
SYN1	10.209	0.00413556	Si treatment	15.939	0.00399228
			Fusion	14.682	0.00500579
			Si treatment*Fusion	0.005	0.94569912
ANXA1	96.898	1.2527 × 10 ⁻⁰⁶	Si treatment	45.870	0.00014171
			Fusion	243.711	2.8262 × 10 ⁻⁰⁷
			Si treatment*Fusion	1.114	0.32213654
MMP9	5.171	0.02810927	Si treatment	1.134	0.31791426
			Fusion	13.560	0.00619729
			Si treatment*Fusion	0.819	0.39182403
INHHA	137.727	3.1788 × 10 ⁻⁰⁷	Si treatment	40.502	0.00021729
			Fusion	372.037	5.4151 × 10 ⁻⁰⁸
			Si treatment*Fusion	0.641	0.44650823
BAX	21.540	0.00034606	Si treatment	36.796	0.00030055
			Fusion	25.245	0.00102124
			Si treatment*Fusion	2.580	0.14686479
BCL2	8.774	0.00654947	Si treatment	13.427	0.00636233
			Fusion	12.786	0.00723255
			Si treatment*Fusion	0.110	0.74867557

(Continued)

TABLE 3 | Continued

Y variable	Overall tests of univariate models		Tests of univariate effects		
	F	Prob.	Source	F	Prob.
DAPK1	2.339	0.14975061	Si treatment	2.106	0.18480454
			Fusion	2.027	0.1923598
			Si treatment*Fusion	2.884	0.12788132
BAD	32.681	7.7268 × 10 ⁻⁰⁵	Si treatment	55.723	7.1629 × 10 ⁻⁰⁵
			Fusion	36.270	0.0003154
			Si treatment*Fusion	6.050	0.03934242

previous analysis: in the condition where the KD of UCA1 is combined with FSK treatment, the expression profile is close to the one of BeWoC cells without FSK and not treated with the siUCA1. Overall, the FSK effects were all oriented in the same direction of the first axis (clear to dark colors), which can thus be interpreted as a mark of FSK-induced trophoblast differentiation. A strong difference Between BeWoA, BeWoB and the control BeWoC comes from the variation along the second axis, showing that in this case, STOX1-overexpressing cells in the presence of forskolin are positioned with increasing abscissae, suggesting that this axis correlate with STOX1-driven differentiation in the presence of forskolin. When UCA1 is KD, the effect of STOX1 are less pronounced on the second axis (red squares, lozenges-BeWoA and circles-BeWoB). In the absence of FSK the STOX effects are less obvious and the dots are all in the middle of the graph.

Interestingly, the gene expression profiles are very peculiar in BeWoB cells under FSK treatment when analyzing UCA1 effects. On the first axis, UCA1 KD is not able to modify strongly the x-axis in these cells (from ~2.3 to 1.5, Δ = 0.8), while in control BeWoC, the modification on the x-axis ranges from ~1.9 to -0.5, Δ = 2.4, and in BeWoA from ~2.2 to 0.5, Δ = 1.7. The effect on gene differentiation was thus less reduced in BeWoB cells, comforting the idea that BeWoB overexpression and UCA1 KD act similarly but not synergistically against trophoblast fusion. This may be associated to the fact that STOX1B overexpression is associated with deficits of syncytialization (Ducat et al., 2020).

DISCUSSION

In the placenta, the STB acts as a barrier between the mother and fetus, and functions in gas exchange, nutrient, waste transport and hormone production. The STB is mitotically inactive and is formed by the constant cell-cell fusion of the underlying mononuclear CTBs. STB fragments are continuously shed into the maternal circulation. Thus, maintenance of the STB requires a finely regulated turnover. Excessive or restricted CTB-STB fusion may lead to PE, IUGR, and implantation failure (Gauster et al., 2009).

Although derived from human choriocarcinoma, the BeWo cells, display structural and physiological features of human primary trophoblast (Burres and Cass, 1986; Ramos et al., 2008; Orendi et al., 2010) and have been largely used as a model to study the process of trophoblasts fusion induced by forskolin

treatment (Chen et al., 2008; Zhou et al., 2013; Wang et al., 2014). Several transcriptomic studies have helped to identify important genes involved in trophoblast fusion (Kudo et al., 2004; Depoix et al., 2011; Shankar et al., 2015; Zheng et al., 2016). However, the majority of these studies have focused on the role of protein-coding genes. The role that ncRNAs could have in the trophoblast fusion remains to be explored.

Here, we have conducted a microarray transcriptomic analysis of BeWo cells under forskolin treatment (BeWo-FSK) and focused our analysis on the differentially expressed ncRNAs relative to controls (BeWo-CO). We identified a number of ncRNAs (antisense-RNAs, lncRNAs, miRNAs) which might be involved in the process of syncytialization *in vivo*. We have generated a network displaying the putative regulatory interactions among the differentially expressed ncRNAs and differentially expressed genes (DEGs) in the BeWo-FSK relative to the BeWo-CO. The analysis of this network shows that the majority of ncRNAs targets are involved in cell proliferation and metabolism. Topological analysis of the network identified miR193b as a principal hub of the network. Hallmarks enrichment analysis shows that most targets of miR193b are down-regulated genes involved in cell cycle progression such as CCND1, CCNA2, or BUB1B. Previous studies have shown that miR193b acts as tumor suppressor by repressing cell proliferation (Mazzu et al., 2017; Zhang et al., 2017; Bhayadia et al., 2018). In the context of placental development, it has been reported that miR193b-3p overexpression significantly decreases the migration and invasion of the trophoblast cells (HTR-8/SVneo) by targeting the 3'UTR of TGF-beta2 (Zhou et al., 2016). The miR193b has been found consistently up-regulated in PE and IUGR placentas in our study and others (Ishibashi et al., 2012; Xu et al., 2014; Zhou et al., 2016; Awamleh et al., 2019). This miRNA is thought to contribute to these pathologies because of its inhibitory effect on the migration and invasion of trophoblasts. Here we show that miR193b is also involved in the process of syncytialization. A prior, and key step in syncytialisation, is the acquisition of fusion competence, which requires the CTB to exit the cell cycle (Lu et al., 2017). Therefore, by targeting genes involved in the control of cell cycle progression, miR193b could play a pivotal role in this crucial step of the process of syncytialisation. Overexpression of miR193b in PE could negatively impact placental development by accelerating CTB-STB fusion, thus leading to a premature depletion of the pool of CTBs necessary to ensure the constant renewal of the STB. Alternatively, increased miR193b expression in PE could reflect a mechanism seeking to

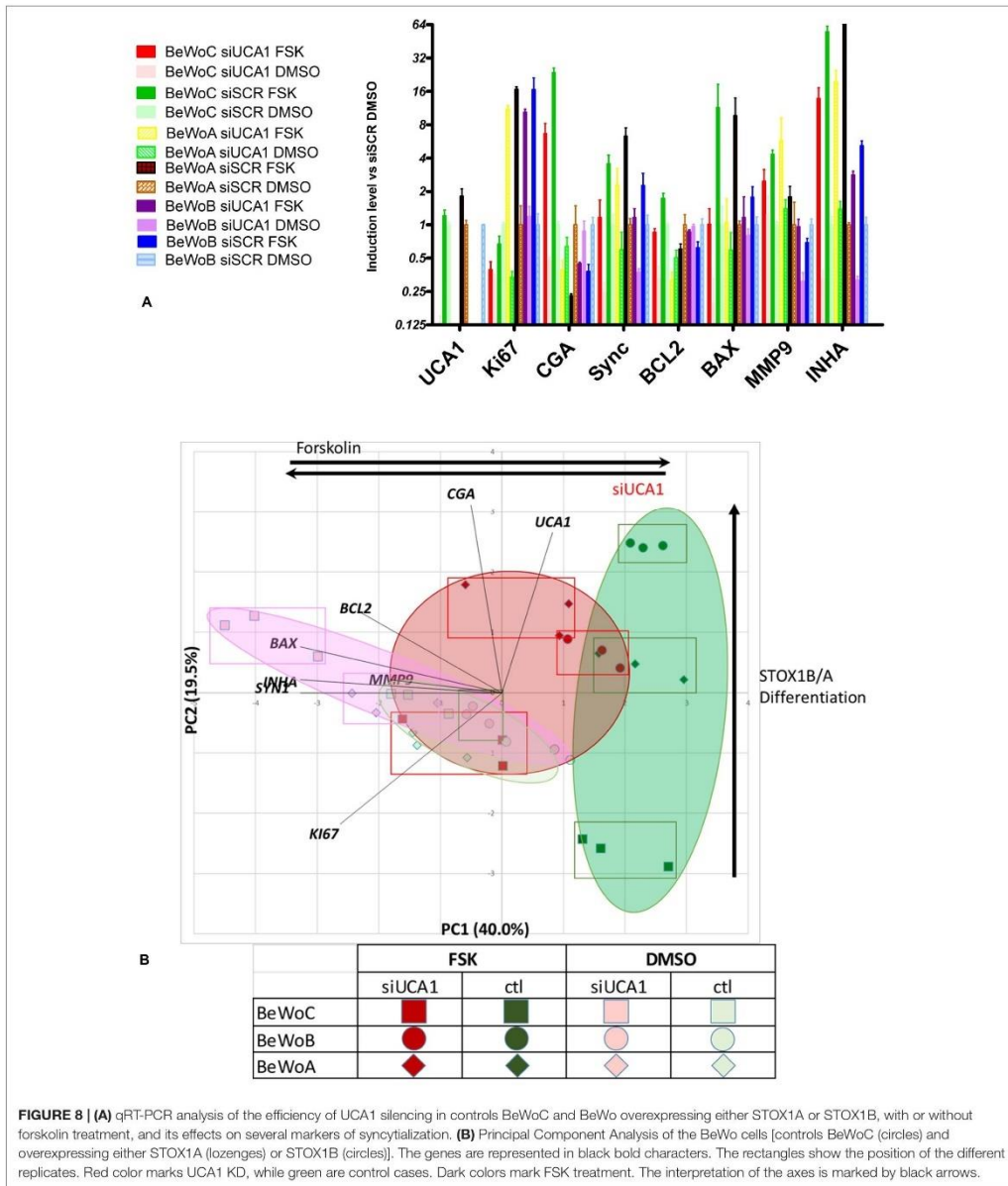


FIGURE 8 | (A) qRT-PCR analysis of the efficiency of UCA1 silencing in controls BeWoC and BeWo overexpressing either STOX1A or STOX1B, with or without forskolin treatment, and its effects on several markers of syncytialization. **(B)** Principal Component Analysis of the BeWo cells [controls BeWoC (circles) and overexpressing either STOX1A (lozenges) or STOX1B (circles)]. The genes are represented in black bold characters. The rectangles show the position of the different replicates. Red color marks UCA1 KD, while green are control cases. Dark colors mark FSK treatment. The interpretation of the axes is marked by black arrows.

compensate an excessive apoptotic shedding of the syncytium by facilitating the entering of CTB into the fusion process.

Since a dysfunctional syncytium could be at the origin of placental diseases, we systematically searched for lncRNAs

involved in the CTBs fusion that were deregulated in placentas from PE or IUGR. An exhaustive literature search, as well and the reanalysis of datasets available in the GEO Database resulted in the identification of three lncRNAs consistently up-regulated

in PE and IUGR and involved in syncytialization: miR193b, miR365a and UCA1.

UCA1 (Urothelial Cancer Associated 1), is a lncRNA initially identified in a bladder cancer cell line (Wang et al., 2006). The involvement of lncRNAs in placental diseases has been previously described for the HELLP syndrome, a serious complication of preeclampsia (van Dijk et al., 2012). In the case of UCA1 high expression has previously been reported in different types of cancer. UCA1 promotes cell proliferation, tumor progression, migration and drug resistance. UCA1 mediates the transcriptional regulation at an epigenetic level by interaction with chromatin modifiers (EZH2, CTCF, YAP, . . .), by direct regulation via chromatin looping and/or by sponging miRNAs (Neve et al., 2018). The oncogenic functions of UCA1 have been extensively studied, but its role in development and differentiation remains unknown. A recent study, using the HTR-8/SVneo and JAR trophoblast cells suggests that UCA1 could inhibit trophoblast cell invasion and proliferation by down-regulating JAK2 (Liu et al., 2020). Knockdown of UCA1 in these cells suppressed the apoptotic rate and accelerated cell proliferation. Increased expression of UCA1 in PE had been reported previously and confirmed by our study (Liu et al., 2020). In addition, increased expression of UCA1, specifically in the STB of preeclamptic placentas, has been reported (Gormley et al., 2017). Thus, these data suggest that similar to miR193b, UCA1 might contribute in driving CTBs toward syncytialisation by inhibiting the genes involved in cell proliferation. The increased expression of UCA1 in the preeclamptic syncytium could reflect an increase in the turnover of the syncytium, to compensate for an increased apoptotic rate (Sharp et al., 2010; Fogarty et al., 2013). However, suppression of UCA1 in the HTR-8/SVneo and JAR cells decreased their apoptotic rates, indicating that UCA1 could also be involved in the induction of apoptosis (Liu et al., 2020). To explore more deeply the role that UCA1 might play in the process of syncytialization, we silenced its expression in the BeWo cells (BeWo-CO and BeWo-FSK) using a specific small interfering RNA (siRNA). Our results show that silencing UCA1 results in the downregulation of proliferation, attenuation of the expression of several markers of syncytialization, and most significantly downregulation of the expression of the antiapoptotic marker BCL2. As mentioned above in the HTR-8/SVneo and JAR cells, the Knockdown of UCA1, suppressed the apoptotic rate and accelerated cell proliferation (Liu et al., 2020). Thus, suppression of UCA1 in BeWo cells seems to have a different impact concerning the proliferation and apoptosis rates. These differences could be attributed to the fact that these cell lines are akin to different types of CTBs or either to particularities linked to the tumoral transformation process undergone by these cells. Nevertheless, our results on the BeWo cells are consistent with other studies indicating that in many cell types, UCA1 stimulates proliferation and inhibits apoptosis (Jun et al., 2018; Liu et al., 2018; Chen et al., 2019; Li et al., 2019; Wang et al., 2019). One limit of our study is that we did not carry out cell visualization experiments of the fusion; we can nevertheless assume that the alterations of syncytialisation marks that we observe here will likely be associated to phenotypic effects, that will have to be further assessed in future works.

Having in hand a model of altered fusion by STOX1A (BeWoA) or STOX1B (BeWoB) overexpression we attempted to evaluate the effect of UCA1 KD in these specific models. The overexpression of STOX1B (inhibiting fusion) led to more limited gene alterations than the other cells when forskolin was added in the Knock down of UCA1, suggesting that the alterations of gene expression induced by STOX1B overexpression render the UCA1 down-regulation alterations less visible.

Interestingly, hypoxia which plays a central role in the development of PE is known to induce UCA1 expression through HIF1A in both cancer cell lines and primary cultures of STB (Yuen et al., 2013; Xue et al., 2014; Zhu et al., 2019; Wang et al., 2020). In addition, it has been shown that UCA1 inhibits ischemia/reperfusion-induced apoptosis in cardiomyocytes (Chen et al., 2019; Wang et al., 2020). Given that ischemia/reperfusion is a known hallmark of severe PE and knowing that UCA1 has been detected as overexpressed specifically in the STB of severe preeclamptic patients (Gormley et al., 2017), it is tempting to speculate that UCA1 overexpression could reflect a protective mechanism aimed to attenuate apoptosis. However, in other cell types UCA1 has proved to exert pleiotropic effects, thus it might be involved in many other aspects of the trophoblast physiology. Although the BeWo cells are a good model to study the cell fusion process they are transformed carcinoma-like cells missing many trophoblast functions. Therefore, a more in-depth analysis of the functions of UCA1 in the placenta requires more physiological models such as primary trophoblast cultures, or placental organocultures. Another direction for future work is the assessment of the specific effects of the short isoforms of UCA1 that appear to be specifically modified when fusion occur. To note, we have recently demonstrated that alternative splicing is a general feature of placental disease, affecting hundreds of genes (Ruano et al., 2021). This could be achieved by lentiviral transformation of the cell lines, or even primary cultures with this short isoform. Finally, to understand better how UCA1 is actually functioning is an interesting challenge for further studies.

METHODS

Cell Culture

BeWo cell lines were cultivated in F12 medium (Life Technologies) supplemented with 10% fetal bovine serum (FBS) and 1% penicillin/streptomycin in 6-cm diameter plates, up to 60% confluence and with 50 µg/ml of geneticin G-418. The generation of the BeWoA (overexpressing constitutively STOX1A), BeWoB (overexpressing constitutively STOX1B) and BeWoC cell lines is described in detail in Ducat et al. (2020). The concentration of forskolin chosen for this study was based on preliminary studies (Ducat et al., 2020). At the end of the treatment, total RNA was extracted as previously described (Ducat et al., 2016). The siRNA against UCA1 was Ambion silencer select provided by ThermoFisher scientific. After plating in 12-well plates (1 ml) at 70% confluency, the cells were transfected the next morning using RNAiMAX transfection

reagent (Invitrogen). Each well was transfected with 200 μ l of OptiMax™ with 1 μ l of RNAiMax and 0.5 μ l of siRNA or si scrambled at 5 pmol/ μ l, following the manufacturer's protocol. To induce syncytialization the cells were treated 1 day later with 20 μ M forskolin or vehicle (DMSO) for 72 h.

Microarray Assay

One hundred ng of RNA per sample were analyzed using the ClariomD (Affymetrix) microarray assay. Library preparation, hybridization and data acquisition were performed by GENOMIC platform according to manufacturer's instructions. Gene and exon level expressions were processed and extracted from the ClariomD microarray using the Transcriptomic Analysis Console (TAC) provided by Affymetrix.

Quantitative Reverse Transcribed-PCR

Five hundred nanograms of total RNA were reverse transcribed with MMLV using the Invitrogen kit and random primers. qPCR was carried out under standard conditions in a LightCycler480 (Roche) in 96 well plates as previously described (Ducat et al., 2020), with a Sybrgreen kit from BioLine (Meridian Bioscience). In the case of UCA1, the analysis was carried out using a TaqMan probe and the Roche LightCycler® TaqMan® Master. The PPIA gene (cyclophilin) was used as reporter in all experiment, since we have shown previously an excellent stability of this gene in trophoblast cells. All the cell qPCR experiments were carried out three to four independent times, and every time in triplicates. Primers for the different genes are listed as **Supplementary Table 4**.

Functional Annotation of the Differentially Expressed Genes (DEGs)

For the functional annotation of the DEGs we performed Over-representation analysis (ORA) using the WebGestalt¹ bioinformatics resource (Liao et al., 2019). Databases interrogated include: Gene Ontology (GO), Kyoto Encyclopedia of Genes and Genomes (KEGG), and Hallmarks. The significance of the detected enrichments was calculated using the Benjamini and Hochberg multiple test adjustment.

Gene Set Enrichment Analysis (GSEA)

GSEA was conducted using GSEA software from the Broad Institute². The BeWo fusion gene set was generated using the top up-regulated and down-regulated genes after 72 h forskolin treatment reported by Shankar et al. (2015). We used as input the gene expression matrix generated by the Transcriptomic Analysis Console (Affymetrix) including all samples and replicates. The permutation value was set as 1,000. *P*-values were corrected for multiple testing and the cutoff for significant enrichment corresponds to an FDR < 0.25.

Prediction of ncRNAs Targets

To identify targets for the differentially expressed ncRNAs in the BeWo-FSK relative to BeWo-Co cells we used *ad hoc* databases.

¹<http://bioinfo.vanderbilt.edu/webgestalt>

²<https://www.gsea-msigdb.org/gsea/index.jsp>

These include miRBase³, starBase v2.0.⁴ and the DianaTools LncBase v.2⁵.

ncRNAs Regulatory Network

The ncRNAs and corresponding differentially expressed targets were used to generate a regulatory network. The network was constructed, visualized and analyzed using the Cytoscape 3.2.1 software⁶ and its complementary applications (Shannon et al., 2003). The centrality parameters of the network were analyzed using the Cytoscape application NetworkAnalyzer (Shannon et al., 2003). Two topological parameters Betweenness Centrality (BC) and node degree were used to identify hub genes. The network is available as a **Supplementary XML File**.

DATA AVAILABILITY STATEMENT

The datasets presented in this study can be found in online repositories. The names of the repository/repositories and accession number(s) can be found below: <https://www.ebi.ac.uk/metagenomics/>, E-MTAB-9416 and <https://www.ncbi.nlm.nih.gov/genbank/>, GSE148088.

ETHICS STATEMENT

This study was approved by the Ethics Committee and CCPPRB (Comité Consultatif de Protection des Personnes dans la Recherche Biomédicale) of Paris Cochin. All patients gave their written consent for the use of their placenta and blood samples. For Angers, the collection and use for research purpose (including genetic analyses) of placentas from pregnancies complicated with IUGR or healthy pregnancy have been approved by the Ethics Committee of Angers. The patients/participants provided their written informed consent to participate in this study.

AUTHOR CONTRIBUTIONS

DV, FM, and CM conceived the work and drafted it. DV performed qRT-PCR experiments. SJ performed the microarray work. GG drafted the manuscript and contributed human samples. CR and CA performed RNA and qPCR experiments and drafted the manuscript. All authors contributed to the article and approved the submitted version.

FUNDING

The Ph.D. projects of CR and CA were funded by the European Union's Horizon 2020 Research and Innovation

³<http://www.mirbase.org/>

⁴<http://starbase.sysu.edu.cn>

⁵<http://diana.imis.athena-innovation.gr/DianaTools/index.php?r=IncBase/index>

⁶<https://cytoscape.org/>

Program under Marie Skłodowska-Curie Actions Innovative Training Network (H2020-MSCA-ITN 2017, Grant No. 765274, acronym iPLACENTA).

SUPPLEMENTARY MATERIAL

The Supplementary Material for this article can be found online at: <https://www.frontiersin.org/articles/10.3389/fcell.2021.633937/full#supplementary-material>

REFERENCES

- Apicella, C., Ruano, C. S. M., Mehats, C., Miralles, F., and Vaiman, D. (2019). The role of epigenetics in placental development and the etiology of preeclampsia. *Int. J. Mol. Sci.* 20:2837. doi: 10.3390/ijms20112837
- Awamleh, Z., Gloor, G. B., and Han, V. K. M. (2019). Placental microRNAs in pregnancies with early onset intrauterine growth restriction and preeclampsia: potential impact on gene expression and pathophysiology. *BMC Med. Genomics* 12:91. doi: 10.1186/s12920-019-0548-x
- Basit, S., Wohlfahrt, J., and Boyd, H. A. (2018). Pre-eclampsia and risk of dementia later in life: nationwide cohort study. *BMJ* 363:k4109. doi: 10.1136/bmj.k4109
- Benny, P. A., Alakwaa, F. M., Schlueter, R. J., Lassiter, C. B., and Garmire, L. X. (2020). A review of omics approaches to study preeclampsia. *Placenta* 92, 17–27. doi: 10.1016/j.placenta.2020.01.008
- Bhayadia, R., Krowiorz, K., Haetscher, N., Jammal, R., Emmrich, S., Obulkasim, A., et al. (2018). Endogenous tumor suppressor microRNA-193b: therapeutic and prognostic value in acute myeloid leukemia. *J. Clin. Oncol.* 36, 1007–1016. doi: 10.1200/JCO.2017.75.2204
- Brouwers, L., van der Meiden-van Roest, A. J., Savelkoul, C., Vogelvang, T. E., Lely, A. T., Franx, A., et al. (2018). Recurrence of pre-eclampsia and the risk of future hypertension and cardiovascular disease: a systematic review and meta-analysis. *BJOG* 125, 1642–1654. doi: 10.1111/1471-0528.15394
- Burres, N. S., and Cass, C. E. (1986). Density-dependent inhibition of expression of syncytiotrophoblastic markers by cultured human chorionicarcoma (BeWo) cells. *J. Cell. Physiol.* 128, 375–382. doi: 10.1002/jcp.1041280305
- Chabrun, F., Huetz, N., Dieu, X., Rousseau, G., Bouzille, G., Chao de la Barca, J. M., et al. (2019). Data-mining approach on transcriptomics and methylomics placental analysis highlights genes in fetal growth restriction. *Front. Genet.* 10:1292. doi: 10.3389/fgene.2019.01292
- Chen, J., Hu, Q., Zhang, B. F., Liu, X. P., Yang, S., and Jiang, H. (2019). Long noncoding RNA UCA1 inhibits ischaemia/reperfusion injury induced cardiomyocytes apoptosis via suppression of endoplasmic reticulum stress. *Genes Genomics* 41, 803–810. doi: 10.1007/s13258-019-00806-w
- Chen, Y., Qian, H., Zhang, Y., Ma, Y., Lin, C., and Xiang, Y. (2008). Effect of Ad-TIMP3 on biologic behavior of choriocarcinoma cells in vitro. *J. Reprod. Med.* 53, 608–614.
- Costa, M. A. (2016). Scrutinising the regulators of syncytialization and their expression in pregnancy-related conditions. *Mol. Cell. Endocrinol.* 420, 180–193. doi: 10.1016/j.mce.2015.11.010
- Cox, B., Leavey, K., Nosi, U., Wong, F., and Kingdom, J. (2015). Placental transcriptome in development and pathology: expression, function, and methods of analysis. *Am. J. Obstet. Gynecol.* 213, S138–S151. doi: 10.1016/j.ajog.2015.07.046
- Darendeliler, F. (2019). IUGR: genetic influences, metabolic problems, environmental associations/triggers, current and future management. *Best Pract. Res. Clin. Endocrinol. Metab.* 33:101260. doi: 10.1016/j.beem.2019.01.001
- Depoix, C., Tee, M. K., and Taylor, R. N. (2011). Molecular regulation of human placental growth factor (PLGF) gene expression in placental villi and trophoblast cells is mediated via the protein kinase a pathway. *Reprod. Sci.* 18, 219–228. doi: 10.1177/1933719110389337
- Deysenroth, M. A., Peng, S., Hao, K., Lambertini, L., Marsit, C. J., and Chen, J. (2017). Whole-transcriptome analysis delineates the human placenta gene network and its associations with fetal growth. *BMC Genomics* 18:520. doi: 10.1186/s12864-017-3878-0
- Ducat, A., Couderc, B., Bouter, A., Biquard, L., Aouache, R., Passet, B., et al. (2020). Molecular mechanisms of trophoblast dysfunction mediated by imbalance between STOX1 isoforms. *iScience* 23:101086. doi: 10.1016/j.isci.2020.101086
- Ducat, A., Doridot, L., Calicchio, R., Mehats, C., Vilotte, J. L., Castille, J., et al. (2016). Endothelial cell dysfunction and cardiac hypertrophy in the STOX1 model of preeclampsia. *Sci. Rep.* 6:19196. doi: 10.1038/srep19196
- Fernandes, J. C. R., Acuna, S. M., Aoki, J. I., Floeter-Winter, L. M., and Muxel, S. M. (2019). Long non-coding RNAs in the regulation of gene expression: physiology and disease. *Noncoding RNA* 5:17. doi: 10.3390/ncrna5010017
- Fogarty, N. M., Ferguson-Smith, A. C., and Burton, G. J. (2013). Syncytial knots (Tennney-Parker changes) in the human placenta: evidence of loss of transcriptional activity and oxidative damage. *Am. J. Pathol.* 183, 144–152. doi: 10.1016/j.ajpath.2013.03.016
- Gauster, M., Moser, G., Orendi, K., and Huppertz, B. (2009). Factors involved in regulating trophoblast fusion: potential role in the development of preeclampsia. *Placenta* 30 Suppl. A, S49–S54. doi: 10.1016/j.placenta.2008.10.011
- George, E. M., and Bidwell, G. L. (2013). STOX1: a new player in preeclampsia? *Hypertension* 61, 561–563. doi: 10.1161/HYPERTENSIONAHA.111.00721
- Gibbs, L., Leavey, K., Benton, S. J., Gynspan, D., Bainbridge, S. A., and Cox, B. J. (2019). Placental transcriptional and histologic subtypes of normotensive fetal growth restriction are comparable to preeclampsia. *Am. J. Obstet. Gynecol.* 220, e1–e110. doi: 10.1016/j.ajog.2018.10.003
- Goldenberg, R. L., Culhane, J. F., Iams, J. D., and Romero, R. (2008). Epidemiology and causes of preterm birth. *Lancet* 371, 75–84. doi: 10.1016/S0140-6736(08)60074-4
- Gormley, M., Ona, K., Kapidzic, M., Garrido-Gomez, T., Zdravkovic, T., and Fisher, S. J. (2017). Preeclampsia: novel insights from global RNA profiling of trophoblast subpopulations. *Am. J. Obstet. Gynecol.* 217, e1–e200. doi: 10.1016/j.ajog.2017.03.017
- Guller, S., Ma, Y. Y., Fu, H. H., Krikun, G., Abrahams, V. M., and Mor, G. (2008). The placental syncytium and the pathophysiology of preeclampsia and intrauterine growth restriction: a novel assay to assess syncytial protein expression. *Ann. N. Y. Acad. Sci.* 1127, 129–133. doi: 10.1196/annals.143.4.015
- Hayder, H., O'Brien, J., Nadeem, U., and Peng, C. (2018). MicroRNAs: crucial regulators of placental development. *Reproduction* 155, R259–R271. doi: 10.1530/REP-17-0603
- Hombach, S., and Kretz, M. (2016). Non-coding RNAs: classification, biology and functioning. *Adv. Exp. Med. Biol.* 937, 3–17. doi: 10.1007/978-3-319-42059-2_1
- Ishibashi, O., Ohkuchi, A., Ali, M. M., Kurashina, R., Luo, S. S., Ishikawa, T., et al. (2012). Hydroxysteroid (17-beta) dehydrogenase 1 is dysregulated by miR-210 and miR-518c that are aberrantly expressed in preeclamptic placentas: a novel marker for predicting preeclampsia. *Hypertension* 59, 265–273. doi: 10.1161/HYPERTENSIONAHA.111.180232
- Jun, T., Zheng, F. S., Ren, K. M., Zhang, H. Y., Zhao, J. G., and Zhao, J. Z. (2018). Suppression of long non-coding RNA UCA1 inhibits proliferation and invasion and induces apoptosis in human lung cancer cells. *Eur. Rev. Med. Pharmacol. Sci.* 22, 7274–7281.
- Kudo, Y., Boyd, C. A., Sargent, I. L., Redman, C. W., Lee, J. M., and Freeman, T. C. (2004). An analysis using DNA microarray of the time course of gene expression during syncytialization of a human placental cell line (BeWo). *Placenta* 25, 479–488. doi: 10.1016/j.placenta.2003.12.001

Li, J. L., Liu, X. L., Guo, S. F., Yang, Y., Zhu, Y. L., and Li, J. Z. (2019). Long noncoding RNA UCA1 regulates proliferation and apoptosis in multiple myeloma by targeting miR-331-3p/IL6R axis for the activation of JAK2/STAT3 pathway. *Eur. Rev. Med. Pharmacol. Sci.* 23, 9238–9250.

Liao, Y., Wang, J., Jaehrig, E. J., Shi, Z., and Zhang, B. (2019). WebGestalt 2019: gene set analysis toolkit with revamped UIs and APIs. *Nucleic Acids Res.* 47, W199–W205. doi: 10.1093/nar/gkz401

Liu, J., Luo, C., Zhang, C., Cai, Q., Lin, J., Zhu, T., et al. (2020). Upregulated lncRNA UCA1 inhibits trophoblast cell invasion and proliferation by downregulating JAK2. *J. Cell. Physiol.* 235, 7410–7419. doi: 10.1002/jcp.29643

Liu, Q., Li, Y., Lv, W., Zhang, G., Tian, X., Li, X., et al. (2018). UCA1 promotes cell proliferation and invasion and inhibits apoptosis through regulation of the miR129-SOX4 pathway in renal cell carcinoma. *Oncol. Targets Ther.* 11, 2475–2487. doi: 10.2147/OTT.S160192

Lu, X., Wang, R., Zhu, C., Wang, H., Lin, H. Y., Gu, Y., et al. (2017). Fine-tuned and cell-cycle-restricted expression of fusogenic protein Syncytin-2 maintains functional placental syncytia. *Cell Rep.* 21, 1150–1159. doi: 10.1016/j.celrep.2017.10.019

Majewska, M., Lipka, A., Pauksztó, L., Jastrzebski, J. P., Szeszko, K., Gowkielewicz, M., et al. (2019). Placenta transcriptome profiling in intrauterine growth restriction (IUGR). *Int. J. Mol. Sci.* 20:1510. doi: 10.3390/ijms20061510

Mazzu, Y. Z., Hu, Y., Soni, R. K., Mojica, K. M., Qin, L. X., Agius, P., et al. (2017). miR-193b-regulated signaling networks serve as tumor suppressors in liposarcoma and promote adipogenesis in adipose-derived stem cells. *Cancer Res.* 77, 5728–5740. doi: 10.1158/0008-5472.CAN-16-2253

Medina-Bastidas, D., Guzman-Huerta, M., Borboa-Olivares, H., Ruiz-Cruz, C., Parra-Hernandez, S., Flores-Pliego, A., et al. (2020). Placental microarray profiling reveals common mRNA and lncRNA expression patterns in preeclampsia and intrauterine growth restriction. *Int. J. Mol. Sci.* 21:3597. doi: 10.3390/ijms21103597

Nardoza, L. M. M., Zamarian, A. C. P., and Araujo Junior, E. (2017). New definition of fetal growth restriction: consensus regarding a major obstetric complication. *Rev. Bras. Ginecol. Obstet.* 39, 315–316. doi: 10.1055/s-0037-1603741

Neve, B., Jonckheere, N., Vincent, A., and Van Seuningen, I. (2018). Epigenetic regulation by lncRNAs: an overview focused on UCA1 in colorectal cancer. *Cancers (Basel)* 10:440. doi: 10.3390/cancers10110440

Newstead, J., von Dadelszen, P., and Magee, L. A. (2007). Preeclampsia and future cardiovascular risk. *Expert Rev. Cardiovasc. Ther.* 5, 283–294. doi: 10.1586/14779072.5.2.283

Orendi, K., Gauster, M., Moser, G., Meiri, H., and Huppertz, B. (2010). The choriocarcinoma cell line BeWo: syncytial fusion and expression of syncytium-specific proteins. *Reproduction* 140, 759–766. doi: 10.1530/REP-10-0221

Ramos, A. J., Cantero, M. R., Zhang, P., Raychowdhury, M. K., Green, A., MacPhee, D., et al. (2008). Morphological and electrical properties of human trophoblast choriocarcinoma. BeWo cells. *Placenta* 29, 492–502. doi: 10.1016/j.placenta.2008.02.013

Rana, S., Lemoine, E., Granger, J. P., and Karumanchi, S. A. (2019). Preeclampsia: pathophysiology, challenges, and perspectives. *Circ. Res.* 124, 1094–1112. doi: 10.1161/CIRCRESAHA.118.313276

Roland, C. S., Hu, J., Ren, C. E., Chen, H., Li, J., Vavoutis, M. S., et al. (2016). Morphological changes of placental syncytium and their implications for the pathogenesis of preeclampsia. *Cell. Mol. Life Sci.* 73, 365–376. doi: 10.1007/s00018-015-2069-x

Ruano, C. S. M., Apicella, C., Jacques, S., Gascoïn, G., Gaspar, C., Miralles, F., et al. (2021). Alternative splicing in normal and pathological human placentas is correlated to genetic variants. *Hum. Genet.* 140, 827–848. doi: 10.1007/s00439-020-02248-x

Shankar, K., Kang, P., Zhong, Y., Borengasser, S. J., Wingfield, C., Saben, J., et al. (2015). Transcriptomic and epigenomic landscapes during cell fusion in BeWo trophoblast cells. *Placenta* 36, 1342–1351. doi: 10.1016/j.placenta.2015.10.010

Shannon, P., Markiel, A., Ozier, O., Baliga, N. S., Wang, J. T., Ramage, D., et al. (2003). Cytoscape: a software environment for integrated models of biomolecular interaction networks. *Genome Res.* 13, 2498–2504. doi: 10.1101/gr.1239303

Sharp, A. N., Heazell, A. E., Crocker, I. P., and Mor, G. (2010). Placental apoptosis in health and disease. *Am. J. Reprod. Immunol.* 64, 159–169. doi: 10.1111/j.1600-0897.2010.00837.x

Steegers, E. A., von Dadelszen, P., Duvekot, J. J., and Pijnenborg, R. (2010). Pre-eclampsia. *Lancet* 376, 631–644. doi: 10.1016/S0140-6736(10)60279-6

Turco, M. Y., and Moffett, A. (2019). Development of the human placenta. *Development* 146, doi: 10.1242/dev.163428

Vaiman, D., and Miralles, F. (2016). Targeting STOX1 in the therapy of preeclampsia. *Expert Opin. Ther. Targets* 20, 1433–1443. doi: 10.1080/14728222.2016.1253682

van Dijk, M., Thulluru, H. K., Mulders, J., Michel, O. J., Poutsma, A., Windhorst, S., et al. (2012). HELLP babies link a novel lincRNA to the trophoblast cell cycle. *J. Clin. Invest.* 122, 4003–4011. doi: 10.1172/JCI65171

Wang, C. J., Zhu, C. C., Xu, J., Wang, M., Zhao, W. Y., Liu, Q., et al. (2019). The lncRNA UCA1 promotes proliferation, migration, immune escape and inhibits apoptosis in gastric cancer by sponging anti-tumor miRNAs. *Mol. Cancer* 18:115. doi: 10.1186/s12943-019-1059-2

Wang, Q. S., Zhou, J., and Li, X. (2020). lncRNA UCA1 protects cardiomyocytes against hypoxia/reoxygenation induced apoptosis through inhibiting miR-143/MDM2/p53 axis. *Genomics* 112, 574–580. doi: 10.1016/j.ygeno.2019.04.009

Wang, R., Dang, Y. L., Zheng, R., Li, Y., Li, W., Lu, X., et al. (2014). Live cell imaging of in vitro human trophoblast syncytialization. *Biol. Reprod.* 90:117. doi: 10.1095/biolreprod.113.114892

Wang, X. S., Zhang, Z., Wang, H. C., Cai, J. L., Xu, Q. W., Li, M. Q., et al. (2006). Rapid identification of UCA1 as a very sensitive and specific unique marker for human bladder carcinoma. *Clin. Cancer Res.* 12, 4851–4858. doi: 10.1158/1078-0432.CCR-06-0134

Xu, P., Zhao, Y., Liu, M., Wang, Y., Wang, H., Li, Y. X., et al. (2014). Variations of microRNAs in human placentas and plasma from preeclamptic pregnancy. *Hypertension* 63, 1276–1284. doi: 10.1161/HYPERTENSIONAHA.113.02647

Xue, M., Chen, W., and Li, X. (2016). Urothelial cancer associated 1: a long noncoding RNA with a crucial role in cancer. *J. Cancer Res. Clin. Oncol.* 142, 1407–1419. doi: 10.1007/s00432-015-2042-y

Xue, M., Li, X., Li, Z., and Chen, W. (2014). Urothelial carcinoma associated 1 is a hypoxia-inducible factor-1alpha-targeted long noncoding RNA that enhances hypoxic bladder cancer cell proliferation, migration, and invasion. *Tumour Biol.* 35, 6901–6912. doi: 10.1007/s13277-014-1925-x

Yuen, R. K., Chen, B., Blair, J. D., Robinson, W. P., and Nelson, D. M. (2013). Hypoxia alters the epigenetic profile in cultured human placental trophoblasts. *Epigenetics* 8, 192–202. doi: 10.4161/epi.23400

Zhang, J., Qin, J., and Su, Y. (2017). miR-193b-3p possesses anti-tumor activity in ovarian carcinoma cells by targeting p21-activated kinase 3. *Biomed. Pharmacother.* 96, 1275–1282. doi: 10.1016/j.biopha.2017.11.086

Zheng, R., Li, Y., Sun, H., Lu, X., Sun, B. F., Wang, R., et al. (2016). Deep RNA sequencing analysis of syncytialization-related genes during BeWo cell fusion. *Reproduction* doi: 10.1530/REP-16-0343

Zhou, X., Li, Q., Xu, J., Zhang, X., Zhang, H., Xiang, Y., et al. (2016). The aberrantly expressed miR-193b-3p contributes to preeclampsia through regulating transforming growth factor-beta signaling. *Sci. Rep.* 6:19910. doi: 10.1038/srep19910

Zhou, Z., Zhang, Q., Lu, X., Wang, R., Wang, H., Wang, Y. L., et al. (2013). The proprotein convertase furin is required for trophoblast syncytialization. *Cell Death Dis.* 4:e593. doi: 10.1038/cddis.2013.106

Zhu, T. T., Sun, R. L., Yin, Y. L., Quan, J. P., Song, P., Xu, J., et al. (2019). Long noncoding RNA UCA1 promotes the proliferation of hypoxic human pulmonary artery smooth muscle cells. *Pflugers Arch.* 471, 347–355. doi: 10.1007/s00424-018-2219-8

Conflict of Interest: The authors declare that the research was conducted in the absence of any commercial or financial relationships that could be construed as a potential conflict of interest.

Copyright © 2021 Apicella, Ruano, Jacques, Gascoïn, Méhats, Vaiman and Miralles. This is an open-access article distributed under the terms of the Creative Commons Attribution License (CC BY). The use, distribution or reproduction in other forums is permitted, provided the original author(s) and the copyright owner(s) are credited and that the original publication in this journal is cited, in accordance with accepted academic practice. No use, distribution or reproduction is permitted which does not comply with these terms.

Discussion and Future Perspectives

The scope of this PhD thesis was to improve knowledge and understanding of the placenta, a relatively neglected human organ, and of placental pathologies such as PE and IUGR. Four main axes have been developed through a multi-omics approach: epigenetics, single nuclei transcriptomics, genome-wide alternative splicing, and long non-coding RNAs analyses.

Firstly, this journey started with the analysis of DNA methylation of healthy and pathological placentas. At the beginning, only 16 samples were available for analysis in Paris. But our preliminary data caught the attention of several groups from the iPlacenta Consortium and opened the possibility to increase our number of samples. Six valuable preeclamptic placental samples were then kindly shared by Pr. Basky Thilaganathan and Dr. Veronica Giorgione, from St. Georges University. With these additional pathological samples and the collection of additional healthy samples at the Maternity Port Royal-Cochin in Paris, we increased our initial dataset to a total of 32 samples. This doubling of samples gave us a boost of happiness and confidence and the DNAm analyzes were continued. Later, repeated analytical problems with batch experimental effects and other confounding factors, in particular related to the difference in mean GA between the groups, call into question the choice of the appropriate methods to discriminate the CpGs linked specifically to the pathology. The addition of earlier term placental samples in our dataset appeared to be the best way to deal with the GA issue. We identified in the public databank GEO a DNAm dataset that includes 42 placental samples of early gestational term from unaffected and chorioamnionitis-affected placental villi. Thus, we decided to add this dataset to reach a total of 73 samples in our analyses.

Since DNAm pattern can be influenced by many variables, such as age, mother characteristics, cell type, etc, we sought to collect as much information as possible to be included in our regression model. We were especially interested in cell composition since DNAm is specifically linked to the cell type (Baron et al., 2006). Most of the published placental DNAm studies so far have

not considered the influence of subtype proportion in their analysis. Whether or not cell variability is considered can have a significant impact on the results of the mDNA profile, in particular when the pathology can affect cell composition. Cell deconvolution helped us to identify proportions of syncytiotrophoblast, trophoblast, stromal, endothelial cell, etc in our dataset using the work of Yuan et coll. (Yuan et al., 2021) as a reference. This reference, built on a DNAm study performed after physical separation of cell types in the placenta, provides a set of CpG signatures for each of the cell types mentioned. Although there are some pitfalls in producing this dataset due to the complexity of syncytiotrophoblasts, this was the most accurate list of cells type-specific DNAm marks at that time.

A multivariate linear regression was next performed using 16 covariates from clinical, technical, and inferred variables, leading us to a signature subset of 142 CpGs for PE-affected placentas. Several different studies have analysed DNAm in preeclampsia in a genome-wide manner, however, very low or none overlap is observed between these studies, with a reproducibility rate of around 30% (Wilson et al., 2017). Most of these studies do not take in account confounding variables. Another consideration is the high DNAm profile variability between individuals and even within the same placental sample (Avila et al., 2010). Indeed, site-to-site expression differences within the same placenta have been observed (Pidoux et al., 2004). This site-to-site variability may reflect a relative placenta plasticity which favours fast adaptation to the environment without impairing the fetal development (Rondinone et al., 2021). This environmental sensing may be a main source of variation under the model of “polycreodism”, which states that the environmental status influences the cell lineage commitment during embryo development, thus influencing the cell repertoire present in the placenta (Lappalainen & Greally, 2017) and DNAm may be part of this process. Also, adding the complexity of PE and/or IUGR pathophysiology to the difficulty of accurately profiling DNAm in healthy placenta is challenging. Thus, a consensus on the description of the disease, the use of well-characterized covariates in methylation studies and validation with gene expression can help in the further characterization of the disease at the methylation level with better reproducibility.

As mentioned before, 6 valuable frozen biopsies from PE-affected placentas were shared by Pr. Basky Thilaganathan and Dr. Veronica Giorgione from St. Georges University, London. This gave us the opportunity to perform in the last 6-months of this thesis, a single-nucleus transcriptomic analysis including these 4 PE-affected samples along with 8 biopsies of unaffected placentas of third trimester pregnancy. After quality checks and filtering, 71,719 unique transcriptomes were obtained and used in the downstream analyses. Given the short period of time between the data collection and the end of my thesis, we focused some of our downstream analyses on the SCT nuclei. While the two most populated SCT clusters presented a global gene-signature related to growth and prolactin response, we were able to identify SCT subsets with specific functional signatures, such as tryptophan metabolism, endocytosis, steroid hormone production, and inflammatory pathways among others, suggesting high transcriptional compartmentalization —spatial and/or temporal— in the placental syncytium.

A total of 21 different cell clusters were found in our data set, suggesting a high heterogeneity within the placenta. Comparing with previous work in single-cell data in first trimester placenta, we observed an increased functional heterogeneity not observed before.

When comparing gene expression in unaffected and PE-affected at the cell-type level, we detected DEGs within all the cell subpopulations. However, the two most populated SCT clusters and a specific cluster of VCTs displayed the highest number of DEGs (~1,800 genes). A total of 637 DEGs were common to these three clusters, involved in oxidative phosphorylation pathways. Oxidative stress caused by periods of hypoxia and reoxygenation have been described in PE, due to improper vascular remodelling (Hung, Skepper, Charnock-Jones, & Burton, 2002; van Patot, Ebensperger, Gassmann, & Llanos, 2012). In PE, an oxidative environment is thought to provoke morphological and functional dysregulations of the syncytial layer, such as increased levels of apoptosis, high levels

of shedding into the maternal circulation and increased concentrations of unfolded proteins (Mukherjee et al., 2021; Redman, Staff, & Roberts, 2020).

Furthermore, preliminary inference of cell states in the trophoblast showed RNA velocity differences in these clusters between the two sample groups. The computational methods on this topic are still in their infancy, but the fascinating idea of being able to determine the future of cells was too exciting to not to put it in my thesis. At a first glance, the observed differences are in line with previous observations showing increased VCTs proliferation and decrease of the SCT differentiation state (Redline & Patterson, 1995). To conclude, this snRNA-seq analysis of third trimester placenta points to a defect in the syncytiotrophoblast layer in PE. SCT nuclei, embedded in the syncytial frontier in contact with the maternal blood, display a variety of transcriptomic profiles and functions, ranging from invasion, fusion, immunosuppression, hormone regulation and apoptosis. We also observed specific dysregulations in these SCT nuclei in PE-affected placentas, suggesting that stressed SCT is a key element in the development of the disease.

While performing these two main projects, other two side projects were developed in order to gain further knowledge in placental regarding alternative splicing and the role of ncRNAs in syncytialization.

Placental soluble fms-like tyrosine kinase 1 (sFlt1), an antagonist of VEGF and placental growth factor (PlGF), is upregulated in PE (Maynard et al., 2003) and measuring maternal serum concentrations of sFlt-1 and PlGF can differentiate healthy women from women with PE (Levine et al., 2004). sFLT1 is thought to be generated through alternative splicing. We hypothesized that global deregulation in alternative splicing may be a common feature in diseased placenta. We analysed bulk transcriptomes of 17 unaffected placentas, 7 PE-, and 13 IUGR-affected placentas at the exon-level and observed differentially splicing in 1,060 genes in PE and 1,409 genes in IUGR compared to control samples (Ruano et al., 2021). Spliced genes in PE are enriched in genes related to extracellular matrix, circulatory system development, and neuronal physiology while IUGR spliced

genes are enriched in genes involved in steroidogenesis, hormone metabolisms and anion transport. We also found 52 cis sQTLs and 52 trans sQTLs, suggesting some of the splicing differences are genetically based. However, experimental validation by gene editing, for example, is needed to confirm the genetic influence in the production of these alternative splicing forms.

Finally, we performed a genome-wide analysis of the ncRNAs in pathological placentas and identified a new actor, UCA-1, in the syncytialization process (Apicella et al., 2021). This study suggested that ncRNAs may also be key in placental biology and disease development. Off note, differentially expressed lncRNAs were detected as the topmost dysregulated genes in our snRNA-seq data.

These omics approaches provide a holistic perspective of cell, tissue, and organ function. The future integration of the omics placental datasets we generated will help to underpin the biological processes in healthy and diseased placentas in a multi-layered view.

Conclusion

Under the supervision and expertise of Dr Céline Mehats and Dr Daniel Vaiman, we aimed to understand the placenta from different and novel perspectives. I was able to learn and develop new skills and gained knowledge in the new computational ways of understanding the biology and the placenta. The rapid development of new technologies and are opening a wide variety of future perspectives in larger omics scales in which integration of genomics, transcriptomics, epigenomics and other “omics” such as metabolomics or immunomics could be of high interest. Moreover, new techniques, such as single-molecule protein profiles could have an outstanding breakthrough in the assessment and understanding of molecular biology and the placenta.

It has been such an inspiring journey, a great challenge, and great satisfaction to contribute to this field and to understand, slightly bit better, this amazing organ.

ANNEX.1

Annex 1.1: Information about the samples used to assess DNAm profile

	GA	Sex	Term	Batch	Group	Series
GSM3179712	32	Male	PT	3	chorioamnionitis	GSEO (3)
GSM3179713	30	Female	PT	3	CTRL	GSEO (3)
GSM3179714	32	Female	PT	3	CTRL	GSEO (3)
GSM3179715	32	Female	PT	3	CTRL	GSEO (3)
GSM3179717	32	Male	PT	3	chorioamniotitis	GSEO (3)
GSM3179718	37	Male	PT	3	CTRL	GSEO (3)
GSM3179719	28	Female	PT	3	chorioamnionitis	GSEO (3)
GSM3179720	37	Male	T	3	CTRL	GSEO (3)
GSM3179721	28	Male	PT	3	chorioamnionitis	GSEO (3)
GSM3179722	33	Female	PT	3	chorioamnionitis	GSEO (3)
GSM3179723	33	Male	PT	3	CTRL	GSEO (3)
GSM3179724	29	Female	PT	3	CTRL	GSEO (3)
GSM3179726	32	Female	PT	3	chorioamnionitis	GSEO (3)
GSM3179727	32	Male	PT	3	CTRL	GSEO (3)
GSM3179728	37	Female	T	3	CTRL	GSEO (3)
GSM3179729	29	Male	PT	3	chorioamnionitis	GSEO (3)
GSM3179731	32	Female	PT	3	chorioamnionitis	GSEO (3)
GSM3179732	33	Female	PT	3	chorioamnionitis	GSEO (3)
GSM3179733	33	Female	PT	3	CTRL	GSEO (3)
GSM3179734	32	Female	PT	3	chorioamnionitis	GSEO (3)
GSM3179735	29	Male	PT	3	chorioamnionitis	GSEO (3)
GSM3179736	33	Male	PT	3	CTRL	GSEO (3)
GSM3179737	28	Female	PT	3	chorioamnionitis	GSEO (3)
GSM3179738	30	Female	PT	3	chorioamnionitis	GSEO (3)
GSM3179739	28	Male	PT	3	CTRL	GSEO (3)
GSM3179740	29	Female	PT	3	chorioamnionitis	GSEO (3)
GSM3179741	33	Male	PT	3	CTRL	GSEO (3)
GSM3179742	29	Male	PT	3	chorioamnionitis	GSEO (3)
GSM3179743	36	Male	PT	3	CTRL	GSEO (3)
GSM3179744	30	Female	PT	3	CTRL	GSEO (3)
GSM3179745	30	Female	PT	3	chorioamnionitis	GSEO (3)
GSM3179746	32	Male	PT	3	chorioamnionitis	GSEO (3)
GSM3179747	30	Female	PT	3	chorioamnionitis	GSEO (3)
GSM3179748	28	Male	PT	3	CTRL	GSEO (3)
GSM3179749	28	Male	PT	3	chorioamnionitis	GSEO (3)
GSM3179750	32	Male	PT	3	CTRL	GSEO (3)
GSM3179751	32	Male	PT	3	chorioamnionitis	GSEO (3)
GSM3179752	32	Female	PT	3	CTRL	GSEO (3)
GSM3179753	31	Male	PT	3	CTRL	GSEO (3)
GSM3179757	36	Male	PT	3	chorioamnionitis	GSEO (3)
GSM3179758	33	Male	PT	3	CTRL	GSEO (3)
GSM3179759	30	Male	PT	3	chorioamnionitis	GSEO (3)
PT99	38.5	Male	T	2	IUGR	Cochin (1)
PT91	38.5	Female	T	2	CTRL	Cochin (1)

PT122	38.5	Male	T	2	CTRL	Cochin (1)
PT05071	38.5	Male	T	2	CTRL	Cochin (1)
PT97	38.5	Male	T	2	IUGR	Cochin (1)
PT07012	38.5	Male	T	2	CTRL	Cochin (1)
PT09003	37	Female	T	2	CTRL	Cochin (1)
PT08003	38.5	Male	T	2	CTRL	Cochin (1)
PT124	38.5	Female	T	2	CTRL	Cochin (1)
PT05062	38.5	Female	T	2	CTRL	Cochin (1)
PT2929211	38	Male	T	2	PE	St.Georges (2)
PT2305656	36	Male	PT	2	PE	St.Georges (2)
PT2751222	36	Male	PT	2	PE	St.Georges (2)
PT2242133	35	Male	PT	2	PE	St.Georges (2)
PT2924935	36	Female	PT	2	PE	St.Georges (2)
PT2695585	32	Male	PT	2	PE	St.Georges (2)
PT85	39	Male	T	1	CTRL	Cochin (1)
PT117	39	Female	T	1	CTRL	Cochin (1)
PT125	39	Female	T	1	CTRL	Cochin (1)
PT09010	38	Female	T	1	CTRL	Cochin (1)
PT05048	38	Male	T	1	CTRL	Cochin (1)
PT05054	38	Female	T	1	CTRL	Cochin (1)
PT90	38	Female	T	1	PE	Cochin (1)
PT07008	39	Female	T	1	PE	Cochin (1)
PT88	33	Male	PT	1	PE	Cochin (1)
PT184	33	Female	PT	1	PE	Cochin (1)
PT07007	33	Female	PT	1	PE	Cochin (1)
PT07009	30	Female	PT	1	PE	Cochin (1)
PT70	30	Male	PT	1	PE_IUGR	Cochin (1)
PT96	30	Female	PT	1	PE_IUGR	Cochin (1)
PT11016	33	Male	PT	1	PE_IUGR	Cochin (1)

ANNEX.2

Annex 2.1: Number of nuclei per cluster per individual sample and total number of nuclei

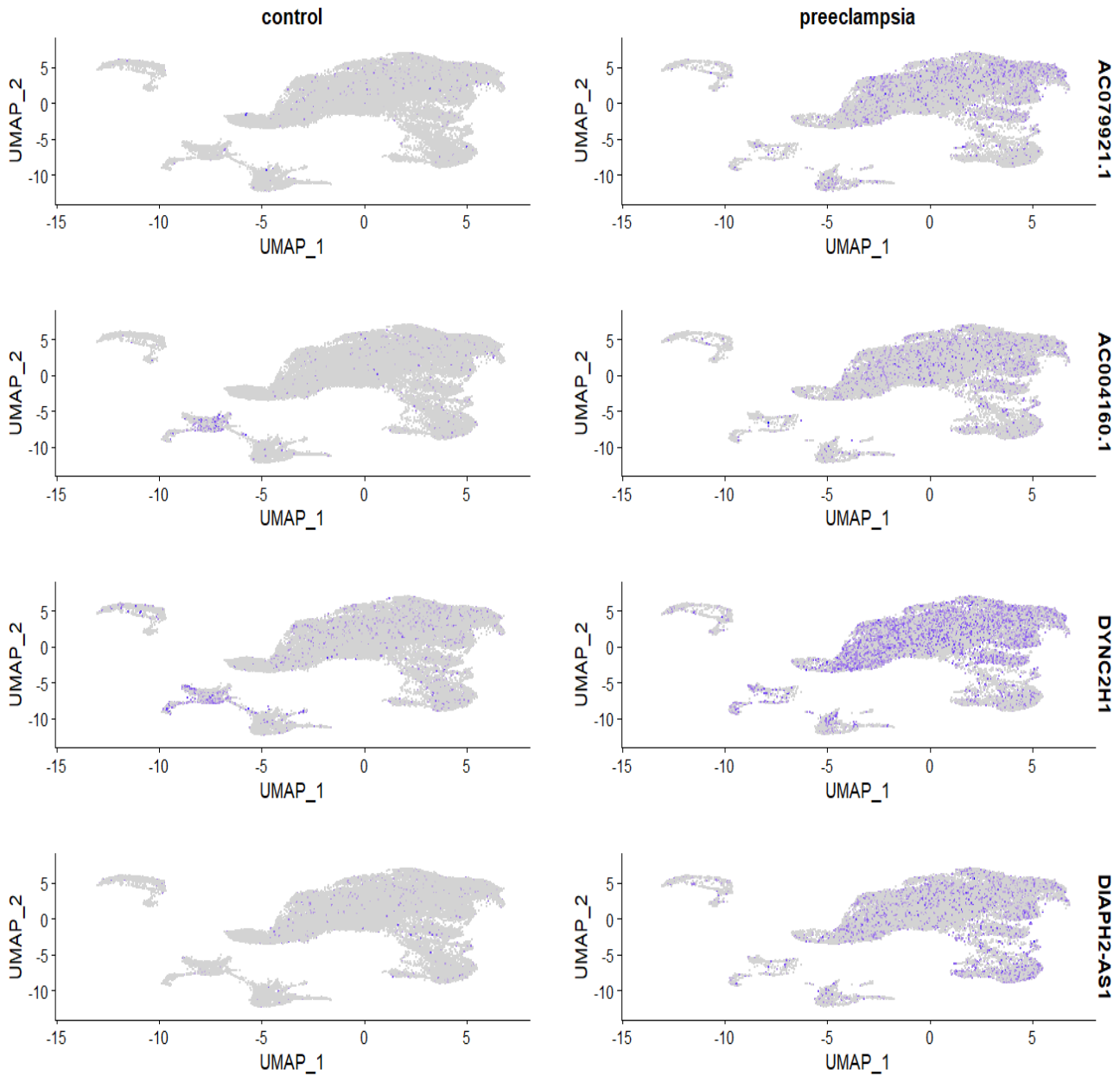
	Cell type	pces1	pces2	pces3	pces4	ppreclam1	ppreclam2	ppreclam3	ppreclam4	pvb1	pvb2	pvb3	pvb4
0	SCT_1	571	1169	1269	1411	1734	794	1979	1692	466	1180	1521	1320
1	SCT_2	614	906	796	1205	1323	557	1345	1396	462	1051	1138	947
10	EVTs_1	38	190	209	218	330	188	247	319	9	191	225	204
11	SCT_3	114	212	189	192	343	143	282	154	22	164	143	241
12	EVTs_2	749	25	62	22	80	441	85	170	224	85	35	110
13	VCTs_1	19	152	161	226	140	84	323	255	13	164	176	174
14	SCT_ETVs	12	86	85	217	30	50	174	94	30	222	258	102
15	Decidualized_stromal	26	152	65	137	134	64	106	150	10	125	97	255
16	Endothelial_Fetal	46	4	53	40	200	84	26	64	64	30	50	39
17	T_cells	160	28	24	23	64	45	17	59	51	24	26	29
18	SCT_4	83	5	20	5	30	70	17	11	36	28	8	40
19	Decidua_Hofabauer_SCT	8	13	45	35	52	26	7	29	5	18	51	27
2	Hofbauer	852	495	390	551	834	255	649	578	482	632	546	455
20	EVTs_3	6	3	21	5	82	29	37	11	2	12	5	17
3	SCT_5	66	409	309	603	904	342	938	477	91	470	515	444
4	Perivascular	968	20	96	64	324	364	125	651	1173	106	88	162
5	VCTs_2	244	136	440	325	638	305	143	300	169	210	356	270
6	Fibroblast	372	187	239	178	691	165	275	265	237	288	116	188
7	T_cells_NK	1018	31	152	42	85	346	34	403	795	62	44	130
8	SCT_6	312	285	272	145	117	289	119	147	127	345	279	189
9	SCT_7	209	156	129	299	294	170	319	275	126	162	243	186
Total		6487	4664	5026	5943	8429	4811	7247	7500	4594	5569	5920	5529

Annex 2.2: Top cluster markers. Cell type has been characterized by cell enrichment of the markers used.

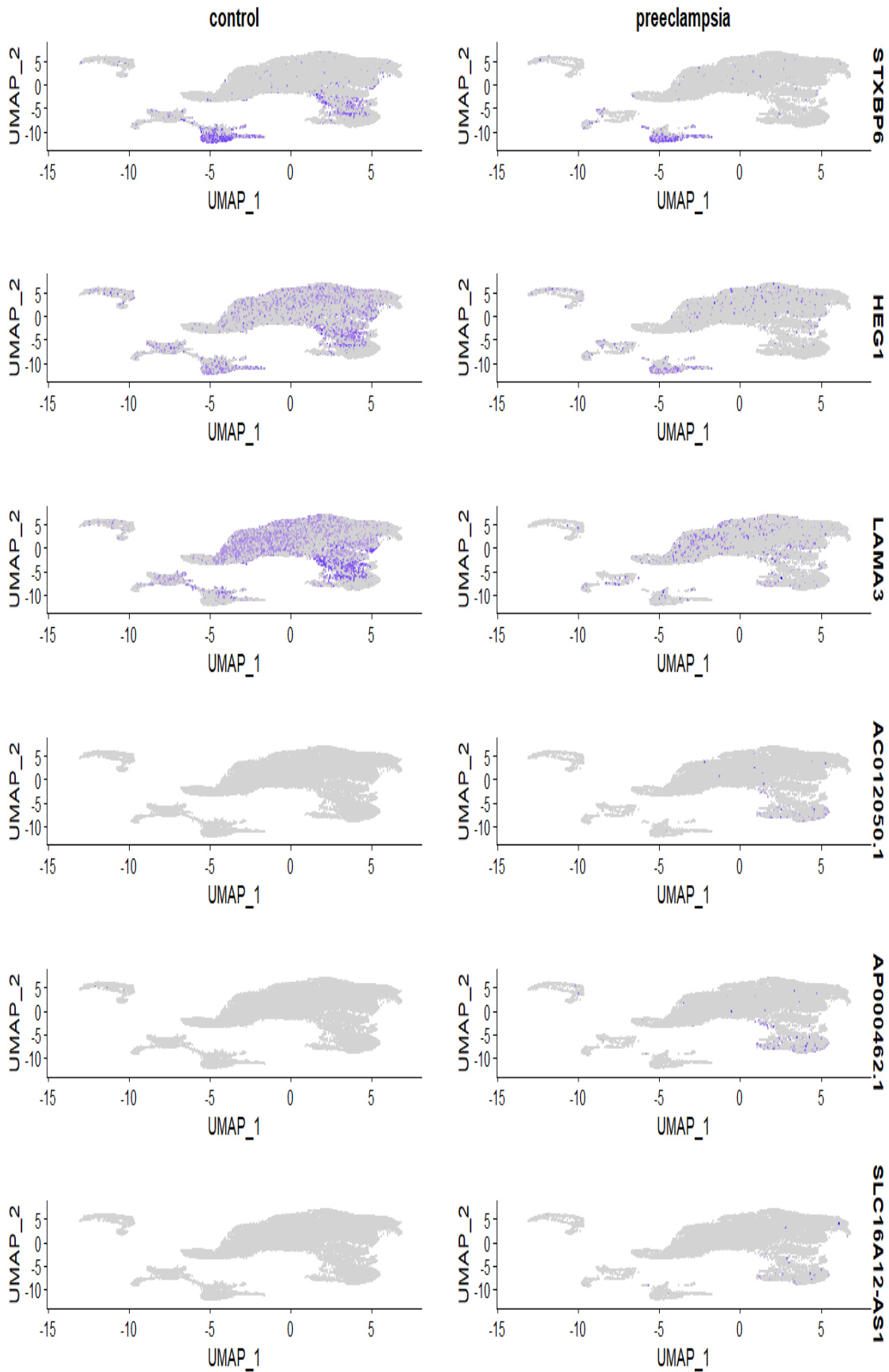
cluster	avg_log2FC	pct.1	pct.2	p_val_adj	gene	cell_type
0	0.83211436	0.597	0.424	0	ADGRL3	Syncytiotrophoblast_1
0	0.66581474	0.512	0.346	0	ACOXL	Syncytiotrophoblast_1
0	0.76513584	0.738	0.579	0	TRPV6	Syncytiotrophoblast_1
0	0.56412384	0.735	0.582	0	PSG6	Syncytiotrophoblast_1
0	0.59145577	0.739	0.589	0	PSG4	Syncytiotrophoblast_1
1	1.42869327	0.614	0.265	0	LINC02291	Syncytiotrophoblast_2
1	1.72132417	0.705	0.357	0	LINC01483	Syncytiotrophoblast_2
1	1.27803745	0.678	0.343	0	KLRD1	Syncytiotrophoblast_2
1	1.51264873	0.671	0.359	0	LVRN	Syncytiotrophoblast_2
1	0.89632904	0.712	0.424	0	DYSF	Syncytiotrophoblast_2
2	0.88984505	0.811	0.589	0	SH3PXD2A	Extravillous trophoblast
2	0.79966273	0.544	0.329	0	NEURL1	Extravillous trophoblast
2	0.8225896	0.489	0.29	7.97E-277	SLCO2A1	Extravillous trophoblast
2	1.21346525	0.756	0.559	0	HPGD	Extravillous trophoblast
2	0.72275447	0.613	0.422	9.14E-248	IL1RAP	Extravillous trophoblast
3	3.09717569	0.977	0.528	0	PDE4D	Syncytiotrophoblast_3
3	1.61735908	0.479	0.095	0	GRB14	Syncytiotrophoblast_3
3	1.32231945	0.749	0.436	0	ADGRL3	Syncytiotrophoblast_3
3	1.09589214	0.541	0.259	0	ARRDC3-AS1	Syncytiotrophoblast_3
3	0.91778397	0.633	0.352	0	CEBPB	Syncytiotrophoblast_3
4	2.26506622	0.796	0.317	0	TENM3	Extravillous trophoblast_2
4	2.00940077	0.623	0.207	0	UBASH3B	Extravillous trophoblast_2
4	1.49473818	0.604	0.192	0	SEMA6D	Extravillous trophoblast_2
4	2.22052136	0.537	0.151	0	CACNA2D3	Extravillous trophoblast_2
4	2.6341065	0.674	0.289	0	FN1	Extravillous trophoblast_2
5	3.47892026	0.906	0.18	0	SEMA6D	Villous Cytotrophoblast
5	3.28352423	0.942	0.234	0	ARL15	Villous Cytotrophoblast
5	3.22905495	0.912	0.209	0	TBL1X	Villous Cytotrophoblast
5	3.27342106	0.937	0.238	0	KANK1	Villous Cytotrophoblast
5	3.10203575	0.947	0.25	0	MSI2	Villous Cytotrophoblast
6	2.71882113	0.998	0.369	0	SERPINE1	Syncytiotrophoblast_4_EVTS
6	1.18569328	0.652	0.346	0	FOSB	Syncytiotrophoblast_4_EVTS
6	0.7635889	0.773	0.523	8.93E-210	FOS	Syncytiotrophoblast_4_EVTS
6	0.6847266	0.557	0.364	4.86E-132	ATF3	Syncytiotrophoblast_4_EVTS
6	0.75390767	0.662	0.479	1.40E-132	AC020916.1	Syncytiotrophoblast_4_EVTS
7	3.32794606	0.731	0.168	0	MEG3	Decidualized_Stromal
7	2.85895484	0.634	0.087	0	MEG8	Decidualized_Stromal

7	1.97351492	0.632	0.117	0	SPTBN1	Decidualized_Stromal
7	3.09588744	0.541	0.029	0	CDH11	Decidualized_Stromal
8	4.06034297	0.898	0.054	0	PECAM1	Endothelial_Fetal
8	4.5604797	0.896	0.062	0	LDB2	Endothelial_Fetal
8	4.69725026	0.903	0.081	0	EGFL7	Endothelial_Fetal
8	3.80285332	0.922	0.102	0	LRMDA	Endothelial_Fetal
8	4.04793524	0.938	0.151	0	MAG1	Endothelial_Fetal
9	3.40956211	0.785	0.098	0	AC073114.1	T_cells
9	2.3453575	0.628	0.046	0	AL353138.1	T_cells
9	1.97081346	0.735	0.216	0	AC093866.1	T_cells
9	2.17390523	0.519	0.034	0	PTCHD4	T_cells
9	1.38021675	0.664	0.314	0	GAS7	T_cells
10	3.36428552	1	0.292	0	PLAC1	Syncytiotrophoblast_5
10	0.85805507	0.566	0.314	8.38E-157	LINC02291	Syncytiotrophoblast_5
10	0.54842914	0.669	0.422	3.40E-114	RAB3B	Syncytiotrophoblast_5
10	0.9434258	0.815	0.57	5.36E-209	ADAMTS6	Syncytiotrophoblast_5
10	0.69487777	0.646	0.406	3.15E-123	LINC01483	Syncytiotrophoblast_5
11	3.17240088	0.997	0.146	0	AL691420.1	SCT_8
11	0.80929249	0.651	0.372	2.75E-170	ACOXL	SCT_8
11	0.7698362	0.903	0.649	6.60E-204	CHODL	SCT_8
11	0.58327001	0.615	0.397	1.15E-99	AC211486.5	SCT_8
12	3.69628524	0.791	0.055	0	ZEB2	Hofbauer
12	3.2295836	0.809	0.112	0	LRMDA	Hofbauer
12	4.24831	0.776	0.088	0	PLXDC2	Hofbauer
12	2.90356681	0.693	0.015	0	DOCK2	Hofbauer
12	3.25877644	0.759	0.104	0	DOCK4	Hofbauer
14	2.81444258	0.486	0.096	0	LINC01619	Syncytiotrophoblast_6
14	2.55207621	0.364	0.046	0	LINC01208	Syncytiotrophoblast_6
14	2.5125817	0.364	0.06	0	CD96	Syncytiotrophoblast_6
14	2.05294369	0.415	0.119	3.04E-278	GRB14	Syncytiotrophoblast_6
14	2.15320721	0.299	0.044	0	AL136456.1	Syncytiotrophoblast_6
15	3.74129822	0.992	0.104	0	ADAMTSL1	Perivascular
15	0.74051004	0.669	0.375	3.66E-103	ACOXL	Perivascular
15	0.53229213	0.695	0.409	4.29E-87	LINC01483	Perivascular
15	0.58651356	0.716	0.432	1.83E-82	FLT4	Perivascular
15	0.91109861	0.6	0.317	3.42E-109	LINC02291	Perivascular
17	3.85449321	0.851	0.059	0	SOX5	Fibroblast
17	4.08161288	0.836	0.048	0	CACNA1C	Fibroblast
17	4.17799642	0.876	0.105	0	PRKG1	Fibroblast
17	3.9018399	0.818	0.054	0	EBF1	Fibroblast
17	4.159521	0.711	0.019	0	GUCY1A2	Fibroblast
18	3.90782298	0.762	0.013	0	SKAP1	T_Cells_NK
18	3.76114076	0.773	0.037	0	PTPRC	T_Cells_NK
18	3.37133749	0.759	0.059	0	CELF2	T_Cells_NK
18	3.71065016	0.674	0.009	0	CD247	T_Cells_NK
18	3.24216819	0.748	0.098	0	FYN	T_Cells_NK

19	3.35681417	0.848	0.077	0	SLC22A11	Syncytiotrophoblast_7
19	4.06741225	0.832	0.152	0	FAR2	Syncytiotrophoblast_7
19	3.13930595	0.639	0.01	0	ERVFRD-1	Syncytiotrophoblast_7
19	2.82282013	0.693	0.079	0	SLC13A4	Syncytiotrophoblast_7
19	3.38629978	0.772	0.209	4.82E-181	GNA12	Syncytiotrophoblast_7
20	2.93425278	0.326	0.099	2.72E-32	DHFR	Syncytiotrophoblast_8
20	2.43729951	0.678	0.462	4.10E-35	TFPI2	Syncytiotrophoblast_8
20	2.08745516	0.348	0.148	6.36E-20	RPL37A	Syncytiotrophoblast_8
20	2.01281658	0.261	0.064	5.58E-33	MT-ND4L	Syncytiotrophoblast_8
20	2.70098602	0.33	0.16	3.10E-13	PEG10	Syncytiotrophoblast_8



Annex 2.3: Featureplot by pathology of the top DEGs observed to be upregulated in the SCT_2 preeclampsia cluster.





Annex 2.4: Featureplot by pathology of the DEGs observed most downregulated (STXBP6, HEG1, LAMA3) and most upregulated (AC012050.1, AP000462.1, SLC16A12-AS1) in the VCTs_2 preeclampsia cluster.

ANNEX.3

International Journal of
Molecular Sciences

Review

The Role of Epigenetics in Placental Development and the Etiology of Preeclampsia

Clara Apicella [†], Camino S. M. Ruano [†], Céline Méhats , Francisco Miralles and Daniel Vaiman ^{* }

Institut Cochin, U1016 INSERM, UMR8104 CNRS, Université Paris Descartes, 24 rue du faubourg St Jacques, 75014 Paris, France; clara.apicella@inserm.fr (C.A.); camino.ruano@inserm.fr (C.S.M.R.); celine.mehats@inserm.fr (C.M.); francisco.miralles@inserm.fr (F.M.)

* Correspondence: daniel.vaiman@inserm.fr; Tel.: +33-1-4441-2301; Fax: +33-1-4441-2302

† These authors contributed equally to this work.

Received: 3 May 2019; Accepted: 3 June 2019; Published: 11 June 2019



Abstract: In this review, we comprehensively present the function of epigenetic regulations in normal placental development as well as in a prominent disease of placental origin, preeclampsia (PE). We describe current progress concerning the impact of DNA methylation, non-coding RNA (with a special emphasis on long non-coding RNA (lncRNA) and microRNA (miRNA)) and more marginally histone post-translational modifications, in the processes leading to normal and abnormal placental function. We also explore the potential use of epigenetic marks circulating in the maternal blood flow as putative biomarkers able to prognosticate the onset of PE, as well as classifying it according to its severity. The correlation between epigenetic marks and impacts on gene expression is systematically evaluated for the different epigenetic marks analyzed.

Keywords: preeclampsia; epigenetics; DNA methylation; non coding RNAs; miRNAs; histone post translational modifications; HOX genes; H19; miR-210

1. Introduction

PE affects ~2–5% of the pregnancies. This disease, characterized in the classical definition by hypertension and proteinuria, surging from the mid-gestation at the earliest, is often seen as a two-stage disease, where a placental dysfunction occurs, first without observable symptoms and is followed later by a symptomatic phase from the 20th week of gestation at the earliest. The placenta is central to the disease development [1]. During pregnancy, the cytotrophoblasts (CTs) invade and remodel the structure of the spiral arteries of the myometrium [2]. These changes cause a significant increase in blood flow to the placenta. In a classical vision of the disease etiology, it is said that deep invasion is deficient in preeclampsia [3]. It is generally acknowledged that in preeclamptic pregnancies, placentation is disrupted because the CTs fail to properly invade the myometrium and transform the spiral arteries [4]. This decreases the blood flow and alters the oxygenation of the placenta (causing hypoxia and hyperoxia events), triggering oxidative stress, necrosis and inflammation [5]. In a very stimulating paper, B. Huppertz challenges this classical understanding of PE etiology, by dissociating the defect of deep trophoblast invasion from preeclampsia but rather associating this defect with the Fetal Growth Restriction (FGR) phenotype [6]. In this vision, preeclampsia would rather be caused by a combination of *villous* trophoblast defects (which are not involved in invasion, contrary to *extravillous* trophoblast) and maternal susceptibility. He based his reasoning on the fact that invasion defects are actually not histologically visible in many cases of preeclampsia. This may be connected to mouse models of preeclampsia where no obvious fetal growth restriction occurs, consistently with the fact

that invasion is not important in rodent [7]. More accepted than this vision, the same paper strengthens the idea that hyperoxia rather than hypoxia is a major actor of the disease [6,8].

The preeclamptic placenta releases vasoactive molecules, pro-inflammatory cytokines, microparticles and syncytial fragments into the maternal circulation which ultimately cause a systemic endothelial dysfunction [9]. Epigenetics plays an important role in the regulation of the development and physiology of the placenta [10]. Besides, substantial epigenetic alterations, in the preeclamptic placenta and other affected tissues have been described and are likely playing a substantial role in the evolution of the disease [11–14].

2. Epigenetics and Normal Placental Development

2.1. Description of the Placenta and Placental Cells

The placenta is a temporary organ connecting the developing fetus to the uterine wall through the umbilical cord, to allow for nutrient absorption, thermal regulation, waste disposal and gas exchange via the mother's blood supply. In addition, the placenta produces hormones that support pregnancy and it acts as a barrier to fight against internal infection [15].

The human placenta at term has a discoid shape, an average diameter of 15–20 cm, a thickness of 2.5 cm in the center and a weight of about 500 g. Its surfaces are the chorionic plate on the fetus side and to which the umbilical cord is attached and the basal plate facing the maternal endometrium. Between the endometrium and the basal plate there is a cavity filled with maternal blood, the intervillous space, into which branched chorionic villi project. The chorionic villi are the structural and functional unit of the placenta. Their core is made of fibroblasts, mesenchymal cells, endothelial cells, immune cells such as Hofbauer cells (supposed to be macrophage-like) and fetal-placental vessels. The villi are covered by two layers of trophoblasts. The inner layer is composed of villous cytotrophoblasts (vCTs), which are highly proliferative and can differentiate into either outer layer villous syncytiotrophoblasts (SCT), which are in direct contact with the maternal blood or extravillous trophoblasts (EVTs), as shown in Figure 1.

2.2. Human Placental Development

The development of the human placenta has been described in detail elsewhere [16–18]. Briefly, the blastocyst implants into the uterine endometrium (decidua) via the trophoctoderm cells adjacent to the inner cell mass (ICM). From the trophoctoderm, the syncytium (SCT) emerges and spreads. Subsequently, CTs proliferate rapidly to form large finger-like projections (villi) that penetrate the entire depth of the SCT. Ultimately, the villi become filled with mesenchyme originated from the extraembryonic mesoderm. This mesenchyme will form fetal blood vessels which connect to the fetal circulation via the umbilical cord. The intervillous space subsequently becomes filled with maternal blood. The vCTs situated at the tips of the anchoring villi proliferate and stratify, forming highly compact cell columns breached only by channels carrying maternal blood toward and away from the placenta (Figure 1). The trophoblast cells within this structure are referred to as EVT, according to their external location relative to the chorionic villi. EVTs situated close to the decidua, stop proliferating and develop invasive properties. These invasive EVTs migrate deeply into the decidua, where they transform the uterine vasculature in order to supply the placenta maternal blood, a critical step in establishing uteroplacental circulation. As pregnancy progresses, the number of vCTs decreases and few is observable at term underneath the SCT.

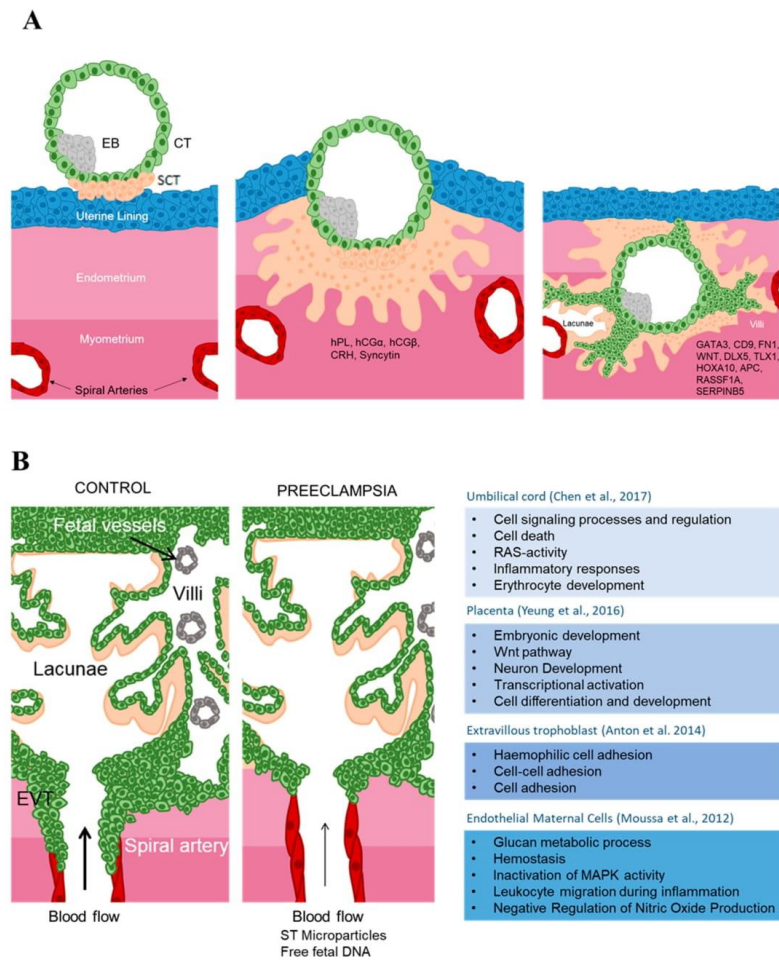


Figure 1. (A) Blastocyst implantation and Placenta Development: After recognizing the uterine lining, the blastocyst is formed by the embryoblast (EB) and the cytotrophoblast (CT). The cytotrophoblast starts to differentiate into Syncytiotrophoblast (SCT). SCT invades the endometrium towards the maternal spiral arteries located in the myometrium. deregulation of numerous genes is observed [19]. Lacunae develop in the syncytiotrophoblast, which will eventually constitute the intervillous space. Genes upregulated during villi formation are presented on the right figure [20]. Other cytotrophoblasts will invade the maternal spiral arteries by differentiating into Extravillous trophoblast. (B) Gene Ontology of genes differentially methylated in PE compared to control samples: (Left) in normal pregnancies, extravillous trophoblast (EVT) invades the maternal spiral arteries allowing for an increased blood stream towards the extravillous space. Nutrients cross the placenta, are directed towards the embryonic vessels and collected in the umbilical cord. In PE, decreased invasion of the EVTs induces poor spiral artery remodeling, leading to poor blood flow towards the placenta. Increased amount of microparticles from the syncytiotrophoblast and increased amount of free fetal DNA is observed in the maternal blood. (Right) Gene ontology of differentially methylated genes found in PE samples in different tissues affected during pregnancy: Umbilical cord, placenta, EVT, Endothelial Maternal cells (see text for detail).

2.3. Epigenetics Mechanisms in Placental Development

Epigenetic mechanisms are involved in the regulation of gene expression both during development and in differentiated tissues [21,22]. These mechanisms include DNA methylation, histone modifications and biogenesis and action of noncoding RNAs (ncRNAs). They regulate gene expression by modulating the accessibility to DNA of transcription factors and other regulatory proteins. In addition, ncRNAs also regulate gene expression at a post-transcriptional level. Epigenetic mechanisms are essential for cellular differentiation and therefore development, as summarized in Table 1

Table 1. Epigenetic mechanisms in placental development.

Epigenetic Mechanism	Target	Cell Type	Biological Relevance	Reference
H3K9/27me3	MMP-2, MMP-9	Human placenta	Related to trophoblasts motility and invasion	[23]
H3K4 acetylation + H3K9 methylation	Maspin	Human placenta	Negatively correlated with human trophoblasts motility and invasion	[24,25]
Acetylated H3	Pregnancy-Specific Glycoproteins	JEG-3	Inhibition of HDACs in JEG-3 cells up-regulated PSG protein and mRNA expression levels	[26]
HDAC3	GCMA	Cell Line	HDAC3 associates with the proximal GCMA-binding site (pGBS) in the syncytin promoter and inhibits its expression	[27]
Acetylation of H2A and H2B		Murine TSCs	Decreases the EMT and invasiveness of murine TSCs while maintaining their stemness phenotype	[28]
H3K4Me2; H4K20me3	Genome Wide	SCTs	H3K4Me2 co-localizes with active RNAP II in the majority of STB nuclei	[29]
H3K27me3	Genome Wide	vCT	H3K27me3 highly represented in vCT	[30]
lncRNA TUG1	RND3	HTR-8/SVneo, JEG-3	TUG1 epigenetically silences RND3 transcription by interacting with EZH2 involved in cellular proliferation, migration and invasion in trophoblasts	[31]
lncRNA RFAIN	Clq	HTR8/SVneo	Inhibition of proliferation and invasion. Inhibits Clq expression	[32]
lncRNA MALAT1		JEG-3	Regulates proliferation, migration, invasion and apoptosis	[33]
lncRNA MEG3		HTR8/SVneo and JEG-3	Regulates migration and apoptosis	[34]
lncRNA MIR503HG		JEG-3	Regulates migration and invasion	[35]
lncRNA LINC00629		JEG-3	Regulates migration and invasion	[35]
lncRNA SPRY4-IT1	HuR	HTR8/SVneo	Regulates migration and apoptosis/interferes with the β -catenin Wnt signaling	[36,37]
lncRNA H19	Binds small RNAs and proteins	vCT, JAR	Regulates proliferation and apoptosis	[38]
miR-141-3p and miR-200a-3p	Transthyretin (TTR)	syncytialized BeWo	Inhibits TTR expression by directly binding to the 3'UTR of TTR. Regulate thyroxin uptake by the SCT	[39]
miR-34	Plasminogen activator inhibitor-1 (PAI-1), SERPINA3	JAR	Regulates invasion	[40,41]
miR-155	Cyclin D1	HTR-8/SVneo	attenuates trophoblast proliferation	[42]
miR-17_92, miR-106a_363, miR-106b_25	GCM1	JEG3 cells	attenuate differentiation of trophoblasts	[43]
miR-675	NOMO1, Igf1R	JEG3 cells	restricts trophoblast proliferation	[44]
C19MC miR cluster		HTR8/SVneo	impaired migration	[45]
methylation of gene body	DAXX	Human placenta	Loss of methylation during both vCT syncytialization to SCT and EVTs differentiation to invasive EVTs	[46]
methylation of gene promoter	APC	Human placenta and choriocarcinoma cells	trophoblast invasiveness	[47]
hypomethylated promoter	MASPIN	Human placenta	inhibits EVTs migration and invasion	[24,25,48]
Hypermethylated promoter	RASSF1A	Human placenta; JAR; JEG3	Possible role in cytotrophoblast development through its effects on ID2 genes involved in immune response,	[49]
Genome wide methylation	PMDs (Partially Methylated Domains)	human placenta: Chorionic Villi	Epithelial-mesenchymal transition and inflammation	[50–52]
Genome wide methylation	Genome Wide	human SCTs compared to vCTS	hypomethylated SCTs compared to vCTS	[53]
Genome wide methylation	Genome Wide	BeWo and BeWo + Forskolin	DNA methylation status of numerous genes regulated at the expression level were altered by forskolin-induced fusion	[54]
Methylation	HOX genes: TLX1, HOXA10, DLX5	Human placenta	Increased methylation across gestation correlates with decreased expression. Involved in SCTs differentiation	[46]
Genome wide methylation	Genome Wide	Side-population trophoblasts, vCTS and EVTs	Each cell population has a distinctive methylome	[55,56]
Methylation	Cdx2; Eomes; Plet1; Tcfap2c	Mice trophoblast stem cells (TSCs)	methylation regulates the expression of genes involved in the establishment of the TSCs	[57–59]
Methylation	Genome Wide	Blastocyst	hypomethylation of the trophoctoderm compared to the inner cell mass	[60]

2.3.1. DNA Methylation

The best studied epigenetic mechanism in the placenta is DNA methylation, the covalent addition of a methyl group to a cytosine, usually in the context of cytosine-phospho-guanine (CpG) dinucleotides. Several reviews have been dedicated to the role of this mechanism in placental development [10,12,61]. Also, several high-throughput analyses have been performed to analyze the methylation epigenetics of the developing placenta (Table 2, Supplementary Table S1 for the details).

Table 2. Summary of DNA methylation studies in developing placenta using genome-wide approaches.

Sample	Method	GEO ID	Findings	Reference
First-trimester and term placenta and maternal blood	Illumina HM450		2944 hypermethylated CpG sites in the first and 5218 in third trimester placenta.	[62]
First-trimester placenta and maternal blood	MeDIP-Seq and Illumina HM450		3759 CpG sites in 2188 regions were differentially methylated	[63]
Placenta (first, second and third trimester)	Illumina HM450 and MethylC-Seq & RNA-Seq	GSE39777	Identification of partially methylated domains (PMDs) and differences between placenta and other tissues	[51]
Placenta (first, second and third trimester)	Illumina HM27		Increase in overall genome methylation observed from first to third trimester.	[64]
Term placenta	MeDIP + custom microarray		Tissue-specific differentially methylated regions in the placenta	[65]
Various human trophoblast populations	Illumina HiSeq 2000	GSE109682	Human trophoblasts are different from somatic cells in terms of global CpG methylation	[56]
Methylation profiles of E18.5 term placenta of WT and Hltf ^{-/-} mouse	Illumina HiSeq 2000 (Mus musculus)	CSE114145	Hltf-gene deletion alters the epigenetic landscape of the placenta.	[66]
Fetal placental tissue of both sexes in GR ^{+/+} vs. GR ^{+/-} mice	Illumina HiSeq 2000	GSE123188	GR mutation in mice changes the epigenome of placental tissue in a sex-specific manner	[67]
Human placentas	Illumina HM450	GSE108567	Adjusting for batch effects in DNA methylation	[68]
Epigenetic mechanism of mouse embryo development	Illumina HiSeq 2500 (Mus musculus)	GSE104243	H3K27me3 and DNA methylation in extraembryonic and embryonic lineages	[69]
Samples from different normal human tissues	Illumina HM450	GSE103413	Identifying candidate imprinted genes	Database, unpublished
Bisulphite and oxidative bisulphite converted placental DNA	Illumina HM450	GSE93429	Hydroxymethylcytosine and methylcytosine profiles in the human placenta	[70]
Methylation in first and third trimester placental samples	Illumina Genome Analyzer Iix	GSE98752	Complex Association between DNA Methylation and Gene Expression	[71]
DNA Methylation in Human Fetal Tissues and Human IPSC	Illumina HM450	GSE76641	DNA methylation and transcriptional trajectories in human development.	[72]
DNA methylation of fetal membranes, trophoblasts and villi 2nd trimester	Illumina HM450	GSE98938	Genome-scale fluctuations in the cytotrophoblast epigenome	Database, unpublished
Developing mouse placenta	Illumina HiSeq 2000	GSE84350	DNA Methylation Divergence and Tissue Specialization in the Developing Mouse Placenta	[73]
Villous cytotrophoblasts samples	Illumina HM450	GSE93208	DNA methylation profiling of first trimester villous cytotrophoblasts	[52]
Placental tissue collected at term.	Illumina HM450	GSE71719	DNA methylation and hydroxymethylation assessment.	[74]
DNA from chorionic villus from the 1st trimester and maternal blood cell samples	Illumina HiSeq 2000 (Homo sapiens)	GSE58826	DNA Methylation Predictors of Gene Expression in the 1st Trimester Chorionic Villus	Database, unpublished
Methylation patterns of human placenta, blood neutrophils and somatic tissue	Illumina HiSeq 2000 (Homo sapiens)	GSE59988	The human placenta exhibits a dichotomized DNA methylation pattern compared to somatic tissues	[75]
mRNA and DNA methylation profiling of Dnmt3a/3b-null trophoblasts	Illumina HiSeq 2000 (Mus musculus)	GSE66049	Maternal DNA methylation in early trophoblast development	[76]
Imprinted differentially methylated regions in hu-man villous trophoblast and blood samples	Illumina MiSeq (Homo sapiens)	GSE76273	Polymorphic imprinted methylation in the human placenta	[77]
Placental villous explant culture in different growth conditions	Illumina HM450	GSE60885	Genome-wide DNA methylation identifies trophoblast invasion-related genes.	[78]
Trophoblast methylation in NLRP7 knockdown	Illumina HM450	GSE45727	NLRP7 alters CpG methylation	[79]
Bisulphite converted DNA	Illumina HumanMethylation27 BeadChip	GSE36829	Epigenome analysis of placenta samples from newborns	Database, unpublished
First trimester, second trimester and full-term placentas	Illumina HumanMethylation27 BeadChip	GSE31781	Widespread changes in promoter methylation profile in human placentas.	[80]
Chorionic villus and maternal blood cell samples	Illumina HumanMethylation27 BeadChip	CSE23311	DNA Methylation Analysis in Human Chorionic Villus and Maternal Blood Cells	[81]

Differentiation of Stem Cells

Contrary to mice, a Trophoblast Stem Cell (TSC) population has not yet been clearly identified in humans, thus limiting our capacity to study the role of DNA methylation in the early stages of trophoblast differentiation. A recent study has addressed this question using a side-population trophoblasts, a candidate human TSC [55], isolated from first trimester placenta. The comparison of

the methylomes of this side-population trophoblasts and the methylomes of vCTs and EVT_s all isolated from the same first trimester placenta, showed that each population had a distinctive methylome [56]. In comparison to mature vCT_s, side-population trophoblasts, showed differential methylation of genes and miRNAs involved in cell cycle regulation, differentiation and regulation of pluripotency. In addition, the comparison of the methylomes and transcriptomes of vCT_s and EVT_s revealed the methylation of genes involved in epithelial-mesenchymal transition (EMT) and metastatic cancer pathways, which could be involved in the acquisition of the invasive capacities of the EVT_s. However, this study, as many others, failed to establish a systematic correlation between hypermethylation of the genes and downregulated expression. Therefore, the authors conclude that although CpG methylation is involved in the trophoblasts differentiation, it cannot be the only regulatory process.

Regulation of Homeotic Genes

Several studies have identified and established the importance of the transcription factors of the homeobox gene family (HOX) in the development of human placenta [82–86]. Most HOX genes have been found stably hypo-methylated throughout gestation, suggesting that DNA methylation is not the primary mechanism involved in regulating HOX genes expression in the placenta. However, these genes show variable methylation patterns across gestation, with a general trend towards an increase in methylation over gestation. Three genes (*TLX1*, *HOXA10* and *DLX5*) present slightly increased methylation while their mRNA expression decreases throughout pregnancy, supporting a role for DNA methylation in their regulation [46]. Down-regulation of these genes using siRNAs specific for *DLX5*, *HOXA10* and *TLX1* in primary trophoblasts leads to loss of proliferation and to an increase in mRNA expression of differentiation markers, such as *ERVW-1*. This suggests that loss of these proteins is required for proper SCT development [46].

Placental Development and Cancer Pathways

The early steps of placentation are reminiscent of the invasive properties of malignant tumors. Studies on DNA methylation in cancer cells and placental cells have highlighted similarities in their epigenomes, particularly, a widespread hypomethylation throughout the genome and focal hypermethylation at CpG islands. Hypomethylation within the placenta is not uniform but occurs in large domains (>100 kb) called partially methylated domains (PMDs) which are regions of reduced DNA methylation that cover approximately 40% of the placental genome [51]. PMDs are unique to a few different tissue types that include the placenta, cultured and cancer cells [50,51,87]. Placental genes within PMDs tend to be tissue-specific and show higher promoter DNA methylation and reduced expression as compared with somatic tissues [51]. A genome-wide comparison of DNA methylation changes in placental tissues during pregnancy and in 13 types of tumor tissues during neoplastic transformation revealed that megabase-scale patterns of hypomethylation distinguish first from third trimester chorionic villi in the placenta [52]. These patterns mirror those that distinguish many tumors from the corresponding normal tissues. The genomic regions affected by this hypomethylation encompass genes involved in pathways related to EMT, immune response and inflammation, all of them associated to cancer phenotypes. Moreover, the authors observed that hypomethylated blocks distinguish vCT_s before 8–10 weeks of gestation and after 12–14 weeks of gestation. The analogy between early placentation and malignant tumors at the epigenetic level is further stressed by studies analyzing the methylation status of the promoters of several tumor suppressor genes (*RASSF1A*, *SERPINB5* also known as *APC* and *Maspin*, respectively) in the developing placenta and human choriocarcinoma cell lines (JAR and JEG3) [25,49]. These studies show that promoter DNA-methylation regulates the expression of these tumor suppressor genes which in turn affects the migration and invasive capacities of the trophoblastic cells (As summarized in Table 1).

2.3.2. Non-coding RNAs and Epigenetic Regulation of Placenta Development

Definition

A non-coding RNA (ncRNA) is defined as an RNA molecule that is not translated into a protein. Classes of non-coding RNAs include transfer RNAs (tRNAs) and ribosomal RNAs (rRNAs), small RNAs such as microRNAs (miRNAs), siRNAs, piRNAs, snoRNAs, snRNAs, exRNAs, scaRNAs and the long ncRNAs [88]. The role of these molecules in placental development, physiology and pathology has been recently reviewed in detail [89]. Here we will discuss solely the role of miRNAs and long ncRNAs in the epigenetic control of placental development.

MiRNA and Normal Human Placental Development

The miRNAs are single stranded RNA molecules of 19–24 nucleotides, which act primarily by degrading mRNA transcripts or inhibiting translation of miRNA in to proteins [90]. To date, more than 2000 human miRNAs have been discovered, which appear to regulate 50% of human RNAs [91]. A large number of miRNAs detected in the placenta are expressed from a gene cluster located on chromosome 19 (C19MC) [92,93]. This cluster includes 46 intronic miRNA genes that express 58 miRNA species. These miRNAs are primate-specific, and they are expressed almost exclusively in the placenta (and are thus termed trophomiRs). In the human placenta, the expression of C19MC miRNAs is detected as early as 5 weeks of pregnancy and the expression gradually increases as pregnancy progresses [94]. An imprinted, paternally expressed, CpG-rich domain has a regulatory role in C19MC expression [95]. This DMR, is hypermethylated in cell lines that do not express C19MCs [96]. The C19MC region contains genomic transposable elements called “Alu repeats”, which have been implicated in recombination and gene duplication events. Because of their sequence complementarity it has been proposed that several C19MC miRNAs could be responsible of the targeting and degradation of transcribed Alu elements. Also, the C19MC miRNAs are expressed in embryonic and in stem cells but their expression drops considerably when these cells differentiate, which may indicate a role in the maintenance of an undifferentiated state [97–101]. Several members of the C19MC cluster are expressed at much higher levels in vCT compared with EVT and overexpression of the C19MC cluster results in reduced migration of the extravillous trophoblast line HTR8/SVneo [45]. The chromosome 14 miRNA cluster (C14MC) is another miRNA cluster that is expressed in the placenta [102]. This cluster includes the miRNAs: miR-127, miR-345, miR-370, miR-431 and miR-665. These miRNAs have been involved in the regulation of the immune suppressive, anti-inflammatory response and also in the regulation of the ischemia/hypoxia response [103]. The expression of the C14MC members generally declines during pregnancy [104].

The miR-675 is expressed from the first exon of the H19 long non-coding RNA. Up-regulation of miR-675, which is controlled by the stress-response RNA-binding protein HuR, restricts murine placental growth. Deficiency of H19, promotes placental growth and miR-675 overexpression decreases cell proliferation, likely through targeting Igf1R [105]. Consistent with these findings, the expression of miR-675 rises toward the end of murine pregnancy, when placental growth decelerates. In addition, miR-675 restricts proliferation in JEG3 cells, likely through binding to the nodal modulator 1 (NOMO1) protein [44].

Several other miRNAs are likely involved in placental development by inhibiting genes associated to regulation of trophoblast fate, invasion and proliferation (Let-7a, miR-377, miR-145, members of the miR-17_92 cluster, members of the miR-106a_363 and miR-106b_25 clusters, miR-155, miR-34, miR-141-3p and miR-200a-3p) [106,107]. As additional examples of regulation, mir-431 inhibits invasion of trophoblast cells by targeting the ZEB1 gene [108], miR-106a~303 inhibits trophoblast differentiation by targeting hCYP19A1 and hGCM1 [43], miR-34 targets SERPINA3, a key gene in a variety of biological processes and highly deregulated in placental diseases [41].

These miRNAs regulate diverse processes such as trophoblast physiology, proliferation and invasion (some mentioned in Table 1 and reviewed in Reference [107]).

lncRNA and Normal Human Placental Development

Long non-coding RNAs (lncRNAs) are RNAs greater than 200 nucleotides in length that do not encode a protein product. They are expressed with cellular and temporal specificity and have been involved in many cellular events, including the regulation of gene expression, post-transcriptional modifications and epigenetic modifications, imprinting and X-chromosome inactivation [109]. They act as scaffolds (binding other RNAs or proteins), signals and antisense decoys and engage in transcriptional interference. Usually a single lncRNA has multiple functions. The function of lncRNAs in placental development is poorly understood, mostly inferred from studies on placental pathologies. Nevertheless, lncRNAs have been involved in a number of critical trophoblast functions, from proliferation, invasion and migration, to cell cycle progression [110]. H19 was one of the first lncRNAs to be discovered [111]. H19 is located within a large imprinted domain on chromosome 11, at ~100 kb downstream of IGF2. H19 and IGF2 are reciprocally imprinted that is, for H19 only the maternal allele is expressed, while for IGF2, only the paternal allele is expressed [112]. H19 expression could be regulated by PLAGL1, a zinc finger transcription factor, in the human placenta [113]. Two major functions have been described for H19, specifically as a modulator for binding small RNAs and proteins [114] and as a source of the miRNA mir-675 (see above). H19 has variable levels of biallelic expression in the placenta (reports suggest between 9% and 25% expression occurs from the imprinted allele) until 10 weeks of gestation by which time H19 expression is mostly restricted to the maternal allele [115]. H19 expression is restricted to intermediate and vCT and is not found within SCTs in the human placenta. H19 down-regulation in trophoblast cells leads to inhibition of proliferation and apoptosis [116]. Many other lncRNAs have been involved in placental development, including lincRNA SPRY4-IT1, MIR503HG, LINC00629, MEG3, MALAT1, RPAIN and TUG1 [31–37]. The study of the expression of these lncRNAs during placental development and the manipulation of their expression in vitro in choriocarcinoma cell made it possible to infer their possible function in the context of placental development (Table 1).

2.3.3. Histone Modifications in the Developing Placenta

Histone modification is the process of modification of histone proteins by enzymes, including post-translational modifications, such as methylation, acetylation, phosphorylation and ubiquitination. Histone modifications participate in gene expression regulation by modulating the degree of chromatin compaction [117].

Our knowledge concerning the role of histones modification in human placentation is scarce and refers mostly to studies in mice. Methylation frequently occurs on histones H3 and H4 on specific lysine (K) and arginine (A) residues. Histone lysine methylation can lead to activation or to inhibition, depending on the position in which it is located. For instance, H3K9, H3K27 and H4K20 are considered as important ‘inactivation’ markers, that is, repressive marks, because of the relationship between these methylations and heterochromatin formation. However, the methylation of H3K4 and H3K36 are considered to be ‘activation’ marks [118,119].

The heterochromatin methylation marker H3K27me3 was found to be highly active in vCT. That was explained by rapid and transient repression of genes at the time of SCT formation. SCTs nuclei were also found enriched for H4K20me3 [30]. However, this report contrasted with another study reporting that the CTs were enriched with H3K4me3 and that the SCTs were transcriptionally activated by the chromatin marker H3K4me2, which co-localized with active RNAP II in the majority of SCT nuclei [29]. In mouse and other mammals, H3 arginine methylation predisposes blastomeres to contribute to the pluripotent cells of the ICM, which appears to require higher global levels of H3 arginine methylation than the TE/trophoblast lineage [120]. Nevertheless, these lower modification levels in the trophoblast lineage are indispensable for normal placental development.

Acetylation, which in most cases occurs in the N-terminal conserved lysine residues, is also an important way to modify the histone proteins, for example, acetylations of lysine residues 9 and 14 of histone H3 and of lysines 5, 8, 12 and 16 of histone H4 by Histone Acetylases (HATs). Acetylation is generally associated with the activation or opening of the chromatin. On the contrary,

de-acetylation of the lysine residues by histone deacetylases (HDACs) leads to chromatin condensation and inactivation of gene transcription. Oxygen (O₂) concentrations strongly influence placental development partially through modifications of the histone methylation codes. Initially, the gestation environment is hypoxic and O₂ concentration increases during development. Hypoxia-inducible factor-1 (HIF-1), consisting of HIF-1 α and ARNT subunits, activates many genes involved in the cellular response to O₂ deprivation [121]. HIF-1 is also known to recruit and regulate HDACs [122,123]. Moreover, HIF-1 has been found to bind specific sites on the promoter of the H3K9 demethylases thereby inducing their expression. In particular, it induces JMJD1A and JMJD2A that remove dimethyl marks on H3K9me₂, JMJD2B [124,125] which removes trimethyl marks (H3K9me₃) and more weakly JMJD2C which converts H3K9me₃ to me₂ [126]. Studies in rodents have shown that HIFs have important roles in the regulation of TSCs differentiation by integrating physiological, transcriptional and epigenetic inputs. Thus, the crosstalk between HIF and the HDACs is required for normal trophoblast differentiation [123,127].

Another example of histone modification during placentation, is the acetylation of histones H2A and H2B by the CREB-binding protein (CBP). CBP acts as an acetyltransferase that decreases the EMT and invasiveness of murine TSCs while maintaining the properties of stem cells [28].

Trophoblastic fusion depends on the regulation of GCMa activity by HATs and HDACs. Human GCMa transcription factor regulates expression of syncytin, which in turn mediates trophoblastic fusion. It has been demonstrated that CBP-mediated GCMa acetylation underlies the activated cAMP/PKA signaling pathway that stimulates trophoblastic fusion [27]. Human pregnancy-specific glycoproteins (PSG) are the major secreted placental proteins expressed by the SCTs and represent early markers of cytotrophoblast differentiation. Pharmacological inhibition of HDACs in JEG-3 cells up-regulated PSG protein and mRNA expression levels. This correlated with an increase in the amount of acetylated histone H3 associated with PSG promoter [26]. Combined acetylation at H3K9 and H3K4 methylation also activates Maspin, a tumor suppressor gene which is negatively correlated with human trophoblasts motility and invasion [24,25]. The invasive capacity exhibited by EVT is attributed in part to the extracellular matrix degradation mediated by matrix metalloproteinases (MMPs) such as MMP-2 and MMP-9. Differential expression of these MMPs and their tissue inhibitors (TIMPs) has been associated to histone H3K9/27me₃ [23].

2.3.4. Imprinting and Placental Development

Placentation and the Materno-Fetal Conflict

Pregnancy in Eutherian mammals is an immunological challenge as reviewed recently [128]. To note, an ancestral inflammatory response in pregnancy and parturition also exist in marsupials (metatherians), as recently observed [129,130]. Other mechanisms are equally conserved in the formation of the placenta, in particular the fusion mechanisms of cytotrophoblasts into syncytiotrophoblasts that are mediated by retroviruses, in eutherians as well as in metatherians [131].

Once the placenta is formed, it will allow nutrients to transit from the mother circulation to the fetal circulation. In the context of the maternal-fetal conflict hypothesis, tightly regulating the placentation process and limiting placental growth is crucial for the mother survival. The genes controlling this regulation are expected to be found different between viviparous and non-viviparous species. For this, mammals appear as an excellent model as a group of ~4500 species divided into egg-laying animals (prototherians, Platypus and Echidnae, 5 species), animals with a short-lived placenta (metatherians, Marsupials ~250 species) and viviparous species with a long-lived placenta (eutherians, i.e., all the other mammals, where gestation length can be up to 22 months in the African elephant). One major difference found between the genome of placental species and non-placental species of mammals is the presence of imprinted genes only in the first group.

Definition of Imprinted Genes and Links with Viviparity

Imprinted genes are genes that are expressed from either the maternal or the paternal allele, mainly through differentially methylation mechanisms. Their existence leads to dramatic phenotypic differences in animal hybrids according to the sense of the cross. For instance, interbreeding of lions and tigers results in two morphologically different animals, if the male is the lion or the male is the tiger, leading to a liger or a tigon, respectively [132]. While the tigon has a size like that of its parents, the liger is the largest existing felid (up to >400 kg) and several hypotheses have been raised to explain this fact, mostly connected to the existence of imprinted genes. Experimentally, in the 80s, Solter and Surani carried out nuclear transfer experiments that demonstrated in mice the necessity of a paternal and maternal genome to foster healthy development [133]. Androgenetic embryos lead to the production of a hypertrophic placenta while gynogenetic embryos had a very small placenta and a stunted embryo. Similarly, in humans, development from two paternal genomes leads to hydatiform moles, where the placenta is composed of grapelike vesicles, whereas parthenogenic development leads to the apparition of teratomas [134].

As far as we know today, imprinting is closely associated to viviparity. The sequencing of the platypus genome in 2008 [135] revealed syntenic regions that are relatively well conserved with the eutherian and marsupials, albeit no evidence of imprinted gene can be found in Monotremes. This may be since acquisition of imprinting in a species seems to be associated to the progressive acquisition of CpG islands (besides other mechanisms, such as chromosome translocations or retrotransposons insertions), that appear absent from the platypus genome [136,137]. In marsupials (metatherians), where the placenta is short-lived, the number of imprinted genes is more limited than in eutherian mammals. Two imprinted regions are well conserved between metatherians and eutherians such as the PEG10 and the H19-IGF2 regions [135]. Similarly, an exhaustive analysis of the transcriptome of chicken failed to identify imprinted genes, while allele specific expression does exist [138,139]. The evidence collected therefore strongly links these genes with the placenta presence. Besides, imprinted genes may have a strictly paternal or strictly maternal expression. Series of invalidation experiments in mice indicated that paternal genes tend to increase placental growth while maternal genes tend to limit this growth [140].

Example of the H19-IGF2 Cluster; Cross Species Conservation of Imprinted Genes

A well-known example of this is the H19-IGF2 cluster localized distally at 11p15.5 in humans and 7qF5 in mice. In both species, the structure of the locus is conserved (about 100 kilobases separating the two genes, with differentially methylated regions inside IGF2 and nearby H19). An IMC (Imprinting Control Region), located 3 kb from the starting point of H19 has also been identified, with seven binding sites for the ZNF transcription factor CTCF. H19 is expressed exclusively from the maternal allele, while IGF2 is expressed from the paternal allele. In mice, a placental specific promoter of IGF2 was discovered. The selective invalidation of this promoter [141] leads to a strong decrease of placental development and placental growth. By contrast, the invalidation of H19, leads to placental and fetal overgrowth [142]. Amongst other imprinted genes that affect placental and fetal growth besides H19 and IGF2 are paternally expressed genes, generally identified in mice (Peg1, Peg3, Rasgrf1, Dlk1) and maternally expressed genes (Igf2r, Gnas, Cdkn1c, Grb10).

Interestingly, in mice, the decoy receptor of IGF2, Igf2r is imprinted and with a maternal profile of expression. In humans, surprisingly, the imprinting status of IGF2R seem to be erratic, polymorphically imprinted according to the human individual analyzed. This was first published in 1993 [143] that showed that 2 out of 14 fetuses had an exclusive expression from the maternal allele. Recently it was shown that IGF2R is duly imprinted in macaques [144], showing that even in primates, the imprinting status can vary between relatively close species. Overall, it appears that many placental imprinted mouse genes are biallelic in their expression in humans [145]. Reciprocally, in a study aiming at identifying novel imprinted genes in the human placentas, we compared variants of the placental DNA versus those of cDNAs from the same placentas using SNP microarrays [146,147]. In addition to

four known imprinted genes (IPW, GRB10, INPP5F and ZNF597), we could identify 8 novel imprinted genes in the human placentas (ZFAT, ZFAT-AS, GLIS3, NTM, MAGI2, ZC3H12C, LIN28b and DSCAM). Using a mouse cross allowing the following of the allelic origin, we found an astonishing variegation of the imprinting status: only Magi2 was imprinted in the mouse species.

Imprinted genes may have a general impact on the global methylation status of the placenta. For instance, recently a polymorphism located at the IGF2/H19 locus was shown associated to placental DNA methylation and birth weight in association with Assisted Reproductive Technologies usage [148].

Imprinted genes deregulation in the placenta is linked to placental diseases, as reviewed in References [149,150]. In a recent study, Christians and coworkers, analyzed a list of 120 imprinted genes in relation with global expression of 117 placental samples, including PE and Intra Uterine Growth Restriction (IUGR) cases [151]. The authors identified a significant correlation between birth weight and the expression level of imprinted genes but without significant differences between paternally versus maternally expressed genes. Imprinted genes were also more heavily deregulated in preeclampsia than other genes and in this case paternally expressed genes were down-regulated, while maternally expressed genes were up-regulated. The trend was similar for IUGR. Interestingly, the two human-specific microRNA clusters (C19MC and C14MC), both appear to be imprinted (paternally and maternally expressed) for C19MC and C14MC, respectively, clusters that have been duly studied by the team of Yoel Sadovsky [45,89,152]. Recently, we identified duplication in the 19q13.42 imprinted region encompassing the C19MC cluster [153], from a male 26 weeks fetus with severe IUGR, suggesting that a double dose of the miRNA could contribute to the disease. This suggests links between miRNA regulation, imprinting status and the putative consequences for fetal health and growth.

3. Epigenetic Alterations in Preeclampsia

3.1. DNA Methylation Alterations in Preeclampsia

Anomalies of DNA methylation in preeclampsia have been analyzed from different cellular sources. Besides the analysis of placental cells, investigators have analyzed circulating maternal blood cells or cell-free DNA, as well as maternal endothelial cells (much less accessible, though) and cord-blood white blood cells (of fetal origin). A list of genes of which methylation was found altered is presented as Table 3.

A summary of epigenetic mechanisms at work in PE is shown in Figure 2.

3.1.1. Methylation Alterations in the Preeclamptic Placenta

Common Alterations of Gene Expression in PE are Associated to Methylation Alterations

Numerous studies revealed altered expression of various genes in the pathological placentas (as synthesized previously [154]). These alterations of gene expression are partly explained by the existence of epigenetic deregulations. In PE, numerous methylation deregulations have been found in the pathological compared to control placentas, some studies (but not all) taking into account the gestational age, a recurrent issue when normal and pathological placentas are compared, for which there is often a more than 6 weeks difference [155–160]. The different techniques used to analyze methylation globally are presented in a previous review [161]. These epigenetic changes probably originate from the abnormal placental environment in PE (or IUGR), characterized by alternations of low oxygen tension and hyperoxia. As mentioned above, hypoxia *per se* induces the expression of the Hypoxia-Inducible factor (HIF1 α), which binds to Hypoxia Responsive Element activating the transcription of various genes related with angiogenesis and metastasis-associated genes [162]. Overall, abnormal oxygen signaling in the placental context leads to increased concentrations of Oxygen Reactive Species (ROS) [163]. Oxidative stress may drive an accelerated ageing of trophoblast cells, which could be key to understand the origin of placental disorders. Indeed, several studies

emphasized alterations of telomere length (a mark of ageing) in preeclamptic pregnancies, with a drastic augmentation of short telomeres in PE, especially in Early Onset PE (EOPE) [164–166]. This senescence may be induced by alterations of the management of oxidative stress [167–169]. The accelerated transformation of vCTs into SCTs will lead to a decrease life expectancy of the placenta and an alteration of its capacity to bring the gestation harmoniously to its normal term.

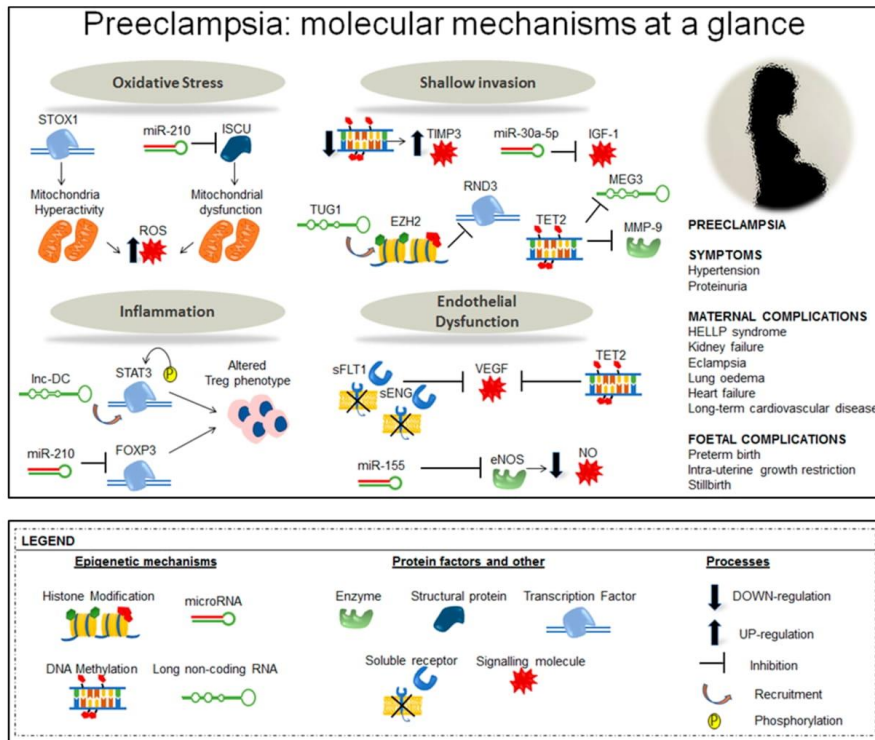


Figure 2. Overview of the molecular mechanisms at play in preeclampsia. Annotations: eNOS = Endothelial Nitric Oxide Synthase; EZH2 = Enhancer of Zeste Homolog 2; FOXP3 = Forkhead box P3; IGF-1 = Insuline-like Growth Factor 1; ISCU = Iron-sulfur cluster; Lnc-DC = Long non-coding RNA DC; miR-30a-5p = microRNA 30a-5p; miR-155 = micro-RNA 155; miR-210 = microRNA 210; MMP-9 = *Matrix Metalloproteinase-9*; NO = Nitric Oxide; RND3 = Rho Family GTPase 3; ROS = Reactive Oxygen Species; TIMP3 = TIMP Metallopeptidase Inhibitor 3; TUG1 = long non-coding RNA taurine-upregulated gene 1; VEGF = Vascular Endothelial Growth Factor.

It is well known that persisting environmental variations induce changes in the epigenetic marks, including DNA methylation. These marks can either be mere biomarkers or participate actively in regulating genes to overcome the changing environmental conditions (although gene expression changes are often disconnected from methylation alterations).

Overall, several of the genome-wide studies showed that the methylation profiles differ between early and late onset of preeclampsia (EOPE and LOPE), suggesting a different etiology between these two types of PE [170–173]. EOPE shows more pronounced genome-wide hypermethylation changes

than LOPE, probably since it is caused by earlier alterations allowing the epigenetic reprogramming to install earlier, in reason of the earlier cellular stress [171,174].

Using the Illumina Methylation 450 BeadChip Array, Yeung and coworkers, identified 303 differentially methylated regions in PE, 214 hyper and 89 hypomethylated, after adjusting for gestational age. The genes located nearby or encompassing hypermethylated regions were enriched in gene-ontology (GO) terms such as “ATP transport”, in KEGG pathways, such as “steroid hormone biosynthesis”, “cellular senescence” and Reactome pathways, such as “Vpr-mediated induction of apoptosis by mitochondrial outer membrane (SLC25A6 and SLC25A4)”. The annotation of clusters also revealed an alteration of clusters of homeobox genes, (especially HOXD genes), Wnt2 cell signaling; fertilization and implantation genes; reactive oxygen species signaling (NOX5) and cell adhesion (ALCAM) genes [158]. Amongst the most recent studies, Leavey and coworkers used a novel approach based upon bioinformatics to sort 48 human PE samples through their transcriptome profile before subjecting them to methylation analysis, using the Illumina Human methylation450K array. This made it possible to the preeclamptic cases into two groups associated to abnormal methylation marks nearby ‘immunological’ genes or more ‘canonical’ EOPE cluster, with for instance abnormally methylated CpG in FLNB, COL17A1, INHBA, SH3PXD2A, as well as in the gene body of FLT1 [160].

In 2015, the study of Zhu and coworkers [175] was the first to analyze simultaneously methylation and hydroxymethylation in the PE placentas. Hydroxymethylation results from the hydroxylation of methyl-Cytosine is a first step towards the active demethylation of DNA through the action of Ten+Eleven Translocation enzyme (TET) proteins, and could play an important role in gene expression regulation [176]. The authors showed that the methylation level is higher in gene promoters and gene bodies in PE versus control placenta. Surprisingly most of the clustering of the genes that were altered, either by methylation or by hydroxymethylation were associated with nervous system development, neurotransmitters, neurogenesis, which are presumably not relevant in a non-neural tissue as the placenta. Nevertheless, positive regulation of vasoconstriction was also enriched as a GO term, as well as regulation of nitrogen compounds, two pathways that have a clear biological sense in terms of placental diseases pathophysiology (association with vascularization and with the modulation of oxidative/nitrosative stresses).

Table 3. Differentially methylated genes in preeclampsia.

Cell Type	Gene	Methylation State in PE	Possible Target	Reference
Placenta and maternal plasma	<i>SERPINB5</i>	Hypomethylated	Trophoblast Invasion	[177]
First-trimester maternal white blood cell and placenta samples	<i>ABCA1</i>	Hypomethylated	Cholesterol transporter in macrophages	[178,179]
First-trimester maternal white blood cell, placenta samples, umbilical cord blood	<i>GNAS</i>	Hypomethylated	Diabetes, hypertension and metabolic diseases	[178,179]
First-trimester maternal white blood cell and placenta samples	<i>TAPBP</i>	Hypomethylated	Peptide loading in the Histocompatibility complex	[178]
First-trimester maternal white blood cell and placenta samples	<i>DYNLL1</i>	Hypomethylated	Phosphate metabolic processing	[178]
First-trimester maternal white blood cell and placenta samples	<i>ORPDI</i>	Hypomethylated	Opioid Receptor	[178]
Placenta	<i>TIMP3</i>	Hypomethylated	Metalloprotease Inhibitor	[180]
Placenta	<i>P2RX4</i>	Hypomethylated	Apoptosis and Inflammation	[170]
Placenta	<i>PAPPA2</i>	Hypomethylated	Insuline-like growth factor regulator	[170]
Placenta	<i>DLX5</i>	Hypomethylated	Trophoblast proliferation and differentiation	[181]
Placenta	<i>KRT15</i>	Hypomethylated	Cytoskeleton	[182]
Placenta	<i>SERPINA3</i>	Hypomethylated	Inhibition of inflammation, pathogen degradation and tissue remodeling	[183]
Placenta	<i>FN1</i>	Hypomethylated	Cell adhesion, trophoblast proliferation, differentiation and apoptosis	[182]
Placenta	<i>TEAD3</i>	Hypomethylated	Cell homeostasis, Inflammation, Coagulation, complement activation	[184]
Placenta	<i>JUNB</i>	Hypomethylated	TNF signaling pathway	[182]
Placenta	<i>PKM2</i>	Hypomethylated	Cellular metabolism	[182]
Placenta	<i>NDRG1</i>	Hypomethylated	Trophoblast invasion	[182]

Table 3. Cont.

Cell Type	Gene	Methylation State in PE	Possible Target	Reference
Placenta	<i>BHLHE40</i>	Hypomethylated	Inhibition of trophoblast differentiation	[171]
Placenta	<i>INHBA</i>	Hypomethylated	Inhibition of trophoblast differentiation	[171]
Placenta	<i>CYP11A1</i>	Hypomethylated	Trophoblast autophagy and steroidogenic pathway	[184]
Placenta	<i>HSD3B1</i>	Hypomethylated	Steroidogenic pathway	[184]
Placenta	<i>TEAD3</i>	Hypomethylated	Steroidogenic pathway	[184]
Placenta	<i>CYP19</i>	Hypomethylated	Steroidogenic pathway	[184]
Placenta	<i>CRH</i>	Hypomethylated	Cortisol bioavailability in the placenta	[184]
Placenta	<i>TFPI-2</i>	Hypomethylated	Block in endothelial dysfunction	[185]
Placenta	<i>VEGF</i>	Hypomethylated	Angiogenesis	[186]
Umbilical cord blood, placenta samples	<i>IGF2</i>	Hypomethylated	Embryonic development and fetal growth	[179,187]
Placenta and Peripheral Blood	<i>GNA12</i>	Hypomethylated	Blood pressure	[188]
Placenta	<i>CAPG</i>	Hypomethylated	Macrophage function	[189]
Placenta	<i>GLI2</i>	Hypomethylated	Embryo development	[189]
Placenta	<i>KRT13</i>	Hypomethylated	Cytoskeleton	[189]
Placenta	<i>LEP</i>	Hypomethylated	Cell homeostasis and metabolism	[190]
Placenta	<i>LP1</i>	Hypomethylated	Lipid metabolism	[191]
Placenta	<i>CEBPα</i>	Hypomethylated	Transcription stimulation of LEP promoter	[191]
Placenta	<i>SH3PX2A</i>	Hypomethylated	Trophoblast invasion and podosome formation	[191]
Placenta	<i>NCAM1</i>	Hypomethylated	Trophoblast-trophoblast interactions and adhesion	[174]
Cord blood samples	<i>HSD11B2</i>	Hypomethylated	Cortisol transmission from the mother to the fetus	[192]
Placenta	<i>WNT2</i>	Hypermethylated	Placentation and cell signaling	[158,193]
Placenta	<i>SPESP1</i>	Hypermethylated	Fertilization	[158]
Placenta	<i>NOX5</i>	Hypermethylated	Reactive Oxygen Species signaling	[158]
Placenta	<i>ALCAM</i>	Hypermethylated	Cell Adhesion	[158]
Placenta	<i>IGF-1</i>	Hypermethylated	Placentation, trophoblast function, fetal growth.	[194]
Placenta	<i>SOX7</i>	Hypermethylated	Embryonic development and cell fate	[155]
Placenta	<i>CDX1</i>	Hypermethylated	Trophoblast invasion restriction	[155]
Placenta	<i>CXCL1</i>	Hypermethylated	Chemokine inducer of angiogenesis	[155]
Placenta	<i>ADORA2B</i>	Hypermethylated	Placenta impairment and fetal growth restriction	[155]
Placenta	<i>FAM3B</i>	Hypermethylated	Cytokine activity	[182]
Placenta	<i>SYNE1</i>	Hypermethylated	Nuclear organization and structural integrity	[182]
Placenta	<i>AGAP1</i>	Hypermethylated	Cellular development, assembly and function	[182]
Placenta	<i>CRHBP</i>	Hypermethylated	Cortisol bioavailability in the placenta	[190]
Placenta and maternal blood	<i>STAT5A</i>	Hypermethylated	Transcription activation	[195]
Placenta and maternal plasma	<i>RASSF1A</i>	Hypermethylated	Tumor suppressor gene	[177]
Placenta	<i>PTPRN2</i>	Hypermethylated	Phosphate metabolic processing	[173]
Placenta	<i>GATA4</i>	Hypermethylated	Placenta Growth	[173]
Placenta	<i>YWHAQ</i>	Hypermethylated	Cellular response to reduce oxygen levels	[196]
Placenta	<i>TNF</i>	Hypermethylated	MMP-9 stimulation, Immune system activation, cell survival, migration and differentiation	[174]
Placenta	<i>COL5A1</i>	Hypermethylated	Extracellular matrix	[174]
Placenta	<i>CDH11</i>	Hypermethylated	Trophoblast anchoring to the decidua, syncytiotrophoblast differentiation	[174]
Placenta	<i>HLA-G</i>	Hypermethylated	Maternal Immune tolerance and immune rejection	[197]

The major modifications of methylation occurring in preeclampsia are presented as Figure 3.

Limits of the Genome-Wide, Multicellular Approach for Preeclampsia Methylation Profiling

As mentioned earlier, a recurrent criticism of genome-wide comparisons between normal and PE placenta is linked to the fact that in general placental samples of PE patients are collected at earlier terms than controls. However, the existence of methylation profiles for control placentas throughout gestation [51] now allows to make the part between the effect of the placental ageing and the effects of the pathology per se. Other limits of these approaches are the complexity of the cell material, the variation between the degree of severity of the disease or the various statistical tests that are used in the different studies. Also, several studies have brought attention to the lack of reproducibility in high-throughput genomic, transcriptomic and epigenomic studies. This has been recently discussed by Komwar and coworkers in a recent study where they analyze the sources of variation in preeclampsia high-throughput studies and propose a methodology to ensure reproducibility and thus facilitate the integration of data across studies [198].

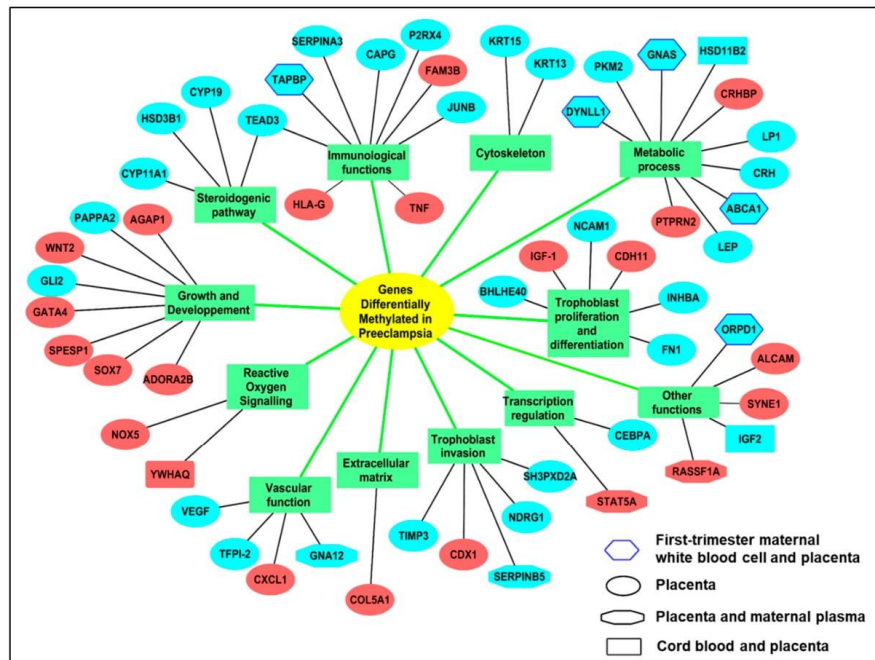


Figure 3. Overview of major methylation alterations in preeclampsia. The main pathways are shown in green boxes. The significant alterations in methylation may be associated either to increased or decreased gene expression (hypermethylated in red and hypomethylated in blue).

Single-Cell Analysis, the Next Frontier to Methylation Epigenomic Approaches

Gene-scale expression studies were recently carried out at the single cell scale [199] and have provided evidence of gene expression shifts during the CT, SCT and EVT differentiation steps, as well as, allowed the reconstructions of differentiation trajectories. This has also been analyzed by genome-scale DNA methylation analysis. Gamage and coworkers have analyzed by RRBS side population trophoblasts, CTs and EVTs from human first trimester placentas [56]. Forty-one genes involved in EMT and metastatic cancer pathways were found methylated between CT and EVTs, possibly contributing to the invasive phenotype of these cells. In the BeWo cell model where fusion can be induced by forskolin, RRBS analysis performed before and after fusion, showed altered methylation of genes involved in cell differentiation and commitment, together with a gain in transcriptionally active histone marks such as H3K4me3 [54]. Such approaches are for the moment difficult to transpose to placenta pathophysiology. Instead, several systems where methylation influences normal placental function have been studied. As an example, we present below the epigenetic regulation of genes involved in placental invasion and PE.

An Example of Specific Gene Alterations of Methylation: Regulation of Invasion

MMPs are well-characterized proteins involved in trophoblast invasion and angiogenesis during pregnancy. They constitute a family of 23 Zn²⁺ and Ca²⁺-dependent proteases that degrade the extracellular matrix. This family of proteins presents abnormal concentration and behavior in placental diseases such as PE [200], placenta accreta and placenta percreta [201,202]. This has been recently reviewed for preeclampsia [203]. A decreased level of MMP-2 and MMP-9 reduces the remodeling of

spiral arteries in early gestation. Besides, other MMPs, such as MMP-1 and MMP-14, may also have a role in this disease. Epigenetic mechanisms are at work for controlling MMP gene expression.

Li and coworkers observed that TET2 is involved in the demethylation of the *MMP-9* promoter, this being associated to the downregulation of the protein and contributing to trophoblast shallow invasion [204].

TIMP3, a MMP inhibitor, shows the highest methylation reduction (over 15%) in EOEPE compared to control placentas with an inverse correlation between methylation level and gene expression suggesting an increased transcription of TIMP3 in PE placentas [180,189]. Low levels of TIMP3 lead to poor invasion of the trophoblast and placenta hypoperfusion. Moreover, TIMP3 may be able to inhibit angiogenesis by blocking vascular endothelial growth factor binding to its receptor contributing to impaired placenta blood vessels development. Also, genetic variations of the gene have been associated with cardiovascular disorders and hypertension.

3.1.2. Maternal Blood Epigenetic Marks in Preeclampsia

Alterations in the levels of many plasma and serum proteins have been associated with PE. In 2013, White and coworkers showed that PE was favoring hypermethylation in white blood maternal cells using the methylation-27k arrays from Illumina [205]. *GRIN2b*, *GABRA1*, *PCDHB7* and *BEX1* were found differentially methylated, with an enrichment of the neuropeptide signaling pathway. The re-analysis of methylation of genes known to be involved in PE revealed that in maternal circulating leukocytes, CpG sites from 4 genes associated with PE, *POMC*, *AGT*, *CALCA* and *DDAH1*, showed differential methylation in PE compared to control, with moderate methylation differences (<6%) [206]. These 4 genes are known to alter immunomodulation and inflammatory response, suggesting that at least alterations of the placental physiology in preeclampsia have epigenomic consequences on maternal circulating cells.

During pregnancy, 3 to 6% of cell-free DNA in the maternal blood plasma is derived from the placenta. Oxidative stress in PE leads to increased trophoblast apoptosis and the release of SCT microparticles and a five to ten-fold increase in circulating fetal DNA in the maternal bloodstream compared with control counterparts [207,208]. These free fetal molecules and their methylation status have been proposed as a non-invasive biomarker of fetal and placental pathologies before the onset of symptoms. This has been shown for *Maspin*, for which the unmethylated version has a median methylation more than 5.7 fold higher in PE than control pregnancies [209,210]. Another epigenetic marker of preeclampsia is the methylation of *RASSF1A* (Ras Association domain-containing protein 1) promoter [177,211,212].

3.1.3. Maternal Endothelial Cells

There is limited access to maternal vessels in pregnancy, nevertheless DNA methylation was assessed from this material in 2012 using the 27K methylation array of Illumina [213]. From 14,495 genes interrogated by the array, 65 genes were identified as hypomethylated in PE. Clustering leads to identify biological processes such as smooth muscle contraction, thrombosis, inflammation, redox homeostasis, sugar metabolism and amino acid metabolism. These alterations of the maternal endothelium suggest potential effects on cardiovascular life of the mother after preeclampsia. Focusing on collagen metabolism, the authors revealed an increased expression of *MMP1* and *MMP8* in vascular smooth muscle cells and infiltrating neutrophils of omental arteries of preeclamptic women, which was associated with reduced methylation in the promoters of both genes in pathological patients compared to control patients [213]. In the same study, several other MMPs, showed reduced hypomethylation in PE patients albeit with lower significance [214,215]. Moreover, pregnant women under dietary supplementation may restore the reduced methylation in the promoters of these genes and be protected against the development of PE. Interestingly, all these MMPs genes are located in chromosome 11, which may be indicative of a specific sensitivity of this chromosome to epigenetic changes caused by oxidative stress during the development of the pathology. The same team reported

the reduced methylation in the promoter region of *TBXAS1* gene in correlation with increased gene and protein expression of thromboxane synthase in vascular smooth muscle, endothelium and infiltrating neutrophils [215]. Increased levels of thromboxane synthase induce the overproduction of thromboxane A₂, a potent vasoconstrictor and platelet activator, contributing to hypertension and coagulation abnormalities classically related to PE.

3.1.4. Cord Blood Cells

In 2014, Nomura and coworkers analyzed the global methylation profile of cord blood cells using the LUMA technique [161] and failed to observe an actual difference but with a limited number of controls samples (5) [216]. Genome-Wide Methylation analysis using the 450K microarray tool on neonatal cord blood DNA showed a significant genome-scale hypomethylation in neonatal cord blood DNA associated with EOPE, with 51,486 hypomethylated and 12,563 hypermethylated CpGs [187]. In this study the most differential methylated genes were associated with inflammatory pathways, cholesterol and lipid metabolism, including *IL12B*, *FAS*, *PIK31* and *IGF1*. Deregulation of both metabolic pathways may increase the risk of cardiovascular diseases in the fetus [187]. The same microarray approach allowed to identify 5001 mostly hypermethylated regions in umbilical cord white blood cells and 869 mostly hypomethylated regions in the placenta [217]. In the cord blood cells, the gene networks enriched were involved in cardiovascular system development, cell cycle, cancer, cell morphology, infectious diseases, suggesting specific alterations that could have long-term consequences on the fetal health.

Some studies focused on mitochondrial DNA, showing hypomethylation in PE cord blood cells. The most affected loci are keys in mitochondria functionality: D-loop (control of mitochondrial DNA replication), Cytochrome C oxidase subunit 1 gene (respiratory chain) and *TF/RNR1* locus (necessary for protein synthesis) [218]. Increased copy of mitochondria is observed in the placenta and maternal blood during PE suggesting an adaptive response to stress [219,220]. This is also observed in mouse models of PE [221]. Hypomethylation in the D-loop may lead to increased mitochondrial replication explaining the pathological increase of mitochondrial DNA. Methylation assay in endothelial colony-forming cells present in cord blood from PE presents differential methylation level in genes related to RNA metabolic processes, cellular protein modification processes and in positive regulation transcription, as assessed with the EPIC Illumina array, interrogating over 850,000 CpG [222]. However, at later passages, an increased number of genes are abnormally methylated. This suggests that preeclampsia may drive an altered epigenetic program in endothelial cell precursors that will be the building bricks of the newborn vascular system and program later complications.

3.2. Non Coding RNAs

Non-coding RNAs have been found to be differentially expressed in preeclampsia by a number of sources. Some studies have focused on investigating differential expression patterns between PE placental samples of different severities versus control groups looking for miRNAs or lncRNA [223–226], without generally identifying consensual signatures. With the aim of identifying potential biomarkers that could be used diagnostically to predict preeclampsia onset, many groups have set out instead to identify molecules differentially expressed in the plasma of patients, which could potentially be detected by mean of a simple blood test [227]. lncRNA and miRNA are the two classes of non-coding RNAs that have dominated the scene of non-coding molecules in preeclampsia. Other classes of non-coding RNAs have been identified, such as circular RNAs, that appeared recently in the context of PE development and future research will help understand the role of these molecules in the regulation of gene expression and disease [228].

3.2.1. LncRNAs in Preeclampsia

Long non-coding RNAs are RNA molecules longer than 200 nucleotides which are involved in regulation of cell function through a wide range of mechanisms. lncRNAs are expressed in the nucleus

as single stranded RNA molecules, which can either function in their native form or undergo maturation through the addition of a 5' cap and polyA tail; however, they are never translated into a protein product [229]. They regulate cell function by a wide range of mechanisms: alteration of the stability of target mRNAs, direct recruitment of chromatin modification enzymes, segregation of transcription factors through specific binding sites contained within the lncRNA sequence, warehousing miRNA as 'miRNA sponges', a function shared with circular RNAs [230]. For a complete overview please see Reference [231].

Transcriptomic analyses of placenta and decidua total RNAs allowed identifying differentially expressed lncRNAs between PE and control patients, often with a difference between EOPE and LOPE [228,232,233]. Most of these lncRNAs had been previously identified in the field of cancer research, often associated with cell proliferation, migration and invasion [234]. As mentioned above, given the parallels between the features of cancer cells and the trophoblasts during placentation such as fast proliferation of the trophoblast, migration and invasion of the maternal tissues, immunotolerance [235–238], this did not come as a surprise and has prompted extensive *in vitro* research to elucidate the roles of these lncRNAs in trophoblast physiology.

In the present review, we will focus on a few lncRNAs that have been well characterized: MALAT-1, MEG3, RNA-ATB. Finally, we will give a brief overview on how in PE some lncRNAs regulate gene expression by altering chromatin methylation state of their target genes, through direct recruitment of histone methyltransferases, bringing as examples PVT1, TUG1 and DIAPH2-AS1. H19 was discussed above for its important role in placental development and miRNA encoding lncRNA.

MALAT-1

Metastasis associated lung adenocarcinoma transcript-1 (MALAT-1) was firstly identified in lung cancer; it is a lncRNA of over 8 kb [239]. MALAT-1 normally localizes in the nucleus where it forms nuclear aggregates called speckles involved in the regulation of splicing factors availability [240]. MALAT-1 is overexpressed in placental pathologies associated with uncontrolled trophoblast invasion [241], which prompted Chen and coworkers [33] to investigate its expression in PE. Comparing RNA levels in 18 PE placentas with matched controls, MALAT-1 was found significantly downregulated in PE placentas. Overexpression and downregulation of MALAT-1 in JEG-3 regulates cell proliferation and invasion, while inhibiting apoptosis [33]. These findings suggest that MALAT-1 deregulation could lead to poor invasion of the maternal endometrium, affecting the spiral arteries' remodeling and placenta development. Li and coworkers [242] have shown that the role of MALAT-1 is not restricted solely to the trophoblast but has a key role in regulating the angiogenesis and vascularization of the maternal decidua and fetal umbilical vasculature. MALAT-1 is expressed by mesenchymal stem cells (MSCs) in the maternal decidua and in the umbilical cord. These cells are pluripotent progenitors which are able of self-renewal and proliferation, differentiate to promote tissue regeneration, form *de novo* vasculature, angiogenesis and regulate immune system responses [243]. Li and coworkers (2017) observed a decreased MALAT-1 expression in MSCs from decidua and umbilical cord of preeclamptic pregnancies and set out to investigate its function in these cells. Similarly, MALAT-1 promotes proliferation and protects from apoptosis in isolated MSCs. Interestingly, coculture of MSCs with trophoblast cell line HTR-8/SVneo clearly showed how MALAT-1 overexpression could promote migration and invasion of the trophoblasts towards the MSCs layer. Coculture of the endothelial cell line HUVECs (Human Umbilical Vein Endothelial Cells) in supernatant obtained from MSCs which either expressed or had downregulated MALAT-1 showed how MALAT-1 promotes tube formation this process being dependent on Vascular Endothelial Growth Factor secretion. Finally, MALAT-1 over-expression increased the levels of the IDO protein, which activated macrophage maturation, proving its role in immune system regulation. These findings combined with the work of Chen and coworkers (2015) beautifully illustrates how MALAT-1 has a symmetric regulatory function in placentation: on the one hand, it promotes trophoblast proliferation, invasive and migratory potential and on the other hand, its expression in MSCs cells helps to attract and promote trophoblast

invasion, stimulates tube formation, promotes angiogenesis and vascularization. Increase in Reactive Oxygen Species caused MALAT-1 and VEGF downregulation in MSCs exposed to oxidative stress in a dose-dependent manner [242]. MALAT-1 downregulation in preeclampsia could therefore have a huge impact on placentation and further development of the placenta over the course of gestation. It is possible that a first triggering event maybe of immunological nature, causes an increase of oxidative stress during implantation which will then alter the expression level of many targets, including MALAT-1; based on the data, this consequent deregulation would have an impact on both trophoblast and MSCs physiology, culminating in preeclampsia.

MEG3

Maternally Expressed 3 (MEG3) is an imprinted lncRNA which is expressed in many different cell types and tissues and acts as a tumor suppressor and is downregulated in many types of cancer. Physiologically, MEG3 acts by stabilising p53 and activating apoptotic responses [244]. Zhang and coworkers [34] analysed MEG3 RNA levels in 30 placentas from preeclamptic women, compared to 30 control samples and found a statistically significant 80% downregulation. These results were consistent with those of Yu and coworkers [245] studying a cohort of 20 preeclamptic and 20 control placentas, finding that MEG3 RNA was only 28% of the RNA levels of the control group. To elucidate in more detail the function of MEG3 in placenta, Zhang and coworkers (2015) overexpressed MEG3 in two trophoblast cell lines (JEG3 and HTR-8/SVneo), showing enhanced antiapoptotic effects, while downregulation of MEG3 increased the apoptotic cells. Analysis of protein markers showed how MEG3 downregulation increased the levels of pro-apoptotic proteins such as Caspase-3 and Bax. These results contrast with what is observed in cancer, where MEG3 expression is rather associated with the activation of proapoptotic pathways, possibly suggesting a different mode of action of MEG3 in these cell types. Yu and coworkers [245] focused on the link between MEG3 expression and endothelial-mesenchymal transition (EMT). During implantation and placentation, the trophoblasts undergo EMT in order to be able to migrate and invade the maternal tissues. MEG3 downregulation correlated with increased E-cadherin levels and downregulation of mesenchymal markers such as N-cadherin, vimentin, slug (encoded by the gene SNAI2), in placental RNA and protein extracts, placental sections and in vitro tests (HTR-8/SVneo trophoblast cell line). Changes in MEG3 expression did not influence proliferation but MEG3 overexpression promoted migration and trophoblast invasion through matrigel matrixes [34,224]. Altogether, MEG3 protects from apoptosis, promotes migration and invasion by regulating endothelial-mesenchymal transition in trophoblast cells and therefore its downregulation possibly affects trophoblast invasion and placentation, playing a key role in preeclampsia. Consistently, the imprinting control region (IG-DMR) of the DLK1-MEG3 cluster was very recently found hypermethylated in human umbilical veins from preeclamptic pregnancies, with an altered expression of both imprinted genes, a lower secretion of nitrite, VEGF and a higher secretion of endothelin 1 (ET1) all factors able to mediate pathological mechanisms in the offspring from preeclampsias [246].

RNA-ATB

As with many other lncRNAs, lncRNA-activated by TGF β (RNA-ATB) was first discovered in cancer, upregulated in hepatocellular carcinoma, it promotes cell proliferation, migration and invasion [247]. It has been reported that in hepatocells RNA-ATB is expressed in response to TGF β and in fibroblasts; it can create positive feedback regulation by promoting TGF β paracrine release. Lnc RNA-ATB was found to be significantly downregulated in placental samples from women with preeclampsia. Moreover patients with EOPE showed an even stronger deregulation [248]. Given the proliferative, invasive and migratory features of trophoblasts and in particular extravillous trophoblast, Liu and coworkers (2017) investigated lncRNA-ATB function in trophoblast cell line HTR-8/SVneo, which is a standard in vitro model of extravillous trophoblast. While overexpression of lncRNA-ATB increased the proliferative, migratory and invasive potential of HTR-8/SVneo cells, the downregulation

caused a steep decrease in proliferation, migration and invasion, proving that this gene has an important role on the physiology of the extravillous trophoblast and that its deregulation could explain an aberrant implantation and endometrium invasion in preeclampsia, potentially being linked to incomplete spiral artery remodeling. Whether RNA-ATB regulates trophoblast function through the interaction with members of the miR200 family is yet to be determined. However, increased miR200 has been found to affect the development of endometrium receptivity, negatively impacting implantation [249]. In labor, miR200 is upregulated in the human uterus and has been associated with pre-term labor in murine studies [250]. It seems likely that an interaction between RNA-ATB and miR200 is required for correct placental development, gestation and delivery.

PVT1, TUG1 and DIAPH2-AS1: Regulating Gene Expression through Recruitment of Chromatin Remodeling Complexes

lncRNAs work through different mechanisms, depending on the specific lncRNA, the cell type, the downstream targets [231]. In the past few years a few lncRNAs have been identified in preeclampsia as potential modulators, among which PVT1, TUG1 and DIAPH2-AS1 adopt the same mechanism of action. lncRNA TUG1 is downregulated in preeclamptic placentas. Interference of TUG1 in trophoblast cell lines (JEG3 and HTR-8/SVneo) negatively affected cell proliferation and growth, migration and invasion, network formation, while it increased apoptosis [31]. Transcriptome analysis by RNA-sequencing of HTR-8/SVneo cells in which TUG1 was downregulated showed a prevalence of affected genes involved in cell growth, migration and apoptosis. Xu and coworkers (2017) identified RND3 as main downstream factor involved in the phenotypic effects of TUG1 downregulation. RND3 mRNA and protein levels were strongly upregulated in response to TUG1 interference in vitro and RND3 mRNA was upregulated in preeclamptic placenta. RND3 is also known as RhoE, a GTPase that acts as a tumor suppressor, negatively regulating proliferation, migration and invasion [251]. In vitro experiments beautifully elucidated the mechanism by which TUG1 modulates RND3 expression—TUG1 directly interacts with the histone modification factor Enhancer of Zeste Homolog 2 (EZH2) and recruits it to the RND3 promoter, where EZH2 drives the silencing of RND3 by tri-methylating H3K27, resulting in strong RND3 downregulation [31]. A year later, Xu and coworkers [252] identified another lncRNA PVT1, strongly downregulated in preeclamptic placenta, whose downregulation negatively affects proliferation and increases apoptosis of trophoblast cell lines. PVT1 was found to recruit EZH2 to the promoter of the transcription factor ANGPTL4, driving its repression by increase in repressive chromatin markers: this could partially explain the phenotypic effects of PVT1 deregulation. Feng and coworkers [253] uncovered a complicated regulatory network behind PAX3 deregulation in preeclampsia which is linked with decreased proliferation, invasion and migration of trophoblast cells [254]. PAX3 is a transcription factor downregulated in preeclamptic placentas and this correlates with DNA hypermethylation of the promoter region [171,254]. In this study, Feng and coworkers (2019) found that in preeclamptic placentas lncRNA DIAPH2-AS1 is upregulated along with the transcription factor HOXD8. In vitro experiments in HTR-8/SVneo cells clarified the regulatory network: under hypoxia the transcription factor HOXD8 is upregulated and induces expression of the lncRNA DIAPH2-AS1. DIAPH2-AS1 recruits lysine-specific demethylase 1 (LSD1) to the promoter of PAX3 where it alters the chromatin modification state, decreasing methylation of Histone H3. LSD1 can also modify DNA methyl-transferase 1 (DNMT1), stabilizing it. ChIP experiments showed enrichment of LSD1 and DNMT1 at the PAX3 promoter, which correlated with increased DNA methylation and mRNA repression. Interference of DIAPH2-AS1 was enough to reverse the phenotype and increase PAX3 levels [253]. These studies underscore that different epigenetic mechanisms regulate gene expression. It is possible that certain mechanisms are favored in different cell types and future studies will help identify the conserved regulatory networks that plays a role in the etiology of preeclampsia.

3.2.2. micro RNA and Preeclampsia

microRNAs in Preeclampsia

The first study on microRNAs (miRs) in preeclampsia was published in 2007. In this study, the expression levels of a subset of 157 miRNAs expressed in the placenta were tested by qRT-PCR in human placental samples from pregnancies without any complications, with PE, and with PE and small for gestational age (SGA) outcomes. 153 miRNA were detected in the placenta RNA samples and three of them were found to be upregulated in PE: miR-210, miR-155, miR-200b [255]. The first global transcriptomic analysis of microRNAs was performed with 20 PE placental samples and 20 controls, with microarray technology by Zhu and collaborators in 2009. Comparing gene expression profiles of the severe PE group with controls, 11 microRNAs were upregulated and 23 downregulated. Among them, many microRNAs are organized in chromosomal clusters: downregulated clusters are found in 13q31.3, 14q32.31, Xq26.2, Xq26.3, while upregulated clusters are found in 19q13.42 suggesting co-regulation profiles [256]. An integrative analysis was conducted comparing distinct datasets with the aim of identifying microRNAs–transcripts regulatory networks in preeclampsia. resulting in the construction of a map of putative microRNA–gene target interactions in developmental process, response to nutrient levels, cell differentiation, cell junction, membrane components [257].

Although many studies followed, most of them aimed at identifying differentially expressed miRs in placenta and in plasma samples from PE women. Fewer studies have focused in other cell types present in the placenta. For example, in fetal endothelial cells downregulation of miR-29a-3p and miR-29c-3p and upregulation of miR-146a is observed in PE patients [258]. Both miR-29a and miR-29c show proangiogenic functions by stimulating HUVECs proliferation and tube formation through VEGFA-induced and FGF2-induced cell migration pathways [259]. However, other studies suggest an antiangiogenic role of miR-29c through downregulation of the IGF-1 proteins at the post-transcriptional level [260,261]. On the other hand, miR-146a inhibits the de-novo formation of blood vessels in-vitro and reduces tube formation ability in HUVECs [260,261]. The study of the role that miRs may have in the different cell types present in the placenta is indispensable to understand the role of this molecules in the development of the disease. In the long term, it has also been shown that miRNA profiles in the neonate is altered following an hypertensive pregnancy; for instance the level of mir-146a at birth predict microvascular development three months later [262].

Many studies followed, aimed at identifying differentially expressed miRs in placenta and in plasma samples from PE women.

In this review, we will discuss the most well characterized microRNAs miR-210, miR-155 and give an overview of some of the research that has been carried out on circulating microRNAs, given their potential as clinically relevant biomarkers.

miR-210

miR-210 is a microRNA involved in the regulation of mitochondrial function and hypoxia response. It has been well characterized, in placentas as well as in different cancer and tissue types [263]. Most of the knowledge on the regulatory pathways that involve miR-210 comes from oncology research. miR-210 has been soon identified as one of the early hypoxia-response miRs, being directly regulated by the Hypoxia inducible factor 1 α (HIF-1 α) [264]. Under hypoxic conditions, miR-210 alters mitochondrial function promoting a metabolic switch to glycolysis. This is achieved by negative targeting of genes involved in the electron-transport chain, namely iron- sulfur cluster scaffold homolog (ISCU) and cytochrome C oxidase assembly protein (COX10). As a result, miR-210 also increases the levels of Reactive Oxygen Species (ROS) [265]. Under hypoxia, miR-210 and HIF-1 α establish a positive feedback regulation that maintains expression of both factors. This is achieved by miR-210 downregulation of the mRNA of Glycerol-3-Phosphate Dehydrogenase 1-Like, which would otherwise contribute to targeting HIF1 α to the proteasome for degradation. Conversely, stabilized HIF1 α directly activates miR-210 expression [266].

In endothelial cells, miR-210 is involved in regulating angiogenesis and vascularization which are fundamental processes in placenta development. Hypoxia causes miR-210 activation which protects endothelial cells from apoptosis and stimulates chemotaxis driven by VEGF, migration and tube formation [267]. In preeclampsia, miR-210 was first identified as upregulated in placenta samples by Pineles and collaborators (2007) using qPCR. In the first comprehensive study carried out with microarray technologies, miR-210 was consistently found upregulated in placenta of severe preeclamptic women, however in mild preeclampsia it was found to be downregulated, which might suggest different mechanisms at play or rather different metabolic states of the placenta, with a more pronounced ischemia in severe preeclamptic placentas [256]. Moreover, subsequent analyses identified significantly upregulated miR-210 in plasma samples from patients with preeclampsia [181]. In the context of PE miR-210 is involved in the mitochondrial dysfunction observed, which causes metabolic imbalance, excessive ROS production and cell damage. Similarly to what happens in cancer, miR-210 negatively regulates ISCU which is downregulated in preeclampsia samples, directly affecting mitochondrial architecture and functionality [268–270]. The deregulation of miR-210 was also found in the placentas of mice from a preeclamptic model [134].

miR-210 is also an important modulator of trophoblast physiology. In vitro studies using isolated primary trophoblasts and trophoblast cell line JAR, proved how hypoxia induces an increase in miR-210 levels. Artificial overexpression of miR-210 in JAR cells caused a significant downregulation of migration and invasion. In trophoblast cells, hypoxia and ROS can activate HIF1 α but more importantly NF κ -B p50—which is found upregulated in preeclamptic placenta tissues. NF κ -B p50 binds a consensus sequence in the miR-210 promoter, activating its expression. In trophoblasts, miR-210 interacts with a perfect match with the 3'-UTR of the transcription factor homeobox-A9 (HOXA9), causing both degradation of the mRNA and downregulation of translation. Another direct target is Ephrin-A3 (EFNA3), a ligand of the Ephrin binding receptors, in this case miR-210 binds the 3'UTR of the gene with an imperfect match, causing only translational downregulation. These two transcription factors activate expression profiles involved in migration, invasion and vascularisation [181]. Therefore, in trophoblast, miR-210 expression correlates with a negative regulation of migration and invasion, mediated by downregulation of EFNA3 and HOXA9, in response to hypoxia, ROS and activated NF κ -B signaling.

Further studies have identified additional downstream targets of miR-210 in preeclampsia, which are downregulated in preeclamptic samples and whose expression is altered upon miR-210 activation in cell models. A few examples are inflammation related molecules STAT6 and IL-4 [271], potassium channel modulatory factor 1 (KCMF1) [272], thrombospondin type I domain containing 7A (THSD7A) [273].

This mounting body of evidence highlights a key role of miR-210 in the development and maintenance of a preeclamptic phenotype. However it is still not clear which is the triggering event. It is possible that complications during implantation trigger an immune response which would create a pro-inflammatory environment, activating NF κ -B signaling, causing aberrant expression of miR-210 and all consequent downstream cascades. Recently, Chen and collaborator (2019) analysed the inflammatory profile of preeclamptic women, compared to patients which experienced healthy pregnancy [274]. The concentrations of proinflammatory cytokines (IL-6, IL-17) were higher in plasma samples from peripheral blood in the preeclampsia group. Moreover, Transforming Growth Factor β 1 (TGF β 1) levels were higher as well. TGF β 1 has the function of promoting the prevalence of a subset of regulatory T cells (Tregs) that maintain immunotolerance, allowing a successful implantation and avoiding an immune response against the foetal tissues. These Tregs are characterised by expression of the fork-head box p3 (Foxp3) transcription factor, which promotes an immunotolerant phenotype [275]. However, proinflammatory signals such as IL-6 cause the activation of T cells at the expense of Foxp3-positive Tregs, causing an activation of inflammatory responses. Zhao and coworkers showed that miR210 was upregulated in preeclamptic placentas and Foxp3 mRNA and protein levels were found downregulated, previous studies had shown evidence of direct regulation of Fox3p by miR210,

suggesting a pivotal role of this microRNA in regulating the threshold of immunotolerance by altering the balance of Foxp3+ Tregs/activated Tcells [276].

miR-155

miR-155 is upregulated in preeclamptic placentas [255]. This upregulation correlates inversely with the level of cysteine-rich protein 61(CYR61) [277], which is a factor secreted by different cell types, including trophoblast, involved in promoting migration, invasion, angiogenesis and vascularisation [278,279]. miR-155 directly targets the 3'-UTR of CYR61 mRNA with a perfect match, causing transcriptional and translational repression. In vitro experiments (HTR-8/SVneo trophoblast cell line) showed how miR-155 inhibits CYR61-mediated expression of VEGF, inhibiting trophoblast migration [277]. Decreased trophoblast-mediated secretion of VEGF would negatively affect angiogenesis and vascularisation in the site of placenta development.

miR-155 regulates trophoblast proliferation and migration also by directly targeting the cell cycle gene Cyclin D1 [172]. Cyclin D1 is involved in cell cycle progression, migration and invasion of trophoblast lineages, downregulated in preeclamptic placentas at both mRNA and protein levels [280–282]. In vitro studies have shown how miR-155 through direct targeting of the 3'UTR of CyclinD mRNA downregulates mRNA and protein levels, negatively affecting migration, causing cell cycle arrest and decrease in proliferation in HTR-8/SVneo cells [42]. Exiting cell cycle is a step of terminal differentiation, which suggests how miR-155 overexpression, as found in preeclampsia, could lead to a premature differentiation of cytotrophoblasts, possibly inducing syncytialization. This phenomenon would cause depletion of the cytotrophoblast pool, accelerating placental aging.

In sum, miR-155 modulates proliferation, migration and invasion of trophoblasts and its expression can affect the phenotype of endothelial cells by negatively regulating VEGF release. miR-155 deregulation could have catastrophic consequences in placentation, deeply affecting trophoblast infiltration, vascularization and angiogenesis of the developing placenta.

Circulating miR-155

Maternal plasma from preeclamptic women presented significantly statistically higher levels of miR-155 [283]. In blood, microRNAs are quite stable and can travel through circulation, to be uptaken by different cell types, such as endothelial and immune cells, regulating gene expression [284]. Yang, Zhang and Ding (2017) showed how plasma levels of miR-155 positively correlate with proinflammatory cytokine interleukin-17 (IL-17) and with proteinuria and urine podocytes counts in women with preeclampsia. Similarly to miR-210, miR-155 promoter presents a binding site for NFκ-B and can be activated by this inflammation master regulator, which could suggest a similar pattern of regulation for miR-155 and pro-inflammatory factors, other than a direct interaction between these genes [285].

miR-155 in Endothelial Cells

Endothelial cells play a fundamental role in placentation given the copious vascularisation and angiogenesis that takes place in the maternal endometrium during placentation. In preeclampsia, pro-inflammatory factors and secreted molecules from the preeclamptic placenta produce an excessive activation of the maternal endothelium, resulting in endothelial dysfunction, culminating in inflammation, blood pressure changes, downstream systemic effects [286]. miR-155 has been found to be downregulated in human umbilical vein endothelial cells (HUVECs) from preeclamptic women, compared to HUVECs from healthy pregnant women [287]. This downregulation correlated with an increase in Angiotensin II Receptor 1 (AT1R) and increased phosphorylation of Extracellular Signal-regulated Kinases1/2 (ERKs), identifying AT1R as direct target of miR-155 [287]. Activation of the Angiotensin II- AT1R through ERK1/2 in endothelial cells causes cell cycle arrest and initiation of senescence pathways; miR-155 depletion-dependent increase in AT1R will render endothelial cells more sensitive to blood level of Angiotensin II, promoting endothelial damage [288].

miR-155 has been implicated in regulating Nitric Oxide (NO) production in endothelial cells. NO is a potent vasodilator and reduced levels of NO have been associated with preeclampsia etiology [289,290]. In vitro studies using HUVECs proved how endothelial Nitric Oxide synthase (eNOS) mRNA is a direct target of miR-155; proinflammatory stimuli upregulate miR-155 expression in these cells in vitro, downregulating eNOS and NO production [290]. As mentioned above, microRNAs can be found in plasma and miR-155 is upregulated in plasma of women with preeclampsia [69]. microRNAs can be free in circulation or travel inside vesicles and exosomes, which can be uptaken by target cells, activating signaling pathways, affecting expression profiles [291]. Shen and collaborators (2018) elegantly showed how exosomes from plasma samples of preeclamptic patients can affect eNOS mRNA and protein levels in HUVECs [292]. In particular, treatment of HUVECs in vitro with isolated exosomes from plasma of preeclamptic patients (compared to exosomes from control group) caused a statistically significant decrease in eNOS mRNA and protein levels, which correlated with decreased NO production. When analysing the composition of the exosomes, miR-155 was found to be upregulated in the preeclamptic group. Follow up in vitro tests proved how miR-155 located in the exosomes affects eNOS regulation in endothelial cells.

miR-155 in Vascular Smooth Muscle Cells

In arteries and arterioles, endothelial cells are interspaced by vascular smooth muscle cells (VSMCs) which thanks to their contractile properties allow vasoconstriction and vasodilation to occur, accommodating for changes in blood pressure. VSMCs generally present a contractile phenotype characterised by elongated spindle-like morphology, high concentration of contractile filaments. In response to external stimuli, they can switch to a synthetic phenotype characterised by loss of contractility markers, rhomboid morphology, increased proliferative and migratory potential; in this state VSMCs cells lose the ability to modulate vascular resistance [293]. Phenotypic regulation of VSMCs is driven by soluble guanylate cyclase (sGC) which increases intracellular levels of guanosine monophosphate (cGMP), key messenger molecule. cGMP is the substrate of cyclic GMP-dependent protein kinase (PKG) which activates downstream signaling pathways promoting VSMCs contractile phenotype. Nitric Oxide produced by endothelial cells positively modulates sGC activity, favouring vasodilation through enhancement of the VSMCs contractile phenotype [294,295].

In the presence of proinflammatory cytokine Transforming Necrosis Factor α (TNF α), miR-155 was found to be directly activated by NF κ -B in in vitro model of VSMCs. The upregulated miR-155 directly interacts with the 3'-UTR of the mRNA of PKG1 [296] and of the β 1 subunit of guanylate cyclase (sGC β 1), resulting in translational repression and mRNA degradation [297]. As a consequence of sGC β 1 downregulation, intracellular cGMP levels are strongly decreased and the downregulation of PKG1 inhibits downstream pathways [296,297]. Park and collaborators (2019) co-cultured HUVECs and VSMCs, observing higher cGMP accumulation in VSMCs, which is mediated by Nitric Oxide stimulation, produced by the endothelial cells [297]. This could be countered by ectopic miR-155 expression in VSMCs. miR-155 overexpressing in response to TNF α , mediating inhibition of the sGC/PKG pathway, causes downregulation of contractile protein markers. This results in a shift of VSMCs to a synthetic phenotype, assuming a rhomboid morphology, increasing proliferation and migration rates. Interestingly the pro-contractile effects of Nitric Oxide could be cancelled by miR-155 expression [296,297]. In placental vessels of preeclamptic placenta sGC β 1 mRNA levels are downregulated [297], given the evidence provided on miR-155 repression of the sGC/PKG pathway, we can imagine that PKG1 might be downregulated as well. In response to inflammation, both endothelial and smooth muscle cells are affected and in preeclampsia they overexpress miR-155 which alters their ability to produce and respond to vasodilation stimuli. Taken together, this evidence highlights the pivotal role of inflammation and miR-155 in the etiology of the preeclamptic phenotype.

Potential Biomarkers: microRNAs Circulating in Maternal Plasma

Since the identification of circulating small RNAs in plasma samples, the prospect of their potential use as diagnostic and predictive biomarkers has fueled extensive research [298]. In the context of preeclampsia, the finding that small microRNAs with placental origin can travel in the blood circulation and affect systemically different cell types opens new avenues for the understanding of the mechanisms of this complex disease [299,300].

In Table 4 are listed some of the microRNAs that have been found deregulated in plasma samples of preeclamptic patients. In several studies, groups of microRNAs differentially expressed have been analyzed for their potential as predictive biomarkers of the preeclamptic phenotype [301–305]. These studies show how blood levels elevation of PE-associated microRNAs can be predictive for the preeclamptic phenotype starting from the second trimester. Li and collaborators (2015) evaluated the predictive values of the upregulated micro-RNAs miR-152, miR-183 and miR-210 by plotting the corresponding receiver operating characteristic curves. In the second trimester samples, the Area Under the Curve (AUC) indicated strong predictive values and were respectively 0.93 for miR-210, 0.97 for miR-183 and 0.94 for miR-152. Interestingly, different studies investigated the predictive power of miR-210 and, even though all results highlighted its key role in preeclampsia and potential as diagnostic marker, the AUCs varied in a range between 0.7 and 0.94 [301–303,305]. This variation might be due to differences in patient cohorts, samples collections and handling; however, the fact that miR-210 still emerged as predictive biomarker is encouraging.

Winger and collaborators (2018) collected peripheral blood cells in preeclamptic and control patient group, analysing the expression levels of a subset of 30 microRNAs previously identified altered in preeclampsia. 48 samples were divided in a training and a validation group. Analysis of differentially expressed microRNAs in the training cohort identified a panel of 8 microRNAs with good prediction values (AUC > 0.75) and p value ≤ 0.05 : miR-1267, miR-148a, miR-196a, miR-33a, miR-575, miR-582, miR-210, miR-16. The panel was successfully validated and the use of the 8 microRNAs combined increased the prediction power of the tests [305].

From Table 4, it is possible to appreciate the heterogeneity of findings across different studies. These discrepancies in the repertoires of circulating miRNAs complicate the identification of useful biomarkers. This heterogeneity could partly be explained by the fact that preeclampsia is a complex systemic disease that develops over months of gestation; therefore, the panel of circulating molecules in blood samples might vary considerably depending of the time point at which samples are collected. Another possible explanation might reside in the wide range of different methodologies used for the extraction of circulating RNAs which introduce technical variability [306,307]. Moreover, there is mounting evidence on how the current techniques are able to detect only a small fraction of the total bulk of circulating RNAs (WO2009093254A2). Therefore, further research is still required to improve our technical knowledge so to design better, more consistent methodologies for the identification of circulating biomarkers, that might one day allow the design of diagnostic panels for effective early detection and prevention of preeclampsia.

3.2.3. Additional Considerations on the Analysis of lncRNA Functions

Possible Caveats of the Current Trophoblast In Vitro Models

Many of the lncRNAs found to be deregulated in preeclamptic placenta have previously been identified in cancers, where they have a role in regulating proliferation, migration, invasion and apoptosis. Most of these PE-associated lncRNAs have pro-survival and pro-migration properties, therefore downregulation is associated with activation of apoptosis, decreased migratory potential and proliferative rate.

Once they have been found to be downregulated in preeclamptic placenta, the main objective has been to investigate the molecular function of these lncRNAs in the context of placenta physiology and preeclampsia. In vitro studies have seen the use of classical cellular models of trophoblast, either

choriocarcinoma cell lines (JEG3 and BeWo) or artificially immortalized cell lines (HTR-8/SVneo). Through these in vitro studies it has been established that most of these lncRNAs regulate proliferation, invasion and migration of the trophoblast.

Table 4. Deregulated miRNA in preeclampsia.

microRNA	PE Placenta	PE Plasma	Function	Gene targets	AUC	References
miR-214	DOWN					[308]
miR-152		DOWN				[300]
miR-218	DOWN					[308]
miR-590	DOWN					[308]
miR-18a	DOWN	DOWN	Promoting trophoblast migration	SMAD2		[225,308]
miR-19a	DOWN					[308]
miR-19b1		DOWN	TGFβ-signaling	SMAD factors		[225]
miR-379	DOWN					[308]
miR-411	DOWN					[308]
miR-195	DOWN					[308]
miR-223	DOWN					[308]
miR-363	DOWN					[308]
miR-542-3p	DOWN					[308]
miR-144		DOWN	Ischemia, hypoxia			[225]
miR-15b		DOWN	Angiotensin-renin system			[225]
miR-181a	UP	UP				[225,308]
miR-584	UP					[308]
miR-30a-3p	UP					[308]
miR-151	UP					[308]
miR-31	UP					[308]
miR-210	UP	UP		PTPN2	0.7 < AUC < 0.9	[225,255,300,302,303,305,308,309]
miR-17-3p	UP					[308]
miR-193b	UP					[308]
miR-638	UP					[308]
miR-525	UP					[308]
miR-515-3p	UP					[308]
miR-519e	UP					[308]
miR-517-5p	UP	UP			AUC = 0.7	[304]
miR-518b	UP	UP				[225,304,308]
miR-524	UP					[308]
miR-296	UP					[308]
miR-362	UP					[308]
miR-574-5p		UP			AUC > 0.7	[302]
miR-1233-3p		UP			AUC > 0.6	[302]
miR-155		UP			AUC > 0.7	[225,303]
miR-1267		UP			AUC > 0.8	[305]
miR-148a		UP	Immune response	HLA-G	AUC > 0.9	[305,310]
miR-196a		UP			AUC = 1	[305]
miR-33a		UP			AUC = 1	[305]
miR-575		UP			AUC > 0.9	[305]
miR-582		UP	Trophoblast invasion, migration	VEGF	1	[305,311]
miR-152	UP	UP	Immune response	HLA-G	AUC > 0.9	[256,301,312]
miR-183	UP	UP	Cell differentiation, apoptosis, invasion		AUC > 0.9	[255,301,313]
miR-215		UP				[225]
miR-650		UP				[225]
miR-21	UP	UP	Apoptosis			[225,314]
miR-29a		UP				[225]
miR-300		UP	Trophoblast differentiation	ETS-1		[315]

Annotations: AUC = Area Under the Curve; SMAD2 = Mothers Against Decapentaplegic Homolog 2; PTPN2 = Tyrosine-protein phosphatase non-receptor type 2; HLA-G = Histocompatibility antigen, alpha chain G; VEGF = Vascular endothelial growth factor; ETS-1 = E26 oncogene homolog 1; TGFβ = Tumor growth factor β.

Have we completely unfolded the role of PE-associated lncRNA in the human placenta? Since lncRNAs have been previously identified in cancers, it is possible that the functions we have attributed them in the placenta are actually a result of the fact that we are analyzing them in cell lines that are cancer-like. Therefore, there is still the possibility that these lncRNAs have additional distinct functions in placenta that could be highlighted using more physiological placenta models. The recent development of placenta organoids from stem cells rises the hope for exciting new avenues, to explore these questions [316].

What about the Syncytiotrophoblast?

Migration, apoptosis, invasiveness and proliferation are functions shared between cancer cells and by cytotrophoblast (CTB) especially by the extravillous trophoblast (EVT) in the placenta, the *in vitro* investigations into PE associated lncRNAs have so far focused on EVT cell line models (e.g., JEG3, HTR-8/SVneo). However, it is important to highlight how transcriptomic data from placenta samples are a result of overall placenta gene expression levels. The extracted placental RNA comes from all the different cell types present in the tissue and the most abundant cell populations are represented by cytotrophoblasts and syncytiotrophoblasts (SCT). Even though it is true that CTB and EVT cells are fundamental for implantation and correct placental development, the syncytiotrophoblast is the functional core of the placenta itself, constituting the barrier for nutrient exchanges between fetal and maternal vasculatures and acting as secretory organ that hormonally regulates progression of gestation. Liu and coworkers (2017), in their work on RNA-ATB, showed a strong *in situ* hybridization staining of lncRNA-ATB in the syncytiotrophoblast layer of the placenta, reinforcing the idea that the syncytiotrophoblast might be equally affected by deregulation in the lncRNAs species [248]. Yu and coworkers (2018) work on MEG3 showed how MEG3 downregulation observed in preeclampsia correlates with an increase in adhesion molecule E-cadherin [224]. While it is true that this molecule is important for endothelial-mesenchymal transition, and its alteration would affect trophoblast invasion and EVT migration, E-cadherin downregulation after cytotrophoblast cell-cell interaction has been implicated in CTB syncytialization [317]. Suggesting that MEG3 might affect STB physiology as well.

Therefore, there are still potentially interesting questions to be raised: what are the effects of downregulated lncRNAs on the physiology of the CTB and SCT? Do we see an alteration of the proliferative state of the CTB, does this cause premature placental aging? Does this deregulation affect the differentiation potential of the CTB, affecting the balance between CTB renewal and SCT terminal differentiation? Do these lncRNAs have other functions, exclusive to placenta, other than the ones shared with cancer?

3.3. Histone Modifications

Few studies addressed the question of histone code modifications in PE. Chakraborty and coll. evidenced a HIF-KDM3A-MMP12 signaling cascade that promotes trophoblast invasion and trophoblast-directed uterine spiral artery remodeling in rat placenta and human placental cells. Hypoxia drives HIF activation and KDM3A expression, which in return will alter the histone methylation status of genes promoting development of the invasive trophoblast lineage and tissue remodeling, illustrated with trophoblast-derived MMP12 activation [318]. Hypoxia was also shown to affect the histone demethylase JMJD6 (Jumonji domain containing protein 6) and JMJD6 demethylase activity was shown to be drastically reduced in PE placenta as compared to Control Placenta [319]. Very recently, the expressions of HDACs were investigated in PE placentas and only HDAC9 was found downregulated both at the mRNA and protein levels in syncytiotrophoblast cells. Knock-down of HDAC9 in HTR-8/SVneo cells inhibits trophoblast cell migration and invasion. TIMP3, an inhibitory of MMP involved in invasion and tissue remodeling, is a direct target of HDAC9, identified by ChIP and is upregulated in the absence of HDAC9 [320].

3.4. Imprinting

Overall, preeclampsia cannot be considered an imprinting disease, despite the fact that a recent study showed that imprinted genes are more differentially expressed in PE than other genes, with paternally expressed genes (inducing placental growth) rather down-regulated and maternally expressed genes upregulated [151]. A systematic analysis of preeclampsia placental gene expression and imprinted genes was carried out in 2017 [321], which revealed altered expression of DLX5 in human PE placentas but with a rather mild deregulation (~2 fold). To be mentioned as well, the first gene identified by positional cloning in preeclampsia, STOX1, is imprinted in specific placental cell

subtypes [322,323]. The mutation originally found in STOX1 has rather a gain-of-function effect [323] and in fact, overexpression of STOX1 induces a preeclamptic expression profile and a preeclamptic phenotype in cells or in mice, respectively [7,324]. To note, however, we have no evidence that Stox1 is imprinted in mice, therefore it is suspected that the mere ectopic and untimely overexpression of this factor is the cause of the disease. The idea that an imprinted gene is implicated in preeclampsia has been cleverly substantiated by Jennifer Graves as early as 1998 [325] and she gave theoretical reasons why this should be the case. The future will tell us if more examples of imprinted preeclampsia-associated genes exist in the human genome.

4. Perspectives and Conclusions

The recent years have seen the emergence of an increasing number of studies focused on the role of epigenetics in the regulation of placental development and on its potential implication in placental pathologies. However, we still lack a precise picture on how these epigenetic modifications correlate with gene expression. In particular, we have a limited knowledge on how DNA-methylation or Histone modifications impact gene expression in normal and pathological placenta development. In addition, our knowledge on the mechanisms regulating the dynamics of the instauration of the different epigenetic marks across development is very scarce. Nevertheless, recent studies have started to reveal how epigenetics is involved in the regulation of important processes in placental development such as cell fate determination, *syncytialization* or EVT migration and invasion. The emergence of new technologies allowing the study of the epigenetic and transcriptomic profiles of the different cells types of the placenta will certainly greatly contribute to improve our understanding of epigenetics in placenta. Moreover, in the context of PE, to date, the studies analyzing epigenetic modifications have focused on the placenta, however the antiangiogenic and cytotoxic factors released by the PE placenta have the potential to induce epigenetics modifications in maternal target tissues (blood cells, endothelial cells). This could impact the future maternal and fetal health and deserves to be studied in detail. Overall, the comprehension of epigenetic regulation in preeclampsia both at the level of the placenta and other involved organs could provide new biomarkers and therapeutic targets to improve the management of this disease. For the moment, this has not been successfully applied as diagnostic or prognostic of preeclampsia. One explanation of this observation could be that the extraction of circulating RNAs from the plasma is still immature technologically, leading to discrepant results between various laboratories and absence of consensus in defining a panel of diagnostic miRNA. This may evolve in the future, leading to substantial exploitation of these markers in complex diseases, including preeclampsia.

Supplementary Materials: Supplementary materials can be found at <http://www.mdpi.com/1422-0067/20/11/2837/s1>. Table S1. High-throughput studies analyzing methylation profiles of different relevant tissues in the context of preeclampsia [42,43,47,54–73].

Funding: F.M., C.M. and D.V. are funded by INSERM, C.S.M.R. and C.A. are PhD students, funded by the H2020 European project ‘iPLACENTA,’ headed by Colin Murdoch.

Conflicts of Interest: The authors declare no conflict of interest. The funders had no role in the design of the study; in the collection, analyses, or interpretation of data; in the writing of the manuscript, or in the decision to publish the results.

References

1. Steegers, E.A.; von Dadelszen, P.; Duvekot, J.J.; Pijnenborg, R. Pre-eclampsia. *Lancet* **2010**, *376*, 631–644. [CrossRef]
2. Roland, C.S.; Hu, J.; Ren, C.E.; Chen, H.; Li, J.; Varvoutis, M.S.; Leaphart, L.W.; Byck, D.B.; Zhu, X.; Jiang, S.W. Morphological changes of placental syncytium and their implications for the pathogenesis of preeclampsia. *Cell. Mol. Life Sci.* **2016**, *73*, 365–376. [CrossRef] [PubMed]
3. Redman, C.W.; Sargent, I.L. Latest advances in understanding preeclampsia. *Science* **2005**, *308*, 1592–1594. [CrossRef] [PubMed]

4. Fisher, S.J. Why is placentation abnormal in preeclampsia? *Am. J. Obstet. Gynecol.* **2015**, *213*, S115–S122. [[CrossRef](#)] [[PubMed](#)]
5. Huppertz, B. Placental origins of preeclampsia: Challenging the current hypothesis. *Hypertension* **2008**, *51*, 970–975. [[CrossRef](#)] [[PubMed](#)]
6. Huppertz, B. The Critical Role of Abnormal Trophoblast Development in the Etiology of Preeclampsia. *Curr. Pharm. Biotechnol.* **2018**, *19*, 771–780. [[CrossRef](#)] [[PubMed](#)]
7. Doridot, L.; Passet, B.; Mehats, C.; Rigourd, V.; Barbaux, S.; Ducat, A.; Mondon, F.; Vilotte, M.; Castille, J.; Breuiller-Fouche, M.; et al. Preeclampsia-like symptoms induced in mice by fetoplacental expression of STOX1 are reversed by aspirin treatment. *Hypertension* **2013**, *61*, 662–668. [[CrossRef](#)] [[PubMed](#)]
8. Sibley, C.P.; Pardi, G.; Cetin, I.; Todros, T.; Piccoli, E.; Kaufmann, P.; Huppertz, B.; Bulfamante, G.; Cribiu, F.M.; Ayuk, P.; et al. Pathogenesis of intrauterine growth restriction (IUGR)-conclusions derived from a European Union Biomed 2 Concerted Action project 'Importance of Oxygen Supply in Intrauterine Growth Restricted Pregnancies'-a workshop report. *Placenta* **2002**, *23* (Suppl. A), S75–S79. [[CrossRef](#)]
9. Possomato-Vieira, J.S.; Khalil, R.A. Mechanisms of Endothelial Dysfunction in Hypertensive Pregnancy and Preeclampsia. *Adv. Pharmacol.* **2016**, *77*, 361–431.
10. Nelissen, E.C.; van Montfoort, A.P.; Dumoulin, J.C.; Evers, J.L. Epigenetics and the placenta. *Hum. Reprod. Update* **2011**, *17*, 397–417. [[CrossRef](#)]
11. Vaiman, D. Genes, epigenetics and miRNA regulation in the placenta. *Placenta* **2017**, *52*, 127–133. [[CrossRef](#)] [[PubMed](#)]
12. Robinson, W.P.; Price, E.M. The human placental methylome. *Cold Spring Harb. Perspect. Med.* **2015**, *5*, a023044. [[CrossRef](#)] [[PubMed](#)]
13. Januar, V.; Desoye, G.; Novakovic, B.; Cvitic, S.; Saffery, R. Epigenetic regulation of human placental function and pregnancy outcome: Considerations for causal inference. *Am. J. Obstet. Gynecol.* **2015**, *213*, S182–S196. [[CrossRef](#)] [[PubMed](#)]
14. Fu, G.; Brkic, J.; Hayder, H.; Peng, C. MicroRNAs in Human Placental Development and Pregnancy Complications. *Int. J. Mol. Sci.* **2013**, *14*, 5519–5544. [[CrossRef](#)] [[PubMed](#)]
15. Burton, G.J.; Fowden, A.L. The placenta: A multifaceted, transient organ. *Philos. Trans. R. Soc. Lond. B Biol. Sci.* **2015**, *370*, 20140066. [[CrossRef](#)]
16. James, J.L.; Carter, A.M.; Chamley, L.W. Human placentation from nidation to 5 weeks of gestation. Part I: What do we know about formative placental development following implantation? *Placenta* **2012**, *33*, 327–334. [[CrossRef](#)]
17. Knofler, M. Critical growth factors and signalling pathways controlling human trophoblast invasion. *Int. J. Dev. Biol.* **2010**, *54*, 269–280. [[CrossRef](#)]
18. Knofler, M.; Pollheimer, J. Human placental trophoblast invasion and differentiation: A particular focus on Wnt signaling. *Front. Genet.* **2013**, *4*, 190. [[CrossRef](#)]
19. Rouault, C.; Clement, K.; Guesnon, M.; Henegar, C.; Charles, M.-A.; Heude, B.; Evain-Brion, D.; Degrelle, S.A.; Fournier, T. Transcriptomic signatures of villous cytotrophoblast and syncytiotrophoblast in term human placenta. *Placenta* **2016**, *44*, 83–90. [[CrossRef](#)]
20. Khan, M.A.; Manna, S.; Malhotra, N.; Sengupta, J.; Ghosh, D. Expressional regulation of genes linked to immunity & programmed development in human early placental villi. *Indian J. Med. Res.* **2014**, *139*, 125–140.
21. Henikoff, S.; Gready, J.M. Epigenetics, cellular memory and gene regulation. *Curr. Biol.* **2016**, *26*, R644–R648. [[CrossRef](#)] [[PubMed](#)]
22. Zhang, G.; Pradhan, S. Mammalian epigenetic mechanisms. *IUBMB Life* **2014**, *66*, 240–256. [[CrossRef](#)] [[PubMed](#)]
23. Rahat, B.; Sharma, R.; Bagga, R.; Hamid, A.; Kaur, J. Imbalance between matrix metalloproteinases and their tissue inhibitors in preeclampsia and gestational trophoblastic diseases. *Reproduction* **2016**, *152*, 11–22. [[CrossRef](#)] [[PubMed](#)]
24. Dokras, A.; Gardner, L.M.; Kirschmann, D.A.; Sefter, E.A.; Hendrix, M.J. The tumour suppressor gene maspin is differentially regulated in cytotrophoblasts during human placental development. *Placenta* **2002**, *23*, 274–280. [[CrossRef](#)] [[PubMed](#)]
25. Dokras, A.; Coffin, J.; Field, L.; Frakes, A.; Lee, H.; Madan, A.; Nelson, T.; Ryu, G.Y.; Yoon, J.G.; Madan, A. Epigenetic regulation of maspin expression in the human placenta. *Mol. Hum. Reprod.* **2006**, *12*, 611–617. [[CrossRef](#)] [[PubMed](#)]

26. Camolotto, S.A.; Racca, A.C.; Ridano, M.E.; Genti-Raimondi, S.; Panzetta-Dutari, G.M. PSG gene expression is up-regulated by lysine acetylation involving histone and nonhistone proteins. *PLoS ONE* **2013**, *8*, e55992. [[CrossRef](#)] [[PubMed](#)]
27. Chuang, H.C.; Chang, C.W.; Chang, G.D.; Yao, T.P.; Chen, H. Histone deacetylase 3 binds to and regulates the GCMA transcription factor. *Nucleic Acids Res.* **2006**, *34*, 1459–1469. [[CrossRef](#)] [[PubMed](#)]
28. Abell, A.N.; Jordan, N.V.; Huang, W.; Prat, A.; Midland, A.A.; Johnson, N.L.; Granger, D.A.; Mieczkowski, P.A.; Perou, C.M.; Gomez, S.M.; et al. MAP3K4/CBP-regulated H2B acetylation controls epithelial-mesenchymal transition in trophoblast stem cells. *Cell Stem Cell* **2011**, *8*, 525–537. [[CrossRef](#)]
29. Ellery, P.M.; Cindrova-Davies, T.; Jauniaux, E.; Ferguson-Smith, A.C.; Burton, G.J. Evidence for transcriptional activity in the syncytiotrophoblast of the human placenta. *Placenta* **2009**, *30*, 329–334. [[CrossRef](#)]
30. Fogarty, N.M.; Burton, G.J.; Ferguson-Smith, A.C. Different epigenetic states define syncytiotrophoblast and cytotrophoblast nuclei in the trophoblast of the human placenta. *Placenta* **2015**, *36*, 796–802. [[CrossRef](#)]
31. Xu, Y.; Ge, Z.; Zhang, E.; Zuo, Q.; Huang, S.; Yang, N.; Wu, D.; Zhang, Y.; Chen, Y.; Xu, H.; et al. The lncRNA TUG1 modulates proliferation in trophoblast cells via epigenetic suppression of RND3. *Cell Death Dis.* **2017**, *8*, e3104. [[CrossRef](#)] [[PubMed](#)]
32. Song, X.; Rui, C.; Meng, L.; Zhang, R.; Shen, R.; Ding, H.; Li, J.; Li, J.; Long, W. Long non-coding RNA RPAIN regulates the invasion and apoptosis of trophoblast cell lines via complement protein C1q. *Oncotarget* **2017**, *8*, 7637–7646. [[CrossRef](#)] [[PubMed](#)]
33. Chen, H.; Meng, T.; Liu, X.; Sun, M.; Tong, C.; Liu, J.; Wang, H.; Du, J. Long non-coding RNA MALAT-1 is downregulated in preeclampsia and regulates proliferation, apoptosis, migration and invasion of JEG-3 trophoblast cells. *Int. J. Clin. Exp. Pathol.* **2015**, *8*, 12718–12727. [[PubMed](#)]
34. Zhang, Y.; Zou, Y.; Wang, W.; Zuo, Q.; Jiang, Z.; Sun, M.; De, W.; Sun, L. Down-regulated long non-coding RNA MEG3 and its effect on promoting apoptosis and suppressing migration of trophoblast cells. *J. Cell. Biochem.* **2015**, *116*, 542–550. [[CrossRef](#)] [[PubMed](#)]
35. Muys, B.R.; Lorenzi, J.C.; Zanette, D.L.; Lima e Bueno Rde, B.; de Araujo, L.F.; Dinarte-Santos, A.R.; Alves, C.P.; Ramao, A.; de Molfetta, G.A.; Vidal, D.O.; et al. Placenta-Enriched lncRNAs MIR503HG and LINC00629 Decrease Migration and Invasion Potential of JEG-3 Cell Line. *PLoS ONE* **2016**, *11*, e0151560. [[CrossRef](#)] [[PubMed](#)]
36. Zou, Y.; Jiang, Z.; Yu, X.; Sun, M.; Zhang, Y.; Zuo, Q.; Zhou, J.; Yang, N.; Han, P.; Ge, Z.; et al. Upregulation of long noncoding RNA SPRY4-IT1 modulates proliferation, migration, apoptosis, and network formation in trophoblast cells HTR-8SV/neo. *PLoS ONE* **2013**, *8*, e79598. [[CrossRef](#)] [[PubMed](#)]
37. Zuo, Q.; Huang, S.; Zou, Y.; Xu, Y.; Jiang, Z.; Zou, S.; Xu, H.; Sun, L. The lnc RNA SPRY4-IT1 Modulates Trophoblast Cell Invasion and Migration by Affecting the Epithelial-Mesenchymal Transition. *Sci. Rep.* **2016**, *6*, 37183. [[CrossRef](#)] [[PubMed](#)]
38. Yu, L.L.; Chang, K.; Lu, L.S.; Zhao, D.; Han, J.; Zheng, Y.R.; Yan, Y.H.; Yi, P.; Guo, J.X.; Zhou, Y.G.; et al. Lentivirus-mediated RNA interference targeting the H19 gene inhibits cell proliferation and apoptosis in human choriocarcinoma cell line JAR. *BMC Cell Biol.* **2013**, *14*, 26. [[CrossRef](#)] [[PubMed](#)]
39. Saha, S.; Chakraborty, S.; Bhattacharya, A.; Biswas, A.; Ain, R. MicroRNA regulation of Transthyretin in trophoblast differentiation and Intra-Uterine Growth Restriction. *Sci. Rep.* **2017**, *7*, 16548. [[CrossRef](#)]
40. Umemura, K.; Ishioka, S.; Endo, T.; Ezaka, Y.; Takahashi, M.; Saito, T. Roles of microRNA-34a in the pathogenesis of placenta accreta. *J. Obstet. Gynaecol. Res.* **2013**, *39*, 67–74. [[CrossRef](#)]
41. Doridot, L.; Houry, D.; Gaillard, H.; Chelbi, S.T.; Barbaux, S.; Vaiman, D. miR-34a expression, epigenetic regulation, and function in human placental diseases. *Epigenetics* **2014**, *9*, 142–151. [[CrossRef](#)] [[PubMed](#)]
42. Dai, Y.; Qiu, Z.; Diao, Z.; Shen, L.; Xue, P.; Sun, H.; Hu, Y. MicroRNA-155 inhibits proliferation and migration of human extravillous trophoblast derived HTR-8/SVneo cells via down-regulating cyclin D1. *Placenta* **2012**, *33*, 824–829. [[CrossRef](#)]
43. Kumar, P.; Luo, Y.; Tudela, C.; Alexander, J.M.; Mendelson, C.R. The c-Myc-regulated microRNA-17~92 (miR-17~92) and miR-106a~363 clusters target hCYP19A1 and hGCM1 to inhibit human trophoblast differentiation. *Mol. Cell. Biol.* **2013**, *33*, 1782–1796. [[CrossRef](#)] [[PubMed](#)]
44. Gao, W.L.; Liu, M.; Yang, Y.; Yang, H.; Liao, Q.; Bai, Y.; Li, Y.X.; Li, D.; Peng, C.; Wang, Y.L. The imprinted H19 gene regulates human placental trophoblast cell proliferation via encoding miR-675 that targets Nodal Modulator 1 (NOMO1). *RNA Biol.* **2012**, *9*, 1002–1010. [[CrossRef](#)] [[PubMed](#)]

45. Xie, L.; Mouillet, J.F.; Chu, T.; Parks, W.T.; Sadovsky, E.; Knofler, M.; Sadovsky, Y. C19MC microRNAs regulate the migration of human trophoblasts. *Endocrinology* **2014**, *155*, 4975–4985. [[CrossRef](#)] [[PubMed](#)]
46. Novakovic, B.; Fournier, T.; Harris, L.K.; James, J.; Roberts, C.T.; Yong, H.E.J.; Kalionis, B.; Evain-Brion, D.; Ebeling, P.R.; Wallace, E.M.; et al. Increased methylation and decreased expression of homeobox genes TLX1, HOXA10 and DLX5 in human placenta are associated with trophoblast differentiation. *Sci. Rep.* **2017**, *7*, 4523. [[CrossRef](#)] [[PubMed](#)]
47. Wong, N.C.; Novakovic, B.; Weinrich, B.; Dewi, C.; Andronikos, R.; Sibson, M.; Macrae, F.; Morley, R.; Pertile, M.D.; Craig, J.M.; et al. Methylation of the adenomatous polyposis coli (APC) gene in human placenta and hypermethylation in choriocarcinoma cells. *Cancer Lett.* **2008**, *268*, 56–62. [[CrossRef](#)] [[PubMed](#)]
48. Shi, X.; Liu, H.; Cao, J.; Liu, Q.; Tang, G.; Liu, W.; Liu, H.; Deng, D.; Qiao, F.; Wu, Y. Promoter Hypomethylation of Maspin Inhibits Migration and Invasion of Extravillous Trophoblast Cells during Placentation. *PLoS ONE* **2015**, *10*, e0135359. [[CrossRef](#)] [[PubMed](#)]
49. Chiu, R.W.; Chim, S.S.; Wong, I.H.; Wong, C.S.; Lee, W.S.; To, K.F.; Tong, J.H.; Yuen, R.K.; Shum, A.S.; Chan, J.K.; et al. Hypermethylation of RASSF1A in human and rhesus placentas. *Am. J. Pathol.* **2007**, *170*, 941–950. [[CrossRef](#)] [[PubMed](#)]
50. Lister, R.; Pelizzola, M.; Kida, Y.S.; Hawkins, R.D.; Nery, J.R.; Hon, G.; Antosiewicz-Bourget, J.; O'Malley, R.; Castanon, R.; Klugman, S.; et al. Hotspots of aberrant epigenomic reprogramming in human induced pluripotent stem cells. *Nature* **2011**, *471*, 68–73. [[CrossRef](#)] [[PubMed](#)]
51. Schroeder, D.I.; Blair, J.D.; Lott, P.; Yu, H.O.; Hong, D.; Crary, F.; Ashwood, P.; Walker, C.; Korf, I.; Robinson, W.P.; et al. The human placenta methylome. *Proc. Natl. Acad. Sci. USA* **2013**, *110*, 6037–6042. [[CrossRef](#)] [[PubMed](#)]
52. Nordor, A.V.; Nehar-Belaid, D.; Richon, S.; Klatzmann, D.; Bellet, D.; Dangles-Marie, V.; Fournier, T.; Aryee, M.J. The early pregnancy placenta foreshadows DNA methylation alterations of solid tumors. *Epigenetics* **2017**, *12*, 793–803. [[CrossRef](#)] [[PubMed](#)]
53. Yuen, R.K.; Chen, B.; Blair, J.D.; Robinson, W.P.; Nelson, D.M. Hypoxia alters the epigenetic profile in cultured human placental trophoblasts. *Epigenetics* **2013**, *8*, 192–202. [[CrossRef](#)] [[PubMed](#)]
54. Shankar, K.; Kang, P.; Zhong, Y.; Borengasser, S.J.; Wingfield, C.; Saben, J.; Gomez-Acevedo, H.; Thakali, K.M. Transcriptomic and epigenomic landscapes during cell fusion in BeWo trophoblast cells. *Placenta* **2015**, *36*, 1342–1351. [[CrossRef](#)] [[PubMed](#)]
55. James, J.L.; Hurley, D.G.; Gamage, T.K.; Zhang, T.; Vather, R.; Pantham, P.; Murthi, P.; Chamley, L.W. Isolation and characterisation of a novel trophoblast side-population from first trimester placentae. *Reproduction* **2015**, *150*, 449–462. [[CrossRef](#)] [[PubMed](#)]
56. Gamage, T.K.; Schierding, W.; Hurley, D.; Tsai, P.; Ludgate, J.L.; Bhoopathur, C.; Chamley, L.W.; Weeks, R.J.; Macaulay, E.C.; James, J.L. The role of DNA methylation in human trophoblast differentiation. *Epigenetics* **2018**. [[CrossRef](#)] [[PubMed](#)]
57. Ng, R.K.; Dean, W.; Dawson, C.; Lucifero, D.; Madeja, Z.; Reik, W.; Hemberger, M. Epigenetic restriction of embryonic cell lineage fate by methylation of Elf5. *Nat. Cell Biol.* **2008**, *10*, 1280–1290. [[CrossRef](#)] [[PubMed](#)]
58. Senner, C.E.; Krueger, F.; Oxley, D.; Andrews, S.; Hemberger, M. DNA methylation profiles define stem cell identity and reveal a tight embryonic-extraembryonic lineage boundary. *Stem Cells* **2012**, *30*, 2732–2745. [[CrossRef](#)]
59. Murray, R.; Bryant, J.; Titcombe, P.; Barton, S.J.; Inskip, H.; Harvey, N.C.; Cooper, C.; Lillycrop, K.; Hanson, M.; Godfrey, K.M. DNA methylation at birth within the promoter of ANRIL predicts markers of cardiovascular risk at 9 years. *Clin. Epigenet.* **2016**, *8*, 90. [[CrossRef](#)]
60. Santos, J.; Pereira, C.F.; Di-Gregorio, A.; Spruce, T.; Alder, O.; Rodriguez, T.; Azuara, V.; Merckenschlager, M.; Fisher, A.G. Differences in the epigenetic and reprogramming properties of pluripotent and extra-embryonic stem cells implicate chromatin remodelling as an important early event in the developing mouse embryo. *Epigenet. Chromatin* **2010**, *3*, 1. [[CrossRef](#)]
61. Bianco-Miotto, T.; Mayne, B.T.; Buckberry, S.; Breen, J.; Rodriguez Lopez, C.M.; Roberts, C.T. Recent progress towards understanding the role of DNA methylation in human placental development. *Reproduction* **2016**, *152*, R23–R30. [[CrossRef](#)] [[PubMed](#)]
62. Ou, X.; Wang, H.; Qu, D.; Chen, Y.; Gao, J.; Sun, H. Epigenome-wide DNA methylation assay reveals placental epigenetic markers for noninvasive fetal single-nucleotide polymorphism genotyping in maternal plasma. *Transfusion* **2014**, *54*, 2523–2533. [[CrossRef](#)] [[PubMed](#)]

63. Xiang, Y.; Zhang, J.; Li, Q.; Zhou, X.; Wang, T.; Xu, M.; Xia, S.; Xing, Q.; Wang, L.; He, L.; et al. DNA methylome profiling of maternal peripheral blood and placentas reveal potential fetal DNA markers for non-invasive prenatal testing. *Mol. Hum. Reprod.* **2014**, *20*, 875–884. [[CrossRef](#)] [[PubMed](#)]
64. Novakovic, B.; Yuen, R.K.; Gordon, L.; Penaherrera, M.S.; Sharkey, A.; Moffett, A.; Craig, J.M.; Robinson, W.P.; Saffery, R. Evidence for widespread changes in promoter methylation profile in human placenta in response to increasing gestational age and environmental/stochastic factors. *BMC Genom.* **2011**, *12*, 529. [[CrossRef](#)] [[PubMed](#)]
65. Rakan, V.K.; Down, T.A.; Thorne, N.P.; Flicek, P.; Kulesha, E.; Graf, S.; Tomazou, E.M.; Backdahl, L.; Johnson, N.; Herberth, M.; et al. An integrated resource for genome-wide identification and analysis of human tissue-specific differentially methylated regions (tDMRs). *Genome Res.* **2008**, *18*, 1518–1529. [[CrossRef](#)] [[PubMed](#)]
66. Kaur, G.; Helmer, R.A.; Smith, L.A.; Martinez-Zaguilan, R.; Dufour, J.M.; Chilton, B.S. Alternative splicing of helicase-like transcription factor (Hltf): Intron retention-dependent activation of immune tolerance at the fetomaternal interface. *PLoS ONE* **2018**, *13*, e0200211. [[CrossRef](#)] [[PubMed](#)]
67. Schmidt, M.; Lax, E.; Zhou, R.; Cheishvili, D.; Ruder, A.M.; Ludi, A.; Lapert, F.; Macedo da Cruz, A.; Sandrini, P.; Calzoni, T.; et al. Fetal glucocorticoid receptor (Nr3c1) deficiency alters the landscape of DNA methylation of murine placenta in a sex-dependent manner and is associated to anxiety-like behavior in adulthood. *Transl. Psychiatry* **2019**, *9*, 23. [[CrossRef](#)]
68. Price, E.M.; Cotton, A.M.; Penaherrera, M.S.; McFadden, D.E.; Kobor, M.S.; Robinson, W. Different measures of “genome-wide” DNA methylation exhibit unique properties in placental and somatic tissues. *Epigenetics* **2012**, *7*, 652–663. [[CrossRef](#)] [[PubMed](#)]
69. Yang, A.; Sun, Y.; Mao, C.; Yang, S.; Huang, M.; Deng, M.; Ding, N.; Yang, X.; Zhang, M.; Jin, S.; et al. Folate Protects Hepatocytes of Hyperhomocysteinemia Mice From Apoptosis via Cystic Fibrosis Transmembrane Conductance Regulator (CFTR)-Activated Endoplasmic Reticulum Stress. *J. Cell. Biochem.* **2017**, *118*, 2921–2932. [[CrossRef](#)] [[PubMed](#)]
70. Hernandez Mora, J.R.; Sanchez-Delgado, M.; Petazzi, P.; Moran, S.; Esteller, M.; Iglesias-Platas, I.; Monk, D. Profiling of oxBS-450K 5-hydroxymethylcytosine in human placenta and brain reveals enrichment at imprinted loci. *Epigenetics* **2018**, *13*, 182–191. [[CrossRef](#)]
71. Lim, Y.C.; Li, J.; Ni, Y.; Liang, Q.; Zhang, J.; Yeo, G.S.H.; Lyu, J.; Jin, S.; Ding, C. A complex association between DNA methylation and gene expression in human placenta at first and third trimesters. *PLoS ONE* **2017**, *12*, e0181155. [[CrossRef](#)] [[PubMed](#)]
72. Roost, M.S.; Sliker, R.C.; Bialecka, M.; van Iperen, L.; Gomes Fernandes, M.M.; He, N.; Suchiman, H.E.D.; Szuhai, K.; Carlotti, F.; de Koning, E.J.P.; et al. DNA methylation and transcriptional trajectories during human development and reprogramming of isogenic pluripotent stem cells. *Nat. Commun.* **2017**, *8*, 908. [[CrossRef](#)] [[PubMed](#)]
73. Decato, B.E.; Lopez-Tello, J.; Sferruzzi-Perri, A.N.; Smith, A.D.; Dean, M.D. DNA Methylation Divergence and Tissue Specialization in the Developing Mouse Placenta. *Mol. Biol. Evol.* **2017**, *34*, 1702–1712. [[CrossRef](#)] [[PubMed](#)]
74. Green, B.B.; Houseman, E.A.; Johnson, K.C.; Guerin, D.J.; Armstrong, D.A.; Christensen, B.C.; Marsit, C.J. Hydroxymethylation is uniquely distributed within term placenta, and is associated with gene expression. *FASEB J.* **2016**, *30*, 2874–2884. [[CrossRef](#)] [[PubMed](#)]
75. Chatterjee, A.; Macaulay, E.C.; Rodger, E.J.; Stockwell, P.A.; Parry, M.F.; Roberts, H.E.; Slatter, T.L.; Hung, N.A.; Devenish, C.J.; Morison, I.M. Placental Hypomethylation Is More Pronounced in Genomic Loci Devoid of Retroelements. *G3 (Bethesda)* **2016**, *6*, 1911–1921. [[CrossRef](#)] [[PubMed](#)]
76. Branco, M.R.; King, M.; Perez-Garcia, V.; Bogutz, A.B.; Caley, M.; Fineberg, E.; Lefebvre, L.; Cook, S.J.; Dean, W.; Hemberger, M.; et al. Maternal DNA Methylation Regulates Early Trophoblast Development. *Dev. Cell* **2016**, *36*, 152–163. [[CrossRef](#)] [[PubMed](#)]
77. Hanna, C.W.; Penaherrera, M.S.; Saadeh, H.; Andrews, S.; McFadden, D.E.; Kelsey, G.; Robinson, W.P. Pervasive polymorphic imprinted methylation in the human placenta. *Genome Res.* **2016**, *26*, 756–767. [[CrossRef](#)] [[PubMed](#)]
78. Hu, Y.; Blair, J.D.; Yuen, R.K.; Robinson, W.P.; von Dadelszen, P. Genome-wide DNA methylation identifies trophoblast invasion-related genes: Claudin-4 and Fucosyltransferase IV control mobility via altering matrix metalloproteinase activity. *Mol. Hum. Reprod.* **2015**, *21*, 452–465. [[CrossRef](#)]

79. Mahadevan, S.; Wen, S.; Wan, Y.W.; Peng, H.H.; Ota, S.; Liu, Z.; Iacovino, M.; Mahen, E.M.; Kyba, M.; Sadikovic, B.; et al. NLRP7 affects trophoblast lineage differentiation, binds to overexpressed YY1 and alters CpG methylation. *Hum. Mol. Genet.* **2014**, *23*, 706–716. [[CrossRef](#)] [[PubMed](#)]
80. Novakovic, B.; Gordon, L.; Wong, N.C.; Moffett, A.; Manuelpillai, U.; Craig, J.M.; Sharkey, A.; Saffery, R. Wide-ranging DNA methylation differences of primary trophoblast cell populations and derived cell lines: Implications and opportunities for understanding trophoblast function. *Mol. Hum. Reprod.* **2011**, *17*, 344–353. [[CrossRef](#)] [[PubMed](#)]
81. Amorim, R.P.; Araujo, M.G.L.; Valero, J.; Lopes-Cendes, I.; Pascoal, V.D.B.; Malva, J.O.; da Silva Fernandes, M.J. Silencing of P2X7R by RNA interference in the hippocampus can attenuate morphological and behavioral impact of pilocarpine-induced epilepsy. *Purinergic Signal.* **2017**, *13*, 467–478. [[CrossRef](#)] [[PubMed](#)]
82. Oudejans, C.B.; Pannese, M.; Simeone, A.; Meijer, C.J.; Boncinelli, E. The three most downstream genes of the Hox-3 cluster are expressed in human extraembryonic tissues including trophoblast of androgenetic origin. *Development* **1990**, *108*, 471–477. [[PubMed](#)]
83. Chui, A.; Pathirage, N.A.; Johnson, B.; Cocquebert, M.; Fournier, T.; Evain-Brion, D.; Roald, B.; Manuelpillai, U.; Brennecke, S.P.; Kalionis, B.; et al. Homeobox gene distal-less 3 is expressed in proliferating and differentiating cells of the human placenta. *Placenta* **2010**, *31*, 691–697. [[CrossRef](#)] [[PubMed](#)]
84. Grati, F.R.; Sirchia, S.M.; Gentilin, B.; Rossella, F.; Ramoscelli, L.; Antonazzo, P.; Cavallari, U.; Bulfamante, G.; Cetin, I.; Simoni, G.; et al. Biparental expression of ESX1L gene in placentas from normal and intrauterine growth-restricted pregnancies. *Eur. J. Hum. Genet.* **2004**, *12*, 272–278. [[CrossRef](#)] [[PubMed](#)]
85. Quinn, L.M.; Johnson, B.V.; Nicholl, J.; Sutherland, G.R.; Kalionis, B. Isolation and identification of homeobox genes from the human placenta including a novel member of the Distal-less family, DLX4. *Gene* **1997**, *187*, 55–61. [[CrossRef](#)]
86. Rajaraman, G.; Murthi, P.; Quinn, L.; Brennecke, S.P.; Kalionis, B. Homeodomain protein HLX is expressed primarily in cytotrophoblast cell types in the early pregnancy human placenta. *Reprod. Fertil. Dev.* **2008**, *20*, 357–367. [[CrossRef](#)] [[PubMed](#)]
87. Schroeder, D.I.; LaSalle, J.M. How has the study of the human placenta aided our understanding of partially methylated genes? *Epigenomics* **2013**, *5*, 645–654. [[CrossRef](#)] [[PubMed](#)]
88. Hombach, S.; Kretz, M. Non-coding RNAs: Classification, Biology and Functioning. *Adv. Exp. Med. Biol.* **2016**, *937*, 3–17. [[PubMed](#)]
89. Sadovsky, Y.; Mouillet, J.F.; Ouyang, Y.; Bayer, A.; Coyne, C.B. The Function of TrophomiRs and Other MicroRNAs in the Human Placenta. *Cold Spring Harb. Perspect. Med.* **2015**, *5*, a023036. [[CrossRef](#)] [[PubMed](#)]
90. Guo, H.; Ingolia, N.T.; Weissman, J.S.; Bartel, D.P. Mammalian microRNAs predominantly act to decrease target mRNA levels. *Nature* **2010**, *466*, 835–840. [[CrossRef](#)]
91. Krol, J.; Loedige, I.; Filipowicz, W. The widespread regulation of microRNA biogenesis, function and decay. *Nat. Rev. Genet.* **2010**, *11*, 597–610. [[CrossRef](#)] [[PubMed](#)]
92. Bentwich, I.; Avniel, A.; Karov, Y.; Aharonov, R.; Gilad, S.; Barad, O.; Barzilai, A.; Einat, P.; Einav, U.; Meiri, E.; et al. Identification of hundreds of conserved and nonconserved human microRNAs. *Nat. Genet.* **2005**, *37*, 766–770. [[CrossRef](#)] [[PubMed](#)]
93. Donker, R.B.; Mouillet, J.F.; Chu, T.; Hubel, C.A.; Stolz, D.B.; Morelli, A.E.; Sadovsky, Y. The expression profile of C19MC microRNAs in primary human trophoblast cells and exosomes. *Mol. Hum. Reprod.* **2012**, *18*, 417–424. [[CrossRef](#)] [[PubMed](#)]
94. Zhang, R.; Wang, Y.Q.; Su, B. Molecular evolution of a primate-specific microRNA family. *Mol. Biol. Evol.* **2008**, *25*, 1493–1502. [[CrossRef](#)] [[PubMed](#)]
95. Noguer-Dance, M.; Abu-Amero, S.; Al-Khtib, M.; Lefevre, A.; Coullin, P.; Moore, G.E.; Cavaille, J. The primate-specific microRNA gene cluster (C19MC) is imprinted in the placenta. *Hum. Mol. Genet.* **2010**, *19*, 3566–3582. [[CrossRef](#)] [[PubMed](#)]
96. Tsai, K.W.; Kao, H.W.; Chen, H.C.; Chen, S.J.; Lin, W.C. Epigenetic control of the expression of a primate-specific microRNA cluster in human cancer cells. *Epigenetics* **2009**, *4*, 587–592. [[CrossRef](#)]
97. Bar, M.; Wyman, S.K.; Fritz, B.R.; Qi, J.; Garg, K.S.; Parkin, R.K.; Kroh, E.M.; Bendoraite, A.; Mitchell, P.S.; Nelson, A.M.; et al. MicroRNA discovery and profiling in human embryonic stem cells by deep sequencing of small RNA libraries. *Stem Cells* **2008**, *26*, 2496–2505. [[CrossRef](#)] [[PubMed](#)]

98. Laurent, L.C.; Chen, J.; Ulitsky, I.; Mueller, F.J.; Lu, C.; Shamir, R.; Fan, J.B.; Loring, J.F. Comprehensive microRNA profiling reveals a unique human embryonic stem cell signature dominated by a single seed sequence. *Stem Cells* **2008**, *26*, 1506–1516. [[CrossRef](#)] [[PubMed](#)]
99. Morin, R.D.; O'Connor, M.D.; Griffith, M.; Kuchenbauer, F.; Delaney, A.; Prabhu, A.L.; Zhao, Y.; McDonald, H.; Zeng, T.; Hirst, M.; et al. Application of massively parallel sequencing to microRNA profiling and discovery in human embryonic stem cells. *Genome Res.* **2008**, *18*, 610–621. [[CrossRef](#)] [[PubMed](#)]
100. Ren, J.; Jin, P.; Wang, E.; Marincola, F.M.; Stroncek, D.F. MicroRNA and gene expression patterns in the differentiation of human embryonic stem cells. *J. Transl. Med.* **2009**, *7*, 20. [[CrossRef](#)] [[PubMed](#)]
101. Stadler, B.; Ivanovska, I.; Mehta, K.; Song, S.; Nelson, A.; Tan, Y.; Mathieu, J.; Darby, C.; Blau, C.A.; Ware, C.; et al. Characterization of microRNAs involved in embryonic stem cell states. *Stem Cells Dev.* **2010**, *19*, 935–950. [[CrossRef](#)]
102. Morales-Prieto, D.M.; Ospina-Prieto, S.; Chaiwangyen, W.; Schoenleben, M.; Markert, U.R. Pregnancy-associated miRNA-clusters. *J. Reprod. Immunol.* **2013**, *97*, 51–61. [[CrossRef](#)] [[PubMed](#)]
103. Gu, Y.; Sun, J.; Groome, L.J.; Wang, Y. Differential miRNA expression profiles between the first and third trimester human placentas. *Am. J. Physiol. Endocrinol. Metab.* **2013**, *304*, E836–E843. [[CrossRef](#)] [[PubMed](#)]
104. Liang, Y.; Ridzon, D.; Wong, L.; Chen, C. Characterization of microRNA expression profiles in normal human tissues. *BMC Genom.* **2007**, *8*, 166. [[CrossRef](#)] [[PubMed](#)]
105. Keniry, A.; Oxley, D.; Monnier, P.; Kyba, M.; Dandolo, L.; Smits, G.; Reik, W. The H19 lincRNA is a developmental reservoir of miR-675 that suppresses growth and Igf1r. *Nat. Cell Biol.* **2012**, *14*, 659–665. [[CrossRef](#)] [[PubMed](#)]
106. Forbes, K.; Farokhnia, F.; Aplin, J.D.; Westwood, M. Dicer-dependent miRNAs provide an endogenous restraint on cytotrophoblast proliferation. *Placenta* **2012**, *33*, 581–585. [[CrossRef](#)] [[PubMed](#)]
107. Doridot, L.; Miralles, F.; Barbaux, S.; Vaiman, D. Trophoblasts, invasion, and microRNA. *Front. Genet.* **2013**, *4*, 248. [[CrossRef](#)] [[PubMed](#)]
108. Yang, X.; Meng, T. MicroRNA-431 affects trophoblast migration and invasion by targeting ZEB1 in preeclampsia. *Gene* **2019**, *683*, 225–232. [[CrossRef](#)] [[PubMed](#)]
109. Ransohoff, J.D.; Wei, Y.; Khavari, P.A. The functions and unique features of long intergenic non-coding RNA. *Nat. Rev. Mol. Cell Biol.* **2018**, *19*, 143–157. [[CrossRef](#)] [[PubMed](#)]
110. McAninch, D.; Roberts, C.T.; Bianco-Miotto, T. Mechanistic Insight into Long Noncoding RNAs and the Placenta. *Int. J. Mol. Sci.* **2017**, *18*, 1371. [[CrossRef](#)]
111. Brannan, C.I.; Dees, E.C.; Ingram, R.S.; Tilghman, S.M. The product of the H19 gene may function as an RNA. *Mol. Cell. Biol.* **1990**, *10*, 28–36. [[CrossRef](#)] [[PubMed](#)]
112. Gabory, A.; Jammes, H.; Dandolo, L. The H19 locus: Role of an imprinted non-coding RNA in growth and development. *Bioessays* **2010**, *32*, 473–480. [[CrossRef](#)] [[PubMed](#)]
113. Iglesias-Platas, I.; Martin-Trujillo, A.; Petazzi, P.; Guillaumet-Adkins, A.; Esteller, M.; Monk, D. Altered expression of the imprinted transcription factor PLAGL1 deregulates a network of genes in the human IUGR placenta. *Hum. Mol. Genet.* **2014**, *23*, 6275–6285. [[CrossRef](#)] [[PubMed](#)]
114. Kallen, A.N.; Zhou, X.B.; Xu, J.; Qiao, C.; Ma, J.; Yan, L.; Lu, L.; Liu, C.; Yi, J.S.; Zhang, H.; et al. The imprinted H19 lincRNA antagonizes let-7 microRNAs. *Mol. Cell* **2013**, *52*, 101–112. [[CrossRef](#)] [[PubMed](#)]
115. Jinno, Y.; Ikeda, Y.; Yun, K.; Maw, M.; Masuzaki, H.; Fukuda, H.; Inuzuka, K.; Fujishita, A.; Ohtani, Y.; Okimoto, T.; et al. Establishment of functional imprinting of the H19 gene in human developing placentae. *Nat. Genet.* **1995**, *10*, 318–324. [[CrossRef](#)]
116. Yu, L.; Chen, M.; Zhao, D.; Yi, P.; Lu, L.; Han, J.; Zheng, X.; Zhou, Y.; Li, L. The H19 gene imprinting in normal pregnancy and pre-eclampsia. *Placenta* **2009**, *30*, 443–447. [[CrossRef](#)]
117. Jenuwein, T.; Allis, C.D. Translating the histone code. *Science* **2001**, *293*, 1074–1080. [[CrossRef](#)]
118. Mellor, J.; Dudek, P.; Clynes, D. A glimpse into the epigenetic landscape of gene regulation. *Curr. Opin. Genet. Dev.* **2008**, *18*, 116–122. [[CrossRef](#)]
119. Grewal, S.I.; Jia, S. Heterochromatin revisited. *Nat. Rev. Genet.* **2007**, *8*, 35–46. [[CrossRef](#)]
120. Torres-Padilla, M.E.; Parfitt, D.E.; Kouzarides, T.; Zernicka-Goetz, M. Histone arginine methylation regulates pluripotency in the early mouse embryo. *Nature* **2007**, *445*, 214–218. [[CrossRef](#)]
121. Semenza, G.L. HIF-1 and mechanisms of hypoxia sensing. *Curr. Opin. Cell Biol.* **2001**, *13*, 167–171. [[CrossRef](#)]

122. Charron, C.E.; Chou, P.C.; Coutts, D.J.; Kumar, V.; To, M.; Akashi, K.; Pinhu, L.; Griffiths, M.; Adcock, I.M.; Barnes, P.J.; et al. Hypoxia-inducible factor 1alpha induces corticosteroid-insensitive inflammation via reduction of histone deacetylase-2 transcription. *J. Biol. Chem.* **2009**, *284*, 36047–36054. [[CrossRef](#)] [[PubMed](#)]
123. Maltepe, E.; Krampitz, G.W.; Okazaki, K.M.; Red-Horse, K.; Mak, W.; Simon, M.C.; Fisher, S.J. Hypoxia-inducible factor-dependent histone deacetylase activity determines stem cell fate in the placenta. *Development* **2005**, *132*, 3393–3403. [[CrossRef](#)] [[PubMed](#)]
124. Pollard, P.J.; Loenarz, C.; Mole, D.R.; McDonough, M.A.; Gleadle, J.M.; Schofield, C.J.; Ratcliffe, P.J. Regulation of Jumoni-domain-containing histone demethylases by hypoxia-inducible factor (HIF)-1alpha. *Biochem. J.* **2008**, *416*, 387–394. [[CrossRef](#)] [[PubMed](#)]
125. Wellmann, S.; Bettkober, M.; Zelmer, A.; Seeger, K.; Faigle, M.; Eltzschig, H.K.; Buhner, C. Hypoxia upregulates the histone demethylase JMJD1A via HIF-1. *Biochem. Biophys. Res. Commun.* **2008**, *372*, 892–897. [[CrossRef](#)] [[PubMed](#)]
126. Xia, M.; Yao, L.; Zhang, Q.; Wang, F.; Mei, H.; Guo, X.; Huang, W. Long noncoding RNA HOTAIR promotes metastasis of renal cell carcinoma by up-regulating histone H3K27 demethylase JMJD3. *Oncotarget* **2017**, *8*, 19795–19802. [[CrossRef](#)] [[PubMed](#)]
127. Maltepe, E.; Bakardjiev, A.I.; Fisher, S.J. The placenta: Transcriptional, epigenetic, and physiological integration during development. *J. Clin. Investig.* **2010**, *120*, 1016–1025. [[CrossRef](#)] [[PubMed](#)]
128. Franasiak, J.M.; Scott, R.T. Contribution of immunology to implantation failure of euploid embryos. *Fertil. Steril.* **2017**, *107*, 1279–1283. [[CrossRef](#)] [[PubMed](#)]
129. Griffith, O.W.; Chavan, A.R.; Protopapas, S.; Maziarz, J.; Romero, R.; Wagner, G.P. Embryo implantation evolved from an ancestral inflammatory attachment reaction. *Proc. Natl. Acad. Sci. USA* **2017**, *114*, E6566–E6575. [[CrossRef](#)] [[PubMed](#)]
130. Hansen, V.L.; Faber, L.S.; Salehpoor, A.A.; Miller, R.D. A pronounced uterine pro-inflammatory response at parturition is an ancient feature in mammals. *Proc. Biol. Sci.* **2017**, *284*, 20171694. [[CrossRef](#)] [[PubMed](#)]
131. Cornelis, G.; Funk, M.; Vernochet, C.; Leal, F.; Tarazona, O.A.; Meurice, G.; Heidmann, O.; Dupressoir, A.; Miralles, A.; Ramirez-Pinilla, M.P.; et al. An endogenous retroviral envelope syncytin and its cognate receptor identified in the viviparous placental Mabuya lizard. *Proc. Natl. Acad. Sci. USA* **2017**, *114*, E10991–E11000. [[CrossRef](#)] [[PubMed](#)]
132. McKinnell, Z.; Wessel, G. Ligers and tignons and.....what?.....oh my! *Mol. Reprod. Dev.* **2012**, *79*, Fm i. [[CrossRef](#)] [[PubMed](#)]
133. Surani, M.A.; Barton, S.C.; Norris, M.L. Development of reconstituted mouse eggs suggests imprinting of the genome during gametogenesis. *Nature* **1984**, *308*, 548–550. [[CrossRef](#)] [[PubMed](#)]
134. Wake, N.; Arima, T.; Matsuda, T. Involvement of IGF2 and H19 imprinting in choriocarcinoma development. *Int. J. Gynaecol. Obstet.* **1998**, *60* (Suppl. 1), S1–S8. [[CrossRef](#)]
135. Warren, W.C.; Hillier, L.W.; Marshall Graves, J.A.; Birney, E.; Ponting, C.P.; Grutzner, F.; Belov, K.; Miller, W.; Clarke, L.; Chinwalla, A.T.; et al. Genome analysis of the platypus reveals unique signatures of evolution. *Nature* **2008**, *453*, 175–183. [[CrossRef](#)] [[PubMed](#)]
136. Suzuki, S.; Shaw, G.; Kaneko-Ishino, T.; Ishino, F.; Renfree, M.B. The evolution of mammalian genomic imprinting was accompanied by the acquisition of novel CpG islands. *Genome Biol. Evol.* **2011**, *3*, 1276–1283. [[CrossRef](#)] [[PubMed](#)]
137. Renfree, M.B.; Suzuki, S.; Kaneko-Ishino, T. The origin and evolution of genomic imprinting and viviparity in mammals. *Philos. Trans. R. Soc. Lond. B Biol. Sci.* **2013**, *368*, 20120151. [[CrossRef](#)] [[PubMed](#)]
138. Fresard, L.; Leroux, S.; Servin, B.; Gourichon, D.; Dehais, P.; Cristobal, M.S.; Marsaud, N.; Vignoles, F.; Bed'hom, B.; Coville, J.L.; et al. Transcriptome-wide investigation of genomic imprinting in chicken. *Nucleic Acids Res.* **2014**, *42*, 3768–3782. [[CrossRef](#)] [[PubMed](#)]
139. Zhuo, Z.; Lamont, S.J.; Abasht, B. RNA-Seq Analyses Identify Frequent Allele Specific Expression and No Evidence of Genomic Imprinting in Specific Embryonic Tissues of Chicken. *Sci. Rep.* **2017**, *7*, 11944. [[CrossRef](#)] [[PubMed](#)]
140. Piedrahita, J.A. The role of imprinted genes in fetal growth abnormalities. *Birth Defects Res. A Clin. Mol. Teratol.* **2011**, *91*, 682–692. [[CrossRef](#)] [[PubMed](#)]
141. Constancia, M.; Hemberger, M.; Hughes, J.; Dean, W.; Ferguson-Smith, A.; Fundele, R.; Stewart, F.; Kelsey, G.; Fowden, A.; Sibley, C.; et al. Placental-specific IGF-II is a major modulator of placental and fetal growth. *Nature* **2002**, *417*, 945–948. [[CrossRef](#)] [[PubMed](#)]

142. Ripoché, M.A.; Kress, C.; Poirier, F.; Dandolo, L. Deletion of the H19 transcription unit reveals the existence of a putative imprinting control element. *Genes Dev.* **1997**, *11*, 1596–1604. [[CrossRef](#)] [[PubMed](#)]
143. Xu, Y.; Goodyer, C.G.; Deal, C.; Polychronakos, C. Functional polymorphism in the parental imprinting of the human IGF2R gene. *Biochem. Biophys. Res. Commun.* **1993**, *197*, 747–754. [[CrossRef](#)] [[PubMed](#)]
144. Cheong, C.Y.; Chng, K.; Ng, S.; Chew, S.B.; Chan, L.; Ferguson-Smith, A.C. Germline and somatic imprinting in the nonhuman primate highlights species differences in oocyte methylation. *Genome Res.* **2015**, *25*, 611–623. [[CrossRef](#)] [[PubMed](#)]
145. Monk, D.; Arnaud, P.; Apostolidou, S.; Hills, F.A.; Kelsey, G.; Stanier, P.; Feil, R.; Moore, G.E. Limited evolutionary conservation of imprinting in the human placenta. *Proc. Natl. Acad. Sci. USA* **2006**, *103*, 6623–6628. [[CrossRef](#)]
146. Barbaux, S.; Gascoïn-Lachambre, G.; Buffat, C.; Monnier, P.; Mondon, F.; Tonanny, M.B.; Pinard, A.; Auer, J.; Bessières, B.; Barlier, A.; et al. A genome-wide approach reveals novel imprinted genes expressed in the human placenta. *Epigenetics* **2012**, *7*, 1079–1090. [[CrossRef](#)]
147. Allach El Khattabi, L.; Backer, S.; Pinard, A.; Dieudonne, M.N.; Tsatsaris, V.; Vaiman, D.; Dandolo, L.; Bloch-Gallego, E.; Jammes, H.; Barbaux, S. A genome-wide search for new imprinted genes in the human placenta identifies DSCAM as the first imprinted gene on chromosome 21. *Eur. J. Hum. Genet.* **2019**, *27*, 49–60. [[CrossRef](#)]
148. Marjonen, H.; Auvinen, P.; Kahila, H.; Tsuiko, O.; Koks, S.; Tiirats, A.; Viltrop, T.; Tuuri, T.; Soderstrom-Anttila, V.; Suikkari, A.M.; et al. rs10732516 polymorphism at the IGF2/H19 locus associates with genotype-specific effects on placental DNA methylation and birth weight of newborns conceived by assisted reproductive technology. *Clin. Epigenet.* **2018**, *10*, 80. [[CrossRef](#)]
149. Peters, J. The role of genomic imprinting in biology and disease: An expanding view. *Nat. Rev. Genet.* **2014**, *15*, 517–530. [[CrossRef](#)]
150. Monk, D. Genomic imprinting in the human placenta. *Am. J. Obstet. Gynecol.* **2015**, *213*, S152–S162. [[CrossRef](#)]
151. Christians, J.K.; Leavey, K.; Cox, B.J. Associations between imprinted gene expression in the placenta, human fetal growth and preeclampsia. *Biol. Lett.* **2017**, *13*, 20170643. [[CrossRef](#)] [[PubMed](#)]
152. Xie, L.; Sadovsky, Y. The function of miR-519d in cell migration, invasion, and proliferation suggests a role in early placentation. *Placenta* **2016**, *48*, 34–37. [[CrossRef](#)] [[PubMed](#)]
153. Petre, G.; Lores, P.; Sartelet, H.; Truffot, A.; Poreau, B.; Brandeis, S.; Martinez, G.; Satre, V.; Harbuz, R.; Ray, P.F.; et al. Genomic duplication in the 19q13.42 imprinted region identified as a new genetic cause of intrauterine growth restriction. *Clin. Genet.* **2018**. [[CrossRef](#)] [[PubMed](#)]
154. Vaiman, D.; Calicchio, R.; Miralles, F. Landscape of transcriptional deregulations in the preeclamptic placenta. *PLoS ONE* **2013**, *8*, e65498. [[CrossRef](#)] [[PubMed](#)]
155. Jia, R.Z.; Zhang, X.; Hu, P.; Liu, X.M.; Hua, X.D.; Wang, X.; Ding, H.J. Screening for differential methylation status in human placenta in preeclampsia using a CpG island plus promoter microarray. *Int. J. Mol. Med.* **2012**, *30*, 133–141.
156. Anton, L.; Olarérin-George, A.O.; Schwartz, N.; Srinivas, S.; Bastek, J.; Hogenesch, J.B.; Elovitz, M.A. miR-210 inhibits trophoblast invasion and is a serum biomarker for preeclampsia. *Am. J. Pathol.* **2013**, *183*, 1437–1445. [[CrossRef](#)]
157. Liu, L.; Zhang, X.; Rong, C.; Rui, C.; Ji, H.; Qian, Y.J.; Jia, R.; Sun, L. Distinct DNA methylomes of human placentas between pre-eclampsia and gestational diabetes mellitus. *Cell. Physiol. Biochem.* **2014**, *34*, 1877–1889. [[CrossRef](#)]
158. Yeung, K.R.; Chiu, C.L.; Pidsley, R.; Makris, A.; Hennessy, A.; Lind, J.M. DNA methylation profiles in preeclampsia and healthy control placentas. *Am. J. Physiol. Heart Circ. Physiol.* **2016**, *310*, H1295–H1303. [[CrossRef](#)]
159. Zhu, Y.; Song, X.; Wang, J.; Li, Y.; Yang, Y.; Yang, T.; Ma, H.; Wang, L.; Zhang, G.; Cho, W.C.; et al. Placental mesenchymal stem cells of fetal origin deposit epigenetic alterations during long-term culture under serum-free condition. *Expert Opin. Biol. Ther.* **2015**, *15*, 163–180. [[CrossRef](#)]
160. Leavey, K.; Wilson, S.L.; Bainbridge, S.A.; Robinson, W.P.; Cox, B.J. Epigenetic regulation of placental gene expression in transcriptional subtypes of preeclampsia. *Clin. Epigenet.* **2018**, *10*, 28. [[CrossRef](#)]
161. Calicchio, R.; Doridot, L.; Miralles, F.; Mehats, C.; Vaiman, D. DNA methylation, an epigenetic mode of gene expression regulation in reproductive science. *Curr. Pharm. Des.* **2014**, *20*, 1726–1750. [[CrossRef](#)] [[PubMed](#)]

162. Horiuchi, A.; Hayashi, T.; Kikuchi, N.; Hayashi, A.; Fuseya, C.; Shiozawa, T.; Konishi, I. Hypoxia upregulates ovarian cancer invasiveness via the binding of HIF-1alpha to a hypoxia-induced, methylation-free hypoxia response element of S100A4 gene. *Int. J. Cancer* **2012**, *131*, 1755–1767. [[CrossRef](#)] [[PubMed](#)]
163. Aouache, R.; Biquard, L.; Vaiman, D.; Miralles, F. Oxidative Stress in Preeclampsia and Placental Diseases. *Int. J. Mol. Sci.* **2018**, *19*, 1496. [[CrossRef](#)] [[PubMed](#)]
164. Biron-Shental, T.; Sukenik Halevy, R.; Goldberg-Bittman, L.; Kidron, D.; Fejgin, M.D.; Amiel, A. Telomeres are shorter in placental trophoblasts of pregnancies complicated with intrauterine growth restriction (IUGR). *Early Hum. Dev.* **2010**, *86*, 451–456. [[CrossRef](#)] [[PubMed](#)]
165. Sukenik-Halevy, R.; Amiel, A.; Kidron, D.; Liberman, M.; Ganor-Paz, Y.; Biron-Shental, T. Telomere homeostasis in trophoblasts and in cord blood cells from pregnancies complicated with preeclampsia. *Am. J. Obstet. Gynecol.* **2016**, *214*, 283.e1–283.e7. [[CrossRef](#)]
166. Farladansky-Gershnel, S.; Gal, H.; Kidron, D.; Krizhanovsky, V.; Amiel, A.; Sukenik-Halevy, R.; Biron-Shental, T. Telomere Homeostasis and Senescence Markers Are Differently Expressed in Placentas From Pregnancies With Early- Versus Late-Onset Preeclampsia. *Reprod. Sci.* **2018**, 1933719118811644. [[CrossRef](#)]
167. Cindrova-Davies, T.; Fogarty, N.M.E.; Jones, C.J.P.; Kingdom, J.; Burton, G.J. Evidence of oxidative stress-induced senescence in mature, post-mature and pathological human placentas. *Placenta* **2018**, *68*, 15–22. [[CrossRef](#)]
168. Londero, A.P.; Orsaria, M.; Marzinotto, S.; Grassi, T.; Fruscalzo, A.; Calcagno, A.; Bertozzi, S.; Nardini, N.; Stella, E.; Lelle, R.J.; et al. Placental aging and oxidation damage in a tissue micro-array model: An immunohistochemistry study. *Histochem. Cell Biol.* **2016**, *146*, 191–204. [[CrossRef](#)]
169. Burton, G.J.; Yung, H.W.; Murray, A.J. Mitochondrial—Endoplasmic reticulum interactions in the trophoblast: Stress and senescence. *Placenta* **2017**, *52*, 146–155. [[CrossRef](#)]
170. Chu, T.; Bunce, K.; Shaw, P.; Shridhar, V.; Althouse, A.; Hubel, C.; Peters, D. Comprehensive analysis of preeclampsia-associated DNA methylation in the placenta. *PLoS ONE* **2014**, *9*, e107318. [[CrossRef](#)]
171. Blair, J.D.; Yuen, R.K.; Lim, B.K.; McFadden, D.E.; von Dadelszen, P.; Robinson, W.P. Widespread DNA hypomethylation at gene enhancer regions in placentas associated with early-onset pre-eclampsia. *Mol. Hum. Reprod.* **2013**, *19*, 697–708. [[CrossRef](#)] [[PubMed](#)]
172. Yung, H.W.; Atkinson, D.; Champion-Smith, T.; Olovsson, M.; Charnock-Jones, D.S.; Burton, G.J. Differential activation of placental unfolded protein response pathways implies heterogeneity in causation of early- and late-onset pre-eclampsia. *J. Pathol.* **2014**, *234*, 262–276. [[CrossRef](#)] [[PubMed](#)]
173. Zhu, L.; Lv, R.; Kong, L.; Cheng, H.; Lan, F.; Li, X. Genome-Wide Mapping of 5mC and 5hmC Identified Differentially Modified Genomic Regions in Late-Onset Severe Preeclampsia: A Pilot Study. *PLoS ONE* **2015**, *10*, e0134119. [[CrossRef](#)] [[PubMed](#)]
174. Anton, L.; Brown, A.G.; Bartolomei, M.S.; Elovitz, M.A. Differential methylation of genes associated with cell adhesion in preeclamptic placentas. *PLoS ONE* **2014**, *9*, e100148. [[CrossRef](#)] [[PubMed](#)]
175. Nie, X.; Zhang, K.; Wang, L.; Ou, G.; Zhu, H.; Gao, W.Q. Transcription factor STOX1 regulates proliferation of inner ear epithelial cells via the AKT pathway. *Cell Prolif.* **2015**, *48*, 209–220. [[CrossRef](#)] [[PubMed](#)]
176. Guibert, S.; Weber, M. Functions of DNA methylation and hydroxymethylation in mammalian development. *Curr. Top. Dev. Biol.* **2013**, *104*, 47–83. [[PubMed](#)]
177. Bellido, M.L.; Radpour, R.; Lapaire, O.; De Bie, I.; Hosli, I.; Bitzer, J.; Hmadcha, A.; Zhong, X.Y.; Holzgreve, W. MALDI-TOF mass array analysis of RASSF1A and SERPINB5 methylation patterns in human placenta and plasma. *Biol. Reprod.* **2010**, *82*, 745–750. [[CrossRef](#)] [[PubMed](#)]
178. Anderson, C.M.; Ralph, J.L.; Wright, M.L.; Linggi, B.; Ohm, J.E. DNA methylation as a biomarker for preeclampsia. *Biol. Res. Nurs.* **2014**, *16*, 409–420. [[CrossRef](#)] [[PubMed](#)]
179. He, J.; Zhang, A.; Fang, M.; Fang, R.; Ge, J.; Jiang, Y.; Zhang, H.; Han, C.; Ye, X.; Yu, D.; et al. Methylation levels at IGF2 and GNAS DMRs in infants born to preeclamptic pregnancies. *BMC Genom.* **2013**, *14*, 472. [[CrossRef](#)]
180. Xiang, Y.; Zhang, X.; Li, Q.; Xu, J.; Zhou, X.; Wang, T.; Xing, Q.; Liu, Y.; Wang, L.; He, L.; et al. Promoter hypomethylation of TIMP3 is associated with pre-eclampsia in a Chinese population. *Mol. Hum. Reprod.* **2013**, *19*, 153–159. [[CrossRef](#)]
181. Zhang, Y.; Fei, M.; Xue, G.; Zhou, Q.; Jia, Y.; Li, L.; Xin, H.; Sun, S. Elevated levels of hypoxia-inducible microRNA-210 in pre-eclampsia: New insights into molecular mechanisms for the disease. *J. Cell. Mol. Med.* **2012**, *16*, 249–259. [[CrossRef](#)] [[PubMed](#)]

182. Wilson, S.L.; Leavey, K.; Cox, B.; Robinson, W.P. Mining DNA methylation alterations towards a classification of placental pathologies. *Hum. Mol. Genet.* **2018**, *27*, 135–146. [[CrossRef](#)] [[PubMed](#)]
183. Chelbi, S.T.; Wilson, M.L.; Veillard, A.C.; Ingles, S.A.; Zhang, J.; Mondon, F.; Gascoin-Lachambre, G.; Doridot, L.; Mignot, T.M.; Rebourcet, R.; et al. Genetic and epigenetic mechanisms collaborate to control SERPINA3 expression and its association with placental diseases. *Hum. Mol. Genet.* **2012**, *21*, 1968–1978. [[CrossRef](#)] [[PubMed](#)]
184. Hogg, K.; Blair, J.D.; McFadden, D.E.; von Dadelszen, P.; Robinson, W.P. Early onset pre-eclampsia is associated with altered DNA methylation of cortisol-signalling and steroidogenic genes in the placenta. *PLoS ONE* **2013**, *8*, e62969. [[CrossRef](#)] [[PubMed](#)]
185. Xirong, X.; Tao, X.; Wang, Y.; Zhu, L.; Ye, Y.; Liu, H.; Zhou, Q.; Li, X.; Xiong, Y. Hypomethylation of tissue factor pathway inhibitor 2 in human placenta of preeclampsia. *Thrombosis Res.* **2017**, *152*, 7–13.
186. Sundrani, D.P.; Reddy, U.S.; Joshi, A.A.; Mehendale, S.S.; Chavan-Gautam, P.M.; Hardikar, A.A. Differential placental methylation and expression of VEGF, FLT-1 and KDR genes in human term and preterm preeclampsia. *Clin. Epigenet.* **2013**, *5*. [[CrossRef](#)]
187. Ching, T.; Ha, J.; Song, M.A.; Tiirikainen, M.; Molnar, J.; Berry, M.J.; Towner, D.; Garmire, L.X. Genome-scale hypomethylation in the cord blood DNAs associated with early onset preeclampsia. *Clin. Epigenet.* **2015**, *7*, 21. [[CrossRef](#)]
188. Ye, W.; Shen, L.; Xiong, Y.; Zhou, Y.; Gu, H.; Yang, Z. Preeclampsia is Associated with Decreased Methylation of the GNA12 Promoter. *Ann. Hum. Genet.* **2016**, *80*, 7–10. [[CrossRef](#)]
189. Yuen, R.K.; Penaherrera, M.S.; von Dadelszen, P.; McFadden, D.E.; Robinson, W.P. DNA methylation profiling of human placentas reveals promoter hypomethylation of multiple genes in early-onset preeclampsia. *Eur. J. Hum. Genet.* **2010**, *18*, 1006–1012. [[CrossRef](#)]
190. Hogg, K.; Blair, J.D.; von Dadelszen, P.; Robinson, W.P. Hypomethylation of the LEP gene in placenta and elevated maternal leptin concentration in early onset pre-eclampsia. *Mol. Cell. Endocrinol.* **2013**, *367*, 64–73. [[CrossRef](#)]
191. Xiang, Y.; Cheng, Y.; Li, X.; Li, Q.; Xu, J.; Zhang, J.; Liu, Y.; Xing, Q.; Wang, L.; He, L.; et al. Up-regulated expression and aberrant DNA methylation of LEP and SH3PXD2A in pre-eclampsia. *PLoS ONE* **2013**, *8*, e59753. [[CrossRef](#)] [[PubMed](#)]
192. Hu, W.; Weng, X.; Dong, M.; Liu, Y.; Li, W.; Huang, H. Alteration in methylation level at 11 β -hydroxysteroid dehydrogenase type 2 gene promoter in infants born to preeclamptic women. *BMC Genet.* **2014**, *15*, 96. [[CrossRef](#)] [[PubMed](#)]
193. Liu, Y.; Ma, Y. Promoter Methylation Status of WNT2 in Placenta from Patients with Preeclampsia. *Med. Sci. Monit. Int. Med. J. Exp. Clin. Res.* **2017**, *23*, 5294–5301. [[CrossRef](#)] [[PubMed](#)]
194. Ma, M.; Zhou, Q.-J.; Xiong, Y.; Li, B.; Li, X.-T. Preeclampsia is associated with hypermethylation of IGF-1 promoter mediated by DNMT1. *Am. J. Transl. Res.* **2018**, *10*, 16–39. [[PubMed](#)]
195. Rahat, B.; Thakur, S.; Bagga, R.; Kaur, J. Epigenetic regulation of STAT5A and its role as fetal DNA epigenetic marker during placental development and dysfunction. *Placenta* **2016**, *44*, 46–53. [[CrossRef](#)]
196. Choux, C.; Carmignac, V.; Bruno, C.; Sagot, P.; Vaiman, D.; Fauque, P. The placenta: Phenotypic and epigenetic modifications induced by Assisted Reproductive Technologies throughout pregnancy. *Clin. Epigenet.* **2015**, *7*, 87. [[CrossRef](#)] [[PubMed](#)]
197. Tang, Y.; Liu, H.; Li, H.; Peng, T.; Gu, W.; Li, X. Hypermethylation of the HLA-G promoter is associated with preeclampsia. *Mol. Hum. Reprod.* **2015**, *21*, 736–744. [[CrossRef](#)]
198. Konwar, C.; Del Gobbo, G.; Yuan, V.; Robinson, W.P. Considerations when processing and interpreting genomics data of the placenta. *Placenta* **2019**. [[CrossRef](#)]
199. Tsang, J.C.H.; Vong, J.S.L.; Ji, L.; Poon, L.C.Y.; Jiang, P.; Lui, K.O.; Ni, Y.B.; To, K.F.; Cheng, Y.K.Y.; Chiu, R.W.K.; et al. Integrative single-cell and cell-free plasma RNA transcriptomics elucidates placental cellular dynamics. *Proc. Natl. Acad. Sci. USA* **2017**, *114*, E7786–E7795. [[CrossRef](#)]
200. Anacker, J.; Segerer, S.E.; Hagemann, C.; Feix, S.; Kapp, M.; Bausch, R.; Kammerer, U. Human decidua and invasive trophoblasts are rich sources of nearly all human matrix metalloproteinases. *Mol. Hum. Reprod.* **2011**, *17*, 637–652. [[CrossRef](#)]
201. Vettraino, I.M.; Roby, J.; Tolley, T.; Parks, W.C. Collagenase-I, stromelysin-I, and matrilysin are expressed within the placenta during multiple stages of human pregnancy. *Placenta* **1996**, *17*, 557–563. [[CrossRef](#)]

202. Kocarslan, S.; Incebiyik, A.; Guldur, M.E.; Ekinci, T.; Ozardali, H.I. What is the role of matrix metalloproteinase-2 in placenta percreta? *J. Obstet. Gynaecol. Res.* **2015**, *41*, 1018–1022. [[CrossRef](#)] [[PubMed](#)]
203. Espino, Y.S.S.; Flores-Pliego, A.; Espejel-Nunez, A.; Medina-Bastidas, D.; Vadillo-Ortega, F.; Zaga-Clavellina, V.; Estrada-Gutierrez, G. New Insights into the Role of Matrix Metalloproteinases in Preeclampsia. *Int. J. Mol. Sci.* **2017**, *18*, 1448. [[CrossRef](#)] [[PubMed](#)]
204. Li, X.; Wu, C.; Shen, Y.; Wang, K.; Tang, L.; Zhou, M.; Yang, M.; Pan, T.; Liu, X.; Xu, W. Ten-eleven translocation 2 demethylates the MMP9 promoter, and its down-regulation in preeclampsia impairs trophoblast migration and invasion. *J. Biol. Chem.* **2018**, *293*, 10059–10070. [[CrossRef](#)] [[PubMed](#)]
205. White, W.M.; Brost, B.; Sun, Z.; Rose, C.; Craici, I.; Wagner, S.J.; Turner, S.T.; Garovic, V.D. Genome-wide methylation profiling demonstrates hypermethylation in maternal leukocyte DNA in preeclamptic compared to normotensive pregnancies. *Hypertens. Pregnancy* **2013**, *32*, 257–269. [[CrossRef](#)] [[PubMed](#)]
206. White, W.M.; Sun, Z.; Borowski, K.S.; Brost, B.C.; Davies, N.P.; Rose, C.H.; Garovic, V.D. Preeclampsia/Eclampsia candidate genes show altered methylation in maternal leukocytes of preeclamptic women at the time of delivery. *Hypertens. Pregnancy* **2016**, *35*, 394–404. [[CrossRef](#)] [[PubMed](#)]
207. Levine, R.J.; Maynard, S.E.; Qian, C.; Lim, K.H.; England, L.J.; Yu, K.F.; Schisterman, E.F.; Thadhani, R.; Sachs, B.P.; Epstein, F.H.; et al. Circulating angiogenic factors and the risk of preeclampsia. *N. Engl. J. Med.* **2004**, *350*, 672–683. [[CrossRef](#)] [[PubMed](#)]
208. Taglauer, E.S.; Wilkins-Haug, L.; Bianchi, D.W. Review: Cell-free fetal DNA in the maternal circulation as an indication of placental health and disease. *Placenta* **2014**, *35* (Suppl.), S64–S68. [[CrossRef](#)]
209. Chim, S.S.; Tong, Y.K.; Chiu, R.W.; Lau, T.K.; Leung, T.N.; Chan, L.Y.; Oudejans, C.B.; Ding, C.; Lo, Y.M. Detection of the placental epigenetic signature of the maspin gene in maternal plasma. *Proc. Natl. Acad. Sci. USA* **2005**, *102*, 14753–14758. [[CrossRef](#)]
210. Qi, Y.H.; Teng, F.; Zhou, Q.; Liu, Y.X.; Wu, J.F.; Yu, S.S.; Zhang, X.; Ma, M.Y.; Zhou, N.; Chen, L.J. Unmethylated-maspin DNA in maternal plasma is associated with severe preeclampsia. *Acta Obstet. Gynecol. Scand.* **2015**, *94*, 983–988. [[CrossRef](#)]
211. Tsui, D.W.; Chan, K.C.; Chim, S.S.; Chan, L.W.; Leung, T.Y.; Lau, T.K.; Lo, Y.M.; Chiu, R.W. Quantitative aberrations of hypermethylated RASSF1A gene sequences in maternal plasma in pre-eclampsia. *Prenat. Diagn.* **2007**, *27*, 1212–1218. [[CrossRef](#)] [[PubMed](#)]
212. Salvianti, F.; Inversetti, A.; Smid, M.; Valsecchi, L.; Candiani, M.; Pazzagli, M.; Cremonesi, L.; Ferrari, M.; Pinzani, P.; Galbiati, S. Prospective evaluation of RASSF1A cell-free DNA as a biomarker of pre-eclampsia. *Placenta* **2015**, *36*, 996–1001. [[CrossRef](#)] [[PubMed](#)]
213. Mousa, A.A.; Archer, K.J.; Cappello, R.; Estrada-Gutierrez, G.; Isaacs, C.R.; Strauss, J.F., 3rd; Walsh, S.W. DNA methylation is altered in maternal blood vessels of women with preeclampsia. *Reprod. Sci.* **2012**, *19*, 1332–1342. [[CrossRef](#)] [[PubMed](#)]
214. Mousa, A.A.; Cappello, R.E.; Estrada-Gutierrez, G.; Shukla, J.; Romero, R.; Strauss, J.F., 3rd; Walsh, S.W. Preeclampsia is associated with alterations in DNA methylation of genes involved in collagen metabolism. *Am. J. Pathol.* **2012**, *181*, 1455–1463. [[CrossRef](#)] [[PubMed](#)]
215. Mousa, A.A.; Strauss, J.F., 3rd; Walsh, S.W. Reduced methylation of the thromboxane synthase gene is correlated with its increased vascular expression in preeclampsia. *Hypertension* **2012**, *59*, 1249–1255.
216. Nomura, Y.; Lambertini, L.; Rialdi, A.; Lee, M.; Mystal, E.Y.; Grabie, M.; Manaster, I.; Huynh, N.; Finik, J.; Davey, M.; et al. Global methylation in the placenta and umbilical cord blood from pregnancies with maternal gestational diabetes, preeclampsia, and obesity. *Reprod. Sci.* **2014**, *21*, 131–137. [[CrossRef](#)]
217. Chen, J.; Steegers-Theunissen, R.P.M.; van Meurs, J.B.; Felix, J.F.; Eggink, A.J.; Herzog, E.M.; Wijnands, K.P.J.; Stubbs, A.; Sliker, R.C.; van der Spek, P.J.; et al. Early- and late-onset preeclampsia and the tissue-specific epigenome of the placenta and newborn. *Placenta* **2017**, *58*, 122–132.
218. Novielli, C.; Mando, C.; Tabano, S.; Anelli, G.M.; Fontana, L.; Antonazzo, P.; Miozzo, M.; Cetin, I. Mitochondrial DNA content and methylation in fetal cord blood of pregnancies with placental insufficiency. *Placenta* **2017**, *55*, 63–70. [[CrossRef](#)]
219. Qiu, C.; Hevner, K.; Enquobahrie, D.A.; Williams, M.A. A case-control study of maternal blood mitochondrial DNA copy number and preeclampsia risk. *Int. J. Mol. Epidemiol. Genet.* **2012**, *3*, 237–244.

220. Vishnyakova, P.A.; Volodina, M.A.; Tarasova, N.V.; Marey, M.V.; Tsvirkun, D.V.; Vavina, O.V.; Khodzhaeva, Z.S.; Kan, N.E.; Menon, R.; Vysokikh, M.Y.; et al. Mitochondrial role in adaptive response to stress conditions in preeclampsia. *Sci. Rep.* **2016**, *6*, 32410. [CrossRef]
221. Doridot, L.; Chatre, L.; Ducat, A.; Vilotte, J.L.; Lombes, A.; Mehats, C.; Barbaux, S.; Calicchio, R.; Ricchetti, M.; Vaiman, D. Nitroso-redox balance and mitochondrial homeostasis are regulated by STOX1, a pre-eclampsia-associated gene. *Antioxid. Redox Signal.* **2014**, *21*, 819–834. [CrossRef] [PubMed]
222. Brodowski, L.; Zindler, T.; von Hardenberg, S.; Schroder-Heurich, B.; von Kaisenberg, C.S.; Frieling, H.; Hubel, C.A.; Dork, T.; von Versen-Hoynck, F. Preeclampsia-Associated Alteration of DNA Methylation in Fetal Endothelial Progenitor Cells. *Front. Cell Dev. Biol.* **2019**, *7*, 32. [CrossRef] [PubMed]
223. Wang, X.; Chen, Y.; Du, L.; Li, X.; Li, X.; Chen, D. Evaluation of circulating placenta-related long noncoding RNAs as potential biomarkers for preeclampsia. *Exp. Ther. Med.* **2018**, *15*, 4309–4317. [CrossRef] [PubMed]
224. Yu, L.; Kuang, L.Y.; He, F.; Du, L.L.; Li, Q.L.; Sun, W.; Zhou, Y.M.; Li, X.M.; Li, X.Y.; Chen, D.J. The Role and Molecular Mechanism of Long Noncoding RNA-MEG3 in the Pathogenesis of Preeclampsia. *Reprod. Sci.* **2018**, *25*, 1619–1628. [CrossRef] [PubMed]
225. Jairajpuri, D.S.; Malalla, Z.H.; Mahmood, N.; Almawi, W.Y. Circulating microRNA expression as predictor of preeclampsia and its severity. *Gene* **2017**, *627*, 543–548. [CrossRef] [PubMed]
226. Lykoudi, A.; Kolialexi, A.; Lambrou, G.I.; Braoudaki, M.; Siristatidis, C.; Papaioanou, G.K.; Tzetis, M.; Mavrou, A.; Papantoniou, N. Dysregulated placental microRNAs in Early and Late onset Preeclampsia. *Placenta* **2018**, *61*, 24–32. [CrossRef] [PubMed]
227. Purwosunu, Y.; Sekizawa, A.; Okazaki, S.; Farina, A.; Wibowo, N.; Nakamura, M.; Rizzo, N.; Saito, H.; Okai, T. Prediction of preeclampsia by analysis of cell-free messenger RNA in maternal plasma. *Am. J. Obstet. Gynecol.* **2009**, *200*, 386.e1–386.e7. [CrossRef] [PubMed]
228. Tong, J.; Zhao, W.; Lv, H.; Li, W.P.; Chen, Z.J.; Zhang, C. Transcriptomic Profiling in Human Decidua of Severe Preeclampsia Detected by RNA Sequencing. *J. Cell. Biochem.* **2018**, *119*, 607–615. [CrossRef] [PubMed]
229. Zhang, Y.; Yang, L.; Chen, L.L. Life without A tail: New formats of long noncoding RNAs. *Int. J. Biochem. Cell Biol.* **2014**, *54*, 338–349. [CrossRef] [PubMed]
230. Hansen, T.B.; Jensen, T.I.; Clausen, B.H.; Bramsen, J.B.; Finsen, B.; Damgaard, C.K.; Kjems, J. Natural RNA circles function as efficient microRNA sponges. *Nature* **2013**, *495*, 384–388. [CrossRef] [PubMed]
231. Marchese, F.P.; Raimondi, I.; Huarte, M. The multidimensional mechanisms of long noncoding RNA function. *Genome Biol.* **2017**, *18*, 206. [CrossRef] [PubMed]
232. He, X.; He, Y.; Xi, B.; Zheng, J.; Zeng, X.; Cai, Q.; OuYang, Y.; Wang, C.; Zhou, X.; Huang, H.; et al. LncRNAs expression in preeclampsia placenta reveals the potential role of LncRNAs contributing to preeclampsia pathogenesis. *PLoS ONE* **2013**, *8*, e81437. [CrossRef] [PubMed]
233. Long, W.; Rui, C.; Song, X.; Dai, X.; Xue, X.; Lu, Y.; Shen, R.; Li, J.; Ding, H. Distinct expression profiles of lncRNAs between early-onset preeclampsia and preterm controls. *Clin. Chim. Acta* **2016**, *463*, 193–199. [CrossRef] [PubMed]
234. Hosseini, E.S.; Meryet-Figuere, M.; Sabzalipoor, H.; Kashani, H.H.; Nikzad, H.; Asemi, Z. Dysregulated expression of long noncoding RNAs in gynecologic cancers. *Mol. Cancer* **2017**, *16*, 107. [CrossRef] [PubMed]
235. Amigorena, S. © 1998 Nature Publishing Group. *Nature Medicine*. 1998. Available online: <http://www.nature.com/naturemedicine> (accessed on 3 May 2019).
236. Mullen, C.A. Review: Analogies between trophoblastic and malignant cells. *Am. J. Reprod. Immunol.* **1998**, *39*, 41–49. [CrossRef] [PubMed]
237. Ferretti, C.; Bruni, L.; Dangles-Marie, V.; Pecking, A.P.; Bellet, D. Molecular circuits shared by placental and cancer cells, and their implications in the proliferative, invasive and migratory capacities of trophoblasts. *Hum. Reprod. Update* **2007**, *13*, 121–141. [CrossRef] [PubMed]
238. Genbacev, O.; Zhou, Y.; Ludlow, J.W.; Fisher, S.J. Regulation of human placental development by oxygen tension. *Science* **1997**, *277*, 1669–1672. [CrossRef] [PubMed]
239. Ji, P.; Diederichs, S.; Wang, W.; Böing, S.; Metzger, R.; Schneider, P.M.; Tidow, N.; Brandt, B.; Buerger, H.; Bulk, E.; et al. MALAT-1, a novel noncoding RNA, and thymosin β 4 predict metastasis and survival in early-stage non-small cell lung cancer. *Oncogene* **2003**, *22*, 8031–8041. [CrossRef] [PubMed]
240. Miyagawa, R.; Tano, K.; Mizuno, R.; Nakamura, Y.; Ijiri, K.; Rakwal, R.; Shibato, J.; Masuo, Y.; Mayeda, A.; Hirose, T.; et al. Identification of cis- and trans-acting factors involved in the localization of MALAT-1 noncoding RNA to nuclear speckles. *RNA* **2012**, *18*, 738–751. [CrossRef]

241. Tseng, J.-J.; Hsieh, Y.-T.; Hsu, S.-L.; Chou, M.-M. Metastasis associated lung adenocarcinoma transcript 1 is up-regulated in placenta previa increta/percreta and strongly associated with trophoblast-like cell invasion in vitro. *Mol. Hum. Reprod.* **2009**, *15*, 725–731. [[CrossRef](#)]
242. Li, X.; Song, Y.; Liu, F.; Liu, D.; Miao, H.; Ren, J.; Xu, J.; Ding, L.; Hu, Y.; Wang, Z.; et al. Long Non-Coding RNA MALAT1 Promotes Proliferation, Angiogenesis, and Immunosuppressive Properties of Mesenchymal Stem Cells by Inducing VEGF and IDO. *J. Cell. Biochem.* **2017**, *118*, 2780–2791. [[CrossRef](#)] [[PubMed](#)]
243. Hass, R.; Kasper, C.; Böhm, S.; Jacobs, R. Different populations and sources of human mesenchymal stem cells (MSC): A comparison of adult and neonatal tissue-derived MSC. *Cell Commun. Signal.* **2011**, *9*, 12. [[CrossRef](#)] [[PubMed](#)]
244. Zhou, Y.; Zhang, X.; Klibanski, A. MEG3 noncoding RNA: A tumor suppressor. *J. Mol. Endocrinol.* **2012**, *48*, 45–53. [[CrossRef](#)] [[PubMed](#)]
245. Davatzikos, C.; Rathore, S.; Bakas, S.; Pati, S.; Bergman, M.; Kalarot, R.; Sridharan, P.; Gastounioti, A.; Jahani, N.; Cohen, E.; et al. Cancer imaging phenomics toolkit: Quantitative imaging analytics for precision diagnostics and predictive modeling of clinical outcome. *J. Med. Imaging* **2018**, *5*, 011018. [[CrossRef](#)] [[PubMed](#)]
246. Yu, Y.C.; Jiang, Y.; Yang, M.M.; He, S.N.; Xi, X.; Xu, Y.T.; Hu, W.S.; Luo, Q. Hypermethylation of delta-like homolog 1/maternally expressed gene 3 loci in human umbilical veins: Insights into offspring vascular dysfunction born after preeclampsia. *J. Hypertens.* **2019**, *37*, 581–589. [[CrossRef](#)] [[PubMed](#)]
247. Yuan, J.H.; Yang, F.; Wang, F.; Ma, J.Z.; Guo, Y.J.; Tao, Q.F.; Liu, F.; Pan, W.; Wang, T.T.; Zhou, C.C.; et al. A Long Noncoding RNA Activated by TGF- β promotes the invasion-metastasis cascade in hepatocellular carcinoma. *Cancer Cell* **2014**, *25*, 666–681. [[CrossRef](#)] [[PubMed](#)]
248. Liu, X.; Chen, H.; Kong, W.; Zhang, Y.; Cao, L.; Gao, L.; Zhou, R. Down-regulated long non-coding RNA-ATB in preeclampsia and its effect on suppressing migration, proliferation, and tube formation of trophoblast cells. *Placenta* **2017**, *49*, 80–87. [[CrossRef](#)] [[PubMed](#)]
249. Zheng, Q.; Zhang, D.; Yang, Y.U.; Cui, X.; Sun, J.; Liang, C.; Qin, H.; Yang, X.; Liu, S.; Yan, Q. MicroRNA-200c impairs uterine receptivity formation by targeting FUT4 and α 1,3-fucosylation. *Cell Death Differ.* **2017**, *24*, 2161–2172. [[CrossRef](#)] [[PubMed](#)]
250. Renthall, N.E.; Chen, C.-C.; Williams, K.C.; Gerard, R.D.; Prange-Kiel, J.; Mendelson, C.R. miR-200 family and targets, ZEB1 and ZEB2, modulate uterine quiescence and contractility during pregnancy and labor. *Proc. Natl. Acad. Sci. USA* **2010**, *107*, 20828–20833. [[CrossRef](#)]
251. Paysan, L.; Piquet, L.; Saltel, F.; Moreau, V. Rnd3 in Cancer: A Review of the Evidence for Tumor Promoter or Suppressor. *Mol. Cancer Res.* **2016**, *14*, 1033–1044. [[CrossRef](#)]
252. Xu, Y.; Lian, Y.; Zhang, Y.; Huang, S.; Zuo, Q.; Yang, N.; Chen, Y.; Wu, D.; Sun, L. The long non-coding RNA PVT1 represses ANGPTL4 transcription through binding with EZH2 in trophoblast cell. *J. Cell. Mol. Med.* **2018**, *22*, 1272–1282. [[CrossRef](#)] [[PubMed](#)]
253. Feng, Y.; Wang, J.; He, Y.; Zhang, H.; Jiang, M.; Cao, D.; Wang, A. HOXD8/DIAPH2-AS1 epigenetically regulates PAX3 and impairs HTR-8/SVneo cell function under hypoxia. *Biosci. Rep.* **2019**, *39*, BSR20182022. [[CrossRef](#)] [[PubMed](#)]
254. Loupe, J.M.; Miller, P.J.; Bonner, B.P.; Maggi, E.C.; Vijayaraghavan, J.; Crabtree, J.S.; Taylor, C.M.; Zabaleta, J.; Hollenbach, A.D. Comparative transcriptomic analysis reveals the oncogenic fusion protein PAX3-FOXO1 globally alters mRNA and miRNA to enhance myoblast invasion. *Oncogenesis* **2016**, *5*, e246. [[CrossRef](#)] [[PubMed](#)]
255. Pineles, B.L.; Romero, R.; Montenegro, D.; Tarca, A.L.; Han, Y.M.; Kim, Y.M.; Draghici, S.; Espinoza, J.; Kusanovic, J.P.; Mittal, P.; et al. Distinct subsets of microRNAs are expressed differentially in the human placentas of patients with preeclampsia. *Am. J. Obstet. Gynecol.* **2007**, *196*, e261. [[CrossRef](#)] [[PubMed](#)]
256. Zhu, X.m.; Han, T.; Sargent, I.L.; Yin, G.w.; Yao, Y.q. Differential expression profile of microRNAs in human placentas from preeclamptic pregnancies vs normal pregnancies. *Am. J. Obstet. Gynecol.* **2009**, *200*, e661. [[CrossRef](#)]
257. Biró, O.; Nagy, B.; Rigó, J. Identifying miRNA regulatory mechanisms in preeclampsia by systems biology approaches. *Hypertens. Pregnancy* **2017**, *36*, 90–99. [[CrossRef](#)]
258. Zhou, C.; Zou, Q.Y.; Li, H.; Wang, R.F.; Liu, A.X.; Magness, R.R.; Zheng, J. Preeclampsia Downregulates MicroRNAs in Fetal Endothelial Cells: Roles of miR-29a/c-3p in Endothelial Function. *J. Clin. Endocrinol. Metab.* **2017**, *102*, 3470–3479. [[CrossRef](#)] [[PubMed](#)]

259. Yang, Z.; Wu, L.; Zhu, X.; Xu, J.; Jin, R.; Li, G.; Wu, F. MiR-29a modulates the angiogenic properties of human endothelial cells. *Biochem. Biophys. Res. Commun.* **2013**, *434*, 143–149. [[CrossRef](#)]
260. Davis, E.F.; Newton, L.; Lewandowski, A.J.; Lazdam, M.; Kelly, B.A.; Kyriakou, T.; Leeson, P. Pre-eclampsia and offspring cardiovascular health: Mechanistic insights from experimental studies. *Clin. Sci. (Lond.)* **2012**, *123*, 53–72. [[CrossRef](#)]
261. Butalia, S.; Audibert, F.; Cote, A.M.; Firoz, T.; Logan, A.G.; Magee, L.A.; Mundle, W.; Rey, E.; Rabi, D.M.; Daskalopoulou, S.S.; et al. Hypertension Canada's 2018 Guidelines for the Management of Hypertension in Pregnancy. *Can. J. Cardiol.* **2018**, *34*, 526–531. [[CrossRef](#)]
262. Yu, G.Z.; Reilly, S.; Lewandowski, A.J.; Aye, C.Y.L.; Simpson, L.J.; Newton, L.; Davis, E.F.; Zhu, S.J.; Fox, W.R.; Goel, A.; et al. Neonatal Micro-RNA Profile Determines Endothelial Function in Offspring of Hypertensive Pregnancies. *Hypertension* **2018**, *72*, 937–945. [[CrossRef](#)] [[PubMed](#)]
263. BAVELLONI, A.; Ramazzotti, G.; Poli, A.; Piazzini, M.; Focaccia, E.; Blalock, W.; Faenza, I. MiRNA-210: A Current Overview. *Anticancer Res.* **2017**, *37*, 6511–6521. [[PubMed](#)]
264. Kulshreshtha, R.; Ferracin, M.; Wojcik, S.E.; Garzon, R.; Alder, H.; Agosto-Perez, F.J.; Davuluri, R.; Liu, C.-G.; Croce, C.M.; Negrini, M.; et al. A MicroRNA Signature of Hypoxia. *Mol. Cell. Biol.* **2006**, *27*, 1859–1867. [[CrossRef](#)] [[PubMed](#)]
265. Chen, Z.; Li, Y.; Zhang, H.; Huang, P.; Luthra, R. Hypoxia-regulated microRNA-210 modulates mitochondrial function and decreases ISCU and COX10 expression. *Oncogene* **2010**, *29*, 4362–4368. [[CrossRef](#)] [[PubMed](#)]
266. Kelly, T.J.; Souza, A.L.; Clish, C.B.; Puigserver, P. A Hypoxia-Induced Positive Feedback Loop Promotes Hypoxia-Inducible Factor 1 Stability through miR-210 Suppression of Glycerol-3-Phosphate Dehydrogenase 1-Like. *Mol. Cell. Biol.* **2012**, *32*, 898. [[CrossRef](#)]
267. Fasanaro, P.; Di Stefano, V.; Melchionna, R.; Romani, S.; Pompilio, G.; Capogrossi, M.C.; Martelli, F. MicroRNA-210 Modulates Endothelial Cell Response to Hypoxia and Inhibits the Receptor Tyrosine Kinase Ligand Ephrin-A3. *J. Biol. Chem.* **2008**, *283*, 15878–15883. [[CrossRef](#)] [[PubMed](#)]
268. Cabello, C.M.; Bair, W.B.; Lamore, S.D.; Ley, S.; Alexandra, S.; Azimian, S.; Wondrak, G.T. The cinnamon-derived Michael acceptor cinnamic aldehyde impairs melanoma cell proliferation, invasiveness, and tumor growth. *Free Radic. Biol. Med.* **2009**, *46*, 220–231.
269. Lee, D.-C.; Romero, R.; Kim, J.-S.; Tarca, A.L.; Montenegro, D.; Pineles, B.L.; Kim, E.; Lee, J.; Kim, S.Y.; Draghici, S.; et al. miR-210 Targets Iron-Sulfur Cluster Scaffold Homologue in Human Trophoblast Cell Lines. *Am. J. Pathol.* **2011**, *179*, 590–602. [[CrossRef](#)]
270. Muralimanoharan, S.; Maloyan, A.; Mele, J.; Guo, C.; Myatt, L.G.; Myatt, L. MIR-210 modulates mitochondrial respiration in placenta with preeclampsia. *Placenta* **2012**, *33*, 816–823. [[CrossRef](#)]
271. Kopriva, S.E.; Chiasson, V.L.; Mitchell, B.M.; Chatterjee, P. TLR3-Induced Placental miR-210 Down-Regulates the STAT6/Interleukin-4 Pathway. *PLoS ONE* **2013**, *8*, e67760. [[CrossRef](#)]
272. Luo, R.; Shao, X.; Xu, P.; Liu, Y.; Wang, Y.; Zhao, Y.; Liu, M.; Ji, L.; Li, Y.X.; Chang, C.; et al. MicroRNA-210 contributes to preeclampsia by downregulating potassium channel modulatory factor 1. *Hypertension* **2014**, *64*, 839–845. [[CrossRef](#)] [[PubMed](#)]
273. Luo, R.; Wang, Y.; Xu, P.; Cao, G.; Zhao, Y.; Shao, X.; Li, Y.X.; Chang, C.; Peng, C.; Wang, Y.L. Hypoxia-inducible miR-210 contributes to preeclampsia via targeting thrombospondin type I domain containing 7A. *Sci. Rep.* **2016**, *6*, 19588. [[CrossRef](#)] [[PubMed](#)]
274. Chen, J.; Zhao, L.; Wang, D.; Xu, Y.; Gao, H.; Tan, W.; Wang, C. Contribution of regulatory T cells to immune tolerance and association of microRNA-210 and Foxp3 in preeclampsia. *Mol. Med. Rep.* **2019**, *19*, 1150–1158. [[CrossRef](#)]
275. Rudensky, A.Y. Regulatory T Cells and Foxp3. *Immunol. Rev.* **2011**, *241*, 260–268. [[CrossRef](#)] [[PubMed](#)]
276. Zhao, M.; Wang, L.T.; Liang, G.P.; Zhang, P.; Deng, X.J.; Tang, Q.; Zhai, H.Y.; Chang, C.C.; Su, Y.W.; Lu, Q.J. Up-regulation of microRNA-210 induces immune dysfunction via targeting FOXP3 in CD4(+) T cells of psoriasis vulgaris. *Clin. Immunol.* **2014**, *150*, 22–30. [[CrossRef](#)]
277. Zhang, Y.; Diao, Z.; Su, L.; Sun, H.; Li, R.; Cui, H.; Hu, Y. MicroRNA-155 contributes to preeclampsia by down-regulating CYR61. *Am. J. Obstet. Gynecol.* **2010**, *202*, e461–e466. [[CrossRef](#)] [[PubMed](#)]
278. Mo, F.-E.; Muntean, A.G.; Chen, C.-C.; Stolz, D.B.; Watkins, S.C.; Lau, L.F. CYR61 (CCN1) Is Essential for Placental Development and Vascular Integrity. *Mol. Cell. Biol.* **2002**, *22*, 8709–8720. [[CrossRef](#)] [[PubMed](#)]
279. Holbourn, K.; Ravi Acharya, K.; Perbal, B. The CCN family of proteins: Structure–function relationships. *Trends Biochem. Sci.* **2008**, *33*, 561–573. [[CrossRef](#)]

280. Deloia, J.A.; Burlingame, J.M.; Krasnow, J.S. Differential Expression of G1 Cyclins During Human Placentogenesis. *Placenta* **1997**, *18*, 9–16. [[CrossRef](#)]
281. Baldin, V.; Marcote, M.J.; Lukas, J.; Draetta, G.; Pagano, M. Cyclin D1 is a nuclear protein required for cell cycle progression in G1. *Genes Dev.* **2007**, *7*, 812–821. [[CrossRef](#)] [[PubMed](#)]
282. Yung, H.-w.; Calabrese, S.; Hynx, D.; Hemmings, B.A.; Cetin, I.; Charnock-Jones, D.S.; Burton, G.J. Evidence of Placental Translation Inhibition and Endoplasmic Reticulum Stress in the Etiology of Human Intrauterine Growth Restriction. *Am. J. Pathol.* **2008**, *173*, 451–462. [[CrossRef](#)] [[PubMed](#)]
283. Yang, X.; Zhang, J.; Ding, Y. Association of microRNA-155, interleukin 17A, and proteinuria in preeclampsia. *Medicine* **2017**, *96*, e6509. [[CrossRef](#)] [[PubMed](#)]
284. Martin, D.B.; Nelson, P.S.; Knudsen, B.S.; Parkin, R.K.; Noteboom, J.; Kroh, E.M.; O'Brian, K.C.; Drescher, C.W.; Vessella, R.L.; Gentleman, R.; et al. Circulating microRNAs as stable blood-based markers for cancer detection. *Proc. Natl. Acad. Sci. USA* **2008**, *105*, 10513–10518.
285. Dai, Y.; Diao, Z.; Sun, H.; Li, R.; Qiu, Z.; Hu, Y. MicroRNA-155 is involved in the remodelling of human-trophoblast-derived HTR-8/SVneo cells induced by lipopolysaccharides. *Hum. Reprod.* **2011**, *26*, 1882–1891. [[CrossRef](#)] [[PubMed](#)]
286. Chambers, J.C.; Fusi, L.; Haskard, D.O.; Swiet, M.D.; Page, P. Association of Maternal Endothelial Dysfunction With Preeclampsia. *JAMA J. Am. Med. Assoc.* **2014**, *28*, 1607–1612.
287. Cheng, W.; Liu, T.; Jiang, F.; Liu, C.; Zhao, X.; Gao, Y.; Wang, H.; Liu, Z. microRNA-155 regulates angiotensin II type 1 receptor expression in umbilical vein endothelial cells from severely pre-eclamptic pregnant women. *Int. J. Mol. Med.* **2011**, *27*, 393–399. [[PubMed](#)]
288. Shan, H.Y.; Bai, X.J.; Chen, X.M. Angiotensin II induces endothelial cell senescence via the activation of mitogen-activated protein kinases. *Cell Biochem. Funct.* **2008**, *26*, 459–466. [[CrossRef](#)]
289. Seligman, S.P.; Buyon, J.P.; Clancy, R.M.; Young, B.K.; Abramson, S.B. The role of nitric oxide in the pathogenesis of preeclampsia. *Am. J. Obstet. Gynecol.* **1994**, *171*, 944–948. [[CrossRef](#)]
290. Sun, H.X.; Zeng, D.Y.; Li, R.T.; Pang, R.P.; Yang, H.; Hu, Y.L.; Zhang, Q.; Jiang, Y.; Huang, L.Y.; Tang, Y.B.; et al. Essential role of microRNA-155 in regulating endothelium-dependent vasorelaxation by targeting endothelial nitric oxide synthase. *Hypertension* **2012**, *60*, 1407–1414. [[CrossRef](#)]
291. Théry, C.; Zitvogel, L.; Amigorena, S. Exosomes: Composition, biogenesis and function. *Nat. Rev. Immunol.* **2002**, *2*, 569–579. [[CrossRef](#)]
292. Shen, L.; Li, Y.; Li, R.; Diao, Z.; Yany, M.; Wu, M.; Sun, H.; Yan, G.; Hu, Y. Placenta-associated serum exosomal miR-155 derived from patients with preeclampsia inhibits eNOS expression in human umbilical vein endothelial cells. *Int. J. Mol. Med.* **2018**, *41*, 1731–1739. [[CrossRef](#)] [[PubMed](#)]
293. Rensen, S.S.M.; Doevendans, P.A.F.M.; Van Eys, G.J.J.M. Regulation and characteristics of vascular smooth muscle cell phenotypic diversity. *Neth. Heart J.* **2007**, *15*, 100–108. [[CrossRef](#)] [[PubMed](#)]
294. Boerth, N.J.; Dey, N.B.; Cornwell, T.L.; Lincoln, T.M. Cyclic GMP-Dependent Protein Kinase Regulates Vascular Smooth Muscle Cell Phenotype. *J. Vasc. Res.* **1997**, *34*, 245–259. [[CrossRef](#)] [[PubMed](#)]
295. Lincoln, T.M.; Dey, N.B.; Boerth, N.J.; Cornwell, T.L.; Soff, G.A. Nitric oxide—Cyclic GMP pathway regulates vascular smooth muscle cell phenotypic modulation: Implications in vascular diseases. *Acta Physiol. Scand.* **1998**, *164*, 507–515. [[CrossRef](#)] [[PubMed](#)]
296. Choi, S.; Park, M.; Kim, J.; Park, W.; Kim, S.; Lee, D.K.; Hwang, J.Y.; Choe, J.; Won, M.H.; Ryoo, S.; et al. TNF- α elicits phenotypic and functional alterations of vascular smooth muscle cells by miR-155-5p-dependent down-regulation of cGMP-dependent kinase 1. *J. Biol. Chem.* **2018**, *293*, 14812–14822. [[CrossRef](#)] [[PubMed](#)]
297. Park, M.; Choi, S.; Kim, S.; Kim, J.; Lee, D.K.; Park, W.; Kim, T.; Jung, J.; Hwang, J.Y.; Won, M.H.; et al. NF- κ B-responsive miR-155 induces functional impairment of vascular smooth muscle cells by downregulating soluble guanylyl cyclase. *Exp. Mol. Med.* **2019**, *51*, 17. [[CrossRef](#)]
298. Lo, Y.M.; Chiu, R.W. Prenatal diagnosis: Progress through plasma nucleic acids. *Nat. Rev. Genet.* **2007**, *8*, 71–77.
299. Chim, S.S.; Shing, T.K.; Hung, E.C.; Leung, T.Y.; Lau, T.K.; Chiu, R.W.; Lo, Y.M. Detection and characterization of placental microRNAs in maternal plasma. *Clin. Chem.* **2008**, *54*, 482–490. [[CrossRef](#)]
300. Gunel, T.; Zeybek, Y.G.; Akcakaya, P.; Kalelioglu, I.; Benian, A.; Ermis, H.; Aydinli, K. Serum microRNA expression in pregnancies with preeclampsia. *Genet. Mol. Res.* **2011**, *10*, 4034–4040. [[CrossRef](#)]
301. Li, Q.; Long, A.; Jiang, L.; Cai, L.; Xie, L.I.; Gu, J.; Chen, X.; Tan, L. Quantification of preeclampsia-related microRNAs in maternal serum. *Biomed. Rep.* **2015**, *3*, 792–796. [[CrossRef](#)]

302. Munaut, C.; Tebache, L.; Blacher, S.; Noel, A.; Nisolle, M.; Chantraine, F. Dysregulated circulating miRNAs in preeclampsia. *Biomed. Rep.* **2016**, *5*, 686–692. [[CrossRef](#)] [[PubMed](#)]
303. Gan, L.; Liu, Z.; Wei, M.; Chen, Y.; Yang, X.; Chen, L.; Xiao, X. MIR-210 and miR-155 as potential diagnostic markers for pre-eclampsia pregnancies. *Medicine* **2017**, *96*, e7515. [[CrossRef](#)] [[PubMed](#)]
304. Hromadnikova, I.; Kotlabova, K.; Ivankova, K.; Krofta, L. First trimester screening of circulating C19MC microRNAs and the evaluation of their potential to predict the onset of preeclampsia and IUGR. *PLoS ONE* **2017**, *12*, e0171756. [[CrossRef](#)] [[PubMed](#)]
305. Winger, E.E.; Reed, J.L.; Ji, X.; Nicolaidis, K. Peripheral blood cell microRNA quantification during the first trimester predicts preeclampsia: Proof of concept. *PLoS ONE* **2018**, *13*, e0190654. [[CrossRef](#)] [[PubMed](#)]
306. Moldovan, L.; Batte, K.E.; Trgovcich, J.; Wisler, J.; Marsh, C.B.; Piper, M. Methodological challenges in utilizing miRNAs as circulating biomarkers. *J. Cell. Mol. Med.* **2014**, *18*, 371–390. [[CrossRef](#)] [[PubMed](#)]
307. El-Khoury, V.; Pierson, S.; Kaoma, T.; Bernardin, F.; Berchem, G. Assessing cellular and circulating miRNA recovery: The impact of the RNA isolation method and the quantity of input material. *Sci. Rep.* **2016**, *6*, 19529. [[CrossRef](#)] [[PubMed](#)]
308. Xu, P.; Zhao, Y.; Liu, M.; Wang, Y.; Wang, H.; Li, Y.X.; Zhu, X.; Yao, Y.; Wang, H.; Qiao, J.; et al. Variations of microRNAs in human placentas and plasma from preeclamptic pregnancy. *Hypertension* **2014**, *63*, 1276–1284. [[CrossRef](#)]
309. Adel, S.; Mansour, A.; Louka, M.; Matboli, M.; Elmekawi, S.F.; Swelam, N. Evaluation of MicroRNA-210 and Protein tyrosine phosphatase, non-receptor type 2 in Pre-eclampsia. *Gene* **2017**, *596*, 105–109. [[CrossRef](#)]
310. Manaster, I.; Goldman-Wohl, D.; Greenfield, C.; Nachmani, D.; Tsukerman, P.; Hamani, Y.; Yagel, S.; Mandelboim, O. MiRNA-Mediated Control of HLA-G Expression and Function. *PLoS ONE* **2012**, *7*, e33395. [[CrossRef](#)]
311. Su, M.-T.; Tsai, P.-Y.; Tsai, H.-L.; Chen, Y.-C.; Kuo, P.-L. miR-346 and miR-582-3p-regulated EG-VEGF expression and trophoblast invasion via matrix metalloproteinases 2 and 9. *BioFactors* **2017**, *43*, 210–219. [[CrossRef](#)]
312. Tan, Z.; Randall, G.; Fan, J.; Camoretti-Mercado, B.; Brockman-Schneider, R.; Pan, L.; Solway, J.; Gern, J.E.; Lemanske, R.F.; Nicolae, D.; et al. Allele-Specific Targeting of microRNAs to HLA-G and Risk of Asthma. *Am. J. Hum. Genet.* **2007**, *81*, 829–834. [[CrossRef](#)] [[PubMed](#)]
313. Zhang, Q.-H.; Sun, H.-M.; Zheng, R.-Z.; Li, Y.-C.; Zhang, Q.; Cheng, P.; Tang, Z.-H.; Huang, F. Meta-analysis of microRNA-183 family expression in human cancer studies comparing cancer tissues with noncancerous tissues. *Gene* **2013**, *527*, 26–32. [[CrossRef](#)] [[PubMed](#)]
314. Lasabova, Z.; Vazan, M.; Zibolenova, J.; Svecova, I. Overexpression of miR-21 and miR-122 in preeclamptic placentas. *Neuro Endocrinol. Lett.* **2015**, *36*, 695–699. [[PubMed](#)]
315. Gao, S.; Wang, Y.; Han, S.; Zhang, Q. Up-regulated microRNA-300 in maternal whole peripheral blood and placenta associated with pregnancy-induced hypertension and preeclampsia. *Int. J. Clin. Exp. Pathol.* **2017**, *10*, 4232–4242.
316. Turco, M.Y.; Gardner, L.; Kay, R.G.; Hamilton, R.S.; Prater, M.; Hollinshead, M.S.; McWhinnie, A.; Esposito, L.; Fernando, R.; Skelton, H.; et al. Trophoblast organoids as a model for maternal-fetal interactions during human placentation. *Nature* **2018**, *564*, 263–267. [[CrossRef](#)]
317. Coutifaris, C.; Kao, L.C.; Sehdev, H.M.; Chin, U.; Babalola, G.O.; Blaschuk, O.W.; Strauss, J.F. E-cadherin expression during the differentiation of human trophoblasts. *Development (Camb. Engl.)* **1991**, *113*, 767–777.
318. Chakraborty, D.; Cui, W.; Rosario, G.X.; Scott, R.L.; Dhakal, P.; Renaud, S.J.; Tachibana, M.; Rumi, M.A.; Mason, C.W.; Krieg, A.J.; et al. HIF-KDM3A-MMP12 regulatory circuit ensures trophoblast plasticity and placental adaptations to hypoxia. *Proc. Natl. Acad. Sci. USA* **2016**, *113*, E7212–E7221. [[CrossRef](#)]
319. Alahari, S.; Post, M.; Rolfo, A.; Weksberg, R.; Caniggia, I. Compromised JMJD6 Histone Demethylase Activity Affects VHL Gene Repression in Preeclampsia. *J. Clin. Endocrinol. Metab.* **2018**, *103*, 1545–1557. [[CrossRef](#)]
320. Xie, D.; Zhu, J.; Liu, Q.; Li, J.; Song, M.; Wang, K.; Zhou, Q.; Jia, Y.; Li, T. Dysregulation of HDAC9 Represses Trophoblast Cell Migration and Invasion Through TIMP3 Activation in Preeclampsia. *Am. J. Hypertens.* **2019**, *32*, 515–523. [[CrossRef](#)]
321. Zadora, J.; Singh, M.; Herse, F.; Przybyl, L.; Haase, N.; Golic, M.; Yung, H.W.; Huppertz, B.; Cartwright, J.E.; Whitley, G.; et al. Disturbed Placental Imprinting in Preeclampsia Leads to Altered Expression of DLX5, a Human-Specific Early Trophoblast Marker. *Circulation* **2017**, *136*, 1824–1839. [[CrossRef](#)]

322. Van Dijk, M.; Mulders, J.; Poutsma, A.; Konst, A.A.; Lachmeijer, A.M.; Dekker, G.A.; Blankenstein, M.A.; Oudejans, C.B. Maternal segregation of the Dutch preeclampsia locus at 10q22 with a new member of the winged helix gene family. *Nat. Genet.* **2005**, *37*, 514–519. [[CrossRef](#)] [[PubMed](#)]
323. Van Dijk, M.; van Bezu, J.; van Abel, D.; Dunk, C.; Blankenstein, M.A.; Oudejans, C.B.; Lye, S.J. The STOX1 genotype associated with pre-eclampsia leads to a reduction of trophoblast invasion by alpha-T-catenin upregulation. *Hum. Mol. Genet.* **2010**, *19*, 2658–2667. [[CrossRef](#)] [[PubMed](#)]
324. Rigourd, V.; Chauvet, C.; Chelbi, S.T.; Rebourcet, R.; Mondon, F.; Letourneur, F.; Mignot, T.M.; Barbaux, S.; Vaiman, D. STOX1 overexpression in choriocarcinoma cells mimics transcriptional alterations observed in preeclamptic placentas. *PLoS ONE* **2008**, *3*, e3905. [[CrossRef](#)] [[PubMed](#)]
325. Graves, J.A. Genomic imprinting, development and disease—is pre-eclampsia caused by a maternally imprinted gene? *Reprod. Fertil. Dev.* **1998**, *10*, 23–29. [[CrossRef](#)] [[PubMed](#)]



© 2019 by the authors. Licensee MDPI, Basel, Switzerland. This article is an open access article distributed under the terms and conditions of the Creative Commons Attribution (CC BY) license (<http://creativecommons.org/licenses/by/4.0/>).

BIBLIOGRAPHY

- Aghababaei, M., Hogg, K., Perdu, S., Robinson, W. P., & Beristain, A. G. (2015). ADAM12-directed ectodomain shedding of E-cadherin potentiates trophoblast fusion. *Cell Death and Differentiation*, 22(12), 1970–1984. <https://doi.org/10.1038/cdd.2015.44>
- Agrawal, S., Shinar, S., Cerdeira, A. S., Redman, C., & Vatish, M. (2019). Predictive Performance of PIGF (Placental Growth Factor) for Screening Preeclampsia in Asymptomatic Women. *Hypertension*, 74(5), 1124–1135. <https://doi.org/10.1161/HYPERTENSIONAHA.119.13360>
- Alese, M. O., Moodley, J., & Naicker, T. (2021). Preeclampsia and HELLP syndrome, the role of the liver. *The Journal of Maternal-Fetal & Neonatal Medicine : The Official Journal of the European Association of Perinatal Medicine, the Federation of Asia and Oceania Perinatal Societies, the International Society of Perinatal Obstetricians*, 34(1), 117–123. <https://doi.org/10.1080/14767058.2019.1572737>
- Andrus, S. S., & Wolfson, A. B. (2010). Postpartum preeclampsia occurring after resolution of antepartum preeclampsia. *The Journal of Emergency Medicine*, 38(2), 168–170. <https://doi.org/10.1016/j.jemermed.2008.04.039>
- Apicella, C., Ruano, C. S. M., Jacques, S., Gascoin, G., Méhats, C., Vaiman, D., & Miralles, F. (2021). Urothelial Cancer Associated 1 (UCA1) and miR-193 Are Two Non-coding RNAs Involved in Trophoblast Fusion and Placental Diseases. *Frontiers in Cell and Developmental Biology*, 9, 633937. <https://doi.org/10.3389/fcell.2021.633937>
- Apicella, C., Ruano, C. S. M., Méhats, C., Miralles, F., & Vaiman, D. (2019). The Role of Epigenetics in Placental Development and the Etiology of Preeclampsia. *International Journal of Molecular Sciences*, 20(11). <https://doi.org/10.3390/ijms20112837>
- Aplin, J. D., Lewis, R. M., & Jones, C. J. P. B. T.-R. M. in B. S. (2018). *Development of the Human Placental Villus*. <https://doi.org/https://doi.org/10.1016/B978-0-12-801238-3.99857-X>
- Aran, D., Looney, A. P., Liu, L., Wu, E., Fong, V., Hsu, A., ... Bhattacharya, M. (2019). Reference-based analysis of lung single-cell sequencing reveals a transitional profibrotic macrophage. *Nature Immunology*, 20(2), 163–172. <https://doi.org/10.1038/s41590-018-0276-y>
- Avagliano, L., Garò, C., & Marconi, A. M. (2012). Placental Amino Acids Transport in Intrauterine Growth Restriction. *Journal of Pregnancy*, 2012, 972562. <https://doi.org/10.1155/2012/972562>
- Avila, L., Yuen, R. K., Diego-Alvarez, D., Penaherrera, M. S., Jiang, R., & Robinson, W. P. (2010). Evaluating DNA methylation and gene expression variability in the human term placenta. *Placenta*, 31. <https://doi.org/10.1016/j.placenta.2010.09.011>
- Ayorinde, A. A., & Bhattacharya, S. (2017). Inherited predisposition to preeclampsia: Analysis of the Aberdeen intergenerational cohort. *Pregnancy Hypertension*, 8, 37–41. <https://doi.org/10.1016/j.preghy.2017.03.001>

- Backes, C. H., Markham, K., Moorehead, P., Cordero, L., Nankervis, C. A., & Giannone, P. J. (2011). Maternal preeclampsia and neonatal outcomes. *Journal of Pregnancy*, 2011, 214365. <https://doi.org/10.1155/2011/214365>
- Bakken, T. E., Hodge, R. D., Miller, J. A., Yao, Z., Nguyen, T. N., Aevermann, B., ... Tasic, B. (2018). Single-nucleus and single-cell transcriptomes compared in matched cortical cell types. *PLOS ONE*, 13(12), e0209648. Retrieved from <https://doi.org/10.1371/journal.pone.0209648>
- Bamberger, A. M., Schulte, H. M., Thuneke, I., Erdmann, I., Bamberger, C. M., & ASA, S. L. (1997). Expression of the apoptosis-inducing Fas ligand (FasL) in human first and third trimester placenta and choriocarcinoma cells. *The Journal of Clinical Endocrinology and Metabolism*, 82(9), 3173–3175. <https://doi.org/10.1210/jcem.82.9.4360>
- Baron, U., Türbachova, I., Hellwag, A., Eckhardt, F., Berlin, K., Hoffmuller, U., ... Olek, S. (2006). DNA methylation analysis as a tool for cell typing. *Epigenetics*, 1(1), 55–60. <https://doi.org/10.4161/epi.1.1.2643>
- Barrett, H. L., Kubala, M. H., Scholz Romero, K., Denny, K. J., Woodruff, T. M., McIntyre, H. D., ... Nitert, M. D. (2014). Placental lipases in pregnancies complicated by gestational diabetes mellitus (GDM). *PloS One*, 9(8), e104826. <https://doi.org/10.1371/journal.pone.0104826>
- Baumann, M. U., Deborde, S., & Illsley, N. P. (2002). Placental glucose transfer and fetal growth. *Endocrine*, 19(1), 13–22. <https://doi.org/10.1385/ENDO:19:1:13>
- Bergen, V., Soldatov, R. A., Kharchenko, P. V., & Theis, F. J. (2021). RNA velocity—current challenges and future perspectives. *Molecular Systems Biology*, 17(8), e10282. <https://doi.org/https://doi.org/10.15252/msb.202110282>
- Blair, J. D., Yuen, R. K., Lim, B. K., McFadden, D. E., von Dadelszen, P., & Robinson, W. P. (2013). Widespread DNA hypomethylation at gene enhancer regions in placentas associated with early-onset pre-eclampsia. *Mol Hum Reprod*, 19. <https://doi.org/10.1093/molehr/gat044>
- Bouter, A. R., & Duvekot, J. J. (2020). Evaluation of the clinical impact of the revised ISSHP and ACOG definitions on preeclampsia. *Pregnancy Hypertension*, 19, 206–211. <https://doi.org/https://doi.org/10.1016/j.preghy.2019.11.011>
- Brown, C. M., & Garovic, V. D. (2014). Drug treatment of hypertension in pregnancy. *Drugs*, 74(3), 283–296. <https://doi.org/10.1007/s40265-014-0187-7>
- Buckley, A. R., & Buckley, D. J. (2000). Prolactin regulation of apoptosis-associated gene expression in T cells. *Annals of the New York Academy of Sciences*, 917, 522–533. <https://doi.org/10.1111/j.1749-6632.2000.tb05417.x>
- Bulmer, J. N., Innes, B. A., Levey, J., Robson, S. C., & Lash, G. E. (2012). The role of vascular smooth muscle cell apoptosis and migration during uterine spiral artery remodeling in normal human pregnancy. *FASEB Journal : Official Publication of the Federation of American Societies for Experimental Biology*, 26(7), 2975–2985. <https://doi.org/10.1096/fj.12-203679>
- Burton, G. J., & Jauniaux, E. (2004). Placental oxidative stress: from miscarriage to

- preeclampsia. *Journal of the Society for Gynecologic Investigation*, 11(6), 342–352.
<https://doi.org/10.1016/j.jsgi.2004.03.003>
- Burton, G. J., & Jauniaux, E. (2011). Oxidative stress. *Best Practice & Research. Clinical Obstetrics & Gynaecology*, 25(3), 287–299.
<https://doi.org/10.1016/j.bpobgyn.2010.10.016>
- Burton, G. J., Moffett, A., & Keverne, B. (2015). Human evolution: brain, birthweight and the immune system. *Philosophical Transactions of the Royal Society of London. Series B, Biological Sciences*, 370(1663), 20140061. <https://doi.org/10.1098/rstb.2014.0061>
- Burton, G. J., Redman, C. W., Roberts, J. M., & Moffett, A. (2019). Pre-eclampsia: pathophysiology and clinical implications. *BMJ*, 366, l2381.
<https://doi.org/10.1136/bmj.l2381>
- Busche, S., Shao, X., Caron, M., Kwan, T., Allum, F., Cheung, W. A., ... Resource, T. M. T. H. E. (2015). Population whole-genome bisulfite sequencing across two tissues highlights the environment as the principal source of human methylome variation. *Genome Biology*, 16(1), 290. <https://doi.org/10.1186/s13059-015-0856-1>
- Camolotto, S., Racca, A., Rena, V., Nores, R., Patrino, L. C., Genti-Raimondi, S., & Panzetta-Dutari, G. M. (2010). Expression and Transcriptional Regulation of Individual Pregnancy-specific Glycoprotein Genes in Differentiating Trophoblast Cells. *Placenta*, 31(4), 312–319. <https://doi.org/https://doi.org/10.1016/j.placenta.2010.01.004>
- Carter, A. M., Enders, A. C., & Pijnenborg, R. (2015). The role of invasive trophoblast in implantation and placentation of primates. *Philosophical Transactions of the Royal Society of London. Series B, Biological Sciences*, 370(1663), 20140070.
<https://doi.org/10.1098/rstb.2014.0070>
- Chaddha, V., Viero, S., Huppertz, B., & Kingdom, J. (2004). Developmental biology of the placenta and the origins of placental insufficiency. *Seminars in Fetal and Neonatal Medicine*, 9(5), 357–369. <https://doi.org/https://doi.org/10.1016/j.siny.2004.03.006>
- Chang, W., Wang, H., Cui, L., Peng, N.-N., Fan, X., Xue, L.-Q., & Yang, Q. (2016). PLAC1 is involved in human trophoblast syncytialization. *Reproductive Biology*, 16.
<https://doi.org/10.1016/j.repbio.2016.07.001>
- Chappell, S., & Morgan, L. (2006). Searching for genetic clues to the causes of pre-eclampsia. *Clinical Science (London, England : 1979)*, 110(4), 443–458.
<https://doi.org/10.1042/CS20050323>
- Chatuphonprasert, W., Jarukamjorn, K., & Ellinger, I. (2018). Physiology and Pathophysiology of Steroid Biosynthesis, Transport and Metabolism in the Human Placenta . *Frontiers in Pharmacology* , Vol. 9, p. 1027. Retrieved from
<https://www.frontiersin.org/article/10.3389/fphar.2018.01027>
- Chau, K., Hennessy, A., & Makris, A. (2017). Placental growth factor and pre-eclampsia. *Journal of Human Hypertension*, 31(12), 782–786. <https://doi.org/10.1038/jhh.2017.61>
- Chen, M., & Manley, J. L. (2009). Mechanisms of alternative splicing regulation: insights from molecular and genomics approaches. *Nature Reviews. Molecular Cell Biology*, 10(11), 741–754. <https://doi.org/10.1038/nrm2777>

- Chiarello, D. I., Abad, C., Rojas, D., Toledo, F., Vázquez, C. M., Mate, A., ... Marín, R. (2020). Oxidative stress: Normal pregnancy versus preeclampsia. *Biochimica et Biophysica Acta. Molecular Basis of Disease*, 1866(2), 165354. <https://doi.org/10.1016/j.bbadis.2018.12.005>
- Cooke, P. S., Spencer, T. E., Bartol, F. F., & Hayashi, K. (2013). Uterine glands: development, function and experimental model systems. *Molecular Human Reproduction*, 19(9), 547–558. <https://doi.org/10.1093/molehr/gat031>
- Costa, M. A. (2016). The endocrine function of human placenta: an overview. *Reproductive BioMedicine Online*, 32(1), 14–43. <https://doi.org/https://doi.org/10.1016/j.rbmo.2015.10.005>
- Costanzo, V., Bardelli, A., Siena, S., & Abrignani, S. (2018). Exploring the links between cancer and placenta development. *Open Biology*, 8(6), 180081. <https://doi.org/10.1098/rsob.180081>
- Devisme, L., Merlot, B., Ego, A., Houfflin-Debarge, V., Deruelle, P., & Subtil, D. (2013). A case-control study of placental lesions associated with pre-eclampsia. *International Journal of Gynaecology and Obstetrics: The Official Organ of the International Federation of Gynaecology and Obstetrics*, 120(2), 165–168. <https://doi.org/10.1016/j.ijgo.2012.08.023>
- Donker, R. B., Mouillet, J. F., Chu, T., Hubel, C. A., Stolz, D. B., Morelli, A. E., & Sadovsky, Y. (2012). The expression profile of C19MC microRNAs in primary human trophoblast cells and exosomes. *Molecular Human Reproduction*, 18(8), 417–424. <https://doi.org/10.1093/molehr/gas013>
- Doridot, L., Passet, B., Méhats, C., Rigourd, V., Barboux, S., Ducat, A., ... Vaiman, D. (2013). Preeclampsia-like symptoms induced in mice by fetoplacental expression of STOX1 are reversed by aspirin treatment. *Hypertension (Dallas, Tex. : 1979)*, 61(3), 662–668. <https://doi.org/10.1161/HYPERTENSIONAHA.111.202994>
- Dover, N., Gulerman, H. C., Celen, S., Kahyaoglu, S., & Yenicesu, O. (2013). Placental growth factor: as an early second trimester predictive marker for preeclampsia in normal and high-risk pregnancies in a Turkish population. *Journal of Obstetrics and Gynaecology of India*, 63(3), 158–163. <https://doi.org/10.1007/s13224-012-0279-9>
- Ducat, A., Couderc, B., Bouter, A., Biquard, L., Aouache, R., Passet, B., ... Vaiman, D. (2020). Molecular Mechanisms of Trophoblast Dysfunction Mediated by Imbalance between STOX1 Isoforms. *IScience*, 23(5), 101086. <https://doi.org/10.1016/j.isci.2020.101086>
- Economides, D. L., Nicolaides, K. H., Gahl, W. A., Bernardini, I., & Evans, M. I. (1989). Plasma amino acids in appropriate- and small-for-gestational-age fetuses. *American Journal of Obstetrics and Gynecology*, 161(5), 1219–1227. [https://doi.org/10.1016/0002-9378\(89\)90670-4](https://doi.org/10.1016/0002-9378(89)90670-4)
- Edgar, R., Mazor, Y., Rinon, A., Blumenthal, J., Golan, Y., Buzhor, E., ... Shtrichman, R. (2013). LifeMap Discovery™: the embryonic development, stem cells, and regenerative medicine research portal. *PLoS One*, 8(7), e66629. <https://doi.org/10.1371/journal.pone.0066629>

- Feng, Y., Wang, J., He, Y., Zhang, H., Jiang, M., Cao, D., & Wang, A. (2019). HOXD8/DIAPH2-AS1 epigenetically regulates PAX3 and impairs HTR-8/SVneo cell function under hypoxia. *Bioscience Reports*, 39(1), BSR20182022. <https://doi.org/10.1042/BSR20182022>
- Floridon, C., Nielsen, O., Hølund, B., Sweep, F., Sunde, L., Thomsen, S. G., & Teisner, B. (2000). Does plasminogen activator inhibitor-1 (PAI-1) control trophoblast invasion? A study of fetal and maternal tissue in intrauterine, tubal and molar pregnancies. *Placenta*, 21(8), 754–762. <https://doi.org/10.1053/plac.2000.0573>
- Fogarty, N. M. E., Ferguson-Smith, A. C., & Burton, G. J. (2013). Syncytial Knots (Tenney-Parker Changes) in the Human Placenta: Evidence of Loss of Transcriptional Activity and Oxidative Damage. *The American Journal of Pathology*, 183(1), 144–152. <https://doi.org/https://doi.org/10.1016/j.ajpath.2013.03.016>
- Fox, H. (1997). Aging of the placenta. *Archives of Disease in Childhood - Fetal and Neonatal Edition*, 77(3), F171 LP-F175. <https://doi.org/10.1136/fn.77.3.F171>
- Fryer, B. H., & Simon, M. C. (2006). Hypoxia, HIF and the placenta. *Cell Cycle (Georgetown, Tex.)*, 5(5), 495–498. <https://doi.org/10.4161/cc.5.5.2497>
- Gaccioli, F., & Lager, S. (2016). Placental Nutrient Transport and Intrauterine Growth Restriction . *Frontiers in Physiology* , Vol. 7, p. 40. Retrieved from <https://www.frontiersin.org/article/10.3389/fphys.2016.00040>
- Galinsky, R., Polglase, G. R., Hooper, S. B., Black, M. J., & Moss, T. J. M. (2013). The consequences of chorioamnionitis: preterm birth and effects on development. *Journal of Pregnancy*, 2013, 412831. <https://doi.org/10.1155/2013/412831>
- Gamage, T. K. J. B., Schierding, W., Tsai, P., Ludgate, J. L., Chamley, L. W., Weeks, R. J., ... James, J. L. (2018). Human trophoblasts are primarily distinguished from somatic cells by differences in the pattern rather than the degree of global CpG methylation. *Biology Open*, 7(8), bio034884. <https://doi.org/10.1242/bio.034884>
- Gauster, M., Hiden, U., Blaschitz, A., Frank, S., Lang, U., Alvino, G., ... Wadsack, C. (2007). Dysregulation of placental endothelial lipase and lipoprotein lipase in intrauterine growth-restricted pregnancies. *The Journal of Clinical Endocrinology and Metabolism*, 92(6), 2256–2263. <https://doi.org/10.1210/jc.2006-2403>
- George, E. M., & Granger, J. P. (2011). Endothelin: Key Mediator of Hypertension in Preeclampsia. *American Journal of Hypertension*, 24(9), 964–969. <https://doi.org/10.1038/ajh.2011.99>
- Gerbaud, P., Taskén, K., & Pidoux, G. (2015). Spatiotemporal regulation of cAMP signaling controls the human trophoblast fusion. *Frontiers in Pharmacology*, 6, 202. <https://doi.org/10.3389/fphar.2015.00202>
- Ghulmiyyah, L., & Sibai, B. (2012). Maternal Mortality From Preeclampsia/Eclampsia. *Seminars in Perinatology*, 36(1), 56–59. <https://doi.org/https://doi.org/10.1053/j.semperi.2011.09.011>
- Glazier, J. D., Cetin, I., Perugino, G., Ronzoni, S., Grey, A. M., Mahendran, D., ... Sibley, C. P. (1997). Association between the activity of the system A amino acid transporter in the

microvillous plasma membrane of the human placenta and severity of fetal compromise in intrauterine growth restriction. *Pediatric Research*, 42(4), 514–519. <https://doi.org/10.1203/00006450-199710000-00016>

- Goldenberg, R., Jones, B., Griffin, J., Rouse, D., Kamath-Rayne, B., Trivedi, N., & McClure, E. (2014). Reducing Maternal Mortality From Preeclampsia and Eclampsia in Low-Resource Countries: What Should Work? *Acta Obstetrica et Gynecologica Scandinavica*, 94. <https://doi.org/10.1111/aogs.12533>
- Goldman-Wohl, D., & Yagel, S. (2014). United we stand not dividing: The syncytiotrophoblast and cell senescence. *Placenta*, 35(6), 341–344. <https://doi.org/https://doi.org/10.1016/j.placenta.2014.03.012>
- Goll, M. G., & Bestor, T. H. (2005). Eukaryotic cytosine methyltransferases. *Annual Review of Biochemistry*, 74, 481–514. <https://doi.org/10.1146/annurev.biochem.74.010904.153721>
- Gridelet, V., Perrier d’Hauterive, S., Polese, B., Foidart, J.-M., Nisolle, M., & Geenen, V. (2020). Human Chorionic Gonadotrophin: New Pleiotropic Functions for an “Old” Hormone During Pregnancy . *Frontiers in Immunology* , Vol. 11, p. 343. Retrieved from <https://www.frontiersin.org/article/10.3389/fimmu.2020.00343>
- Griffiths, S. K., & Campbell, J. P. (2015). Placental structure, function and drug transfer. *Continuing Education in Anaesthesia Critical Care & Pain*, 15(2), 84–89. <https://doi.org/10.1093/bjaceaccp/mku013>
- Grindberg, R. V, Yee-Greenbaum, J. L., McConnell, M. J., Novotny, M., O’Shaughnessy, A. L., Lambert, G. M., ... Lasken, R. S. (2013). RNA-sequencing from single nuclei. *Proceedings of the National Academy of Sciences*, 110(49), 19802 LP – 19807. <https://doi.org/10.1073/pnas.1319700110>
- Gude, N. M., Roberts, C. T., Kalionis, B., & King, R. G. (2004). Growth and function of the normal human placenta. *Thrombosis Research*, 114(5–6), 397–407. <https://doi.org/10.1016/j.thromres.2004.06.038>
- Guerby, P., Tasta, O., Swiader, A., Pont, F., Bujold, E., Parant, O., ... Negre-Salvayre, A. (2021). Role of oxidative stress in the dysfunction of the placental endothelial nitric oxide synthase in preeclampsia. *Redox Biology*, 40, 101861. <https://doi.org/10.1016/j.redox.2021.101861>
- Gunasekara, C. J., Scott, C. A., Laritsky, E., Baker, M. S., MacKay, H., Duryea, J. D., ... Waterland, R. A. (2019). A genomic atlas of systemic interindividual epigenetic variation in humans. *Genome Biology*, 20(1), 105. <https://doi.org/10.1186/s13059-019-1708-1>
- Guo, H., Zhu, P., Yan, L., Li, R., Hu, B., Lian, Y., ... Qiao, J. (2014). The DNA methylation landscape of human early embryos. *Nature*, 511(7511), 606–610. <https://doi.org/10.1038/nature13544>
- Habib, N., Li, Y., Heidenreich, M., Swiech, L., Avraham-Davidi, I., Trombetta, J. J., ... Regev, A. (2016). Div-Seq: Single-nucleus RNA-Seq reveals dynamics of rare adult newborn neurons. *Science (New York, N.Y.)*, 353(6302), 925–928. <https://doi.org/10.1126/science.aad7038>

- Handy, D. E., Castro, R., & Loscalzo, J. (2011). Epigenetic modifications: basic mechanisms and role in cardiovascular disease. *Circulation*, *123*(19), 2145–2156. <https://doi.org/10.1161/CIRCULATIONAHA.110.956839>
- Harris, L. K., Keogh, R. J., Wareing, M., Baker, P. N., Cartwright, J. E., Aplin, J. D., & Whitley, G. S. J. (2006). Invasive Trophoblasts Stimulate Vascular Smooth Muscle Cell Apoptosis by a Fas Ligand-Dependent Mechanism. *The American Journal of Pathology*, *169*(5), 1863–1874. <https://doi.org/https://doi.org/10.2353/ajpath.2006.060265>
- He, Y., Smith, S. K., Day, K. A., Clark, D. E., Licence, D. R., & Charnock-Jones, D. S. (1999). Alternative splicing of vascular endothelial growth factor (VEGF)-R1 (FLT-1) pre-mRNA is important for the regulation of VEGF activity. *Molecular Endocrinology (Baltimore, Md.)*, *13*(4), 537–545. <https://doi.org/10.1210/mend.13.4.0265>
- Hertig, A. T., Rock, J., & Adams, E. C. (1956). A description of 34 human ova within the first 17 days of development. *American Journal of Anatomy*, *98*(3), 435–493. <https://doi.org/https://doi.org/10.1002/aja.1000980306>
- Hogg, K., Blair, J. D., von Dadelszen, P., & Robinson, W. P. (2013). Hypomethylation of the LEP gene in placenta and elevated maternal leptin concentration in early onset pre-eclampsia. *Molecular and Cellular Endocrinology*, *367*(1–2), 64–73. <https://doi.org/10.1016/j.mce.2012.12.018>
- Hung, T.-H., Skepper, J. N., Charnock-Jones, D. S., & Burton, G. J. (2002). Hypoxia-Reoxygenation. *Circulation Research*, *90*(12), 1274–1281. <https://doi.org/10.1161/01.RES.0000024411.22110.AA>
- Huppertz, B. (2008). Placental Origins of Preeclampsia. *Hypertension*, *51*(4), 970–975. <https://doi.org/10.1161/HYPERTENSIONAHA.107.107607>
- Huppertz, B., Weiss, G., & Moser, G. (2014). Trophoblast invasion and oxygenation of the placenta: measurements versus presumptions. *Journal of Reproductive Immunology*, *101–102*, 74–79. <https://doi.org/https://doi.org/10.1016/j.jri.2013.04.003>
- Jain, V. G., Willis, K. A., Jobe, A., & Ambalavanan, N. (2022). Chorioamnionitis and neonatal outcomes. *Pediatric Research*, *91*(2), 289–296. <https://doi.org/10.1038/s41390-021-01633-0>
- James, J. L., Stone, P. R., & Chamley, L. W. (2006). The regulation of trophoblast differentiation by oxygen in the first trimester of pregnancy. *Human Reproduction Update*, *12*(2), 137–144. <https://doi.org/10.1093/humupd/dmi043>
- Jaremek, A., Jeyarajah, M. J., Jaju Bhattad, G., & Renaud, S. J. (2021). Omics Approaches to Study Formation and Function of Human Placental Syncytiotrophoblast. *Frontiers in Cell and Developmental Biology*, *9*, 674162. <https://doi.org/10.3389/fcell.2021.674162>
- Johnson, M. S., Jackson, D. L., & Schust, D. J. (2018). *Endocrinology of Pregnancy* (M. K. B. T.-E. of R. (Second E. Skinner, Ed.)). <https://doi.org/https://doi.org/10.1016/B978-0-12-801238-3.64672-X>
- Jones, M. J., Islam, S. A., Edgar, R. D., & Kobor, M. S. (2017). *Adjusting for Cell Type Composition in DNA Methylation Data Using a Regression-Based Approach BT - Population Epigenetics: Methods and Protocols* (P. Haggarty & K. Harrison, Eds.).

https://doi.org/10.1007/7651_2015_262

- Kaludjerovic, J., & Ward, W. E. (2012). The Interplay between Estrogen and Fetal Adrenal Cortex. *Journal of Nutrition and Metabolism*, 2012, 837901.
<https://doi.org/10.1155/2012/837901>
- Kanaka-Gatenbein, C., Mastorakos, G., & Chrousos, G. P. (2003). Endocrine-Related Causes and Consequences of Intrauterine Growth Retardation. *Annals of the New York Academy of Sciences*, 997(1), 150–157.
<https://doi.org/https://doi.org/10.1196/annals.1290.017>
- Karahoda, R., Abad, C., Horackova, H., Kastner, P., Zaugg, J., Cerveny, L., ... Staud, F. (2020). Dynamics of Tryptophan Metabolic Pathways in Human Placenta and Placental-Derived Cells: Effect of Gestation Age and Trophoblast Differentiation . *Frontiers in Cell and Developmental Biology* , Vol. 8, p. 937. Retrieved from
<https://www.frontiersin.org/article/10.3389/fcell.2020.574034>
- Karaszi, K., Szabo, S., Juhasz, K., Kiraly, P., Kocsis-Deak, B., Hargitai, B., ... Than, N. G. (2019). Increased placental expression of Placental Protein 5 (PP5) / Tissue Factor Pathway Inhibitor-2 (TFPI-2) in women with preeclampsia and HELLP syndrome: Relevance to impaired trophoblast invasion? *Placenta*, 76, 30–39.
<https://doi.org/https://doi.org/10.1016/j.placenta.2019.01.011>
- Kaufmann, P., Black, S., & Huppertz, B. (2003). Endovascular trophoblast invasion: implications for the pathogenesis of intrauterine growth retardation and preeclampsia. *Biology of Reproduction*, 69(1), 1–7. <https://doi.org/10.1095/biolreprod.102.014977>
- Keaton, S. A., Heilman, P., Bryleva, E. Y., Madaj, Z., Krzyzanowski, S., Grit, J., ... Brundin, L. (2019). Altered Tryptophan Catabolism in Placentas From Women With Pre-eclampsia. *International Journal of Tryptophan Research : IJTR*, 12, 1178646919840321.
<https://doi.org/10.1177/1178646919840321>
- Kim, M., Franke, V., Brandt, B., Lowenstein, E. D., Schöwel, V., Spuler, S., ... Birchmeier, C. (2020). Single-nucleus transcriptomics reveals functional compartmentalization in syncytial skeletal muscle cells. *Nature Communications*, 11(1), 6375.
<https://doi.org/10.1038/s41467-020-20064-9>
- Kingdom, J., Huppertz, B., Seaward, G., & Kaufmann, P. (2000). Development of the placental villous tree and its consequences for fetal growth. *European Journal of Obstetrics, Gynecology, and Reproductive Biology*, 92(1), 35–43.
[https://doi.org/10.1016/s0301-2115\(00\)00423-1](https://doi.org/10.1016/s0301-2115(00)00423-1)
- Knipp, G. T., Audus, K. L., & Soares, M. J. (1999). Nutrient transport across the placenta. *Advanced Drug Delivery Reviews*, 38(1), 41–58.
[https://doi.org/https://doi.org/10.1016/S0169-409X\(99\)00005-8](https://doi.org/https://doi.org/10.1016/S0169-409X(99)00005-8)
- Knöfler, M., Haider, S., Saleh, L., Pollheimer, J., Gamage, T. K. J. B., & James, J. (2019). Human placenta and trophoblast development: key molecular mechanisms and model systems. *Cellular and Molecular Life Sciences*, 76(18), 3479–3496.
<https://doi.org/10.1007/s00018-019-03104-6>
- Kobayashi, H., Sakurai, T., Imai, M., Takahashi, N., Fukuda, A., Yayoi, O., ... Kono, T. (2012).

- Contribution of intragenic DNA methylation in mouse gametic DNA methylomes to establish oocyte-specific heritable marks. *PLoS Genetics*, *8*(1), e1002440. <https://doi.org/10.1371/journal.pgen.1002440>
- Krebs, C., Macara, L. M., Leiser, R., Bowman, A. W., Greer, I. A., & Kingdom, J. C. P. (1996). Intrauterine growth restriction with absent end-diastolic flow velocity in the umbilical artery is associated with maldevelopment of the placental terminal villous tree. *American Journal of Obstetrics and Gynecology*, *175*(6), 1534–1542. [https://doi.org/https://doi.org/10.1016/S0002-9378\(96\)70103-5](https://doi.org/https://doi.org/10.1016/S0002-9378(96)70103-5)
- La Manno, G., Soldatov, R., Zeisel, A., Braun, E., Hochgerner, H., Petukhov, V., ... Kharchenko, P. V. (2018). RNA velocity of single cells. *Nature*, *560*(7719), 494–498. <https://doi.org/10.1038/s41586-018-0414-6>
- Lamarca, B. (2012). Endothelial dysfunction. An important mediator in the pathophysiology of hypertension during pre-eclampsia. *Minerva Ginecologica*, *64*(4), 309–320. Retrieved from <https://pubmed.ncbi.nlm.nih.gov/22728575>
- Lappalainen, T., & Grealley, J. M. (2017). Associating cellular epigenetic models with human phenotypes. *Nature Reviews Genetics*, *18*(7), 441–451. <https://doi.org/10.1038/nrg.2017.32>
- Lee, Y., Choufani, S., Weksberg, R., Wilson, S. L., Yuan, V., Burt, A., ... Horvath, S. (2019). Placental epigenetic clocks: estimating gestational age using placental DNA methylation levels. *Aging*, *11*(12), 4238–4253. <https://doi.org/10.18632/aging.102049>
- Levine, R. J., Maynard, S. E., Qian, C., Lim, K.-H., England, L. J., Yu, K. F., ... Karumanchi, S. A. (2004). Circulating angiogenic factors and the risk of preeclampsia. *The New England Journal of Medicine*, *350*(7), 672–683. <https://doi.org/10.1056/NEJMoa031884>
- Lin, Y.-S., Tang, C.-H., Yang, C.-Y. C., Wu, L.-S., Hung, S.-T., Hwa, H.-L., & Chu, P.-H. (2011). Effect of pre-eclampsia-eclampsia on major cardiovascular events among peripartum women in Taiwan. *The American Journal of Cardiology*, *107*(2), 325–330. <https://doi.org/10.1016/j.amjcard.2010.08.073>
- Loukeris, K., Sela, R., & Baergen, R. N. (2010). Syncytial knots as a reflection of placental maturity: reference values for 20 to 40 weeks' gestational age. *Pediatric and Developmental Pathology : The Official Journal of the Society for Pediatric Pathology and the Paediatric Pathology Society*, *13*(4), 305–309. <https://doi.org/10.2350/09-08-0692-OA.1>
- Lu, X., Wang, R., Zhu, C., Wang, H., Lin, H.-Y., Gu, Y., ... Wang, H. (2017). Fine-Tuned and Cell-Cycle-Restricted Expression of Fusogenic Protein Syncytin-2 Maintains Functional Placental Syncytia. *Cell Reports*, *21*(5), 1150–1159. <https://doi.org/https://doi.org/10.1016/j.celrep.2017.10.019>
- Luttun, A., & Carmeliet, P. (2003). Soluble VEGF receptor Flt1: the elusive preeclampsia factor discovered? *The Journal of Clinical Investigation*, *111*(5), 600–602. <https://doi.org/10.1172/JCI18015>
- MacDorman, M. F., Munson, M. L., & Kirmeyer, S. (2007). Fetal and perinatal mortality, United States, 2004. *National Vital Statistics Reports : From the Centers for Disease*

Control and Prevention, National Center for Health Statistics, National Vital Statistics System, 56(3), 1–19.

- Manandhar, T., Prashad, B., & Pal, M. (2018). Risk Factors for Intrauterine Growth Restriction and Its Neonatal Outcome. *Gynecology & Obstetrics, 08*.
<https://doi.org/10.4172/2161-0932.1000464>
- Männik, J., Vaas, P., Rull, K., Teesalu, P., & Laan, M. (2012). Differential placental expression profile of human Growth Hormone/Chorionic Somatomammotropin genes in pregnancies with pre-eclampsia and gestational diabetes mellitus. *Molecular and Cellular Endocrinology, 355(1)*, 180–187. <https://doi.org/10.1016/j.mce.2012.02.009>
- Marconi, A. M., Paolini, C. L., Zerbe, G., & Battaglia, F. C. (2006). Lactacidemia in Intrauterine Growth Restricted (IUGR) Pregnancies: Relationship to Clinical Severity, Oxygenation and Placental Weight. *Pediatric Research, 59(4)*, 570–574.
<https://doi.org/10.1203/01.pdr.0000205477.70391.3e>
- Marsh, B., & Blelloch, R. (2020). Single nuclei RNA-seq of mouse placental labyrinth development. *ELife, 9*. <https://doi.org/10.7554/eLife.60266>
- Martin, D., & Conrad, K. P. (2000). Expression of endothelial nitric oxide synthase by extravillous trophoblast cells in the human placenta. *Placenta, 21(1)*, 23–31.
<https://doi.org/10.1053/plac.1999.0428>
- Martinez, F., Olvera-Sanchez, S., Esparza-Perusquia, M., Gomez-Chang, E., & Flores-Herrera, O. (2015). Multiple functions of syncytiotrophoblast mitochondria. *Steroids, 103*, 11–22. <https://doi.org/https://doi.org/10.1016/j.steroids.2015.09.006>
- Matsubara, K., Higaki, T., Matsubara, Y., & Nawa, A. (2015). Nitric oxide and reactive oxygen species in the pathogenesis of preeclampsia. *International Journal of Molecular Sciences, 16(3)*, 4600–4614. <https://doi.org/10.3390/ijms16034600>
- Mayhew, T. M. (2014). Turnover of human villous trophoblast in normal pregnancy: what do we know and what do we need to know? *Placenta, 35(4)*, 229–240.
<https://doi.org/10.1016/j.placenta.2014.01.011>
- Mayhew, T. M., & Simpson, R. A. (1994). Quantitative evidence for the spatial dispersal of trophoblast nuclei in human placental villi during gestation. *Placenta, 15(8)*, 837–844.
[https://doi.org/10.1016/s0143-4004\(05\)80185-7](https://doi.org/10.1016/s0143-4004(05)80185-7)
- Maynard, S. E., Min, J.-Y., Merchan, J., Lim, K.-H., Li, J., Mondal, S., ... Karumanchi, S. A. (2003). Excess placental soluble fms-like tyrosine kinase 1 (sFlt1) may contribute to endothelial dysfunction, hypertension, and proteinuria in preeclampsia. *The Journal of Clinical Investigation, 111(5)*, 649–658. <https://doi.org/10.1172/JCI17189>
- Mayne, B. T., Leemaqz, S. Y., Smith, A. K., Breen, J., Roberts, C. T., & Bianco-Miotto, T. (2017). Accelerated placental aging in early onset preeclampsia pregnancies identified by DNA methylation. *Epigenomics, 9(3)*, 279–289. <https://doi.org/10.2217/epi-2016-0103>
- Melincovici, C. S., Boşca, A. B., Şuşman, S., Mărginean, M., Mişu, C., Istrate, M., ... Mişu, C. M. (2018). Vascular endothelial growth factor (VEGF) - key factor in normal and pathological angiogenesis. *Romanian Journal of Morphology and Embryology = Revue*

Roumaine de Morphologie et Embryologie, 59(2), 455–467.

- Mendes, S., Timóteo-Ferreira, F., Almeida, H., & Silva, E. (2019). New Insights into the Process of Placentation and the Role of Oxidative Uterine Microenvironment. *Oxidative Medicine and Cellular Longevity*, 2019, 9174521. <https://doi.org/10.1155/2019/9174521>
- Monk, D., & Moore, G. E. (2004). Intrauterine growth restriction—genetic causes and consequences. *Seminars in Fetal and Neonatal Medicine*, 9(5), 371–378. <https://doi.org/https://doi.org/10.1016/j.siny.2004.03.002>
- Mor, G., & Cardenas, I. (2010). The immune system in pregnancy: a unique complexity. *American Journal of Reproductive Immunology (New York, N.Y. : 1989)*, 63(6), 425–433. <https://doi.org/10.1111/j.1600-0897.2010.00836.x>
- Mukherjee, I., Dhar, R., Singh, S., Sharma, J. B., Nag, T. C., Mridha, A. R., ... Karmakar, S. (2021). Oxidative stress-induced impairment of trophoblast function causes preeclampsia through the unfolded protein response pathway. *Scientific Reports*, 11(1), 18415. <https://doi.org/10.1038/s41598-021-97799-y>
- Munn, D. H., Zhou, M., Attwood, J. T., Bondarev, I., Conway, S. J., Marshall, B., ... Mellor, A. L. (1998). Prevention of allogeneic fetal rejection by tryptophan catabolism. *Science (New York, N.Y.)*, 281(5380), 1191–1193. <https://doi.org/10.1126/science.281.5380.1191>
- Napso, T., Yong, H. E. J., Lopez-Tello, J., & Sferruzzi-Perri, A. N. (2018). The Role of Placental Hormones in Mediating Maternal Adaptations to Support Pregnancy and Lactation . *Frontiers in Physiology* , Vol. 9. Retrieved from <https://www.frontiersin.org/article/10.3389/fphys.2018.01091>
- Nevo, O., Soleymanlou, N., Wu, Y., Xu, J., Kingdom, J., Many, A., ... Caniggia, I. (2006). Increased expression of sFlt-1 in in vivo and in vitro models of human placental hypoxia is mediated by HIF-1. *American Journal of Physiology. Regulatory, Integrative and Comparative Physiology*, 291(4), R1085–R1093. <https://doi.org/10.1152/ajpregu.00794.2005>
- Ng, S.-W., Norwitz, G. A., Pavlicev, M., Tilburgs, T., Simón, C., & Norwitz, E. R. (2020). Endometrial Decidualization: The Primary Driver of Pregnancy Health. *International Journal of Molecular Sciences*, 21(11). <https://doi.org/10.3390/ijms21114092>
- Ng, Y. H., Zhu, H., & Leung, P. C. K. (2012). Twist Modulates Human Trophoblastic Cell Invasion via Regulation of N-Cadherin. *Endocrinology*, 153(2), 925–936. <https://doi.org/10.1210/en.2011-1488>
- Norberg, S., Powell, T. L., & Jansson, T. (1998). Intrauterine growth restriction is associated with a reduced activity of placental taurine transporters. *Pediatric Research*, 44(2), 233–238. <https://doi.org/10.1203/00006450-199808000-00016>
- Novakovic, B., Yuen, R. K., Gordon, L., Penaherrera, M. S., Sharkey, A., & Moffett, A. (2011). Evidence for widespread changes in promoter methylation profile in human placenta in response to increasing gestational age and environmental/stochastic factors. *BMC Genomics*, 12. <https://doi.org/10.1186/1471-2164-12-529>

- O'Brien, M., Baczyk, D., & Kingdom, J. C. (2017). Endothelial Dysfunction in Severe Preeclampsia is Mediated by Soluble Factors, Rather than Extracellular Vesicles. *Scientific Reports*, 7(1), 5887. <https://doi.org/10.1038/s41598-017-06178-z>
- Odigboegwu, O., Pan, L. J., & Chatterjee, P. (2018). Use of Antihypertensive Drugs During Preeclampsia. *Frontiers in Cardiovascular Medicine*, 5, 50. <https://doi.org/10.3389/fcvm.2018.00050>
- Ogunwole, S. M., Mwinnyaa, G., Wang, X., Hong, X., Henderson, J., & Bennett, W. L. (2021). Preeclampsia Across Pregnancies and Associated Risk Factors: Findings From a High-Risk US Birth Cohort. *Journal of the American Heart Association*, 10(17), e019612. <https://doi.org/10.1161/JAHA.120.019612>
- Okae, H., Chiba, H., Hiura, H., Hamada, H., Sato, A., Utsunomiya, T., ... Arima, T. (2014). Genome-wide analysis of DNA methylation dynamics during early human development. *PLoS Genetics*, 10(12), e1004868. <https://doi.org/10.1371/journal.pgen.1004868>
- Olmos-Ortiz, A., Déciga-García, M., Preciado-Martínez, E., Bermejo-Martínez, L., Flores-Espinosa, P., Mancilla-Herrera, I., ... Zaga-Clavellina, V. (2019). Prolactin decreases LPS-induced inflammatory cytokines by inhibiting TLR-4/NFκB signaling in the human placenta. *Molecular Human Reproduction*, 25(10), 660–667. <https://doi.org/10.1093/molehr/gaz038>
- Omata, W., Ackerman IV, W. E., Vandre, D. D., & Robinson, J. M. (2013). Trophoblast Cell Fusion and Differentiation Are Mediated by Both the Protein Kinase C and A Pathways. *PLOS ONE*, 8(11), e81003. Retrieved from <https://doi.org/10.1371/journal.pone.0081003>
- Peleg, D., Kennedy, C. M., & Hunter, S. K. (1998). Intrauterine growth restriction: identification and management. *American Family Physician*, 58(2), 453-460,466-467.
- Peng, C.-C., Chang, J.-H., Lin, H.-Y., Cheng, P.-J., & Su, B.-H. (2018). Intrauterine inflammation, infection, or both (Triple I): A new concept for chorioamnionitis. *Pediatrics and Neonatology*, 59(3), 231–237. <https://doi.org/10.1016/j.pedneo.2017.09.001>
- Pidoux, G., Guibourdenche, J., Frenedo, J.-L., Gerbaud, P., Conti, M., Luton, D., ... Evain-Brion, D. (2004). Impact of Trisomy 21 on Human Trophoblast Behaviour and Hormonal Function. *Placenta*, 25, S79–S84. <https://doi.org/https://doi.org/10.1016/j.placenta.2004.01.007>
- Pijnenborg, R., Vercruyse, L., & Hanssens, M. (2006). The uterine spiral arteries in human pregnancy: facts and controversies. *Placenta*, 27(9–10), 939–958. <https://doi.org/10.1016/j.placenta.2005.12.006>
- Pique-Regi, R., Romero, R., Tarca, A. L., Sandler, E. D., Xu, Y., Garcia-Flores, V., ... Gomez-Lopez, N. (2019). Single cell transcriptional signatures of the human placenta in term and preterm parturition. *ELife*, 8. <https://doi.org/10.7554/eLife.52004>
- Poston, L., & Raijmakers, M. T. M. (2004). Trophoblast Oxidative Stress, Antioxidants and Pregnancy Outcome—A Review. *Placenta*, 25, S72–S78. <https://doi.org/https://doi.org/10.1016/j.placenta.2004.01.003>

- Pötgens, A. J. G., Schmitz, U., Bose, P., Versmold, A., Kaufmann, P., & Frank, H.-G. (2002). Mechanisms of Syncytial Fusion: A Review. *Placenta*, *23*, S107–S113. <https://doi.org/https://doi.org/10.1053/plac.2002.0772>
- Rajakumar, A., Powers, R. W., Hubel, C. A., Shibata, E., von Versen-Höynck, F., Plymire, D., & Jeyabalan, A. (2009). Novel soluble Flt-1 isoforms in plasma and cultured placental explants from normotensive pregnant and preeclamptic women. *Placenta*, *30*(1), 25–34. <https://doi.org/10.1016/j.placenta.2008.10.006>
- Rawn, S. M., & Cross, J. C. (2008). The evolution, regulation, and function of placenta-specific genes. *Annual Review of Cell and Developmental Biology*, *24*, 159–181. <https://doi.org/10.1146/annurev.cellbio.24.110707.175418>
- Redline, R. W. (2012). Distal villous immaturity. *Diagnostic Histopathology*, *18*(5), 189–194. <https://doi.org/https://doi.org/10.1016/j.mpdhp.2012.02.002>
- Redline, R. W., & Patterson, P. (1995). Pre-eclampsia is associated with an excess of proliferative immature intermediate trophoblast. *Human Pathology*, *26*(6), 594–600. [https://doi.org/https://doi.org/10.1016/0046-8177\(95\)90162-0](https://doi.org/https://doi.org/10.1016/0046-8177(95)90162-0)
- Redman, C. W. G., Staff, A. C., & Roberts, J. M. (2020). Syncytiotrophoblast stress in preeclampsia: the convergence point for multiple pathways. *American Journal of Obstetrics and Gynecology*. <https://doi.org/10.1016/j.ajog.2020.09.047>
- Reyes, L., Wolfe, B., & Golos, T. (2017). Hofbauer Cells: Placental Macrophages of Fetal Origin. *Results and Problems in Cell Differentiation*, *62*, 45–60. https://doi.org/10.1007/978-3-319-54090-0_3
- Reynolds, L. P., & Redmer, D. A. (1999). Growth and development of the corpus luteum. *Journal of Reproduction and Fertility. Supplement*, *54*, 181–191.
- Risau, W. (1997). Mechanisms of angiogenesis. *Nature*, *386*(6626), 671–674. <https://doi.org/10.1038/386671a0>
- Ritter, A., Roth, S., Kreis, N.-N., Friemel, A., Hooek, S. C., Steglich Souto, A., ... Yuan, J. (2020). Primary Cilia in Trophoblastic Cells. *Hypertension*, *76*(5), 1491–1505. <https://doi.org/10.1161/HYPERTENSIONAHA.120.15433>
- Roberts, R. M., Ezashi, T., Schulz, L. C., Sugimoto, J., Schust, D. J., Khan, T., & Zhou, J. (2021). Syncytins expressed in human placental trophoblast. *Placenta*, *113*, 8–14. <https://doi.org/https://doi.org/10.1016/j.placenta.2021.01.006>
- Robson, A., Harris, L. K., Innes, B. A., Lash, G. E., Aljunaidy, M. M., Aplin, J. D., ... Bulmer, J. N. (2012). Uterine natural killer cells initiate spiral artery remodeling in human pregnancy. *FASEB Journal : Official Publication of the Federation of American Societies for Experimental Biology*, *26*(12), 4876–4885. <https://doi.org/10.1096/fj.12-210310>
- Roland, C. S., Hu, J., Ren, C.-E., Chen, H., Li, J., Varvoutis, M. S., ... Jiang, S.-W. (2016). Morphological changes of placental syncytium and their implications for the pathogenesis of preeclampsia. *Cellular and Molecular Life Sciences : CMLS*, *73*(2), 365–376. <https://doi.org/10.1007/s00018-015-2069-x>
- Rondinone, O., Murgia, A., Costanza, J., Tabano, S., Camanni, M., Corsaro, L., ... Miozzo, M.

- (2021). Extensive Placental Methylation Profiling in Normal Pregnancies. *International Journal of Molecular Sciences*, 22(4). <https://doi.org/10.3390/ijms22042136>
- Ruano, C. S. M., Apicella, C., Jacques, S., Gascoin, G., Gaspar, C., Miralles, F., ... Vaiman, D. (2021). Alternative splicing in normal and pathological human placentas is correlated to genetic variants. *Human Genetics*, 140(5), 827–848. <https://doi.org/10.1007/s00439-020-02248-x>
- Sadovsky, Y., Mouillet, J.-F., Ouyang, Y., Bayer, A., & Coyne, C. B. (2015). The Function of TrophomiRs and Other MicroRNAs in the Human Placenta. *Cold Spring Harbor Perspectives in Medicine*, 5(8), a023036. <https://doi.org/10.1101/cshperspect.a023036>
- Saito, S., Shiozaki, A., Nakashima, A., Sakai, M., & Sasaki, Y. (2007). The role of the immune system in preeclampsia. *Molecular Aspects of Medicine*, 28(2), 192–209. <https://doi.org/https://doi.org/10.1016/j.mam.2007.02.006>
- Sankar, D., Bhanu, P., Ramalingam, K., Kiran, S., & Ramakrishna, B. (2013). Histomorphological and morphometrical changes of placental terminal villi of normotensive and preeclamptic mothers. *Anatomy & Cell Biology*, 46, 285–290. <https://doi.org/10.5115/acb.2013.46.4.285>
- Shahbazi, M. N. (2020). Mechanisms of human embryo development: from cell fate to tissue shape and back. *Development (Cambridge, England)*, 147(14). <https://doi.org/10.1242/dev.190629>
- Sharma, D., Shastri, S., & Sharma, P. (2016). Intrauterine Growth Restriction: Antenatal and Postnatal Aspects. *Clinical Medicine Insights. Pediatrics*, 10, 67–83. <https://doi.org/10.4137/CMPed.S40070>
- Sheridan, M. A., Yang, Y., Jain, A., Lyons, A. S., Yang, P., Brahmasani, S. R., ... Roberts, R. M. (2019). Early onset preeclampsia in a model for human placental trophoblast. *Proceedings of the National Academy of Sciences*, 116(10), 4336 LP – 4345. <https://doi.org/10.1073/pnas.1816150116>
- Simpson, L. L. (2002). Maternal medical disease: risk of antepartum fetal death. *Seminars in Perinatology*, 26(1), 42–50. <https://doi.org/10.1053/sper.2002.29838>
- Simpson, R. A., Mayhew, T. M., & Barnes, P. R. (1992). From 13 weeks to term, the trophoblast of human placenta grows by the continuous recruitment of new proliferative units: a study of nuclear number using the disector. *Placenta*, 13(5), 501–512. [https://doi.org/10.1016/0143-4004\(92\)90055-x](https://doi.org/10.1016/0143-4004(92)90055-x)
- Slukvin, I. I., Lunn, D. P., Watkins, D. I., & Golos, T. G. (2000). Placental expression of the nonclassical MHC class I molecule Mamu-AG at implantation in the rhesus monkey. *Proceedings of the National Academy of Sciences*, 97(16), 9104 LP – 9109. <https://doi.org/10.1073/pnas.97.16.9104>
- Small, H. Y., Cornelius, D. C., Guzik, T. J., & Delles, C. (2017). Natural killer cells in placentation and cancer: Implications for hypertension during pregnancy. *Placenta*, 56, 59–64. <https://doi.org/https://doi.org/10.1016/j.placenta.2017.03.003>
- Smallwood, S. A., Tomizawa, S.-I., Krueger, F., Ruf, N., Carli, N., Segonds-Pichon, A., ... Kelsey, G. (2011). Dynamic CpG island methylation landscape in oocytes and preimplantation

- embryos. *Nature Genetics*, 43(8), 811–814. <https://doi.org/10.1038/ng.864>
- Smith, J., Sen, S., Weeks, R. J., Eccles, M. R., & Chatterjee, A. (2020). Promoter DNA Hypermethylation and Paradoxical Gene Activation. *Trends in Cancer*, 6(5), 392–406. <https://doi.org/10.1016/j.trecan.2020.02.007>
- Smith, M., Waugh, J., & Nelson-Piercy, C. (2013). Management of postpartum hypertension. *The Obstetrician & Gynaecologist*, 15(1), 45–50. <https://doi.org/https://doi.org/10.1111/j.1744-4667.2012.00144.x>
- Smith, S. D., Dunk, C. E., Aplin, J. D., Harris, L. K., & Jones, R. L. (2009). Evidence for immune cell involvement in decidual spiral arteriole remodeling in early human pregnancy. *The American Journal of Pathology*, 174(5), 1959–1971. <https://doi.org/10.2353/ajpath.2009.080995>
- Souders, C. A., Maynard, S. E., Yan, J., Wang, Y., Boatright, N. K., Sedan, J., ... Simas, T. A. M. (2015). Circulating Levels of sFlt1 Splice Variants as Predictive Markers for the Development of Preeclampsia. *International Journal of Molecular Sciences*, 16(6), 12436–12453. <https://doi.org/10.3390/ijms160612436>
- Souza, D. de, McDaniel, G. M., & Baum, V. C. (2011). CHAPTER 4 - Cardiovascular Physiology (P. J. Davis, F. P. Cladis, & E. K. B. T.-S. A. for I. and C. (Eighth E. Motoyama, Eds.). <https://doi.org/https://doi.org/10.1016/B978-0-323-06612-9.00004-3>
- Staun-Ram, E., & Shalev, E. (2005). Human trophoblast function during the implantation process. *Reproductive Biology and Endocrinology : RB&E*, 3, 56. <https://doi.org/10.1186/1477-7827-3-56>
- Sultana, Z., Maiti, K., Aitken, J., Morris, J., Dedman, L., & Smith, R. (2017). Oxidative stress, placental ageing-related pathologies and adverse pregnancy outcomes. *American Journal of Reproductive Immunology*, 77(5), e12653. <https://doi.org/https://doi.org/10.1111/aji.12653>
- Sundrani, D. P., Reddy, U. S., Joshi, A. A., Mehendale, S. S., Chavan-Gautam, P. M., & Hardikar, A. A. (2013). Differential placental methylation and expression of VEGF, FLT-1 and KDR genes in human term and preterm preeclampsia. *Clin Epigenetics*, 5. <https://doi.org/10.1186/1868-7083-5-6>
- Suryawanshi, H., Morozov, P., Straus, A., Sahasrabudhe, N., Max, K. E. A., Garzia, A., ... Williams, Z. (2018). A single-cell survey of the human first-trimester placenta and decidua. *Science Advances*, 4(10), eaau4788. <https://doi.org/10.1126/sciadv.aau4788>
- Sutton, E. F., Gemmel, M., & Powers, R. W. (2020). Nitric oxide signaling in pregnancy and preeclampsia. *Nitric Oxide*, 95, 55–62. <https://doi.org/https://doi.org/10.1016/j.niox.2019.11.006>
- Sweeney, M., Jones, C. J. P., Greenwood, S. L., Baker, P. N., & Taggart, M. J. (2006). Ultrastructural Features of Smooth Muscle and Endothelial Cells of Isolated Isobaric Human Placental and Maternal Arteries. *Placenta*, 27(6), 635–647. <https://doi.org/https://doi.org/10.1016/j.placenta.2005.05.010>
- Szmitko, P. E., Fedak, P. W. M., Weisel, R. D., Stewart, D. J., Kutryk, M. J. B., & Verma, S. (2003). Endothelial Progenitor Cells. *Circulation*, 107(24), 3093–3100.

<https://doi.org/10.1161/01.CIR.0000074242.66719.4A>

- Thilaganathan, B. (2018). Pre-eclampsia and the cardiovascular–placental axis. *Ultrasound in Obstetrics & Gynecology*, *51*(6), 714–717.
<https://doi.org/https://doi.org/10.1002/uog.19081>
- Torry, D. S., Ahn, H., Barnes, E. L., & Torry, R. J. (1999). Placenta growth factor: potential role in pregnancy. *American Journal of Reproductive Immunology (New York, N.Y. : 1989)*, *41*(1), 79–85. <https://doi.org/10.1111/j.1600-0897.1999.tb00078.x>
- Tsang, J. C. H., Vong, J. S. L., Ji, L., Poon, L. C. Y., Jiang, P., Lui, K. O., ... Lo, Y. M. D. (2017). Integrative single-cell and cell-free plasma RNA transcriptomics elucidates placental cellular dynamics. *Proceedings of the National Academy of Sciences of the United States of America*, *114*(37), E7786–E7795. <https://doi.org/10.1073/pnas.1710470114>
- Tuckey, R. C. (2005). Progesterone synthesis by the human placenta. *Placenta*, *26*(4), 273–281. <https://doi.org/https://doi.org/10.1016/j.placenta.2004.06.012>
- Turbeville, H. R., & Sasser, J. M. (2020). Preeclampsia beyond pregnancy: long-term consequences for mother and child. *American Journal of Physiology-Renal Physiology*, *318*(6), F1315–F1326. <https://doi.org/10.1152/ajprenal.00071.2020>
- Turco, M. Y., & Moffett, A. (2019). Development of the human placenta. *Development (Cambridge, England)*, *146*(22). <https://doi.org/10.1242/dev.163428>
- Turowski, G., & Vogel, M. (2018). Re-view and view on maturation disorders in the placenta. *APMIS*, *126*(7), 602–612. <https://doi.org/https://doi.org/10.1111/apm.12858>
- van den Berg, C. B., Chaves, I., Herzog, E. M., Willemsen, S. P., van der Horst, G. T. J., & Steegers-Theunissen, R. P. M. (2017). Early- and late-onset preeclampsia and the DNA methylation of circadian clock and clock-controlled genes in placental and newborn tissues. *Chronobiology International*, *34*(7), 921–932.
<https://doi.org/10.1080/07420528.2017.1326125>
- van Patot, M. C. T., Ebensperger, G., Gassmann, M., & Llanos, A. J. (2012). The hypoxic placenta. *High Altitude Medicine & Biology*, *13*(3), 176–184.
<https://doi.org/10.1089/ham.2012.1046>
- Vargas, A., Moreau, J., Landry, S., LeBellego, F., Toufaily, C., Rassart, É., ... Barbeau, B. (2009). Syncytin-2 Plays an Important Role in the Fusion of Human Trophoblast Cells. *Journal of Molecular Biology*, *392*(2), 301–318.
<https://doi.org/https://doi.org/10.1016/j.jmb.2009.07.025>
- Vento-Tormo, R., Efremova, M., Botting, R. A., Turco, M. Y., Vento-Tormo, M., Meyer, K. B., ... Teichmann, S. A. (2018). Single-cell reconstruction of the early maternal-fetal interface in humans. *Nature*, *563*(7731), 347–353. <https://doi.org/10.1038/s41586-018-0698-6>
- Vlahos, A., Mansell, T., Saffery, R., & Novakovic, B. (2019). Human placental methylome in the interplay of adverse placental health, environmental exposure, and pregnancy outcome. *PLoS Genetics*, *15*(8), e1008236.
<https://doi.org/10.1371/journal.pgen.1008236>

- Wagner, S. J., Craici, I. M., Grande, J. P., & Garovic, V. D. (2012). From placenta to podocyte: vascular and podocyte pathophysiology in preeclampsia. *Clinical Nephrology*, *78*(3), 241–249. <https://doi.org/10.5414/cn107321>
- Wheelock, M. J., & Johnson, K. R. (2003). Cadherins as Modulators of Cellular Phenotype. *Annual Review of Cell and Developmental Biology*, *19*(1), 207–235. <https://doi.org/10.1146/annurev.cellbio.19.011102.111135>
- Wilson, S. L., Leavey, K., Cox, B., & Robinson, W. P. (2017). The value of DNA methylation profiling in characterizing preeclampsia and intrauterine growth restriction. *BioRxiv*, 151290. <https://doi.org/10.1101/151290>
- Wilson, S. L., & Robinson, W. P. (2018). Utility of DNA methylation to assess placental health. *Placenta*, *64*, S23–S28. <https://doi.org/https://doi.org/10.1016/j.placenta.2017.12.013>
- Wu, H., Kirita, Y., Donnelly, E. L., & Humphreys, B. D. (2019). Advantages of Single-Nucleus over Single-Cell RNA Sequencing of Adult Kidney: Rare Cell Types and Novel Cell States Revealed in Fibrosis. *Journal of the American Society of Nephrology : JASN*, *30*(1), 23–32. <https://doi.org/10.1681/ASN.2018090912>
- Xiang, Y., Cheng, Y., Li, X., Li, Q., Xu, J., Zhang, J., ... Zhao, X. (2013). Up-regulated expression and aberrant DNA methylation of LEP and SH3PXD2A in pre-eclampsia. *PLoS One*, *8*(3), e59753–e59753. <https://doi.org/10.1371/journal.pone.0059753>
- Xie, L., Mouillet, J.-F., Chu, T., Parks, W. T., Sadovsky, E., Knöfler, M., & Sadovsky, Y. (2014). C19MC microRNAs regulate the migration of human trophoblasts. *Endocrinology*, *155*(12), 4975–4985. <https://doi.org/10.1210/en.2014-1501>
- Yong, H. E. J., & Chan, S.-Y. (2020). Current approaches and developments in transcript profiling of the human placenta. *Human Reproduction Update*, *26*(6), 799–840. <https://doi.org/10.1093/humupd/dmaa028>
- Yuan, V., Hui, D., Yin, Y., Peñaherrera, M. S., Beristain, A. G., & Robinson, W. P. (2021). Cell-specific characterization of the placental methylome. *BMC Genomics*, *22*(1), 6. <https://doi.org/10.1186/s12864-020-07186-6>
- Yuan, V., Price, E. M., Del Gobbo, G., Mostafavi, S., Cox, B., Binder, A. M., ... Robinson, W. P. (2019). Accurate ethnicity prediction from placental DNA methylation data. *Epigenetics & Chromatin*, *12*(1), 51. <https://doi.org/10.1186/s13072-019-0296-3>
- Yung, H. W., Colleoni, F., Dommett, E., Cindrova-Davies, T., Kingdom, J., Murray, A. J., & Burton, G. J. (2019). Noncanonical mitochondrial unfolded protein response impairs placental oxidative phosphorylation in early-onset preeclampsia. *Proceedings of the National Academy of Sciences of the United States of America*, *116*(36), 18109–18118. <https://doi.org/10.1073/pnas.1907548116>
- Zakiyah, N., Postma, M. J., Baker, P. N., van Asselt, A. D. I., & Consortium, Impro. (2015). Preeclampsia Diagnosis and Treatment Options: A Review of Published Economic Assessments. *PharmacoEconomics*, *33*(10), 1069–1082. <https://doi.org/10.1007/s40273-015-0291-x>
- Zheng, L., Huang, J., Su, Y., Wang, F., Kong, H., & Xin, H. (2020). Overexpression of tissue

factor pathway inhibitor 2 attenuates trophoblast proliferation and invasion in preeclampsia. *Human Cell*, 33(3), 512–520. <https://doi.org/10.1007/s13577-020-00322-0>

Zhu, L., Lv, R., Kong, L., Cheng, H., Lan, F., & Li, X. (2015). Genome-Wide Mapping of 5mC and 5hmC Identified Differentially Modified Genomic Regions in Late-Onset Severe Preeclampsia: A Pilot Study. *PloS One*, 10(7), e0134119. <https://doi.org/10.1371/journal.pone.0134119>

Zindler, T., Frieling, H., Neyazi, A., Bleich, S., & Friedel, E. (2020). Simulating ComBat: how batch correction can lead to the systematic introduction of false positive results in DNA methylation microarray studies. *BMC Bioinformatics*, 21(1), 271. <https://doi.org/10.1186/s12859-020-03559-6>